Università degli Studi
di Salerno

DIPARTIMENTO DI INGEGNERIA CIVILE
Corso di Laurea Magistrale in Ingegneria Edile-Architettura

Tesi di Ricerca in
TEORIA E PROGETTO DI EDIFICI IN ZONA SISMICA

(classe LM-4 C.U.)

A.A. (2019-2020)

DESIGN AND ASSESSMENT OF MRFs AND DUAL-CBFs EQUIPPED WITH "FREEDAM" CONNECTIONS

Relatore
Prof. Ing. Vincenzo Piluso

Candidata
Maria Maglio
0660100245

Correlatori
Prof.ssa Ing. Elide Nastri
Prof. Ing. Rosario Montuori

Ai miei genitori

"People are not killed by earthquakes alone,
but by collapsed buildings"

November 23, 1980. Irpinia-Basilicata earthquake, Italy.

TABLE OF CONTENTS

LIST OF FIGURES

LIST OF TABLES

CHAPTER 1

INTRODUCTION

1.1 Background

Earthquakes have always existed and many of them have been devastating for humanity. Problems arise when the earthquake finds a vulnerable built environment linked to the structural system, the materials, the time of construction and the reference regulations. The structural engineer has the task of designing safe new buildings and increasing the safety of existing buildings taking into account the possible presence of an earthquake i.e. a dynamic force that induces oscillations in the structure.

Seismic engineering is a relatively recent discipline whose research has led to the development of rules and techniques for the construction of increasingly safer buildings. Today, we possess new materials and valid design and construction techniques thanks to a current advanced state of knowledge and seismic regulations.

One of the main objectives in the design of seismic-resistant structures is the dissipation of the incoming seismic energy to reduce the vulnerability of the building even in case of destructive seismic events. For this reason, modern seismic codes have introduced simplified rules, such as the beam-column hierarchy criterion, promoting the development of plastic hinges at the beam ends constituting the dissipative zones of traditional Moment Resisting Frames (MRFs) [1]. According to the concept of resistance hierarchy, the behavior of the structure is governed by the ductile mechanism, since the fragile mechanism characterized by a higher resistance threshold cannot be activated. The dissipative capacity of a structure depends as much on the number of areas that plasticize as on their ductility, then the optimization of the seismic response of MRFs is achieved when all the beam ends are subjected to yielding, as well as, the base sections of first storey columns. Such mode of collapse is called global type mechanism. However, the European seismic code [2], based on the hierarchy criterion, is not able to ensure the development of this collapse mode but limits itself to preventing the soft-storey mechanisms.

Steel, a ductile and highly resistant material, is the best choice for building earthquake resistant constructions. In fact, even for high-rise buildings, the steel frame construction, designed according to current rules, has shown its ability to withstand a strong seismic events.

The horizontal seismic motion is a bidirectional phenomenon so the building structure must be able to resist horizontal actions coming from any direction. The structural elements must be arranged in plan according to an orthogonal direction that ensures similar characteristics of stiffness and strength in both main directions. An important aspect of the design is the ability to dissipate energy without a significant reduction in overall resistance against horizontal and vertical actions.

According to the traditional strategy for the seismic design of building structures [3, 4] in case of frequent and occasional seismic events whose return period is comparable with the life cycle of structures, the earthquake input energy has to be completely dissipated by means of viscous damping. For such seismic events, the structure has to be designed to remain in elastic range. Conversely, in case of rare and very rare seismic events whose return period is about 500 years and even more, most of the earthquake input energy is dissipated by hysteresis, but leading to severe plastic excursions and related structural damage. Such structural damage has to be compatible with the ductility and the energy dissipation capacity of structures, because, even though structural damage is accepted, collapse prevention has to be assured and the safeguard of human lives has to be guaranteed.

With reference to steel Moment Resisting Frames (MRFs), there is the need to provide the structure with sufficient lateral strength and stiffness in order to remain in elastic range under frequent and occasional seismic events. In particular, adequate lateral stiffness is needed to reduce the damage to non-structural components which is a fundamental requirement for the check against serviceability limit states. Conversely, in case of destructive earthquakes, MRFs have to be designed in order to dissipate the earthquake input energy at the beam ends where cyclic plastic bending has to occur. To this aim, it is recommended that beam-to-column connections are designed with sufficient over-strength [5, 6] with respect to the connected beams, accounting for random material variability, and the occurrence of strain-hardening to guarantee the full development of the ultimate flexural resistance of plastic hinges. In addition, aiming to promote the plastic engagement of the greatest number of dissipative zones by properly controlling the failure mode, modern seismic codes, such as Eurocode 8, requires the application of hierarchy criteria to promote the yielding of beam ends rather than column ends. To date, the classical design philosophy based on weak beam-strong column-strong joint hierarchy has been widely applied in practical seismic design [3, 7] and surely provides some advantages, such as the development of quite stable hysteresis loops of dissipative zones and the prevention of soft-storey mechanisms which, as well known, have to be absolutely avoided because of their poor energy dissipation capacity. However, on the other hand, the traditional design approach provides also several drawbacks [5].

In order to reduce the main drawback of the traditional design strategy, i.e. the occurrence of structural damage, in past decades several strategies have been proposed. In particular, a strategy well suited for application to steel structures is the so-called strategy of supplementary energy dissipation, or passive control [8, 9], where the earthquake input energy is dissipated by viscous damping or hysteretic damping.

1.2 FREEDAM Project

In recent years structural engineering new techniques and materials for the prevention of seismic risk has studied. Particular interest was given to steel structures, among the various applications of this material an important contribution by FREEDAM project was made.

FREEDAM is a project funded by the European Union within the RFCS (Research Fund on Coal and Steel) call, concluded in July 2018 and concerns the design of earthquake-resistant steel structures innovative for the characteristic of the beam-column connection. These are innovative connections as they are equipped with friction dissipators whose purpose is to provide for the dissipation of incoming seismic energy in the event of industrial seismic events. In fact, all dissipation is concentrated in these specifically designed devices and the primary load-bearing structural system, i.e. the beams and columns, remain in the elastic range. This means that even at the end of destructive seismic events the structure remains practically free of damage. This is important because in traditional structures, the areas that are damaged in the structure are the extremities of the beams.

As this research project proposes a new design strategy that involves the design of connections able to withstand without any damage not only frequent and occasional seismic events, but also destructive earthquakes such as those corresponding to rare and very rare events; it is named with the acronym FREEDAM to underline the "FREE From DAMage Connections" aim.

In the recently completed RFCS project FREEDAM (RFSR-CT-2015-00022), has been developed the design and testing of these innovative connections with friction dissipators. The devices have a wide-ranging use while the specific project concerns steel constructions, however it is a technology that can be used both in the construction of new buildings and for the seismic adaptation of existing buildings.

From the technological point of view, the innovation regards the conception of beam-to-column connections. In fact, beam-to-column connections are equipped with friction dampers which can be located either at the bottom flange level or at the levels of the both flanges. Such friction dampers have to be designed to assure the transmission of the beam bending moment required to fulfil serviceability limit state requirements and to withstand without slippage the gravity loads. In addition, they have to be designed in order to assure the dissipation of the earthquake input energy, corresponding to the collapse prevention limit state, without any damage.

The basic idea of the research work is the use of the damping devices under a new perspective. In fact, while the passive control strategies are based on the dissipation of energy by means of damping devices, the design strategy of the FREEDAM project is based on the use of friction dampers conceived in such a way to substitute the traditional dissipative zones of MRFs, i.e. the beam ends.

FREEDAM joints are extremely robust, because they are characterized by a first phase of the response corresponding to the damper slippage and by a second phase in which a secondary resisting mechanism is activated with the bolts acting in shear and the plate elements subjected to bearing. The added value to what has already been achieved at both European and worldwide level is the increase the safety buildings and reduction of the direct and indirect costs related to the development of structural damage in case of rare seismic events or exceptional loads. The friction resistance is calibrated by acting on the number and diameter of bolts and their tightening torque governing the preloading. The flexural resistance results from the product between the damper friction resistance and the lever arm. Such connections exhibit wide and stable hysteresis loops without any damage to the connection steel plate elements, so that they can be referred as “Free from Damage Connections”.

The FREEDAM research project envisaged the characterization of the experimental behaviour of friction materials at different slip rates (static test, dynamic, impact and creep); seismic behaviour of FREEDAM connections (experimental tests on joints, FEM simulations, parametric analyses and definition of the design rules); design of structures with FREEDAM connections: seismic, robustness and sustainability; prototypes study; pseudo-dynamic testing of a real scale structure. The results obtained were: both soft and hard shims, such as the examined M4 and M6, are able to provide a high initial value of the friction coefficient and predictable response; some of the analyzed materials provided a stick-slip response which is completely inappropriate for application to seismic devices; joints were all successful in providing a low damage response thanks also to the adoption of design procedures based on the component method and the principles of capacity design; size of the joints did non seem to provide any unexpected behaviour. Overall similar results were obtained with small or large joints.

The main goal of FREEDAM project has been the development of beam-to-column connections able to withstand destructive seismic events without any damage to the steel components. This can be particularly useful to further promote the use of steel structures in earthquake prone countries of Europe and all over the world.

1.3 FREEDAM Plus

FREEDAM PLUS is aimed at the valorisation and dissemination of the technical knowledge and the design tools developed within FREEDAM project, in order to reach a wider and easier use of dissipative beam-to-column connections in steel seismic resisting systems. During FREEDAM friction dampers to be produced in a ready to install kit have been prototyped. These devices will be advertised during the activities of FREEDAM PLUS project.

To improve the knowledge on the behaviour of the friction connections tested during FREEDAM, few new tests aimed at achieving the Technology Readiness Level TRL8 (system complete and qualified) will be planned. In FREEDAM plus project will be examined which are the limits of application of the current EC3 requirements for friction joints, trying also to find a way to homogenize the requirements of EN1993:1-8 and EN1998-1, in light of the results obtained by FREEDAM project.

Within FREEDAM PLUS practical guidelines will be developed for steel moment resisting and dual frames compliant with the Theory of Plastic Mechanism Control (TPMC) and with the current EC8 rules. The developed codified procedures (for both design of joints and frames) will be applied to a comprehensive set of study cases covering both MRFs and Dual low/medium rise systems and different joint performance levels.

The main goal of FREEDAM PLUS is the valorisation of knowledge for FREE from DAMage steel connections. The dissemination project will take place through collection and organization of informative material concerning the connections equipped with friction dampers, develop pre-normative design recommendations of FREEDAM joints, develop a design handbook to guide professional engineers in all the step of the design of building equipped with FREEDAM connections, develop a software and an app for mobiles to select prequalified solutions from standardised connections, identifying the best FREEDAM kit to equip beam-to-column joints; seminars and workshop.

It is important to point out that the main novelty concerns beam to column connections equipped with friction devices manifactured in shop and bolted to the structural elements (beam and column) directly on site. Then the device is chosen from the catalog according to the beams size. From the design point of view, the approach is based only on few steps design of FREEDAM friction dampers for the actions deriving from the ULS and SLS load combinations; design of the non-dissipative parts of the connections, accounting for the maximum overstrength due to random material variability of the friction material and to the random variability of the bolts preload force.

1.4 Organization of the work

The dissertation is comprised of seven chapters, a conclusive section, three appendices and an annex:

CHAPTER 1 provides the background and motivation, objective and scope, and organization of the work.

CHAPTER 2 illustrates the design criteria and both traditional joints and FREEDAM joints used in the structures.

CHAPTER 3 provides the Theory of Plastic Mechanism Control (TPMC) design algorithms, in particular for two ductility classes established by the Eurocode and applied to two structural types, Moment Resisting Frame (MRF) and Dual-MRF namely.

CHAPTER 4 provides structural configuration of the buildings, applied loads and design assumptions for applications.

CHAPTER 5 provides the TPMC application both with haunched connections and with FREEDAM connections to one study case for MRF and one for D-CBF.

CHAPTER 6 provides the performance evaluation by means of Pushover Analyses of the structures designed by the proposed design procedure (TPMC).

CHAPTER 7 provides the performance evaluation by means of IDA Analyses of the structures designed by the proposed design procedure (TPMC).

CONCLUSIONS present the summary of the work.

APPENDIX A reports the results of all the case studies analyzed, in particular the designed sections, the modal informations, the weight of the structures, the interstorey-drift.

APPENDIX B reports the results of the Pushover Analyses for all the case studies analyzed, in particular seismic forces, resulting curves, the ductility and overstrength information.

APPENDIX C reports the IDA Analyses results in term of inter-storey drift ratio.

ANNEX A shows the catalog of freedam devices that can be used in the design of the structures.

CHAPTER 2

EARTHQUAKE RESISTANT STEEL STRUCTURES

2.1 Introduction

An earthquake can have various effects hence, it is not possible to design an earthquake proof building that will resist all the possible earthquakes. However, it is possible to build structures empowering earthquake resistant features by making use of earthquake engineering techniques that will help increase the chances of survival of both the building and its occupants.

Resistant building steel structures perform well during an earthquake and not cause much of damage. The characteristics that make the steel a perfect structural material for buildings in high seismic risk territories are: high ductility, large levels of energy dissipation, prefabrication and dry connection; qualities that other structural materials cannot boast. Earthquake resistant steel buildings should be designed in one of the Ductility Classes introduced in EN1998-1-1:2019, 4.4.2(3) and 4.4.2, (see Table 11.1), according to their dissipation capacity.

In the new draft of the Eurocode 8 three ductility classes are proposed:

- *DC1 ductility class*, in which the overstrength capacity is taken into account, while the deformation capacity and energy dissipation capacity are disregarded.
- *DC2 ductility class*, in which the local overstrength capacity, the local deformation capacity and the local energy dissipation capacity are taken into account. The purpose is to avoide the soft storey mechanism only.
- *DC3 ductility class*, in which the ability of the structure to form a global plastic mechanism at SD limit state and its local overstrength capacity, local deformation capacity and local energy dissipation capacity are taken into account.

Earthquake-resistant steel structures can be made in three main types.

Moment Resisting Frames (MRFs), are the most common seismic-resistant structures. They are characterized by high dissipation capacity, because of the large number of dissipative zones under cyclic bending represented by the beam end sections. Nevertheless, such structural system could be not able to provide sufficient lateral stiffness, as required to fulfil serviceability limit states.

Concentrically Braced Frames (CBFs), provide the best solution regarding the limitation of the inter-storey drift demands under seismic events having a return period comparable with the lifetime of the structure, because they provide the maximum lateral stiffness when compared with any other structural typology. Nevertheless some uncertainty arises about the adequacy of such structures to assure collapse prevention under severe seismic actions by undergoing large excursions in the nonlinear range (i.e. the fulfilment of ultimate limit state requirements), because they are penalized by the occurrence of buckling of bracing members in compression which governs the shape of the hysteresis loops of such dissipative zones [10].

As an alternative to the basic seismic-resistant structural typologies the *Concentrically Braced Frames Dual system (D-CBF)* constitute a rational solution leading to a design able to satisfy both the requirement for the ultimate limit state and the serviceability limit state. In fact, the exploitation of the dissipative capacity of the beam ends, of the lateral stiffness provided by the diagonals of the braced part and of the dissipation capacity of link elements allow to obtain high global ductility and limited inter-storey drifts, so that both the ultimate and serviceability limit state requirements can be easily satisfied.

In this thesis MRFs and MRF-CBF dual systems, both equipped with friction dampers that without, are investigated.

2.2 Design criteria according to the new Eurocode 8 draft

Structures with dissipative zones shall be designed so that yielding or local buckling or other phenomena due to hysteretic behaviour do not affect the overall stability of the structure. Dissipative zones should have adequate ductility and resistance and may be located in the structural members or the connections. Depending on the ductility class and the behaviour factor q (Table 2.2.1), cross-sectional classes of dissipative elements should be chosen.

Table 2.2.1 - Specific prescriptions for the behaviour factor of different ductility classes and the required cross-section

Ductility class	Value of q	Required cross-sectional class
DC1	$q = 1.5$	-
DC2	$2 < q \leq 3.5$	class 1, 2 for MRFs, CBFs, EBFs and dual frames
DC3	$q > 3.5$	class 1

Low-dissipative structures (DC1) should be designed to resist seismic actions almost in the elastic range. No capacity design rules are provided for this class.

In DC2 ductility class dissipative zones may be in the structural members or in the connections. The connections of the dissipative zones to the rest of the structure should have sufficient overstrength to allow the development of cyclic yielding in the dissipative zones. If dissipative zones are in the connections, the connected members should have sufficient overstrength to allow the development of cyclic yielding in the connections. In particular, this last case is the case of frames equipped with FREEDAM joints.

High-dissipative structure (DC3) should be designed to wide excursions in plastic range, so stresses are amplified with overstrength factors. In particular the material overstrength factor $\gamma_{rm} = 1.25$ for S355; the hardening factor γ_{sh} of the dissipative zones is calculated as $\gamma_{sh} = \frac{(f_y+f_u)}{2f_y} \leq 1.2$ for moment resisting frames with traditional full-strength beam-to-column joints. Conversely, $\gamma_{sh} = 1.0$ in the case of frames equipped with FREEDAM joints.

In the case of frames with concentric bracings (simple and dual), the hardening factor is assumed as equal to $\gamma_{sh} = 1.10$ for all members.

2.2.1 Design rules for Moment Resisting Frames

In DC3 moment resisting frames should be designed so that plastic hinges form in the beams or in the connections of the beams to the columns, but not in the columns. This rule may be neglected in cases:

- at the base of the frame in which $N_{Ed,G}$ in primary columns satisfies the inequality: $N_{Ed,G}/N_{pl,Rd} < 0.3$;
- at the top of primary columns in the upper storey of multi-storey buildings;
- at the top and bottom of primary columns in single storey buildings in which $N_{Ed,G}$ in columns satisfies the inequality: $N_{Ed,G}/N_{pl,Rd} < 0.3$.

If a plastic hinge is expected in the column, its shear force V_{Ed} from the analysis should satisfy:

$$V_{Ed} \leq \begin{cases} 0.5V_{c,Rd} \; for \; class \;\; 1-2 \\ \;\; V_{c,Rd} \; for \; class \; 3-4 \end{cases} \tag{2.1}$$

The non-dimensional slenderness $\bar{\lambda}$ of columns where a plastic hinge is expected to form should not exceed 0,85.

2.2.2 Design rules for Dual Concentrically Braced Frames

In dual structures with both moment resisting frames and braced frames acting in the same direction the horizontal forces should be distributed between the different frames according to their stiffness.

<u>The moment resisting frames should contribute with at least 25 % to the total resistance.</u>

The moment resisting part should be conform to the prescription reported above. The braced frames should respectively conform to the specific prescriptions of CBFs structures reported below.

Design criteria for DC2 and DC3

Concentrically braced frames shall be designed so that yielding of the diagonals in tension takes place before failure of the connections and before yielding or buckling of the beams or columns.

The diagonal elements of bracings should be placed in such a way that the structure exhibits similar behaviour at each storey in opposite senses of the same braced direction under load reversals. To this end, the rule given by the following formula (Formula 11.18 – EC8 1-2 [11]) should be met at each storey:

$$\frac{A^+ - A^-}{A^+ + A^-} \leq 0.05 \tag{2.2}$$

where A^+ and A^- are the areas of the vertical projections of the cross sections of the tension diagonals, when the horizontal seismic actions have a positive or negative direction respectively (see Figure 2.1).

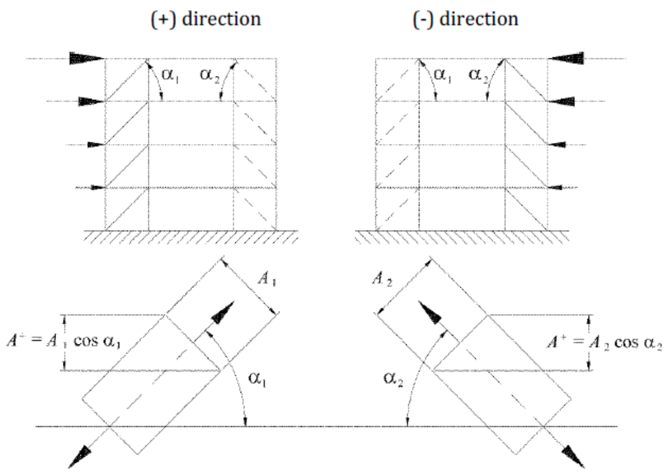

Figure 2.1 - Concentrically braced frame scheme

Eccentricities of diagonal elements in the end connections as respect to the beam-column axes should not be greater than the beam depth and their effects on the members and connections forces should be taken into account. Beams and columns should be considered to resist gravity loads in the persistent and transient design situation, without taking into account the bracing members. In addition, the buckling resistance of diagonal bracings should be verified against the axial forces due to the imposed and variable loads as given in EN1991-1-1, -1-3 and -1-4 at ultimate limit state in non-seismic design situation.

The diagonals should be taken into account using an elastic analysis of the structure for the seismic action according to a) to c):

a) The "tension-only" model may be only used for DC2 frames with X diagonal bracings or split X diagonal bracings;
b) in DC2 frames with V bracings and two-storey X bracings, both the tension and compression diagonals should be taken into account;
c) in DC3 frames, both the tension and compression diagonals should be taken into account.

The compression diagonals in DC2 may be neglected in the analysis provided that the lateral resistance of the building in pre-buckling range of diagonal members is smaller than the resistance of the building evaluated with only the tension diagonals. Both tension and compression diagonals may be taken into account in the analysis of any type of concentric bracing provided that both pre-buckling and post-buckling situations of diagonals are taken into account in both design and modelling.

The cross section of diagonal bracings should be of class 1 in DC3 and class 1 or 2 in DC2 according to EN1993-1-1:2004 [2]. For DC3 frames, a) and b) should be also fulfilled:

a) If circular hollow sections are used for diagonal bracings, their local slenderness D/t should not be greater than, $47{,}4\,\frac{\varepsilon^2}{\gamma_{rm}}$ where D is the external diameter and t the thickness of the cross section and $\varepsilon = \sqrt{235/f_y}$.
b) If either rectangular or square hollow sections are used for diagonal bracings, their maximum local slenderness c/t should not be greater than $19{,}4\,\frac{\varepsilon}{\sqrt{\gamma_{rm}}}$, where c is the side width in accordance with EN1993-1:2005 and t the thickness of the cross section.

The length of the bracing may be taken as the theoretical node-to-node length disregarding the gusset connections at both brace ends. The buckling length should also account for the restraint given by the brace end-connections and the mutual restraint at the mid-length connection between the diagonals of X bracings.

The assumed degree of connection restraint between the diagonals should be verified through analytical calculations, refined finite element simulations or experimental results from the literature.

In frames with tension-compression diagonal bracings (see Figure 11.12 of EC8 1-2), the non-dimensional slenderness $\bar{\lambda}$ hould not be greater than 2,0 in DC3 and 2,5 in DC2.

In structures of up to two storeys with tension-compression diagonal bracings, there is no limitation of non-dimensional slenderness $\bar{\lambda}$.

In frames designed with tension-only bracings, the yield resistance $N_{pl,Rd}$ of the gross cross-section of the diagonals should not be smaller than the axial force N_{Ed} in the bracing member in the seismic design situation.

In frames with tension-compression bracings, the buckling resistance $N_{b,Rd}$ of the bracing members should be such that $N_{b,Rd} \geq N_{Ed}$.

2.3 Traditional joints features

The so-called haunched connections are used in the case of traditional joints. This joints are full-strength and designed to guarantee the formation of all plastic deformations into the beam, which is consistent with EN 1998 strong column-weak beam capacity design rules (i.e. non-dissipative joint). The characteristics are reported in Table 2.2 for haunched connections [12]. In the same tables the details in terms of haunch and rib dimension, stiffness and strength to be accounted for in the design phase are also delivered.

Table 2.2- Details of "Haunched" joints

HAUNCHED CONNECTIONS - Type a

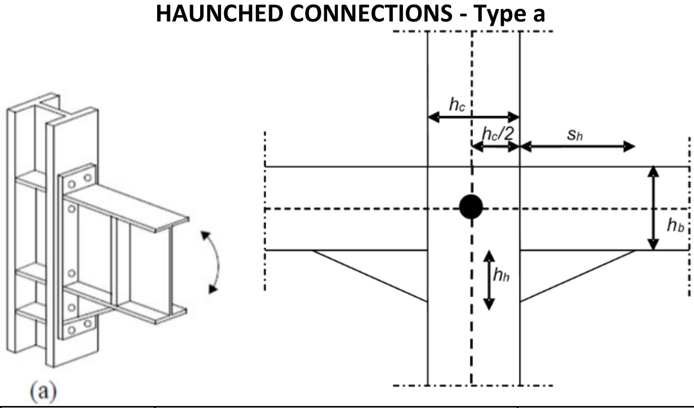

Joint Type	Geometry	Strength		Stiffness	
		Connection:	Panel Zone:	Connection:	Panel Zone:
EH-S: Full-strength with strong panel zone	$\frac{h_h}{h_b} = 0.45$ $\frac{s_h}{h_b} = 0.65$ $z_{wp} = h_b + h_h$	$\frac{M^n_{j,Rd}}{M^e_{pl,b,cf,Rd}} = 1.3$	External nodes: $\frac{V^n_{wp,Rd}\, z_{wp}}{M^e_{pl,b,cf,Rd}} = 1.65$ Internal nodes: $\frac{V^n_{wp,Rd}\, z_{wp}}{2 \cdot M^e_{pl,b,cf,Rd}} = 1.65$	$\frac{s_{con,ini}}{s_b} = 80$	External nodes: $\frac{s_{wp,ini}}{s_b} = 55$ Internal nodes: $\frac{s_{wp,ini}}{2 \cdot s_b} = 55$

Traditional beam-to-column joints have advantages and drawbacks. The advantages derive from the fact that the dissipative zones are costitututed by the beam ends which are able to provide adequate plastic rotation supply, provided that the width-to-thickness ratios b/t of the plate elements constituting the member section are properly limited. Moreover hysteresis loops are wide and stable.

The drawbacks are as follows: the dissipative zones, i.e. the beam ends, are subjected to yielding in case of severe seismic events (life safety or collapse prevention limit states), therefore the primary structural system is subjected to demage and needs to be repaired; the repairing of the yielded ends of the beams is quite difficult and cumbersome; after a destructive seismic event the structure exhibits a significant out of plumb and, therefore, recentering is needed; significant economical losses occurs because of direct and indirect losses.

2.4 Design of FREEDAM joints

In order to overcome the drawbacks of the traditional design approaches, the FREEDAM (FREE from DAMage) design strategy allows, easily, to design rigid frames with fully rigid connections (as in the case of full-strength continuous frames) with a resistance very close to the nominal value of the beam resistance (as in the case of partial – or equal - strength design) and with high energy dissipation supply (as in the case of supplementary energy dissipation strategies) avoiding, in the same time, the structural damage.

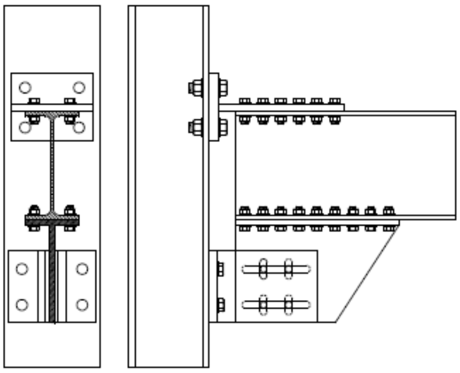

Figure 2.2 - FREEDAM joint scheme

The adoption of FREEDAM connections allows to dissipate the seismic input energy avoiding damage both in the structural members and in the fastening elements of the connecting system, thanks to the inclusion of friction dampers. Such connections are detailed to include at the level of the lower beam flange a friction device realized with steel plates and friction pads pre-stressed with high-strength bolts. In particular, the typical configuration of a FREEDAM beam-to-column joint consists in a modification of the classical detail of a Double Split Tee Joint (DST) where, the bottom tee element, is substituted with a friction damper (Figure 2.2Figure 2.2 - FREEDAM joint scheme).

FREEDAM joints can be designed according to the following equation:

$$M_{f.Ed} \leq M_{j.Rd} = \frac{\mu_{st} n_b n_s P_f}{\gamma_{F2}} h_f \tag{2.3}$$

where μ_{st} is the average value of the static friction coefficient equal to 0.76, n_b is the number of bolts, n_s is the number of the contact surfaces equal to 2, h_f is the lever arm given as the sum of H (Figure 2.3) and h_b (height of the beam), γ_{F2} is the partial safety factor accounting for the randomness of friction and bolt preload, and it is equal to 1.26, P_f is the preloading force that has to be calibrated to assure that the FREEDAM connection resistance is as much close as possible to the design moment $M_{f.Ed}$ at the column face resulting from the seismic load combination. Therefore:

$$P_f \cong \frac{M_{f.Ed}\gamma_{F2}}{\mu_{st} n_b n_s h_f} \tag{2.4}$$

The bolt preloading must not exceed the maximum bolt preloading allowed by code provisions (EN 1993-1-8).

The number of bolts changes according to the standardised devices (Table 2.3). The friction damper to be adopted has to be selected in function of the beam height h_b and of the increase of the lever arm due to the haunch resulting from the damper geometry (Figure 2.3). The characteristics of the prequalified FREEDAM connections are reported in ANNEX A.

Table 2.3 - Number of bolts of the prequalified device

Device	Number of bolts n_b
D1	4
D2	4
D3	6
D4	8
D5	8

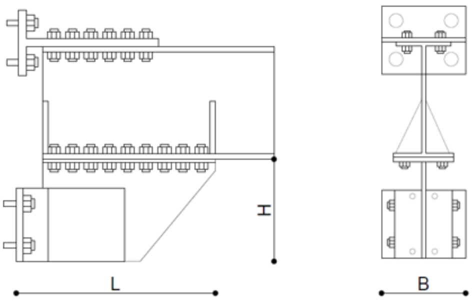

DEVICE	Minimum column size	L [mm]	H [mm]	B [mm]
D1	HE 240 B	505	260	221
D2	HE 280 B	605	360	256
D3	HE 300 B	630	360	276
D4	HE 280 M	820	412	291
D5	HE 320 M	895	512	291
LEGEND				
L	Length			
H	Height			
B	width			

Figure 2.3 - Dimension of prequalified FREEDAM connections

As the aim of FREEDAM joints is the protection of the beam end whose yielding has to be prevented, a local hierarchy criterion to assure that the beam remains in the elastic range must be fulfilled according to the following inequality:

$$M_{b.Rd} \geq \gamma_{Rd} M_{f.Rd} \left(\frac{l-L}{l}\right) \tag{2.5}$$

where $M_{b.Rd}$ is the plastic moment of the beam; l is the distance between the column face and the zero moment point, assumed equal to half beam length; L is the device length (Figure 2.3); γ_{Rd} is the overstrength coefficient accounting for the randomness of both the friction coefficient and the bolts' preload which can be assumed equal to 1.6.

2.4.1 Design Rules for MRFs Equipped with Freedam Joints

Design rules for DC1

Beam and columns are designed as already described in the case of traditional connections. It means that elastic analysis is used without any beam-column hierarchy criterion. However, the FREEDAM joints are designed as described above (Equations (2.3) and (2.4)). It means that the starting solution regarding the beams and the columns to be adopted can be given by the structure designed with traditional joints.

Design rules for DC2 and DC3

In DC2 and DC3, the FREEDAM joints will be designed according to the internal actions arising from the design load combination (Equations (2.3) to (2.5)(2.4). Also in this case the design can start from the knowledge of the structure with traditional joints. The FREEDAM joints standardized typology can be selected from the Table 2.4 according to the beam dimension. Moreover, γ_{Rd} is set equal to 1.6 for DC3 ductility class and 1 for DC2 ductility class.

Table 2.4 - Beam-device couplings

BEAM SIZE	m (Bending Capacity Level)			
	0.3	0.4	0.5	0.6
IPE 270			D1	D1
IPE 300		D1	D1	D1
IPE360	D1	D1	D2	D2
IPE 400	D1	D2	D2	D2
IPE 450	D1	D2	D2	D3
IPE 500	D2	D2	D3	D3
IPE 550	D2	D3	D3	D4
IPE 600	D2	D3	D4	D4
IPE 750 x 147	D3	D4	D5	D5
IPE 750 x 161	D3	D4	D5	D5
IPE 750 x 173	D3	D4	D5	D5
IPE 750 x 185	D4	D5	D5	D5

2.4.2 Specific design rules for Dual CBFs equipped with FREEDAM dampers

Diagonals have to be designed to reduce the interstorey drift that can be very high especially in the 8-storey buildings. According to the new draft of the EC8 the moment-resisting part of the dual system must withstand at least the 25% of the seismic shear. Therefore, the device at the diagonal intersection must be designed with the remaining amount of the shear.

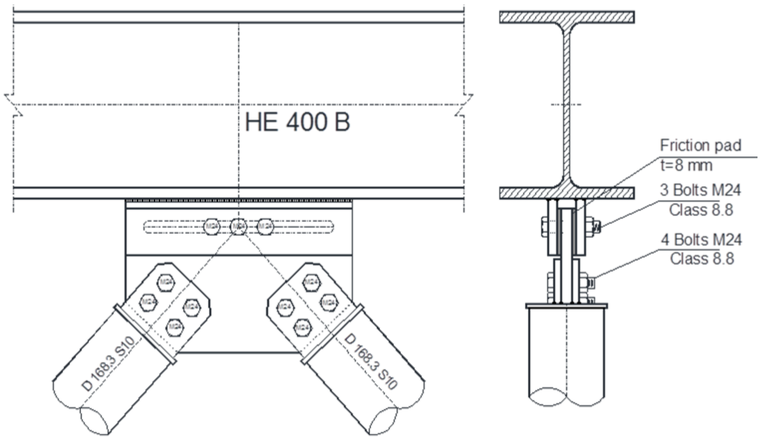

Figure 2.4 - Scheme of the device at brace intersection

The device resistance can be computed according to the following relationship:

$$V_{f.Ed} \leq \frac{\mu_{st} n_b n_s P_f}{\gamma_{F2}} \tag{2.6}$$

where μ_{st} is the average value of the static friction coefficient equal to 0.76, n_b is the number of bolts, n_s is the number of the contact surfaces equal to 2, γ_{F2} is the partial safety factor accounting for the randomness of friction and bolt preload (equal to 1.26), P_f is the preloading force that has to be calibrated to assure that the FREEDAM connection resistance is as much possible close to the design shear $V_{brace.Ed}$ at the storey. In particular:

$$P_f \cong \frac{V_{f.Ed} \gamma_{F2}}{\mu_{st} n_b n_s} \tag{2.7}$$

The dimension of the slotted hole must be calibrated to assure the device sliding; therefore, it has to be compatible with the ductility supply of the column base sections. To this scope, the slotted hole dimension can be computed as 0.04 times the inter-storey height.

Diagonal members should be at least of class 3. No specific limitation are provided for diagonal braces.

Therefore, the friction damper equipping the chevron braces are designed to satisfy the following relationship: $V_{f.Ed} \leq V_{f.Rd}$.

As soon as the design resistance of such dampers has been established, according to the second principle of capacity design, the braces can be designed by considering the maximum friction resistance which the dampers are able to transmit, $V_{f.Cd} = \gamma_{Rd} V_{f.Rd}$. Also here, γ_{Rd} is set equal to 1.6 for DC3 ductility class and 1 for DC2 ductility class.

It is assumed that the braces are pinned; they are designed in order to prevent the occurence of buckling under a compression axial force given by:

$$N_{Ed} = \frac{V_{f.Cd}}{2cos\alpha} \tag{2.8}$$

where α is the brace inclination with respect to the horizontal direction [13].

CHAPTER 3

THEORY OF PLASTIC MECHANISM CONTROL (TPMC)

3.1 Introduction

The 'Theory of Plastic Mechanism Control' (TPMC), initially proposed by Mazzolani and Piluso [14] and subsequently update by Piluso et al. [15], is a useful tool for the seismic design of steel structures.

TPMC is based on the kinematic theorem of plastic collapse extended to the concept of equilibrium curve of mechanism. The kinematic theorem of plastic collapse asserts that the collapse multiplier is the minimum between all kinematically admissible multipliers. Starting from the assumption of a rigid-plastic behaviour, the attention is focused on the structure collapse state. Moreover, according to the TPMC design procedure second order effects are directly accounted for by the concept of the equilibrium curve of the mechanism. The unknowns of the design are the sections of the columns, on each floor, assuring the desired collapse mechanism while beam sections and/or other dissipative zones are assumed as known quantities and designed to withstand the worst condition between the fundamental load combination (ULS) and the seismic combination (SD).

According to the classification on the dissipative capacity of structures by Eurocode 8 [11] only DC2 and DC3 ductility classes are considered for the application of the TPMC. In particular for DC3 ductility class the complete theory (3-TPMC) is adopted because we are considering very dissipative structures wishing to provide a collapse mechanism of global type. To fulfil the philosophy adopted by the new draft of EC8, a simplified theory (2-TPMC) is adopted for DC2 ductility class where the condition to avoid only the soft-storey mechanism is set up. It is important observing that in DC1 ductility class, the TPMC is not adopted because the structures must be designed to remain in the elastic range, so it makes no sense to apply a plastic control design method.

TPMC is herein reported with reference to both Moment Resisting Frames (MRFs) and Dual Concentrically Braced Frames (D-CBFs) with V-braced scheme.

In Figure 3.1 - Global mechanisms for both MRFs and D-CBFsFigure 3.1 the global collapse mechanisms for both MRFs and D-CBFs is reported. Type 1 mechanism (Figure 3.2) affects the storeys of the structure starting from the base. The plastic hinges form at the base and top of the involved columns and at the ends of the beams (and the diagonal bracings for dual systems) of the storeys involved in the mechanism. Type 2 mechanism (Figure 3.3), starts from the upper storeys of the structure. The plastic hinges form at the base of the involved columns and at the ends of the beams (and the diagonal bracing for dual systems) of the storeys involved by the mechanism. Type 3 mechanism

(Figure 3.4), is also called soft-storey mechanism because it invests only one storey. The plastic hinges form at the base and top of the columns of the same storey (and the diagonal bracings for dual systems).

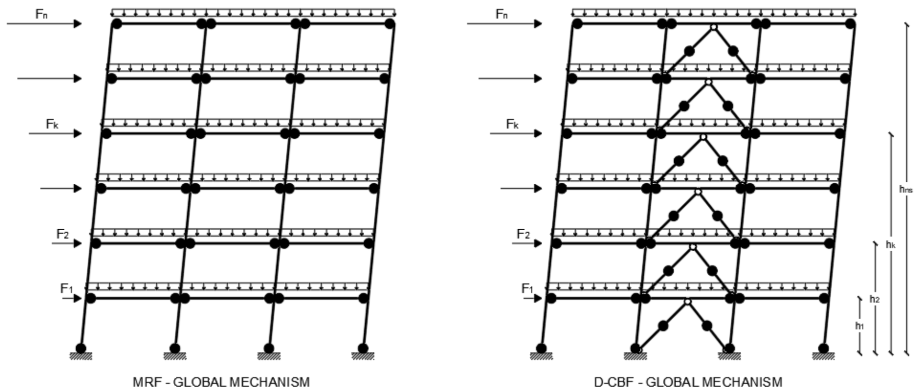

Figure 3.1 - Global mechanisms for both MRFs and D-CBFs

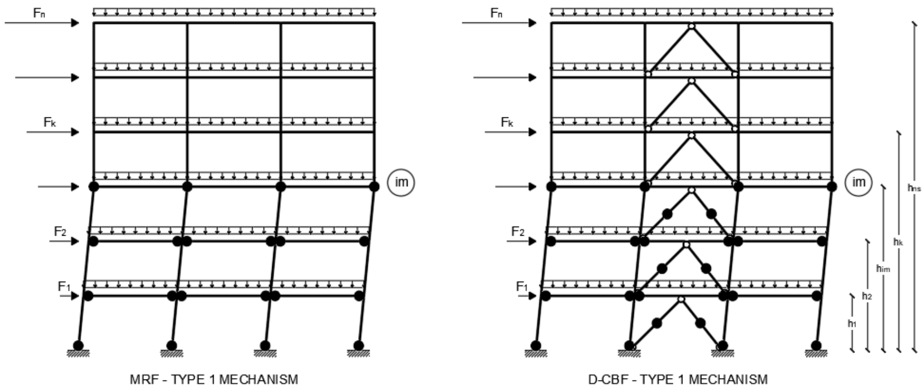

Figure 3.2- Type-1 mechanism for both MRFs and D-CBFs

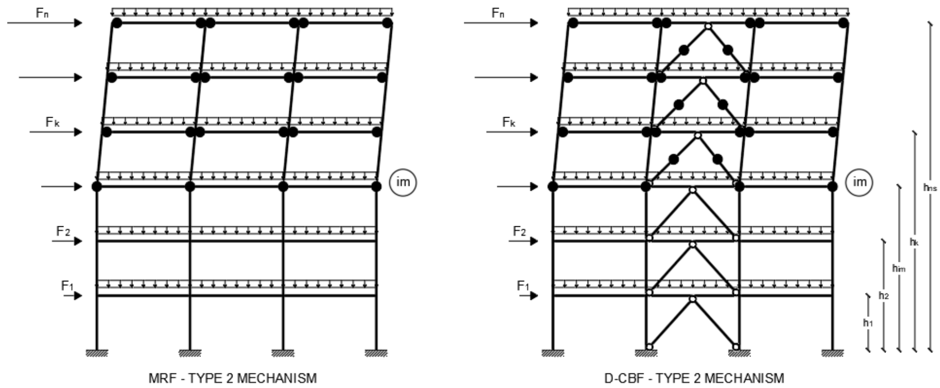

Figure 3.3 - Type-2 mechanism for both MRFs and D-CBFs

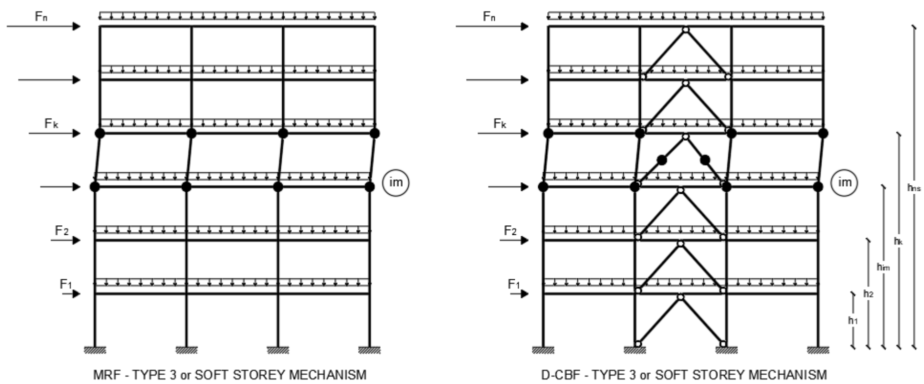

Figure 3.4 - Type-3 mechanism for both MRFs and D-CBFs

Among these considered mechanisms the global mechanism is the more dissipative because all the dissipative zones are involved in the pattern of yielding. The considered dissipative zones are only the beams for the MRFs and the beams and the diagonals in tension and compression for the D-CBFs. Moreover, to attain the complete development of the collapse mechanism also the first storey column bases plastic hinges are activated in plastic range. In the following, the 3-TPMC and 2-TPMC procedures are reported and specialized for both MRFs and D-CBFs. It is important underline that all the local strength and ductility requirement reported in the new EC8 draft must be checked for both the structures designed by 3-TPMC and 2-TPMC as well as the drift limitation. Conversely, all the requirements needed to control the mechanism must not be satisfied as the design philosophy adopted in the mechanism control is out of the traditional rules based on the so-called hierarchy criteria.

3.2 TPMC for DC3 Ductility Class (3-TPMC)

The structures designed by TPMC in DC3 assure a global collapse mechanism (Figure 3.1). For this reason, all the undesired mechanisms must be avoided (Figure 3.2 to Figure 3.4).

Before the complete development of a kinematic mechanism, significant horizontal displacements arise producing non-negligible second order effects. Therefore, the kinematic theorem is supported by the concept of collapse mechanism equilibrium curve. Within the kinematic approach, for any given collapse mechanism, the equilibrium curve of the mechanism can be easily obtained by equating the work of the external forces with the internal one due to the plastic hinges involved in the collapse mechanism. The condition is that second order work due to vertical loads is also included in the determination of the work of external forces.

Reference data:

- i: column index
- j: span index
- n_c: number of columns
- n_b: number of bays
- n_s: number of storeys

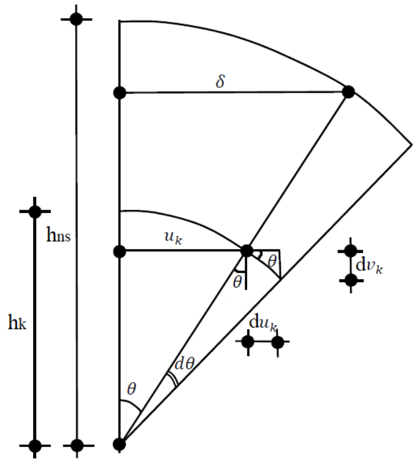

Figure 3.5 – Second-order vertical displacements

When the vertical loads, in seismic combination, acting on the beams respect the following limitation [14]:

$$q_{jk} \leq \frac{4M_{b.jk}}{L_j^2} \tag{3.1}$$

the plastic hinges develop only at the beams ends. Where q_{jk} is the uniformly distributed vertical load applied to the beam of j-th bay and k-th storey; $M_{b.jk}$ is the corresponding beam plastic moment; L_j is the j-th bay span. <u>In this case the previous limitation (3.1) is always verified so we do not consider the external work due to uniformly distributed vertical loads.</u>

In the case of a global mechanism, the work of external forces due to a virtual rotation dθ of the plastic hinges of the columns, starting from a deformed configuration characterized by a rotation θ of the same columns, is given by the following relation (Eq. (3.2)), according to the Figure 3.5:

$$W_e = \alpha \sum_{k=1}^{n_s} F_k h_k \, d\theta + \frac{\delta}{h_{n_s}} \sum_{k=1}^{n_s} V_k h_k \, d\theta \tag{3.2}$$

The first term of equation represents the external work due to seismic horizontal forces, while the second term is the second order work due to vertical loads. This work can be easily expressed when it is recognized that the vector of vertical virtual displacements has the same shape as the vector of horizontal virtual displacements, being in the case of a global mechanism:

$$\delta v_k = \frac{\delta}{h_{ns}} h_k d\theta \tag{3.3}$$

where δv_k is the virtual vertical displacement on the k-th storey.

In the case of a global mechanism the internal work due to the virtual rotation $d\theta$ of the plastic hinges of the columns is:

$$W_i = \left(\sum_{k=1}^{n_s} M_{c.i1} + \sum_{k=1}^{n_s} \sum_{j=1}^{n_b} W_{d.jk} \right) d\theta \tag{3.4}$$

where $M_{c.ik}$ (k = 1) is the plastic moment reduced due to the simultaneous action of the axial force of the i-th column of the k-th storey and $W_{d.jk}$ is the internal work due to the dissipative zones located in j-th bay of k-the storey, to be evaluated depending to the structural typology.

By equating the internal with external work the following relation is obtained:

$$\alpha = \frac{\sum_{k=1}^{n_c} M_{c.1} + \sum_{k=1}^{n_s} \sum_{j=1}^{n_b} W_{d.jk}}{\sum_{k=1}^{n_s} F_k \, h_k} - \frac{1}{h_{ns}} \frac{\sum_{k=1}^{n_s} V_k \, h_k}{\sum_{k=1}^{n_s} F_k \, h_k} \delta \tag{3.5}$$

From this equation it is immediately recognizable that the mechanism equilibrium curve is a straight line which can generally be expressed in the following form:

$$\alpha = \alpha_0 - \gamma \delta \tag{3.6}$$

where α_0 is the kinematically admissible multiplier of the horizontal forces in accordance with a rigid-plastic analysis of the first order; γ is the slope of the collapse mechanism equilibrium curve.

In the case of a global mechanism the kinematically admissible multiplier of the horizontal forces is:

$$\alpha_0{}^{(g)} = \frac{\sum_{i=1}^{n_c} M_{c.1} + \sum_{k=1}^{n_s} \sum_{j=1}^{n_b} W_{d.jk}}{\sum_{k=1}^{n_s} F_k\, h_k} \tag{3.7}$$

while the slope of the equilibrium curve of the mechanism, $\gamma^{(g)}$, is given by:

$$\gamma^{(g)} = \frac{1}{h_{ns}} \frac{\sum_{k=1}^{n_s} V_k\, h_k}{\sum_{k=1}^{n_s} F_k\, h_k} \tag{3.8}$$

The parameters of the equilibrium curve of the collapse mechanism for type 1, type 2 and type 3 mechanisms can be easily obtained in a similar way as follows.

- **Type 1 Collapse Mechanism**

With reference to the i_m-th mechanism of type 1, the multiplier kinematically allowable horizontal forces is given by:

$$\begin{cases} \alpha_{0.1}{}^{(1)} = \dfrac{2\sum_{i=1}^{n_c} M_{c.i1} + \sum_{j=1}^{n_b} W_{d.j1}}{h_1 \sum_{k=1}^{n_s} F_k} & for\ i_m = 1 \\ \alpha_{0.i_m}{}^{(1)} = \dfrac{\sum_{i=1}^{n_c} M_{c.i1} + \sum_{k=1}^{i_m-1} \sum_{j=1}^{n_b} W_{d.jk} + \sum_{i=1}^{n_c} M_{c.iim}}{\sum_{k=1}^{i_m} F_k\, h_k + h_{i_m} \sum_{k=i_m+1}^{i_m} F_k} & for\ i_m > 1 \end{cases} \tag{3.9}$$

while the slope of the equilibrium curve of the mechanism is given by:

$$\gamma_{i_m}^{(1)} = \frac{1}{h_{i_m}} \frac{\sum_{k=1}^{i_m} V_k\, h_k + h_{i_m} \sum_{k=i_m+1}^{n_s} V_k}{\sum_{k=1}^{i_m} F_k\, h_k + h_{i_m} \sum_{k=i_m+1}^{i_m} F_k} \tag{3.10}$$

- **Type 2 Collapse Mechanism**

With reference to the i_m-th mechanism of type 2, the multiplier kinematically allowable horizontal forces is given by:

$$\alpha_{0.i_m}{}^{(2)} = \frac{\sum_{i=1}^{n_c} M_{c.ii_m} + \sum_{k=i_m}^{n_s} \sum_{j=1}^{n_b} W_{d.jk}}{\sum_{k=i_m}^{n_s} F_k \left(h_k - +h_{i_{m-1}}\right)} \tag{3.11}$$

while the slope of the equilibrium curve of the mechanism is:

$$\gamma_{i_m}^{(2)} = \frac{1}{h_{ns} - h_{i_{m-1}}} \frac{\sum_{k=i_m}^{n_s} V_k \left(h_k - h_{i_{m-1}}\right)}{\sum_{k=i_m}^{n_s} F_k \left(h_k - h_{i_{m-1}}\right)} \tag{3.12}$$

It is useful to note that, for the $i_m = 1$ equations (3.11) and (3.12) coincide, respectively, with equations (3.7) and (3.8), because in this case the mechanism coincides with that global one.

- **Type 3 Collapse Mechanism**

With reference to the i_m-th type 3 mechanism, the kinematically admissible multiplier of horizontal forces is given by:

$$\begin{cases} \alpha_{0.1}{}^{(3)} = \dfrac{2\sum_{i=1}^{n_c} M_{c.i1} + \sum_{j=1}^{n_b} W_{d.j1}}{h_1 \sum_{k=1}^{n_s} F_k} & for\ \ i_m = 1 \\ \alpha_{0.i_m}{}^{(3)} = \dfrac{2\sum_{i=1}^{n_c} M_{c.ii_m} + \sum_{j=1}^{n_b} W_{d.ji_m}}{\left(h_{i_m} - h_{i_{m-1}}\right) \sum_{k=i_m}^{n_s} F_k} & for\ \ i_m > 1 \end{cases} \tag{3.13}$$

while the slope of the equilibrium curve of the mechanism is given by:

$$\gamma_{i_m}^{(3)} = \frac{1}{h_{i_m} - h_{i_{m-1}}} \frac{\sum_{k=i_m}^{n_s} V_k}{\sum_{k=i_m}^{n_s} F_k} \tag{3.14}$$

It is important to emphasize that, for any given geometry of the structural system, the slope of the collapse mechanism equilibrium curve draws its minimum value when the developed collapse mechanism is the global one. In accordance with the kinematic theorem of plastic collapse extended to the concept of collapse mechanism equilibrium curve, the design condition that must be satisfied in order to avoid the mechanisms of undesired collapse requires that the equilibrium curve corresponding to the global mechanism must be located below those corresponding to undesired mechanisms up to a maximum displacement at the top, δ_u, compatible with the local resources of ductility of the structure (Figure 3.6 - Design statement for 3-TPMC).

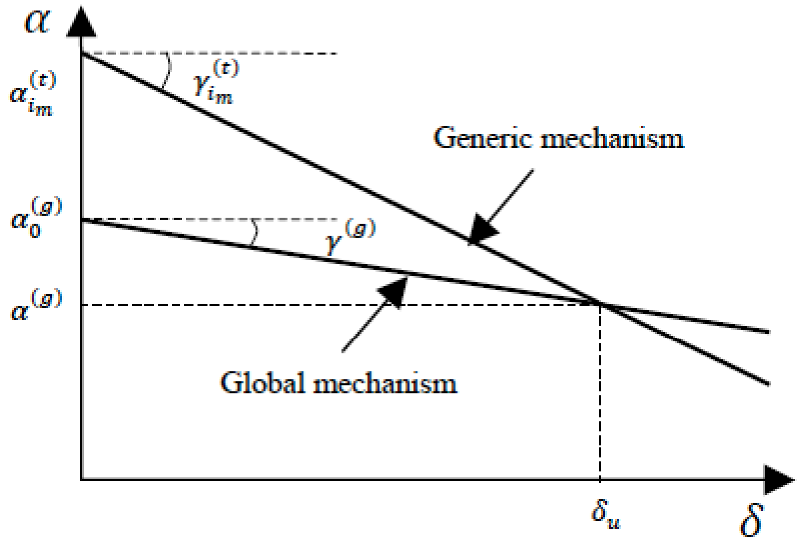

Figure 3.6 - Design statement for 3-TPMC

With this condition we are imposing that the collapse multiplier corresponding to the global mechanism is the smallest among all the kinematically admissible multipliers. Then the global mechanism is the only mechanism that can develop up to the level of displacement considered. The representation reported in Figure 3.6 can be translated in the following inequality:

$$\alpha_0^{(g)} - \gamma^{(g)}\delta_u \leq \alpha_{i_m}^{(t)} - \gamma_{i_m}^{(t)}\delta_u \qquad for \qquad \begin{cases} i_m = 1,2,3.. \\ t = 1,2,3 \end{cases} \qquad (3.15)$$

Eq. (3.15) constitutes the TPMC statement and it is valid independently of the structural typology.

The internal work $W_{d.jk}$ due to the dissipative zones of j-th bay of k-th storey has to be computed accounting for the actual dissipative zones of the structural typology [12, 15, 16]. In particular:

$$\text{for MR-FRAMES: } W_{d.jk} = 2\gamma M_{b.jk}\frac{L_j}{L_{j,k}^*}\begin{cases} W_{d.jk} = 0\ if\ t = 1\ and\ k = 1 \\ W_{d.jk} = 0\ if\ t = 1\ and\ k = i_m \\ W_{d.jk} = 0\ if\ t = 3 \end{cases} \qquad (3.16)$$

$$\text{for D-CBFs: } W_{d.jk} = 2\gamma M_{b.jk}\frac{L_j}{L_{j,k}^*} + \gamma N_{t.jk}e_{t.jk} + N_{c.jk}(\delta_u)e_{c.jk}$$

The rules valid for MRFs apply also for the first term of the dual system. The terms reported in Eq. (3.16) are the following:

- $\gamma = \gamma_{rm} \cdot \gamma_{sh}$ is the overstrength factor used for DC3 ductility class;
- γ_{rm} is the material overstrength factor of the steel in the dissipative zone [11]

$$\begin{cases} \gamma_{\mathrm{rm}} = 1{,}12 \text{ for MRFs and steel S355} \\ \gamma_{\mathrm{rm}} = 1{,}25 \text{ for D} - \text{CBFs and steel S355} \end{cases}$$

- γ_{sh} is the factor accounting for hardening of the dissipative zone [11]

$$\begin{cases} \gamma_{sh} = 1{,}2\ for\ MRFs \\ \gamma_{sh} = 1{,}1\ for\ D - CBFs \end{cases}$$

- L_j is the j-th bay length;
- $L_{j,k}^*$ represents, with reference to k-th storey, the actual length of the j-th bay;
- $N_{t.jk}$ represents the ultimate resistance of the yielded tensile diagonal of j-th braced bay and k-th storey;
- $e_{t.jk}$ is the corresponding axial plastic elongation due to a unit virtual rotation of the plastic hinges of first storey columns;

- $N_{c.jk}(\delta_u)$ is the post-buckling axial resistance of compressed diagonal computed as corresponding to the design ultimate plastic top sway displacement δ_u;
- $e_{c.jk}$ is the corresponding axial shortening due to a unit virtual rotation of the plastic hinges of first storey columns.

3.2.1 Columns design algorithm for the 3-TPMC

The column sections needed to prevent undesired collapse mechanisms have been derived by means of the following design procedure being known all the dissipative zones.

a) Selection of the top sway displacement, $\delta_u = \theta_{pl} \cdot h_{ns}$

- θ_{pl} is the beams plastic rotation, assumed equal to 0,04 rad
- h_{ns} is the total height of the structure.

b) Computation of the slope of mechanism equilibrium curves $\gamma_{im}^{(t)}$ by means of equations (3.10), (3.12) and (3.14).

From Eq. (3.8) we obtain the slope of the equilibrium curve of the global mechanism $\gamma^{(g)}$ which is the minimum among the values of $\gamma_{im}^{(t)}$.

c) Design of the first storey columns sections.

When i_m = 1 the inequality (3.15) is reduced to a single design condition needed to avoid the soft-storey mechanism at the first storey.

Thus, it is possible to design the columns of the first storey in closed form:

$$\alpha_0^{(g)} - \gamma^{(g)}\delta_u \leq \alpha_{0.1}^{(3)} - \gamma_1^{(3)}\delta_u \tag{3.17}$$

By substituting the corresponding terms, we obtain that the design of the columns on the first storey must be such that:

$$\sum_{i=1}^{n_c} M_{c.i.1} \geq \frac{\sum_{k=1}^{n_s}\sum_{j=1}^{n_b} W_{d.jk} + (\gamma_1^{(3)} - \gamma^{(g)})\delta_u \sum_{k=1}^{n_s} F_k\, h_k}{2\frac{\sum_{k=1}^{n_s} F_k\, h_k}{h_1 \sum_{k=1}^{n_s} F_k} - 1} \tag{3.18}$$

d) Computation of the axial load acting in the columns at collapse state i.e., when the global mechanism is fully developed [15].

e) The sum of the plastic moments required on the first storey (Eq. (3.18)) is spread among the columns.

Therefore we can proceed in two ways:

- Distribution by the axial load: $M_{c.i.1} = \frac{N_{c.i.1} \cdot \sum_{i=1}^{n_c} M_{c.i.1}}{\sum_{i=1}^{n_c} N_{c.i.1}}$
- Distribution by the column number: $M_{c.i.1} = \frac{\sum_{i=1}^{n_c} M_{c.i.1}}{n_c}$ For i = 1,2,…,n_c

By known the internal design actions, the sections of the columns can be designed by choosing the appropriate profiles from standard shapes.

From this design it is possible to obtain the sum of the plastic moments of the columns at the first storey, $\sum_{i=1}^{n_c} M^*_{c.i.1}$.

f) Computation of the sum of plastic moment of columns, reduced to the contemporary action of the axial load required at each storey to avoid undesired mechanism by the following conditions:

$$\sum_{i=1}^{n_c} M^{(1)}_{c,ii_m} \geq (\alpha^{(g)} + \gamma^{(1)}_{i_m}\delta_u)\left(\sum_{k=1}^{i_m} F_k\, h_k + h_{i_m}\sum_{k=i_m+1}^{i_m} F_k\right) - \sum_{i=1}^{n_c} M^*_{c.i.1} - \sum_{k=1}^{n_s}\sum_{j=1}^{n_b} W_{d.jk} \tag{3.19}$$

$$\sum_{i=1}^{n_c} M_{c,ii_m}^{(2)} \geq \left(\alpha^{(g)} + \gamma_{i_m}^{(2)} \delta_u\right) - \sum_{k=i_m}^{n_s} F_k \left(h_k - h_{i_{m-1}}\right) - \sum_{k=1}^{n_s} \sum_{j=1}^{n_b} W_{d.jk} \tag{3.20}$$

$$\begin{cases} \displaystyle\sum_{i=1}^{n_c} M_{c.ii_m}^{(3)} \geq \left(\alpha^{(g)} + \gamma_{i_m}^{(3)} \delta_u\right) \frac{\left(h_{i_m} - h_{i_{m-1}}\right)}{2} \sum_{k=i_m}^{n_s} F_k & for\ MRFs \\ \displaystyle\sum_{i=1}^{n_c} M_{c.ii_m}^{(3)} \geq \frac{1}{2} \left[\begin{array}{c} \left(\alpha^{(g)} + \gamma_{i_m}^{(3)} \delta_u\right)\left(h_{i_m} - h_{i_{m-1}}\right) \displaystyle\sum_{k=i_m}^{n_s} F_k \\ -\displaystyle\sum_{j=1}^{n_b} \left(N_{t.jk} e_{t.jk} + N_{c.jk} e_{c.jk}\right) \end{array} \right] & for\ D-CBFs \end{cases} \tag{3.21}$$

It is important underlining that $\alpha^{(g)}$ is computed by Eq. (3.5) by replacing $\sum_{k=1}^{n_c} M_{c.1}$ with $\sum_{i=1}^{n_c} M_{c.i.1}^*$.

g) Selection of the maximum design sum of plastic moment of columns as the maximum of the values provided by Eqs. (3.19)(3.19) to (3.21).

$$\sum_{i=1}^{n_c} M_{c.ii_m} \geq max \left\{ \sum_{i=1}^{n_c} M_{c,ii_m}^{(1)} ; \sum_{i=1}^{n_c} M_{c,ii_m}^{(2)} ; \sum_{i=1}^{n_c} M_{c,ii_m}^{(3)} \right\} \tag{3.22}$$

h) The sum of plastic moment of columns reduced by the simultaneous action of the normal effort, at each storey (for $i_m>1$) given by Eq. (3.22), has to be distributed among the different storey columns, according to the alternative approaches (see point e).

i) Technological condition: starting from the base, columns sections cannot increase along the height of the building.

j) If this condition is not satisfied the procedure must be repeated from point e) because first storey column sections have to be changed according to the higher dimension of the column along the structure height.

Finally, if the structure exibits a collapse mechanism of global type but it does not satisfy the drift limitation it is suggested to increase the beams sections and to repart the procedure [16]. This necessarily leads to an increase in the columns sections and, consequently, to an increase in the lateral stiffness of the structure.

3.3 TPMC for DC2 Ductility Class (2-TPMC)

As previously mentioned, the Theory of Plastic Control Mechanism for structures in ductility class DC2 is simplified to comply with the DC2 design philosophy, namely to verify that the the soft-storey mechanism is avoided at all storeys.

The soft-storey mechanism (Figure 3.4) is a local collapse mechanism for structures subject to seismic action. It occurs when the plastic hinges develop at the ends of the columns of the same storey. It is a not very flexible and therefore very dangerous mechanism that leads the structure to collapse rapidly.

In this case the work of external forces due to a virtual rotation dθ of the plastic hinges of the columns, starting from a deformed configuration characterized by a rotation θ of the same columns, is given by the following relations:

$$W_e = \alpha^{(3)}(h_{im} - h_{im-1}) \sum_{k=im}^{n_s} F_k d\theta + \sum_{k=im}^{n_s} V_k \delta d\theta \tag{3.23}$$

The internal work due to the virtual rotation d_θ of the plastic hinges of the columns is:

$$\begin{cases} W_i = 2\sum_{i=1}^{n_c} M_{c.iim} d\theta & for\ MRFs \\ W_i = 2\sum_{i=1}^{n_c} M_{c.iim} d\theta + \sum_{j=1}^{n_b}\left(N_{t.jk}e_{t.jk} + N_{c.jk}e_{c.jk}\right) & for\ D-CBFs \end{cases} \tag{3.24}$$

For DC2 ductility class we do not use overstrength factors.

By equating the internal and the external work we obtain the following equations:

- For MRFs

$$\alpha^{(3)} = \frac{2\sum_{i=1}^{n_c} M_{c.iim}}{(h_{im} - h_{im-1})\sum_{k=im}^{n_s} F_k} - \frac{\sum_{k=im}^{n_s} V_k \delta}{(h_{im} - h_{im-1})\sum_{k=im}^{n_s} F_k}$$

- For D-CBFs

$$\alpha^{(3)} = \frac{2\sum_{i=1}^{n_c} M_{c.iim} + \sum_{j=1}^{n_b}\left(N_{t.jk}e_{t.jk} + N_{c.jk}e_{c.jk}\right)}{(h_{im} - h_{im-1})\sum_{k=im}^{n_s} F_k} - \frac{\sum_{k=im}^{n_s} V_k \delta}{(h_{im} - h_{im-1})\sum_{k=im}^{n_s} F_k} \tag{3.25}$$

In general form the mechanism equilibrium curve of the type-3 mechanism is expressed as:

$$\alpha_{im}^{(3)} = \alpha_{0.im}^{(3)} - \gamma_{im}^{(3)}\delta \tag{3.26}$$

At this point, according to the kinematic theorem of plastic collapse, it is possible to impose the condition to avoid the soft-storey mechanism:

$$\alpha_0^{(g)} - \gamma^{(g)}\delta_u \le \alpha_{0.i_m}^{(3)} - \gamma_{i_m}^{(3)}\delta_u \tag{3.27}$$

for $i_m = 1,2,3,\dots,n_s$

As can be seen from Figure 3.7 the design condition assures that the global mechanism equilibrium curve is always below the type-3 collapse mechanism curve until the design displacement δ_u.

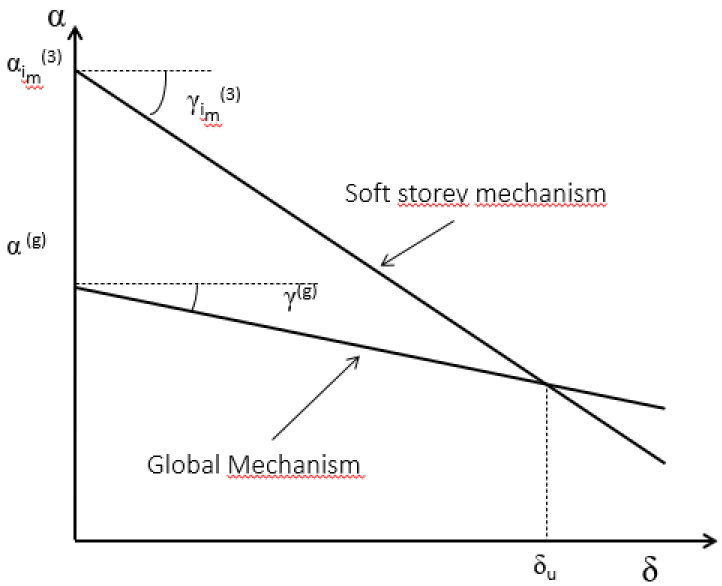

Figure 3.7 – Design statement for 2-TPMC

3.3.1 Columns design algorithm for the 2-TPMC

The column sections needed to prevent Type-3 collapse mechanisms can be derived by means of the following design procedure given that beams and diagonals are already designed.

a) Selection of the top sway displacement, $\delta_u = \theta_{pl} \cdot h_{ns}$

- θ_{pl} is the beams plastic rotation, assumed equal to 0,04 rad
- h_{ns} is the total height of the structure.

b) Computation of the slope of mechanism equilibrium curve $\gamma_{im}^{(3)}$ from the Eqs. (3.8) and (3.14).

c) Design of first storey columns sections.

By replacing Eqs. (3.7), (3.8) and (3.25) in the design condition (Eq. (3.27)) the following design equation is provided to design first storey columns ($i_m = 1$):

$$\sum_{i=1}^{n_c} M_{c,i1}^{(3)} \geq \frac{\sum_{k=1}^{n_s}\sum_{j=1}^{n_b} W_{d.jk} + (\gamma_1^{(3)} - \gamma^{(g)})\delta_u \sum_{k=1}^{n_s} F_k\, h_k}{2\dfrac{\sum_{k=1}^{n_s} F_k\, h_k}{h_1 \sum_{k=1}^{n_s} F_k} - 1} \tag{3.28}$$

where the internal work is specialized as follows for both MRFs and D-CBFs:

$$\begin{cases} W_{d.jk} = 2M_{b.jk}\dfrac{L_j}{L_{j,k}^*} & for\ MRFs \\ W_{d.jk} = 2M_{b.jk}\dfrac{L_j}{L_{j,k}^*} + N_{t.jk}e_{t.jk} + N_{c.jk}(\delta_u)e_{c.jk} & for\ D-CBFs \end{cases} \tag{3.29}$$

From this design it is possible to obtain the sum of the plastic moments of the columns at the first storey, $\sum_{i=1}^{n_c} M_{c.\mathrm{i}.1}^*$.

d) Computation of the axial load acting in the columns at collapse state i.e., when the global mechanism is fully developed [15].

e) The sum of the plastic moments required on the first storey (Eq. (3.28)) is divided among the columns.

f) Computation of the sum of plastic moment of columns, reduced to the contemporary action of the axial load required at each storey to avoid soft-storey mechanism.

By substituting the corresponding terms we obtain the conditions (3.21) for MRF and D-CBFs respectively and $i_m > 1$.

It is important underlining that $\alpha^{(g)}$ is computed by Eq. (3.5) by replacing $\sum_{k=1}^{n_c} M_{c.1}$ with $\sum_{i=1}^{n_c} M_{c.\mathrm{i}.1}^*$.

g) The sum of plastic moment of columns reduced by the simultaneous action of the axial load, at each storey (for i_m>1) given by Eq.(3.21), has to be distributed among the different storey columns (see point e)).

h) Technological condition: starting from the base, columns sections cannot increase along the height of the building.

i) If this condition is not satisfied the procedure must be repeated from point e) because first storey column sections have to be changed according to the higer dimension of the column along the structure height.

Finally, if the structure does not satisfy the drift limitation it is suggested to increase the beams sections and to repeat the procedure. This necessarily leads to an increase in the columns sections and, consequently, to an increase in the lateral stiffness of the structure.

3.4 Application of TPMC to MRFs and D-CBFs with FREEDAM connections

TPMC can be properly applied both to structures with traditional connections and structures equipped whit FREEDAM connections starting from the same equations of the design procedure previously described, with just a few adjustments.

In particular the flexural resistance of beam, $M_{b.Rd.jk}$, is replaced with the flexural resistance referred to the FREEDAMs, $M_{fb.Rd.jk}$, obtained from equations (2.3) to (2.5).

Diagonals of the Daul structures do not become unstable but in the case of a mechanism, friction damper is activated, so the terms referring to chevron braces in eq. (3.16) are to leave out but have to consider the shear resistance of device at the top of chevron braces, $V_{f.Rd.k}$ obtained from equations (2.6) to (2.8).

The internal work $W_{d.jk}$ due to the dissipative zones of j-th bay of k-th storey has to be computed accounting for the actual dissipative zones of the structural typology [13]. In particular:

for MR-FRAMES:

$$W_{d.jk} = 2\gamma_{R_d} M_{fb.Rd.jk} \frac{L_j}{L^*_{j,k}} \begin{cases} W_{d.jk} = 0 \; if \; t = 1 \; and \; k = 1 \\ W_{d.jk} = 0 \; if \; t = 1 \; and \; k = i_m \\ W_{d.jk} = 0 \; if \; t = 3 \end{cases} \tag{3.30}$$

for D-CBFs: $$W_{d.jk} = 2\gamma_{R_d} M_{fb.Rd.jk} \frac{L_j}{L^*_{j,k}} + \gamma_{R_d} V_{f.Rd.k} (h_k - h_{k-1})$$

where γ_{R_d}= 1.6 for DC3 Ductility Class and γ_{R_d}= 1 for DC2 Ductility Class; $M_{fb.Rd.jk}$ is the flexural resistance of the beam-to-column friction damper of j-th beam at k-th storey, $V_{f.Rd.k}$ is the resulting whole shear action due to the braces at k-th storey.

TPMC allows frame to develop the desired global type mechanism (Figure 3.8), by which all the dissipative zones are activated, i.e. the dampers located at the beams end and at the top of braces and plastic hinges at the base sections of first storey columns, while all the other columns remain in elastic range. The beams are designed as non-dissipative members depending on the stresses that FREEDAM are able to transmit to them and so, depending on the case, in order to withstand vertical loads, according to SLU combination, or withstand design seismic forces; whereas the column sections, needed to develop a global type mechanism, are unknown at all storeys.

The undesired mechanism for both MRFs and D-CBFs equipped with FREEDAM connections are pointed out in the Figure 3.9-Figure 3.11. The solid polygons on the beams respresent the FREEDAM dampers actively involved in the kinematic mechanism, the solid rectangles correspond to the activated friction dampers in the braced bay, the solid circles on the columns are the plastic hinges in the same ones.

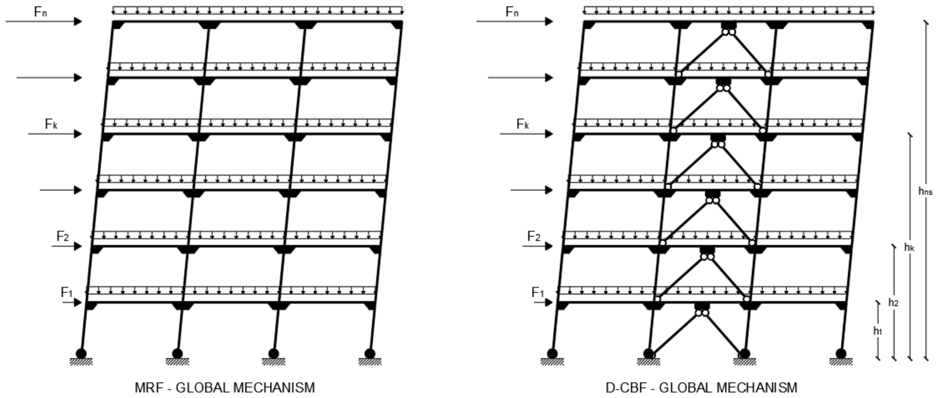

Figure 3.8 - Global mechanisms for both MRFs and D-CBFs equipped with FREEDAM connections

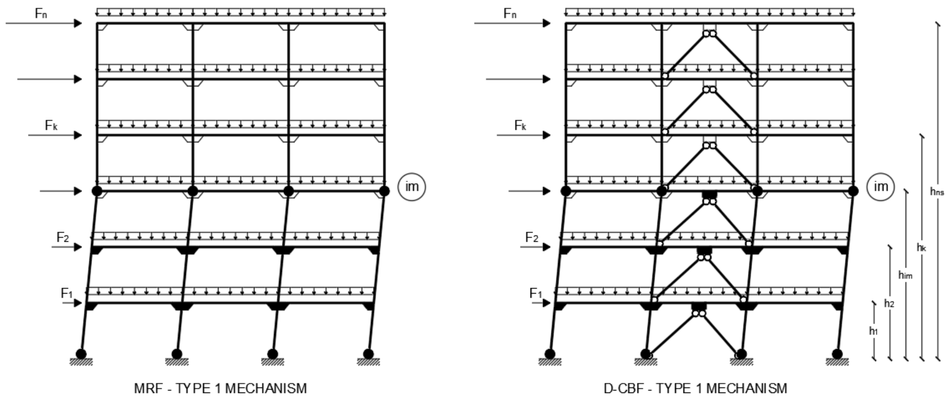

Figure 3.9 – Type 1 mechanism for both MRFs and D-CBFs equipped with FREEDAM connections

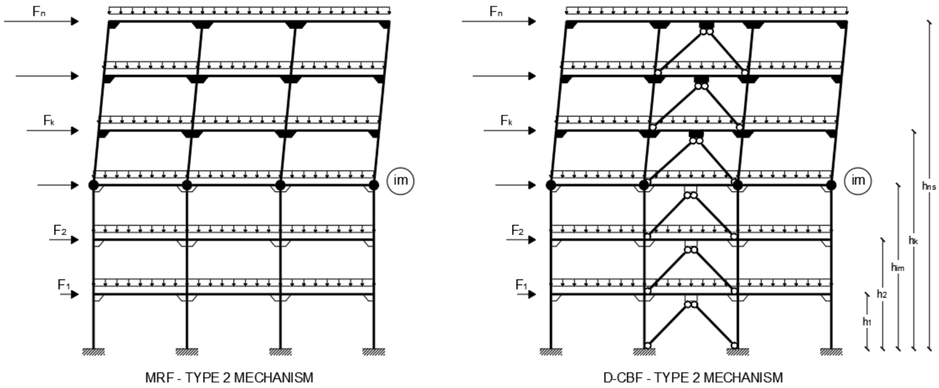

Figure 3.10 – Type 2 mechanism for both MRFs and D-CBFs equipped with FREEDAM connections

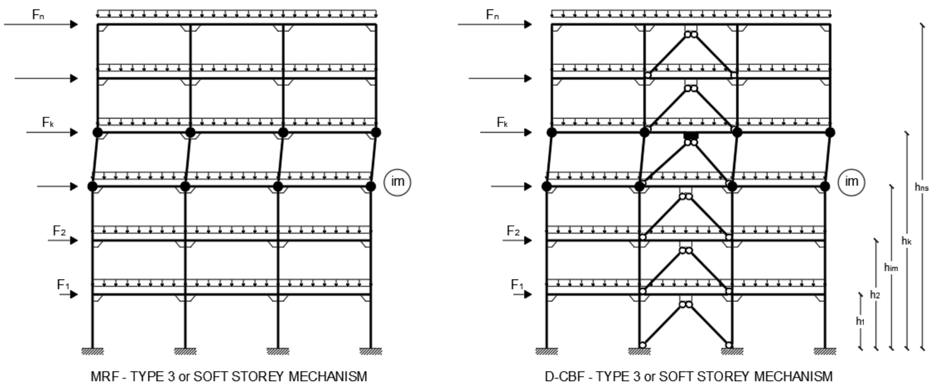

Figure 3.11 – Type 3 mechanism for both MRFs and D-CBFs equipped with FREEDAM connections

CHAPTER 4

DESIGN ASSUMPTIONS FOR APPLICATIONS

4.1 Introduction

The selected structural typologies for numerical applications are Moment Resisting Frames (MRFs) and Dual Concentrically Braced Frames (D-CBFs) with chevron braces. In particular, low-rise (4 storey) and medium-rise structures (8-storey) are designed. Structures are designed according to the Theory of Plastic Mechanism Control (TPMC) both with traditional haunched connections prequalified in the framework of EQUALJOINTS RFCS Project (RFSR-CT-2013-00021) [12] both FREEDAM joints. The design results have been reported and compared in terms of sections, structural weight and dynamic characteristics.

The design of structures with traditional connections will help clarifying the role of FREEDAM connections on the design and performance of seismic resistant structures.

This structural typologies reported in Table 4.1, in two directions of application of the seismic force and in the ductility classes previously exposed, are analyzed. The validation of the procedure has been carried out in two phases. After designing a significant number of structural schemes, the first phase requires that the structures have analysed by means of push-over analysis, while, in a second phase, also incremental dynamic non-linear analyses (IDA) are developed in order to investigate the pattern of yielding under severe seismic motions and the possible influence of higher mode effects. These analyses, constituting the complete validation of the proposed design procedure, will be presented in chapters 6 and 7.

Table 4.1 – Number and code of the structural typologies examined

Nr.	Structure code	Nr Storey
1	4 St_DC2_MRFs_X_TRADITIONAL	4
2	4 St_DC3_MRFs_X_TRADITIONAL	4
3	4 St_DC2_MRFs_Y_TRADITIONAL	4
4	4 St_DC3_MRFs_Y_TRADITIONAL	4
5	8 St_DC2_MRFs_X_TRADITIONAL	8
6	8 St_DC3_MRFs_X_TRADITIONAL	8
7	8 St_DC2_MRFs_Y_TRADITIONAL	8
8	8 St_DC3_MRFs_Y_TRADITIONAL	8
9	4 St_DC2_D-CBFs_X_TRADITIONAL	4
10	4 St_DC3_ D-CBFs _X_TRADITIONAL	4
11	4 St_DC2_ D-CBFs _Y_TRADITIONAL	4
12	4 St_DC3_ D-CBFs _Y_TRADITIONAL	4
13	8 St_DC2_ D-CBFs _X_TRADITIONAL	8
14	8 St_DC3_ D-CBFs _X_TRADITIONAL	8
15	8 St_DC2_ D-CBFs _Y_TRADITIONAL	8
16	8 St_DC3_ D-CBFs _Y_TRADITIONAL	8

17	4 St_DC2_MRFs_X_FREEDAM	4
18	4 St_DC3_MRFs_X_ FREEDAM	4
19	4 St_DC2_MRFs_Y_ FREEDAM	4
20	4 St_DC3_MRFs_Y_ FREEDAM	4
21	8 St_DC2_MRFs_X_ FREEDAM	8
22	8 St_DC3_MRFs_X_ FREEDAM	8
23	8 St_DC2_MRFs_Y_ FREEDAM	8
24	8 St_DC3_MRFs_Y_ FREEDAM	8
25	4 St_DC2_D-CBFs_X_ FREEDAM	4
26	4 St_DC3_ D-CBFs _X_ FREEDAM	4
27	4 St_DC2_ D-CBFs _Y_ FREEDAM	4
28	4 St_DC3_ D-CBFs _Y_ FREEDAM	4
29	8 St_DC2_ D-CBFs _X_ FREEDAM	8
30	8 St_DC3_ D-CBFs _X_ FREEDAM	8
31	8 St_DC2_ D-CBFs _Y_ FREEDAM	8
32	8 St_DC3_ D-CBFs _Y_ FREEDAM	8

4.2 Design assumptions for study cases

The study cases herein investigated are referred to a building whose plan configuration is depicted in Figures 4.1 and 4.2. The seismic resistant structural system is a perimeter system while the inner bays are pinned and designed only for gravity loads.

Regarding the number of storeys, two study cases will be analysed: 1) Low-rise structures with 4 storeys; 2) medium-rise buildings with 8 storeys.

The bay span is equal to 6.00 m; the inter-storey height is equal to 3.50 m. It is assumed that the stairs and the elevator are located outside of the analysed building using an independent structure. The seismic-resistant scheme of the buildings herein analysed are depicted in Figure 4.3 for the X-direction and Figure 4.4 for the Y-direction. The corner right column of each frame is put in the weak direction.

The buildings under investigation are office buildings, i.e. category B according to Eurocode 1 (EC 1-2002) [17]. The adopted steel grade is S355.

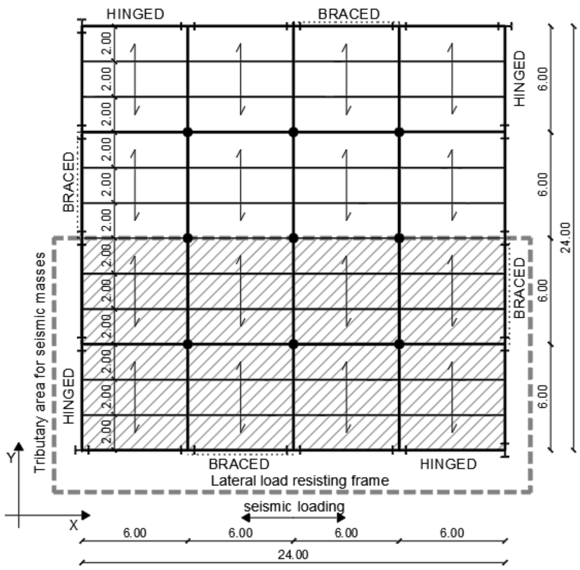

Figure 4.1 – Plan configuration of the building with identification of the lateral load resisting system for X-direction

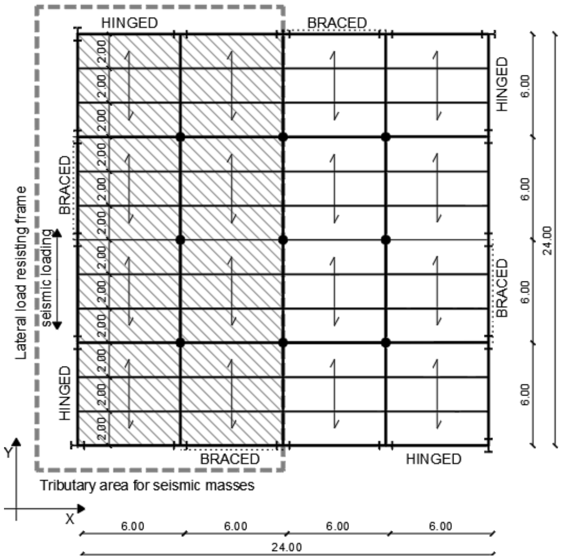

Figure 4.2 – Plan configuration of the building with identification of the lateral load resisting system for Y-direction

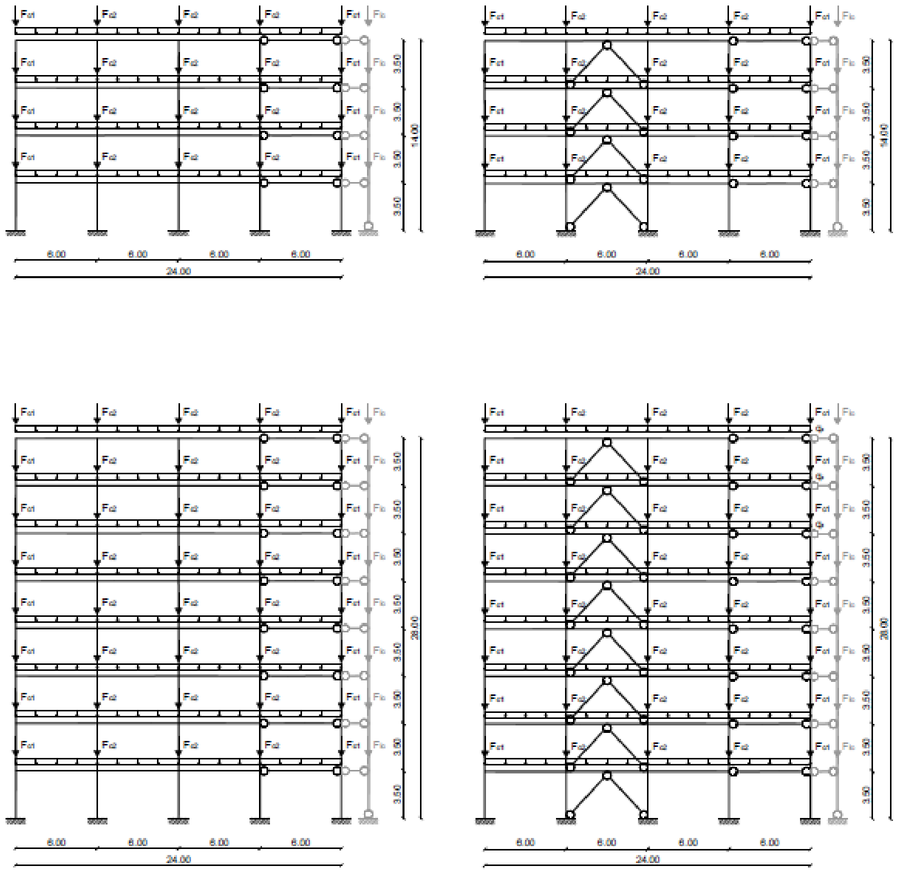

Figure 4.3 – Elevation configuration of the building (MRF and D-CBFs) for X-direction.

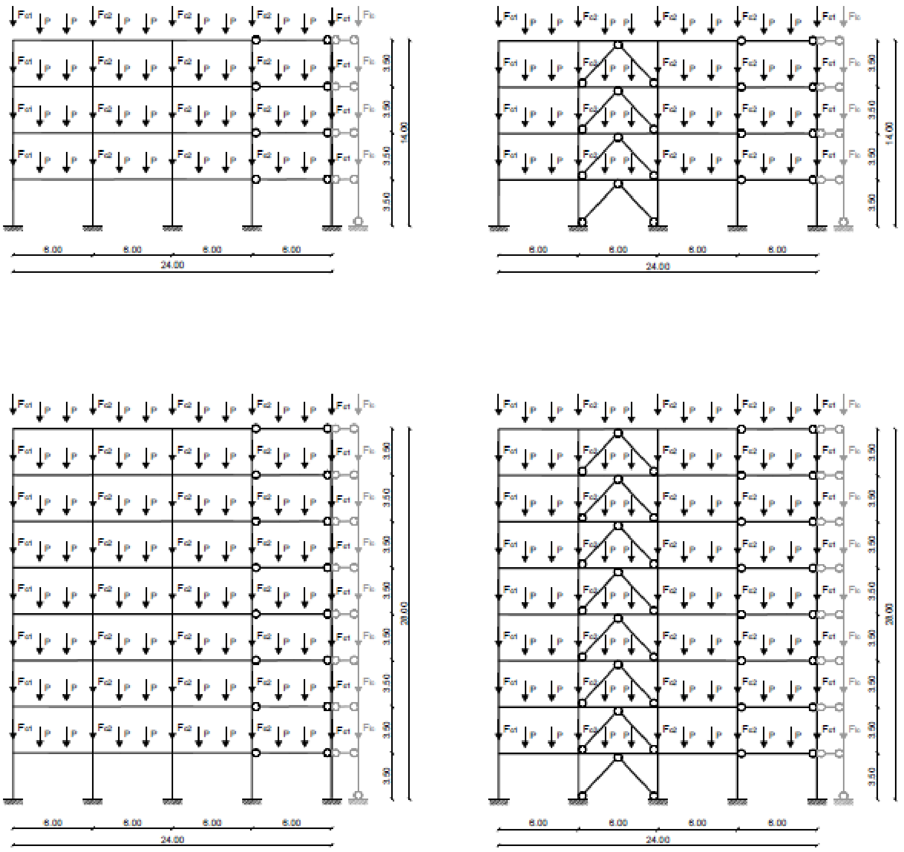

Figure 4.4 – Elevation configuration of the building (MRF and D-CBFs) for Y-direction.

Given the geometry of the structure the following design steps are described:

- Analysis of loads;
- Design of the beams of the gravity load resisting system;
- Computation of concentrated and distributed gravity loads acting on the lateral load resisting frame;
- Computation of gravity loads to be applied to the leaning column;

- Computation of the design seismic forces.

4.3 Assumed permanent and live loads

4.3.1 Permanent loads

➢ **Structural permanent loads**

The floor slab is a composite steel-concrete slab with HI-BOND A55/P600 corrugated steel sheet and C20/25 grade concrete cast (Figure 4.5). The total thickness of the slab is equal to 125 mm. The corrugated sheet is made of S280GD steel, having a thickness equal to 1.2 mm. Therefore, the corresponding loads are:

- Weight of the concrete cast: 2.34 kN/m^2
- Weight of the corrugated steel sheet: 0.16 kN/m^2
- Weight of the structural steel elements: 0.75 kN/m^2

As a consequence, the total structural permanent load is: $\mathbf{3.25}\ \boldsymbol{kN/m^2}$.

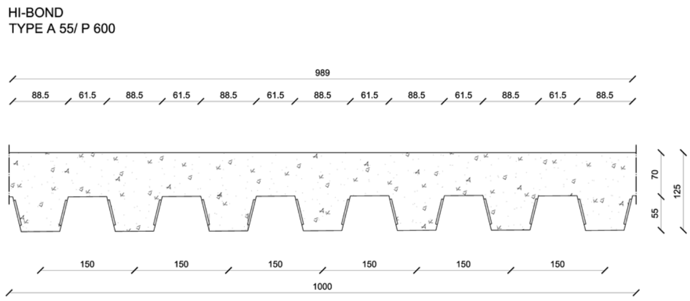

Figure 4.5 - Composite deck section

➢ **Non-structural permanent loads**

- Soundproof insulation

The acoustic insulation is made by soundproof insulation having a thickness equal to 10 mm with a weight per unit volume of 0.30 kN / m^3

- Floor screed

The floor screed is made by lightweight aggregates with a thickness equal to 50 mm and weight per unit volume equal to 7.2 kN/m^3.

- Floor

The floor is made of ceramic with a weight per unit volume equal to 10 kN/m^3 and a thickness equal to 20 mm.

- Thermal insulation

The thermal insulation is made of fibreglass, 100 mm thickness, and weight per unit volume of 0.10 kN/m^3.

- Ceiling

The ceiling is made by plasterboards (thickness 20 mm) with weight per unit volume equal to 0.177 kN/m^2. The values of the non-structural permanent loads are reported in Table 4.2Table 4.2.

Table 4.2 - Non-structural permanent loads.

	Weight per unit volume (kN/m^3)	Thickness (m)	Loads (kN/m^2)
Soundproof insulation	0.30	0.010	0.003
Floor screed	7.20	0.050	0.360
Floor	10.00	0.020	0.200
Thermal insulation	0.10	0.100	0.010
Ceiling			0.177
Total value of non-structural permanent loads			**0.75** kN/m^2

- External walls

The external walls are made by plasterboards (thickness 12,5 mm) with weight per unit volume equal to 1.00 kN/m^2.

- **Summary of permanent loads (g_k)**

The following permanent loads are considered:

- Permanent loads on floors and roof: $\mathbf{3,25+0,75=4,0}\ \boldsymbol{kN/m^2}$
- Permanent loads of external walls: $\mathbf{1,0}\ \boldsymbol{kN/m^2}$

4.3.2 Live loads ($\mathbf{q_k}$)

Live loads for office buildings are equal to: $\mathbf{3.00}\ \boldsymbol{kN/m^2}$

- Internal partition walls

The internal partition walls are made of single metallic warp with single coating panel (KNAUF W111 type). They are made of cold-formed steel profiles with a "C" shape, placed at a spacing of 600 mm. The "C" profiles are integrated by two plasterboards (thickness 12.5 mm) on the outer surfaces. The interspace contains a rock wool insulation layer having 60 mm of thickness and a weight per unit volume equal to 0.7 kN/m^3. The total weight per unit area is 0.292 kN/m^2 (0.25 kN/m^2 for the uninsulated wall and 0.7 kN/m^3 × 0.06 m = 0.042 kN/m^2 for the insulating layer).

The height of the partition wall is equal to about 3.00 m which corresponds to a linear load equal to 0.292 × 3.00 = 0.876 kN/m. Therefore, as the internal partition walls have a unit weight less than 1 kN/m, according to Eurocode 1, it is possible to model their load as a uniform load equal to 0.50 kN/m^2.

Consequently, the characteristic values of live values are:

Current floor: $\boldsymbol{q_k} = \mathbf{3.5}\ \boldsymbol{kN/m^2}$

Roof: $\boldsymbol{q_k} = \mathbf{3.0}\ \boldsymbol{kN/m^2}$

- **Design of the composite steel-concrete slab**

The design load is the sum of non-structural permanent loads and live loads:

$$q_u = 0.75 + 3.00 + 0.50 = 4.25\ kN/m^2 \tag{4.1}$$

The maximum useful load for the composite steel-concrete slabs HI-BOND A55/P600 mm is equal to 4.25 kN/m² in the case of continuous beams on 4 supports with 2.00 m span.

Therefore, the adopted steel-concrete composite slab can withstand the applied loads. The ultimate limit state combination for gravity loads provides:

$$q_d = \gamma_g\,(g_{k1} + g_{k2}) + \gamma_q\, q_k$$
$$= 1.35\ \times (3.25 + 0.75) + 1.5\ \times 3.50 \qquad \textit{floors}$$
$$= 10.65\ kN/m^2$$

$$q_{d.roof} = \gamma_g\,(g_{k1} + g_{k2}) + \gamma_q\, q_k$$
$$= 1.35\ \times (3.25 + 0.75) + 1.5\ \times 3.00 \qquad \textit{roof}$$
$$= 9.9\ kN/m^2$$

- **Design of beams of the gravity load resisting system**

The beams of the gravity load resistant system are designed to withstand the loads corresponding to the ultimate limit state load combination $q_d = 10.65\ kN/m^2$for the floors and $q_{d.roof} = 9.9\ kN/m^2$ for the roof. The reactions corresponding to the internal supports are:

$$R_i = 1.00\ q_d l = 1.00 \times 10.65 \times 2 = 21.30\ kN/m$$
$$R_{i.roof} = 1.00\ q_{d.roof} l = 1.00 \times 9.9 \times 2 = 19.8\ kN/m \qquad (4.2)$$

while the reaction corresponding to the external supports are:

$$R_e = 0.50\ q_d l = 0.50 \times 10.65 \times 2 = 10.65\ kN/m$$
$$R_{e.roof} = 0.50\ q_{d.roof} l = 0.50 \times 9.9 \times 2 = 9.90\ kN/m \qquad (4.3)$$

The reaction R_i per unit of length is the distributed load acting on the secondary beams whose scheme is reported in Figure 4.6

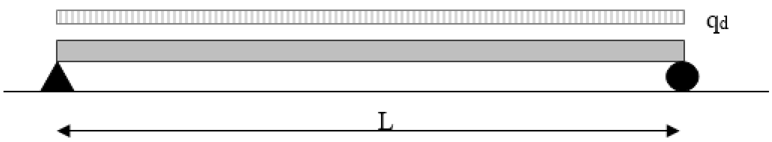

Figure 4.6. The maximum moment in the midspan of the secondary beams, computed for the more loaded beam is:

$$M_{max} = R_i \frac{L^2}{8} = 21.30 \times \frac{6^2}{8} = 95.85\ kN\ m \quad \rightarrow \quad W_{pl} = \frac{M_{max}}{f_y} = \frac{95.85 \times 1000}{355}$$
$$= 270.00\ cm^3 \quad \rightarrow \quad IPE\ 220$$

Notwithstanding the above section has to be increased to fulfil the serviceability requirements concerning the limitation of the maximum deflection which are **1/300 for live loads only and 1/250 for characteristic load combination**.

To this scope, a beam section **IPE 270** is adopted. Therefore, the standard shape selected for secondary beams is IPE 270 profile which is also checked against serviceability requirements. The design flexural resistance of the secondary beams is:

$$M_{Rd} = \frac{484 \times 10^{-3} \times 355}{1.00} \cong 171.82\ kNm \qquad (4.4)$$

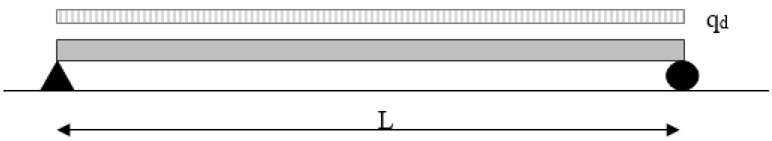

Figure 4.6 - Scheme of secondary beams and primary beams parallel to secondary beams.

The scheme of the primary internal beams is depicted in Figure 4.7, where the concentrated load due to the two adjacent orthogonal secondary beams is $P = 127.8\ kN$. The load acting on the external primary beams is equal to $P = 63.90\ kN$.

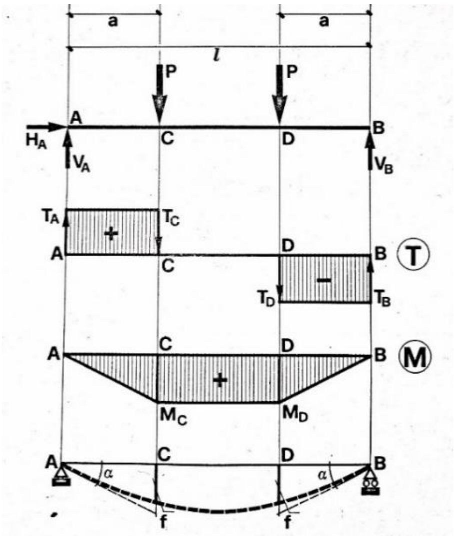

Figure 4.7 - Structural scheme of the primary beams of the gravity load resisting system

The maximum moment acting on these beams is equal to:

$$M_{max} = Pl = 127.8 \times 2 = 255.60\ kNm \ \rightarrow \ W_{pl} = \frac{M_{max}}{f_y} = \frac{255.60 \times 1000}{355}$$
$$= 720.00\ cm^3 \ \rightarrow \ IPE\ 330$$

Also in this case the obtained section has to be is increased to **IPE360** to fulfil the limitation concerning the maximum vertical deflection.

The resistant moment of these beams is:

$$M_{Rd} = \frac{1019.1 \times 10^{-3} \times 355}{1.00} \cong 361.8\ kNm \tag{4.5}$$

The plan configuration of the building with the identification of beam profiles is depicted in Figure 4.8.

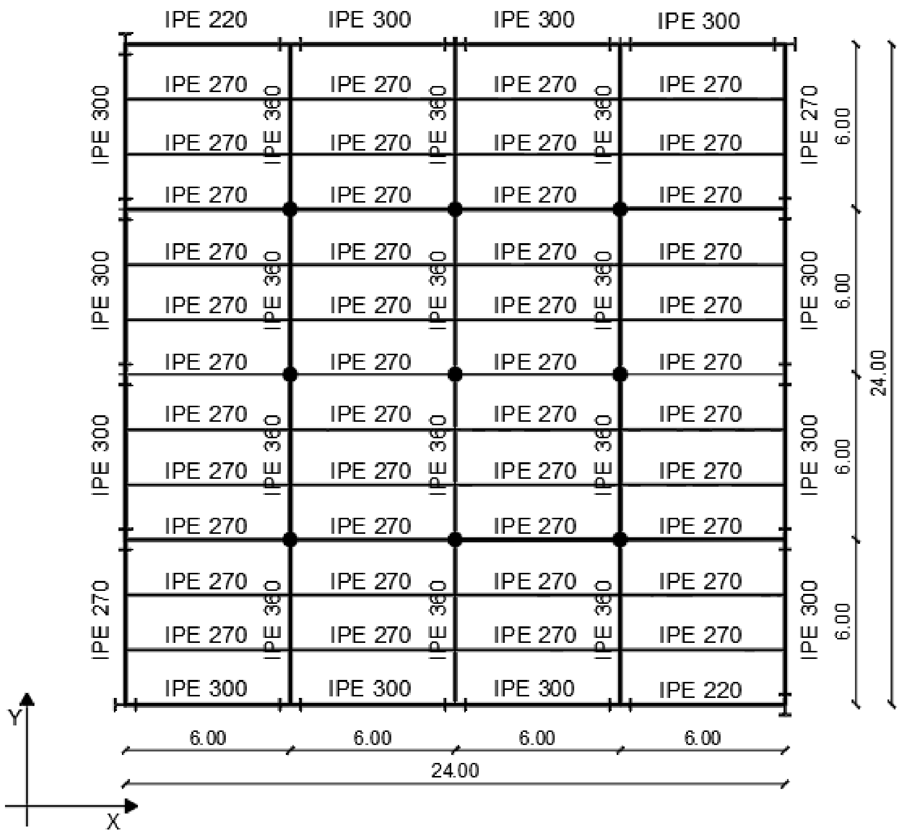

Figure 4.8. Plan configuration of the building with the identification of beam profiles.

4.3.3 Computation of concentrated and distributed vertical loads acting on the lateral load resisting frame

It is important observing that the computation of the loads acting on columns need to consider the weight of the external walls equal to 1.00 kN/m^2 as directly transmitted to the columns. In the roof, the height of the external walls is 1.75 m.

- **Lateral load resisting frame parallel to the secondary beams (X direction)**

With reference to the seismic load combination provided by Eurocode 8, the vertical loads acting on the current floor are evaluated as follows:

$$G_k + \psi_2 Q_k = 4.00 + 0.3 \times 3.5 = 5.05\, kN/m^2 \tag{4.6}$$

while for the roof are evaluated as:

$$G_k + \psi_2 Q_k = 4.00 + 0.3 \times 3.0 = 4.90\, kN/m^2 \tag{4.7}$$

so that it is possible to compute the distributed loads acting on the beams of the current floor of the seismic resistant schemes as:

$$q_d = 0.50 \times 5.05 \times 2 = 5.05 \frac{kN}{m} \tag{4.8}$$

while for the roof are:

$$q_{d.roof} = 0.50 \times 4.90 \times 2 = 4.90\, kN/m \tag{4.9}$$

Concentrated permanent and live loads on the columns are delivered in Table 4.3 and Table 4.4; while the same in seismic combination are delivered in Table 4.5 and Table 4.6.

Table 4.3 - Concentrated loads on beams for the lateral load resisting frame parallel to secondary beams for 4-storey frame.

Storey	$\boldsymbol{F_{c1}}$ (kN)		$\boldsymbol{F_{c2}}$ (kN)		$\boldsymbol{F_{lc}}$ (kN)	
	G_k	Q_k	G_k	Q_k	G_k	Q_k
1-3	45.00	21.00	69.00	42.00	927.00	756.00
4	34.50	18.00	58.50	36.00	895.50	648.00

Table 4.4 - Concentrated loads on beams for the lateral load resisting frame parallel to secondary beams for 8-storey frame.

Storey	$\boldsymbol{F_{c1}}$ (kN)		$\boldsymbol{F_{c2}}$ (kN)		$\boldsymbol{F_{lc}}$ (kN)	
	G_k	Q_k	G_k	Q_k	G_k	Q_k
1-7	45.00	21.00	69.00	42.00	927.00	756.00
8	34.50	18.00	58.50	36.00	895.50	648.00

Table 4.5 - Concentrated loads on beams for the lateral load resisting frame parallel to secondary

beams for 4-storey frame in seismic combination

Storey	F_{c1} (kN)	F_{c2} (kN)	F_{lc} (kN)
	G_k+0.3Q_k	G_k+0.3Q_k	G_k+0.3Q_k
1-3	51.30	81.60	1153.80
4	39.90	69.30	1089.90

Table 4.6 - Concentrated loads on beams for the lateral load resisting frame parallel to secondary beams for 8-storey frame in seismic combination

Storey	F_{c1} (kN)	F_{c2} (kN)	F_{lc} (kN)
	G_k+0.3Q_k	G_k+0.3Q_k	G_k+0.3Q_k
1-7	51.30	81.60	1153.80
8	39.90	69.30	1089.90

- **Lateral load resisting frame orthogonal to the secondary beams (Y direction)**

The lateral load resisting frames arranged orthogonal to secondary beams do not have distributed loads but concentrated loads with a span of 2 m (P).

Concentrated permanent and live loads on the columns are delivered in Table 4.7 and Table 4.8; while the same in seismic combination are delivered in Table 4.9 and Table 4.10Table 4.6.

Table 4.7 - Concentrated loads on beams for the lateral load resisting frame orthogonal to the secondary beams for 4-storey frame.

Storey	P (kN)		F_{c1} (kN)		F_{c2} (kN)		F_{lc} (kN)	
	G_k	Q_k	G_k	Q_k	G_k	Q_k	G_k	Q_k
1-3	24.00	21.00	33.00	10.50	45.00	21.00	927.00	756.00
4	24.00	18.00	22.50	9.00	34.50	18.00	895.50	648.00

Table 4.8. Concentrated loads on beams for the lateral load resisting frame orthogonal to the secondary beams for 8-storey frame.

Storey	P (kN)		F_{c1} (kN)		F_{c2} (kN)		F_{lc} (kN)	
	G_k	Q_k	G_k	Q_k	G_k	Q_k	G_k	Q_k
1-7	24.00	21.00	33.00	10.50	45.00	21.00	927.00	756.00
8	24.00	18.00	22.50	9.00	34.50	18.00	895.50	648.00

Table 4.9 - Concentrated loads on beams for the lateral load resisting frame orthogonal to the secondary beams for 4-storey frame in seismic combination

Storey	P (kN)	F_{c1} (kN)	F_{c2} (kN)	F_{lc} (kN)
	G_k+0.3Q_k	G_k+0.3Q_k	G_k+0.3Q_k	G_k+0.3Q_k
1-3	30.30	36.15	51.30	1153.80
4	29.40	25.20	39.90	1089.90

Table 4.10 - Concentrated loads on beams for the lateral load resisting frame orthogonal to the secondary beams for 8-storey frame in seismic combination

Storey	P (kN)	F_{c1} (kN)	F_{c2} (kN)	F_{lc} (kN)
	G_k+0.3Q_k	G_k+0.3Q_k	G_k+0.3Q_k	G_k+0.3Q_k
1-7	30.30	36.15	51.30	1153.80
8	29.40	25.20	39.90	1089.90

4.4 Global instability checkings

The internal forces and moments should be determined using a first-order analysis [18]. The effects of the deformed geometry (second-order effects) should be considered if they increase the action effects significantly or modify significantly the structural behaviour.

First order analysis may be used for the structure, if the increase of the relevant internal forces or moments or any other change of structural behaviour caused by deformations can be neglected. This condition may be assumed to be fulfilled, if:

$$\alpha_{cr} \geq 10 \tag{4.10}$$

where α_{cr} is the buckling factor by which the design loading would have to be increased to cause elastic instability in a global mode.

The buckling analysis should be perfomed under both the gravity load combination:

$$\gamma_g\, G_k + \gamma_q\, Q_k = 1.35G_k + 1.5Q_k \tag{4.11}$$

and the gravity load combination at SD in seismic condition:

$$G_k + \psi_{2.i}Q_k = G_k + 0.3Q_k \tag{4.12}$$

However, for sway frames could happen that the buckling factor is lower than 10. Therefore, the EC3 suggestes that if:

$$\alpha_{cr} \geq 3 \tag{4.13}$$

second-order sway effects due to vertical loads may be calculated by increasing the horizontal loads H_{Ed} due to imperfections and other possible sway effects according to first order theory by the factor:

$$\frac{1}{1-\frac{1}{\alpha_{cr}}} \tag{4.14}$$

4.4.1 Computation of the loads equivalent to the imperfection

Appropriate allowances should be incorporated in the structural analysis to cover the effects of imperfections, including residual stresses and geometrical imperfections such as lack of verticality, lack of straightness, lack of flatness, lack of fit and any minor eccentricities present in joints of the unloaded structure.

Equivalent geometric imperfections, should be used, with values which reflect the possible effects of all type of imperfections unless these effects are included in the resistance formulae for member design.

The assumed shape of global imperfections may be derived from the elastic buckling mode of a structure in the plane of buckling considered.

For frames sensitive to buckling in a sway mode the effect of imperfections should be allowed for in frame analysis by means of an equivalent imperfection in the form of an initial sway imperfection and individual bow imperfections of members.

The global initial sway imperfection may be determined from:

$$\phi = \phi_0 \alpha_h \alpha_m \tag{4.15}$$

where:

ϕ_0 is the basic value $\phi_0 = 1/200 = 0.005$

α_h is the reduction factor for height h (the whole height of the building) (Figure 4.9)

$$\alpha_h = \frac{2}{\sqrt{h}} \; but \; \frac{2}{3} \leq \alpha_h \leq 1 \tag{4.16}$$

α_m is the reduction factor for the number of columns in a row $\alpha_m = \sqrt{0.5\left(1+\frac{1}{m}\right)}$

m is the number of columns in a row including only those columns which carry a vertical load N_{Ed} not less than the 50% of the average value of the column in the vertical plane considered.

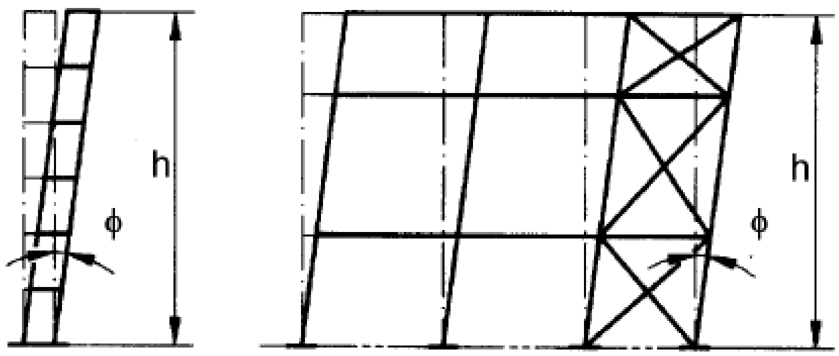

Figure 4.9. Equivalent sway imperfections

For the structures analysed in this document the values of the global initial sway parameters are reported in the Table 4.11.

Table 4.11 - Global sway imperfection parameters

Structure	h (m)	ϕ_0 (-)	α_h (-)	m (-)	α_m (-)	ϕ (-)
4-storey	14	0.005	0.67	5	0.77	0.0026
8-storey	28	0.005	0.67	5	0.77	0.0026

The determination of the horizontal force equivalent imperfection can be computed as follows:

$$H_{Ed} = \phi N_{Ed} \tag{4.17}$$

where $N_{Ed}$is the total axial load acting at each storey in both the gravity load combination at ULS and SD. The values of the aforementioned forces are reported in

Table 4.12 to Table 4.15, for the 4-storey and 8-storey structures, respectively and for both the ULS and SD combinations.

Table 4.12 - Force equivalent to the global sway imperfection for the 4-storey structures for the ULS combination

Storey	N_{Ed} (kN)	ϕ (-)	H_{Ed} (kN)
1-3	3294.00	0.0026	8.51
4	2946.60		7.65

Table 4.13 - Force equivalent to the global sway imperfection for the 8-storey structures for the ULS combination

Storey	N_{Ed} (kN)	ϕ (-)	H_{Ed} (kN)
1-7	3294.00	0.0026	8.51
8	2946.60		7.65

Table 4.14 - Force equivalent to the global sway imperfection for the 4-storey structures for the seismic combination

Storey	N_{Ed} (kN)	ϕ (-)	H_{Ed} (kN)

1-3	1622.40	0.0026	4.19
4	1495.20		3.86

Table 4.15 - Force equivalent to the global sway imperfection for the 8-storey structures for the seismic combination

Storey	N_{Ed} (kN)	ϕ (-)	H_{Ed} (kN)
1-7	1622.40	0.0026	4.19
8	1495.20		3.86

*N_{Ed} are computed for the half structure.

The force equivalent to the sway imperfection must be added in all the load combination to be assigned to the structure being there for seismic or gravity load purpose.

For building frames, sway imperfections may be disregarded when:

$$H_{Ed} \geq 0.15N_{Ed} \quad (4.18)$$

4.5 Computation of the design seismic loads

For each intermediate floor, the masses belonging to the external walls have to be also considered.

Seismic masses were obtained according to Ecurocode 8 [11] provisions as corresponding to the following gravity loads:

$$G_k + \psi_{E.i}Q_k \quad (4.19)$$

where $\psi_{E.i} = 0{,}15$.

The total mass acting at each intermediate storey and at the roof level is delivered in Table 4.16; while Table 4.17 and Table 4.18 show the floor masses for low-rise and medium rise structures, respectively.

Table 4.16 - Seismic masses for the computation of seismic loads

Location	**Type**	**Loads (kN/m^2)**	**W**

			(tonne)
Intermediate stories	Permanent	4.00	264.00
	Variable	3.50	201.60
Roof	Permanent	4.00	247.20
	Variable	3.00	172.80

Table 4.17 - Floor height and floor masses of 4-storey frame

Storey	z_i (m)	$W_{p.i}$ (t)
1	3.50	294.24
2	7.00	294.24
3	10.50	294.24
4	14.00	273.12
	W=	1155.84

Table 4.18 - Floor height and floor masses of 8-storey frame

Storey	z_i (m)	$W_{p.i}$ (t)
1	3.50	294.24
2	7.00	294.24
3	10.50	294.24
4	14.00	294.24
5	17.50	294.24
6	21.00	294.24
7	24.50	294.24
8	28.00	273.12
	W=	2332.80

The first vibration period must be computed by modal analysis.

The design horizontal forces are determined considering for each ductility class a seismic zone whose seismic intensity measure matches the maximum seismic action index S_δ allowed by Eurocode 8 (1-1) according to Table 4.19 and obtained by the following formula:

$$S_\delta = \delta F_\alpha F_T S_{\alpha,475} \tag{4.20}$$

$\delta = 1.0\ for\ CC2$

$F_\alpha = 1.3(1 - 0.01)S_{\alpha RP}$ is the short period site amplification factor (for site category B)

$F_T = 1.0$ is the topography amplification factor (for category B)

$$S_{\alpha,475} = S_{\alpha,ref}\left(\frac{475}{T_{ref}}\right)^{1/k} \tag{4.21}$$

$S_{\alpha,ref}$ is defined in the national annex for the three cases: DC1,DC2,DC3.

It is worthwhile pointing out that the choice of three different seismic zones for the three ductility classes provided by Eurocode 8 is aimed to the evaluation of the accuracy of code provisions concerning the limitation to the maximum seismic action index allowed for the different ductility classes, i.e. for the different design criteria suggested by the code.

It is important notice that the check has to be performed according to the Significant Damage that is an ULS.

Table 4.19 - Seismic action index at Significant Damage and Reference spectral acceleration

Structural type	**Seismic action index at Significant Damage $S_\delta(m/s^2)$**			**Reference spectral acceleration $S_{\alpha,475}\ (m/s^2)$**		
	DC1	DC2	DC3	DC1	DC2	DC3
Moment frames	5.0	6.5	8.5	4.01	5.28	7.03
Dual frames (moment frames with bracing)	5.0	6.5	8.5	4.01	5.28	7.03

To construct the response spectrum for horizontal actions, the spectral parameters must first be identified. Eurocode 8 1-1 [11] defines the values of T_A, F_A, χ. From table 5.4 of EC8 1-1 [11]:

$T_A = 0.02s$ $F_A = 2.5$ $\chi = 4$

The spectral accelerations S_α and S_β should be calculated from formulas:

$$S_\alpha = F_T F_\alpha S_{\alpha,RP} \qquad (4.22)$$
$$S_\beta = F_T F_\beta S_{\beta,RP}$$

in which:

$$S_{\alpha,RP} = \gamma_{LS,CC} S_{\alpha,ref} \qquad (4.23)$$
$$S_{\beta,RP} = \gamma_{LS,CC} S_{\beta,ref}$$

$\gamma_{LS,CC}$ =1 is the performance factor at Significant Damage limite states

$S_{\beta,ref} = f_h S_{\alpha,ref}$ where:

- $f_h = 0.3$ for moderate seismicity levels, in particular if $S_{\alpha,475} < 5$
- $f_h = 0.4$ for high seismicity levels, in particular if $S_{\alpha,475} > 5$

$$F_\beta = 1.6(1 - 0.02) S_{\beta RP} \qquad (4.24)$$

is the site amplification factor for site category B (from table 5.4 of EC8 1-1)

Thanks to the spectral accelerations, it is possible to calculate the other periods:

$$T_C = \frac{S_\beta T_\beta}{S_\alpha} \qquad T_B = 0.10s, \quad if\ \frac{T_C}{\chi} > 0.10s \qquad (4.25)$$

T_D whose value is reported in table 5.3 of EC8 1-1.

In particular, the values of T_D is 2 if $S_{\beta,RP} \leq 1$ m/s^2 while is 1+$S_{\beta,RP}$ if $S_{\beta,RP} > 1$ m/s^2.

The obtained spectra are depicted in Figure 4.10 - Horizontal elastic response spectrum. They corresponds to three different seismic zones whose severity has been selected to match the maximum seismic action index allowed by the code provisions.

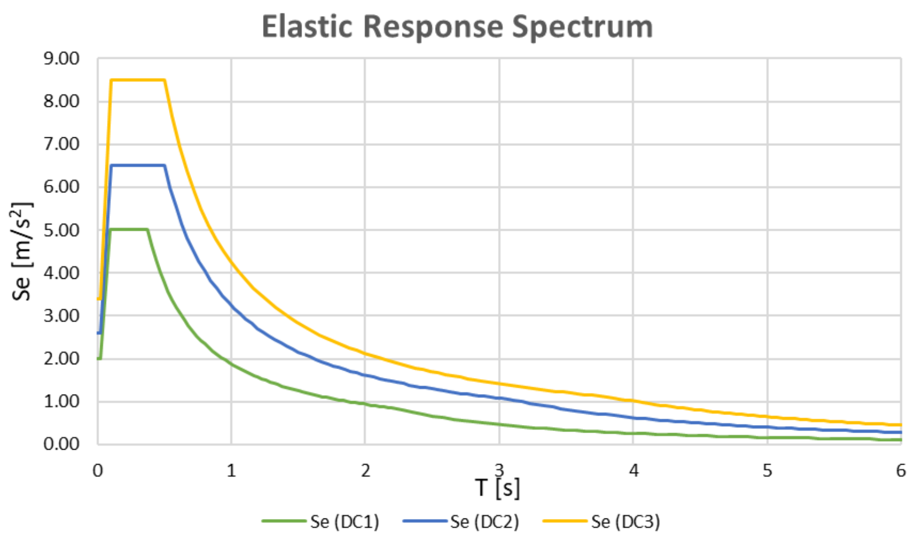

Figure 4.10 - Horizontal elastic response spectrum

The definition of the reduced spectrum occurs using the behaviour factor.

The behaviour factors are reported in Table 4.20 for the Significant Damage and for the ductility classes DC1, DC2 and DC3.

Table 4.20 - Behaviour factor for the different ductility class [19]

Structural type	**Ductility Class**											
	DC1				**DC2**				**DC3**			
	q_s	q_D	q_R	q	q_s	q_D	q_R	q	q_s	q_D	q_R	q
Moment resisting frames (MRFs) Multi-storey MRFs	1.5	1	1	1.5	1.5	1.8	1.3	3.5	1.5	3.3	1.3	6.5
Dual frames MRFs with concentric bracing	1.5	1	1	1.5	1.5	1.8	1.1	3	1.5	2.9	1.1	4.8

For the horizontal components of the seismic action the reduced spectrum, $S_r(T)$, is provided by:

$$S_r(T) = \frac{S_e(T)}{R_q(T)} \geq \beta S_{\alpha,475} \tag{4.26}$$

where:

$0 \leq T \leq T_A$: $R_q(T) = R_{q0} = q_R q_S$

$T_A \leq T \leq T_B$: $R_q(T) = R_{q0} + (q - R_{q0})(T - T_A)/(T_B - T_A)$

$T_B \leq T$: $R_q(T) = q$

It is important observing that β is the lower bound factor for the horizontal reduced spectrum (EC8 1.1): The values to be ascribed to β are given in the relevant parts of EN1998. This lower bound value applies only to forces. Displacement demands should still be evaluated from the displacement spectrum or the elastic response spectrum, in particular for very soft structures. It means that the checking in terms of resistance must be made with the lower bound modified spectrum while the drift and second order effects checking must be done with the spectrum without the lower bound limit. As the β factor has not been already provided in the new Eurocode 8 draft it seems to be rational referring to the former Eurocode 8 [2] version where the suggested lower bound factor value is 0.2 to be applied to the PGA. The value of the PGA has been computed as the ratio between $S_{\alpha,475}$ and F_α.

Therefore, in Figure 4.11-Figure 4.13 and Figure 4.12-Figure 4.14 the reduced design spectra without and with the lower bound are reported with reference to both the MRFs and Dual CBFs.

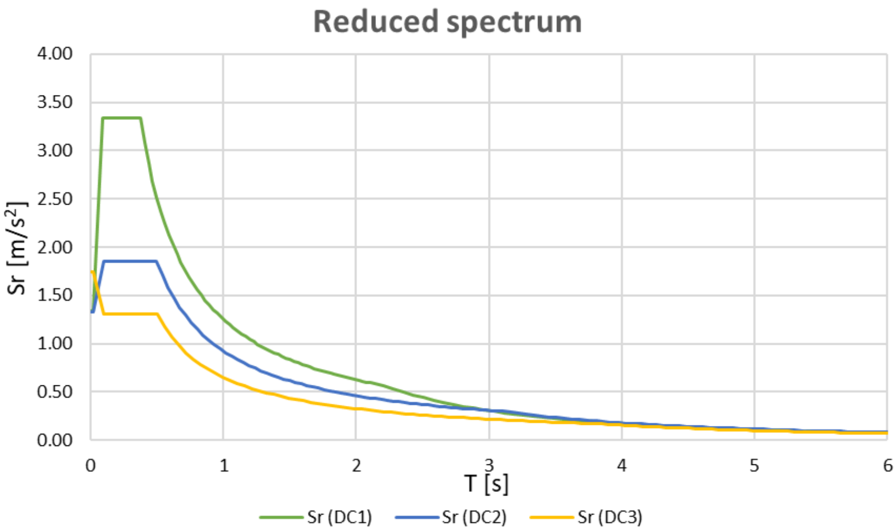

Figure 4.11 - Reduced horizontal elastic response spectrum for the MRFs

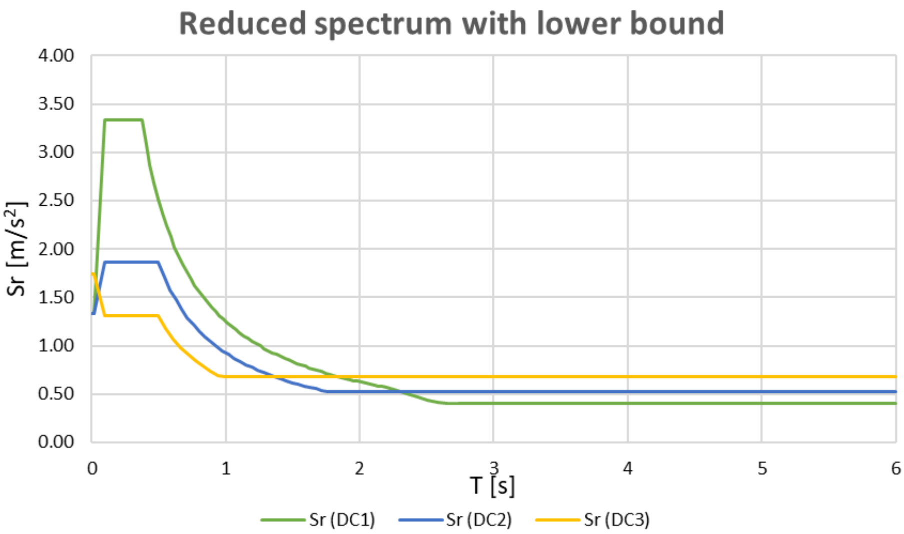

Figure 4.12 - Reduced horizontal elastic response spectrum for the MRFs with the lower bound

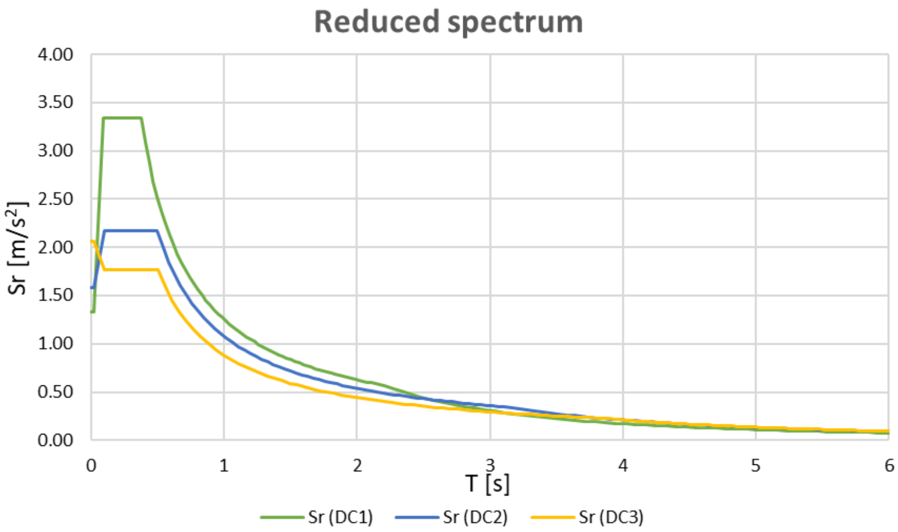

Figure 4.13 - Reduced horizontal elastic response spectrum for the D-CBFs

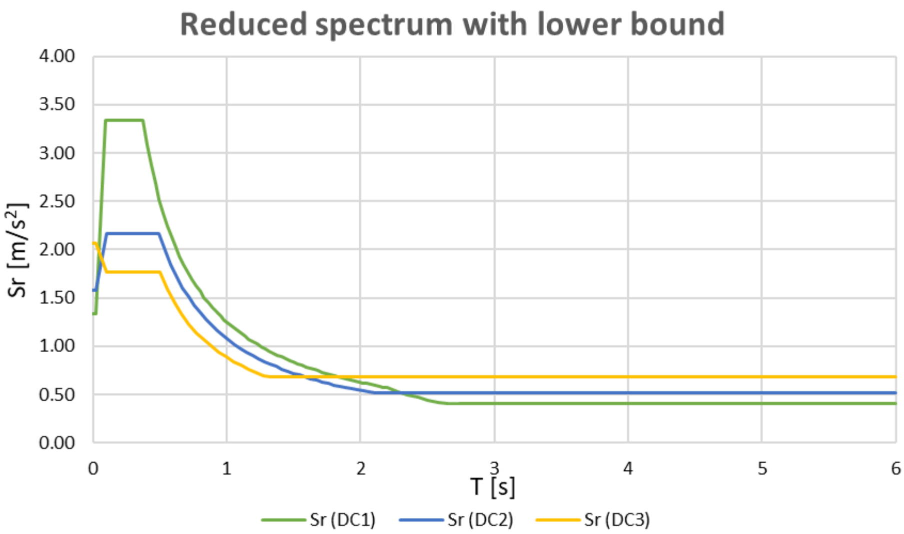

Figure 4.14 - Reduced horizontal elastic response spectrum for the D-CBFs with the lower bound

4.6 Lateral displacements limitation

For the SD Limit state, the inter-storey drift should be limited at any storey of the building by complying with the condition given by Formula (6.3) [19]:

$$d_{r,SD} \leq \lambda_s \, h_s \tag{4.27}$$

where λ_s is a coefficient reflecting the limitation of the inter-storey drift. In general $\lambda_s = 0.02$ for moment frames and dual frames, according to 11.6.3 [EC8 1-2].

CHAPTER 5

CASE STUDIES: 4 St_DC3_MRFs_X & 4 St_DC3_D-CBFs_X (TRADITIONAL & FREEDAM)

5.1 Introduction

The procedure described in CHAPTER 3 was applied to design the structures shown in Table 4.1, the design for case studies numbers 2-10-18-26 are reported in this chapter, while the results obtained for all the other types are shown in APPENDIX A.

With reference to the plan configuration reported in Figure 4.1, the seismic response of the building is herein presented in relation to the seismic actions in x direction only and considering the weight of half the structure. For apply 3-TPMC algorithm the reference is made to the concentrated and distributed vertical loads, in seismic combination, reported in Eqs. (4.8) - (4.9) and in the Table 4.5.

5.2 Design of MF-Frames (4 St_DC3_MRFs_X_TRADITIONAL)

From the modal analysis performed with the software SAP2000 v.22 we obtain the first vibration period adopted for the preliminary design: $T_1 = 1.62$.

The seismic actions of storey have a linear and increasing upward trend according to the simplified first vibration mode. In particular:

$$F_i = F_h \frac{z_i W_{pi}}{\sum_i z_i W_{pi}} \tag{5.1}$$

where $F_h = S_{ed}(T_1)W\lambda$ is the base shear seismic action with $\lambda = 1$. W_{pi} is the weight of each storey and W is the total weight obtained in Table 4.17.

With reference to the design spectrum in Figure 4.11, the design horizontal forces are reported in Table 5.1, starting from a base shear action equal to 238.88 kN (obtained considering half of the structure).

Table 5.1 - Interstorey heights and design seismic horizontal forces at k-th storey

Storey	h_i m	F_k kN
1	3.5	24.59
2	3.5	49.19
3	3.5	73.78
4	3.5	91.32

In the following, the design procedure development is described.

a) Selection of the design displacement

Choosing the maximum design displacement, for which the development of the global collapse mechanism has to be insured, is important because it governs the extent of the second order effects. Furthermore, the complete development of a collapse mechanism can be avoided when the demand for plastic rotation exceeds the structure local ductility. Therefore, it is basic to choose an ultimate design displacement, δ_u, related to the structure local ductility, particularly to the beam-to-column joints, by assuming:

$$\delta_u = \theta_u\, h_{n_s} = 0.04 \times 14 = 0.56\, m \tag{5.2}$$

where θ_u is the joints plastic rotation capacity, in this case equal to $0.04\, rad$.

b) *Calculation of the mechanism equilibrium curves slopes, ${\gamma_{i_m}}^{(t)}$*

The mechanism equilibrium curves slopes, ${\gamma_{i_m}}^{(t)}$, have been evaluated through Equations (3.8), (3.10), (3.12), (3.14) and the values are shown in Table 5.2.

Table 5.2 - Slopes of the mechanism equilibrium curves

Storey	$\boldsymbol{\gamma_{im}^{(1)}}$ **m**$^{-1}$	$\boldsymbol{\gamma_{im}^{(2)}}$ **m**$^{-1}$	$\boldsymbol{\gamma_{im}^{(3)}}$ **m**$^{-1}$
1	7.61	$\boxed{1.58}$	7.61
2	3.50	1.89	6.32
3	2.19	2.57	5.40
4	1.58	4.68	4.68

The value of the slope of global type mechanism equilibrium curve, $\gamma^{(g)}$, is the minimum between all the values of ${\gamma_{i_m}}^{(t)}$:

$$\gamma^{(g)} = 1.58 \tag{5.3}$$

c) *Design of first storey columns sections*

The design of the columns at first storey occurs according to equation (3.18):

$$\sum_{i=1}^{n_c} M_{c.i.1} = \frac{2\sum_{k=1}^{n_s}\sum_{j=1}^{n_b}\gamma M_{b.jk}\frac{L_j}{L_{j,k}^*} + (\gamma_1^{(3)} - \gamma^{(g)})\delta_u \sum_{k=1}^{n_s} F_k\, h_k}{2\frac{\sum_{k=1}^{n_s} F_k\, h_k}{h_1 \sum_{k=1}^{n_s} F_k} - 1} = 3591.68\ kNm \tag{5.4}$$

d) *Computation of the axial load acting in the columns at collapse state i.e., when the global mechanism is fully developed*

According to the global mechanism, the axial forces acting on the columns at collapse depend both on the vertical loads distribution and on the shear actions coming from the plastic hinges developed at the beams end. For this reason, the total amount of axial force that beams pass to columns is the sum of three terms: N_q and N_F, due to the distributed and concentrated loads respectively, acting on beams in the seismic combination (Figure 4.3). The third one, instead, is due to the shear actions that plastic hinges develops at beams ends, N_b.

In the following Table 5.3 to Table 5.6, the three contributions and the total value N_{tot} are reported, with reference to each storey both for internal and external columns.

Table 5.3 – Axial forces acting on first storey columns at collapse state for MRF nr.2

STOREY 1				
Column	N_q **kN**	N_F **kN**	N_b **kN**	N_{tot} **kN**
1	60.15	193.80	593.72	339.77
2	120.30	314.10	0	434.40
3	120.30	314.10	0	434.40
4	120.30	314.10	593.72	1028.12

5	60.15	193.80	0	253.95

Table 5.4 – Axial forces acting on storey 2 columns at collapse state for MRF nr.2

STOREY 2				
Column	N_q **kN**	N_F **kN**	N_b **kN**	N_{tot} **kN**
1	45.00	142.50	425.43	237.93
2	90.00	232.50	0	322.50
3	90.00	232.50	0	322.50
4	90.00	232.50	425.43	747.93
5	45.00	142.50	0	187.50

Table 5.5 – Axial forces acting on storey 3 columns at collapse state for MRF nr.2

STOREY 3				
Column	N_q **kN**	N_F **kN**	N_b **kN**	N_{tot} **kN**
1	29.85	91.20	257.14	136.09
2	59.70	150.90	0	210.60
3	59.70	150.90	0	210.60
4	59.70	150.90	257.14	467.74
5	29.85	91.20	0	121.05

Table 5.6 – Axial forces acting on storey 4 columns at collapse state for MRF nr.2

STOREY 4				
Column	N_q **kN**	N_F **kN**	N_b **kN**	N_{tot} **kN**
1	14.70	39.90	128.57	73.97
2	29.40	69.30	0	98.70
3	29.40	69.30	0	98.70
4	29.40	69.30	128.57	227.27
5	14.70	39.90	0	54.60

e) The sum of the plastic moments required at first storey (Eq.(5.4)(3.18)) is spread among the columns

As already stated, the flexural resistance of the first storey columns, obtained in step c), $\sum_{i=1}^{n_c} M_{c,i,1}$, has to be distributed among the columns. So, the flexural resistance values required for each column, $M_{c,i,1,req}$, the required plastic modulus, $W_{pl,req}$, the obtained plastic modulus, $W_{pl,obt}$, the standard shapes and the flexural resistance achieved both for internal and external columns, $M_{pl,obt}$, are reported in Table 5.7Table 5.7. In these Tables, also the standard sections of first storey columns are delivered.

Table 5.7 – Check of first storey columns to flexural resistance for MRF nr.2

STOREY 1						
Column	N_{tot} **kN**	$M^{(1)}_{reqc,i1}$ **kNm**	$W_{pl,req}$ **cm³**	**sections**	$W_{pl,obt}$ **cm³**	$M_{pl,obt}$ **kNm**
1	339.77	822.92	2318.09	HE 340 B	2408.00	854.84
2	434.40	822.92	2318.09	HE 340 B	2408.00	854.84
3	434.40	822.92	2318.09	HE 340 B	2408.00	854.84
4	1028.12	822.92	2318.09	HE 340 B	2408.00	854.84
5	253.95	300.00	845.07	HE 340 B	985.70	349.92

The sum of the first storey plastic moments, $\sum_{i=1}^{n_c} M^*_{c,i,1}$, coming from Table 5.7, is equal to:

$$\sum_{i=1}^{n_c} M^*_{c,i,1} = 3769.28\ kNm \tag{5.5}$$

Values are greater than the required one because the sections are chosen from standard shapes. At this stage, the value of $\alpha_0{}^{(g)}$ can be evaluate by replacing the values of $\sum_{i=1}^{n_c} M^*_{c,i,1}$ by $\sum_{i=1}^{n_c} M_{c,i,1}$ in Eq. (3.7).

$$\alpha_0{}^{(g)} = \frac{\sum_{i=1}^{n_c} M_{c.1} + 2 \cdot 3 \sum_{k=1}^{n_s} \sum_{j=1}^{n_b} \gamma M_{b.jk} L_j / L_{j,k}^*}{\sum_{k=1}^{n_s} F_k h_k} = 5.29 \quad (5.6)$$

the value of $\alpha^{(g)}$ can be evaluate by replacing both values of $\sum_{i=1}^{n_c} M_{c,i,1}^*$ by $\sum_{i=1}^{n_c} M_{c,i,1}$ in Eq. (3.5)(3.5) with $\delta = \delta_u$ or simply from the following:

$$\alpha^{(g)} = \alpha_0^{(g)} - \gamma^{(g)} \delta_u = 5.29 - 1.58 \cdot 0.56 = 4.40 \quad (5.7)$$

f) - g) Calculation of the sum of the columns plastic moments reduced by a contemporary action of the axial load, $\sum_{i=1}^{n_c} M_{c,i,i_m}^{(t)}$, required at any storey in order to avoid the undesired mechanisms and selection of the maximum one

The sum of the columns plastic moments reduced by a contemporary action of the axial load, required at any storey in order to prevent the undesired mechanisms is obtained from Eqs. (3.19) - (3.21), properly modified for MRF case. This values and the sum of the columns plastic moments which governs the design at each storey are reported in Table 5.8. It is easy to note that the type 1 mechanism always governs the columns design.

Table 5.8 – Required moments at each storey needed to avoid the undesired mechanism and maximum value of $\sum_{i=1}^{n_c} M_{c,i,i_m}^{(t)}$ for MRF nr.2

Storey	$\sum_{i=1}^{n_c} M_{c,i,i_m}^{(1)}$ kNm	$\sum_{i=1}^{n_c} M_{c,i,i_m}^{(2)}$ kNm	$\sum_{i=1}^{n_c} M_{c,i,i_m}^{(3)}$ kNm	$\sum_{i=1}^{n_c} M_{c,i,i_m}^{(t)}$ kNm
1	3769.28	-	3769.28	3769.28
2	3679.94	-2625.61	2977.86	3679.94
3	3128.21	-705.63	2144.68	3128.21
4	2040.38	203.75	1122.06	2040.38

g) Design of the column sections at each storey

The sum of the columns required plastic moment, reduced for the simultaneous axial force, N_{tot}, $M_{c,i,1,req}$, the required plastic modulus, $W_{pl,req}$, and the obtained one, $W_{pl,obt}$, the columns sections chosen from standard shape and their corresponding obtained plastic moments, $M_{c,i,1,obt}$, are shown in the following Table 5.11.

Table 5.9 to Table 5.11.

Table 5.9 – Design of the column sections at storey 2 for MRF nr.2

STOREY 2						
Column	N_{tot} **kN**	$M^{(2)}_{reqc,i1}$ **kNm**	$W_{pl,req}$ **cm³**	**section**	$W_{pl,obt}$ **cm³**	$M_{pl,obt}$ **kNm**
1	237.93	844.99	2380.24	HE 340 B	2408.00	854.84
2	322.50	844.99	2380.24	HE 340 B	2408.00	854.84
3	322.50	844.99	2380.24	HE 340 B	2408.00	854.84
4	747.93	844.99	2380.24	HE 340 B	2408.00	854.84
5	187.50	300.00	845.07	HE 340 B	985.70	349.92

Table 5.10 – Design of the column sections at storey 3 for MRF nr.2

STOREY 3						
Column	N_{tot} **kN**	$M^{(3)}_{reqc,i1}$ **kNm**	$W_{pl,req}$ **cm³**	**section**	$W_{pl,obt}$ **cm³**	$M_{pl,obt}$ **kNm**
1	136.09	719.55	2026.91	HE 320 B	2149.00	762.90
2	210.60	719.55	2026.91	HE 320 B	2149.00	762.90
3	210.60	719.55	2026.91	HE 320 B	2149.00	762.90
4	467.74	719.55	2026.91	HE 320 B	2149.00	762.90
5	121.05	250.00	704.23	HE 320 B	939.10	333.38

Table 5.11 – Design of the column sections at storey 4 for MRF nr.2

STOREY 4

Column	N_{tot} kN	$M^{(4)}_{reqc,i1}$ kNm	$W_{pl,req}$ cm^3	section	$W_{pl,obt}$ cm^3	$M_{pl,obt}$ kNm
1	73.97	447.59	1260.83	HE 320 B	2149.00	762.90
2	98.70	447.59	1260.83	HE 320 B	2149.00	762.90
3	98.70	447.59	1260.83	HE 320 B	2149.00	762.90
4	227.27	447.59	1260.83	HE 320 B	2149.00	762.90
5	54.60	250.00	704.23	HE 320 B	939.10	333.38

h) Control of technological condition

If the obtained first storey columns sections are smaller than the ones required at the other storeys, the technological condition is not verified, so the first storey column sections have to be increased by using some greater sections. As a consequence, the value of $\sum_{i=1}^{n_c} M^*_{c,i,1}$ has to be updated and the procedure has to be repeated from step *c)*. The Tables given in the previous steps show the definitive value, in which the technological condition has been already considered.

The adopted profiles are **HE 340 B** for storeys 1-2 and **HE 320 B** for storeys 3 and 4. The beam sections have be increased until the frame satisfy the interstorey drift requirement set by Eurocode 8 [19]; so the definitive values one are **IPE 330** for storeys 1-2 and **IPE 300** for storeys 3 and 4 (the hinged bay is always IPE 220).

5.3 Design of MR-Frames equipped with FREEDAM beam-to-column dampers (4 St_DC3_MRFs_X_FREEDAM)

Starting from the elements obtained in the previous section, the FREEDAM dampers have been designed. Taking into account the beams and columns dimensions, device D1 was chosen. To evaluate the flexural resistance of the single beams damper, the first step is to consider the maximum moment acting on the beams of each storey, $M_{fb,Ed,max}$, between the ultimate limit state and seismic combination.

Then from equation (2.4(2.4) the preloading force to be used in eq. (2.3) is calculated. A this point the local hierarchy criterion (2.5) must be satisfied.

Table 5.12 – Design of FREEDAM joints for MRF nr.18

Storey	Beam	$M_{fb.Ed.max}$ kNm	P_f kN	$M_{f,Rd}$ kNm	$\gamma_{Rd} M_{f,Rd} l*$ kNm	$M_{b,Rd}$ kNm
1	IPE 330	165.69	69	166.48	219.16	285.53
2	IPE 330	168.25	70	146.86	193.34	285.53
3	IPE 300	115.87	52	102.55	135.21	223.08
4	IPE 300	69.47	31	61.14	80.61	223.08

where l* = (l - L)/l

The local hierarchy criterion is satisfied, otherwise the beam size must be increased.

Once this is done, we design the columns following the 3-TPMC algorithm starting from point c), being the previous points equal to the frame designed with traditional joints (§5.2).

c) Design of first storey column sections

The design of the columns at first storey occurs according to equations (3.18) and (3.30):

$$\sum_{i=1}^{n_c} M_{c.i.1} = \frac{2\sum_{k=1}^{n_s}\sum_{j=1}^{n_b} 2\gamma_{Rd} M_{fb.Rd.jk} \frac{L_j}{L_{j,k}^*} + (\gamma_1^{(3)} - \gamma^{(g)})\delta_u \sum_{k=1}^{n_s} F_k\, h_k}{2\frac{\sum_{k=1}^{n_s} F_k\, h_k}{h_1 \sum_{k=1}^{n_s} F_k} - 1} \tag{5.8}$$
$$= 2670.04\ kNm$$

d) *Computation of the axial load acting in the columns at collapse state i.e., when the global mechanism is fully developed*

The axial loads acting on columns, as already seen, come from vertical loads distribution and the shear actions due to the flexural action that FREEDAMs are able to transmit. In the following Table 5.13Table 5.3 to Table 5.16, the three contributions and the total value N_{tot} are reported, with reference to each storey both for internal and external columns.

Table 5.13 – Axial forces acting on first storey columns at collapse state for MRF nr.18

STOREY 1				
Column	N_q **kN**	N_F **kN**	N_{fb} **kN**	N_{tot} **kN**
1	60.15	193.80	-280.56	26.61
2	120.30	314.10	0	434.40
3	120.30	314.10	0	434.40
4	120.30	314.10	280.56	714.96
5	60.15	193.80	0	253.95

Table 5.14 – Axial forces acting on storey 2 columns at collapse state for MRF nr.18

STOREY 2				
Column	N_q **kN**	N_F **kN**	N_{fb} **kN**	N_{tot} **kN**
1	45.00	142.50	-182.18	5.32
2	90.00	232.50	0	322.50
3	90.00	232.50	0	322.50
4	90.00	232.50	182.18	504.68

5	45.00	142.50	0	187.50

Table 5.15 – Axial forces acting on storey 3 columns at collapse state for MRF nr.18

STOREY 3				
Column	N_q **kN**	N_F **kN**	N_{fb} **kN**	N_{tot} **kN**
1	29.85	91.20	-95.39	25.66
2	59.70	150.90	0	210.60
3	59.70	150.90	0	210.60
4	59.70	150.90	95.39	305.99
5	29.85	91.20	0	121.05

Table 5.16 – Axial forces acting on storey 4 columns at collapse state for MRF nr.18

STOREY 4				
Column	N_q **kN**	N_F **kN**	N_{fb} **kN**	N_{tot} **kN**
1	14.70	91.20	-35.63	18.97
2	29.40	150.90	0	98.70
3	29.40	150.90	0	98.70
4	29.40	150.90	35.63	134.33
5	14.70	91.20	0	54.60

e) The sum of the plastic moments required at first storey (Eq.(5.4)(3.18)) is spread among the columns

The flexural resistance of the first storey columns, obtained in step c), $\sum_{i=1}^{n_c} M_{c,i,1}$, has to be distributed among the columns. In Table 5.17, the standard sections of first storey columns are delivered.

Table 5.17 – Check of first storey columns to flexural resistance for MRF nr.18

STOREY 1

Column	N_{tot} kN	$M^{(1)}_{reqc,i1}$ kNm	$W_{pl,req}$ cm^3	section	$W_{pl,obt}$ cm^3	$M_{pl,obt}$ kNm
1	26.61	592.51	1669.05	HE 300 B	1869.00	663.50
2	434.40	592.51	1669.05	HE 300 B	1869.00	663.50
3	434.40	592.51	1669.05	HE 300 B	1869.00	663.50
4	714.96	592.51	1669.05	HE 300 B	1869.00	663.50
5	253.95	300.00	845.07	HE 300 B	870.10	308.89

The sum of the first storey plastic moments, $\sum_{i=1}^{n_c} M^*_{c,i,1}$, coming from Table 5.17, is equal to:

$$\sum_{i=1}^{n_c} M^*_{c,i,1} = 2962.87\ kNm \tag{5.9}$$

Values are greater than the required one because the sections are chosen from standard shapes. At this stage, the value of $\alpha_0{}^{(g)}$ can be evaluate by replacing the values of $\sum_{i=1}^{n_c} M^*_{c,i,1}$ by $\sum_{i=1}^{n_c} M_{c,i,1}$ in Eq. (3.7).

$$\alpha_0{}^{(g)} = \frac{\sum_{i=1}^{n_c} M_{c.1} + 2 \cdot 3 \sum_{k=1}^{n_s} \sum_{j=1}^{n_b} \gamma M_{b.jk} L_j / L^*_{j,k}}{\sum_{k=1}^{n_s} F_k\, h_k} = 3.13 \tag{5.10}$$

the value of $\alpha^{(g)}$ can be evaluate by replacing both values of $\sum_{i=1}^{n_c} M^*_{c,i,1}$ by $\sum_{i=1}^{n_c} M_{c,i,1}$ in Eq. (3.5) with $\delta = \delta_u$ or simply from the following:

$$\alpha^{(g)} = \alpha_0^{(g)} - \gamma^{(g)}\delta_u = 3.13 - 1.58 \cdot 0.56 = 2.24 \tag{5.11}$$

f) - g) Calculation of the sum of the columns plastic moments reduced by a contemporary action of the axial load, $\sum_{i=1}^{n_c} M^{(t)}_{c,i,i_m}$, required at any storey in order to avoid the undesired mechanisms and selection of the maximum one

The sum of the columns plastic moments reduced by a contemporary action of the axial load, required at any storey in order to prevent the undesired mechanisms is obtained from Eqs. (3.19) – (3.21), properly modified for MRF-FREEDAM case. This values and the sum of the columns plastic moments which governs the design at each storey are reported in Table 5.18.

Table 5.18 – Required moments at each storey needed to avoid the undesired mechanism and maximum value of $\sum_{i=1}^{n_c} M_{c,i,i_m}^{(t)}$ for MRF nr.18

Storey	$\sum_{i=1}^{n_c} M_{c,i,i_m}^{(1)}$ kNm	$\sum_{i=1}^{n_c} M_{c,i,i_m}^{(2)}$ kNm	$\sum_{i=1}^{n_c} M_{c,i,i_m}^{(3)}$ kNm	$\sum_{i=1}^{n_c} M_{c,i,i_m}^{(t)}$ kNm
1	2962.87	-	2962.87	2962.87
2	2021.81	-649.25	2168.50	2168.50
3	1379.85	485.39	1521.11	1521.11
4	631.53	940.80	777.17	940.80

g) *Design of the columns sections at each storey*

The sum of the columns required plastic moment, reduced for the simultaneous axial force, N_{tot}, $M_{c,i,1,req}$, the required plastic modulus, $W_{pl,req}$, and the obtained one, $W_{pl,obt}$, the columns sections chosen from standard shape and their corresponding obtained plastic moments, $M_{c,i,1,obt}$, are shown in the following Table 5.19 to Table 5.21.

Table 5.19 – Design of the column sections at storey 2 for MRF nr.18

STOREY 2						
Column	N_{tot} kN	$M_{reqc,i1}^{(2)}$ kNm	$W_{pl,req}$ cm^3	section	$W_{pl,obt}$ cm^3	$M_{pl,obt}$ kNm
1	5.32	467.13	1315.85	HE 300 B	1869.00	663.50

2	322.50	467.13	1315.85	HE 300 B	1869.00	663.50
3	322.50	467.13	1315.85	HE 300 B	1869.00	663.50
4	504.68	467.13	1315.85	HE 300 B	1869.00	663.50
5	187.50	300.00	845.07	HE 300 B	870.10	308.89

Table 5.20 – Design of the column sections at storey 3 for MRF nr.18

STOREY 3						
Column	N_{tot} **kN**	$M^{(3)}_{reqc,i1}$ **kNm**	$W_{pl,req}$ **cm^3**	**section**	$W_{pl,obt}$ **cm^3**	$M_{pl,obt}$ **kNm**
1	25.66	342.78	965.57	HE 260 B	1283.00	455.47
2	210.60	342.78	965.57	HE 260 B	1283.00	455.47
3	210.60	342.78	965.57	HE 260 B	1283.00	455.47
4	305.99	342.78	965.57	HE 260 B	1283.00	455.47
5	121.05	150.00	422.54	HE 260 B	602.20	213.78

Table 5.21 – Design of the column sections at storey 4 for MRF nr.18

STOREY 4						
Column	N_{tot} **kN**	$M^{(4)}_{reqc,i1}$ **kNm**	$W_{pl,req}$ **cm^3**	**section**	$W_{pl,obt}$ **cm^3**	$M_{pl,obt}$ **kNm**
1	18.97	197.70	556.90	HE 260 B	1283.00	455.47
2	98.70	197.70	556.90	HE 260 B	1283.00	455.47
3	98.70	197.70	556.90	HE 260 B	1283.00	455.47
4	134.33	197.70	556.90	HE 260 B	1283.00	455.47
5	54.60	150.00	422.54	HE 260 B	602.20	213.78

h) Control of technological condition

The Tables given in the previous steps show the definitive value, in which the technological condition has been already considered.

The adopted profiles are **HE 300 B** for storeys 1-2 and **HE 260 B** for storeys 3 and 4. The beam sections satisfy the interstorey drift set by Eurocode 8 [19] therefore they are not incremented.

5.4 Design of MRF-CBF Dual systems (4 St_DC3_D-CBFs_X_TRADITIONAL)

In order to design the MRF-CBF dual systems, since the main structural elements might be different, the procedure starts over again. In this case, the frame lateral stiffness is assured by the concentrically braces, which significantly reduce the interstorey drift.

Diagonals are designed with 75% of the cutting edge resulting from horizontal sesmic force; they must also meet the requirements of Eurocode 8 for DC3 ductility class described in §2.2.2. In particular circular sections have been chosen, so it is very important that their local slenderness D/t should not be greater than, 47,4 $\frac{\varepsilon^2}{\gamma_{rm}}$ where D is the external diameter and t the thickness of the cross section and $\varepsilon = \sqrt{235/f_y}$. For this limitation, the diagonal sections must be increased with respect to those originally planned. Table 5.22 – Design of chevron braces for D-CBF shows the final sections that meet all the project requirements.

Table 5.22 – Design of chevron braces for D-CBF nr.10

Storey	Q kN	N kN	A_{min} cm^2	section	A cm^2	D/t -
1	238.88	275.30	7.75	CHS 88.9x5	13.18	17.78
2	214.29	246.95	6.69	CHS 88.9x5	13.18	17.78
3	165.10	190.27	5.36	CHS 88.9x4	10.67	22.23
4	91.32	105.24	2.69	CHS 88.9x4	10.67	22.23

$$N = \frac{0.75Q}{cos\ \alpha} \tag{5.12}$$

is the axial forces on diagonals, with α = 0.86 rad

$$A_{min} = \frac{N}{f_{yk}} \tag{5.13}$$

$$\varepsilon = \sqrt{\frac{235}{f_{yk}}} = 0.66 \quad \text{with } f_{yk} = 355 \text{ Mpa for S355 steel} \tag{5.14}$$

From the modal analysis performed with the software SAP2000 v.22 we obtain the first vibration period adopted for the preliminary design: T_1 = 0.84 s.

The seismic actions of storey are obtained from eq. (5.1) and with reference to the design spectrum in Figure 4.13. They are reported in Table 5.23Table 5.1, starting from a base shear action equal to 627.14 kN (obtained considering half of the structure).

Table 5.23 - Interstorey heights and design seismic horizontal forces at k-th storey for D-CBF nr.10

Storey	h_i m	F_k kN
1	3.5	64.57
2	3.5	129.14
3	3.5	193.70
4	3.5	239.73

In the following, the design procedure development is described.

a) Selection of the design displacement

Choosing the maximum design displacement, for which the development of the global collapse mechanism has to be insured, is important because it governs the extent of the second order effects.

Furthermore, the complete development of a collapse mechanism can be avoided when the demand for plastic rotation exceeds the structure local ductility. Therefore, it is basic to choose an ultimate design displacement, δ_u, related to the structure local ductility, particularly to the beam-to-column joints, by assuming:

$$\delta_u = \theta_u \, h_{n_s} = 0.04 \times 14 = 0.56\, m \tag{5.15}$$

where θ_u is the joints plastic rotation capacity, in this case equal to $0.04\, rad$.

b) Calculation of the mechanism equilibrium curves slopes, ${\gamma_{i_m}}^{(t)}$

The mechanism equilibrium curves slopes, ${\gamma_{i_m}}^{(t)}$, have been evaluated through Equations (3.8), (3.10), (3.12), (3.14) and the values are shown in Table 5.24.

Table 5.24 - Slopes of the mechanism equilibrium curves for D-CBF

Storey	$\gamma_{im}^{(1)}$ **m^{-1}**	$\gamma_{im}^{(2)}$ **m^{-1}**	$\gamma_{im}^{(3)}$ **m^{-1}**
1	2.90	$\boxed{0.60}$	2.90
2	1.33	0.72	2.41
3	0.83	0.98	2.06
4	0.60	1.78	1.78

The value of the slope of global type mechanism equilibrium curve, $\gamma^{(g)}$, is the minimum between all the values of ${\gamma_{i_m}}^{(t)}$:

$$\gamma^{(g)} = 0.60 \tag{5.16}$$

c) Design of first storey columns sections

The design of the columns at first storey occurs according to equation (3.18) with $W_{d.jk} = 2\gamma M_{b.jk}\frac{L_j}{L^*_{j,k}}+\gamma N_{t.jk}e_{t.jk}+N_{c.jk}(\delta_u)e_{c.jk}$

$$\sum_{i=1}^{n_c} M_{c.i.1} = \frac{\sum_{k=1}^{n_s}\sum_{j=1}^{n_b} W_{b.jk} + (\gamma_1^{(3)} - \gamma^{(g)})\delta_u \sum_{k=1}^{n_s} F_k\, h_k}{2\frac{\sum_{k=1}^{n_s} F_k\, h_k}{h_1 \sum_{k=1}^{n_s} F_k} - 1} = 4718.50\ kNm \tag{5.17}$$

d) Computation of the axial load acting in the columns at collapse state i.e., when the global mechanism is fully developed

In this case, the total axial force that beams pass to columns is the sum of four terms: N_q and N_F, due to the distributed and concentrated loads respectively, acting on beams in the seismic combination (Figure 4.3). The third one, instead, is due to the shear actions that plastic hinges develops at beams ends, N_b; finally, N_{br}, due to the axial force chevron braces transmit to the columns which depends on the contributions of compressed and stretched diagonal. In particular N_{br} = $D_{sg}^{(dx)}$ + $D_{sg}^{(sx)}$, where:

$$\begin{aligned} D_{sg}^{(dx)} &= \frac{N_{t.jk}^{s}\sin\alpha - N_{c.jk}^{s}\sin\alpha}{2} + N_{c.jk}^{s+1}\sin\alpha \\ D_{sg}^{(sx)} &= \frac{N_{t.jk}^{s}\sin\alpha - N_{c.jk}^{s}\sin\alpha}{2} - N_{t.jk}^{s+1}\sin\alpha \end{aligned} \tag{5.18}$$

where with index “s” the storey number has been indicated.

In the following Table 5.25 to Table 5.28, the four contributions and the total value N_{tot} are reported, with reference to each storey both for internal and external columns.

Table 5.25 - Axial forces acting on first storey columns at collapse state for D-CBF nr.10

STOREY 1					
Column	N_q **kN**	N_F **kN**	N_b **kN**	N_{br} **kN**	N_{tot} **kN**

1	60.15	193.80	-523.47	0	269.52
2	120.30	314.10	208.46	-434.72	208.14
3	120.30	314.10	-208.46	901.52	1127.46
4	120.30	314.10	523.47	0	957.87
5	60.15	193.80	0	0	253.95

Table 5.26 - Axial forces acting on storey 2 columns at collapse state for D-CBF nr.10

STOREY 2					
Column	N_q **kN**	N_F **kN**	N_b **kN**	N_{br} **kN**	N_{tot} **kN**
1	45.00	142.50	-392.60	0	205.10
2	90.00	232.50	156.35	-179.69	299.15
3	90.00	232.50	-156.35	646.50	812.65
4	90.00	232.50	392.60	0	715.10
5	45.00	142.50	0	0	187.50

Table 5.27 - Axial forces acting on storey 3 columns at collapse state for D-CBF nr.10

STOREY 3					
Column	N_q **kN**	N_F **kN**	N_b **kN**	N_{br} **kN**	N_{tot} **kN**
1	29.85	91.20	-261.73	0	140.68
2	59.70	150.90	104.23	17.69	297.14
3	59.70	150.90	-104.23	395.40	501.77
4	59.70	150.90	261.73	0	472.33
5	29.85	91.20	0	0	121.05

Table 5.28 - Axial forces acting on storey 4 columns at collapse state for D-CBF nr.10

STOREY 4					
Columns	N_q **kN**	N_F **kN**	N_b **kN**	N_{br} **kN**	N_{tot} **kN**
1	14.70	39.90	-130.87	0	76.27
2	29.40	69.30	52.12	188.85	339.67

3	29.40	69.30	-52.12	188.85	235.44
4	29.40	69.30	130.87	0	229.57
5	14.70	39.90	0	0	54.60

e) The sum of the plastic moments required at first storey (Eq.(5.4)(3.18)) is spread among the columns

As already stated, the flexural resistance of the first storey columns, obtained in step c), $\sum_{i=1}^{n_c} M_{c,i,1}$, has to be distributed among the columns. So, the flexural resistance values required for each column, $M_{c,i,1,req}$, the required plastic modulus, $W_{pl,req}$, the obtained plastic modulus, $W_{pl,obt}$, the standard shapes and the flexural resistance achieved both for internal and external columns, $M_{pl,obt}$, are reported in Table 5.29. In this Table, also the standard sections of first storey columns are delivered.

Table 5.29 – Check of first storey columns to flexural resistance for D-CBF nr.10

STOREY 1						
Column	N_{tot} **kN**	$M^{(1)}_{reqc,i1}$ **kNm**	$W_{pl,req}$ **cm³**	**section**	$W_{pl,obt}$ **cm³**	$M_{pl,obt}$ **kNm**
1	269.52	218.50	615.48	HE 360 B	2683.00	952.47
2	208.14	1400.00	3943.66	HE 450 B	3982.00	1413.61
3	1127.46	1400.00	3943.66	HE 450 B	3982.00	1413.61
4	957.87	1400.00	3943.66	HE 450 B	3982.00	1413.61
5	253.95	300.00	845.07	HE 360 B	1032.00	366.36

The sum of the first storey plastic moments, $\sum_{i=1}^{n_c} M^*_{c,i,1}$, coming from Table 5.29, is equal to:

$$\sum_{i=1}^{n_c} M^*_{c,i,1} = 5559.66\ kNm \tag{5.19}$$

Values are greater than the required one because the sections are chosen from standard shapes. At this stage, the value of $\alpha_0{}^{(g)}$ can be evaluate by replacing the values of $\sum_{i=1}^{n_c} M^*_{c,i,1}$ by $\sum_{i=1}^{n_c} M_{c,i,1}$ in Eq. (3.7).

$$\alpha_0{}^{(g)} = \frac{\sum_{i=1}^{n_c} M_{c.1} + \sum_{k=1}^{n_s} \sum_{j=1}^{n_b} W_{d.jk}}{\sum_{k=1}^{n_s} F_k\, h_k} = 3.14 \tag{5.20}$$

the value of $\alpha^{(g)}$ can be evaluate by replacing both values of $\sum_{i=1}^{n_c} M^*_{c,i,1}$ by $\sum_{i=1}^{n_c} M_{c,i,1}$ in Eq. (3.5) with $\delta = \delta_u$ or simply from the following:

$$\alpha^{(g)} = \alpha_0^{(g)} - \gamma^{(g)}\delta_u = 2.93 - 0.56 \cdot 0.56 = 2.81 \tag{5.21}$$

f) - g) Calculation of the sum of the columns plastic moments reduced by a contemporary action of the axial load, $\sum_{i=1}^{n_c} M^{(t)}_{c,i,i_m}$, required at any storey in order to avoid the undesired mechanisms and selection of the maximum one

The sum of the columns plastic moments reduced by a contemporary action of the axial load, required at any storey in order to prevent the undesired mechanisms is obtained from Eqs. (3.19) - (3.21) properly modified for D-CBF case. This values and the sum of the columns plastic moments which governs the design at each storey are reported in Table 5.30. It is easy to note that the type 1 mechanism always governs the columns design.

Table 5.30 – Required moments at each storey needed to avoid the undesired mechanism and maximum value of $\sum_{i=1}^{n_c} M^{(t)}_{c,i,i_m}$ for D-CBF nr.10

Storey	$\sum_{i=1}^{n_c} M^{(1)}_{c,i,i_m}$ kNm	$\sum_{i=1}^{n_c} M^{(2)}_{c,i,i_m}$ kNm	$\sum_{i=1}^{n_c} M^{(3)}_{c,i,i_m}$ kNm	$\sum_{i=1}^{n_c} M^{(t)}_{c,i,i_m}$ kNm
1	5559.66	-	5559.66	5559.66
2	5330.15	-2847.55	3323.77	5330.15

3	5231.95	-769.37	2381.01	5231.95
4	3565.68	-347.68	975.86	3565.68

g) Design of the columns sections at each storey

The sum of the columns required plastic moment, reduced for the simultaneous axial force, N_{tot}, $M_{c,i,1,req}$, the required plastic modulus, $W_{pl,req}$, and the obtained one, $W_{pl,obt}$, the columns sections chosen from standard shape and their corresponding obtained plastic moments, $M_{c,i,1,obt}$, are shown in the following Table 5.31 to Table 5.33.

Table 5.31 – Design of the column sections at storey 2 for D-CBF nr.10

STOREY 2						
Column	N_{tot} **kN**	$M^{(2)}_{reqc,i1}$ **kNm**	$W_{pl,req}$ **cm³**	**section**	$W_{pl,obt}$ **cm³**	$M_{pl,obt}$ **kNm**
1	205.10	830.15	2338.46	HE 360 B	2683.00	952.47
2	299.15	1400.00	3943.66	HE 450 B	3982.00	1413.61
3	812.65	1400.00	3943.66	HE 450 B	3982.00	1413.61
4	715.10	1400.00	3943.66	HE 450 B	3982.00	1413.61
5	187.50	300.00	845.07	HE 360 B	1032.00	366.36

Table 5.32 – Design of the column sections at storey 3 for D-CBF nr.10

STOREY 3						
Column	N_{tot} **kN**	$M^{(3)}_{reqc,i1}$ **kNm**	$W_{pl,req}$ **cm³**	**section**	$W_{pl,obt}$ **cm³**	$M_{pl,obt}$ **kNm**
1	140.68	701.95	1977.31	HE 320 B	2149.00	762.90
2	297.14	1400.00	3943.66	HE 450 B	3982.00	1413.61
3	501.77	1400.00	3943.66	HE 450 B	3982.00	1413.61
4	472.33	1400.00	3943.66	HE 450 B	3982.00	1413.61
5	121.05	330.00	929.58	HE 320 B	939.10	333.38

Table 5.33 – Design of the column sections at storey 4 for D-CBF nr.10

STOREY 4						
Column	N_{tot} **kN**	$M^{(4)}_{reqc,i1}$ **kNm**	$W_{pl,req}$ **cm³**	**section**	$W_{pl,obt}$ **cm³**	$M_{pl,obt}$ **kNm**
1	76.27	535.68	1508.96	HE 320 B	2149.00	762.90
2	339.67	900.00	2535.21	HE 450 B	3982.00	1413.61
3	235.44	900.00	2535.21	HE 450 B	3982.00	1413.61
4	229.57	900.00	2535.21	HE 450 B	3982.00	1413.61
5	54.60	330.00	929.58	HE 320 B	939.10	333.38

h) Control of technological condition

If the obtained first storey columns sections are smaller than the ones required at the other storeys, the technological condition is not verified, so the first storey column sections have to be increased by using some greater sections. As a consequence, the value of $\sum_{i=1}^{n_c} M^*_{c,i,1}$ has to be updated and the procedure has to be repeated from step *c)*. The Tables given in the previous steps show the definitive value, in which the technological condition has been already considered.

The adopted profiles are **HE 340B** (external columns) and **HE 450B** (internal columns) for storeys 1-2; **HE 320B** (external columns) and **HE 450B** (internal columns) for storeys 3-4. The beam sections have be increased until the frame satisfy the interstorey drift requirement set by Eurocode 8 [19]; so the definitive values one are **IPE 330** for bays 1 and 3; **IPE 270** for bay 2 and IPE 220 for hinged bay.

5.5 Design of MRF-CBF Dual systems equipped with FREEDAM dampers (4 St_DC3_D-CBFs_X_FREEDAM)

FREEDAM dampers are located at beam-to-column joints and at the top of chevron braces with the specific goal of dissipate seismic energy and reduce the lateral displacements. They have been designed starting from the elements obtained in §5.4; taking into account the beams and columns dimensions, device D1 was chosen.

In this case the bracing diagonals have only the purpose of lateral stiffening and in the case of a collapse mechanism they must not become unstable because now the dissipative function is developed by the device placed at the top of chevron braces.

The device at the diagonal intersection must be designed with the 75% of the seismic shear and with the eqs. (2.6) and (2.7). Diagonals have been chosen in order to satisfy the buckling check under axial force deriving from the resistance of the device just designed according to eq. (2.8) The results obtained are shown in Table 5.34.

Table 5.34 – Design of chevron braces equipped with friction dampers

St.	$0.75V_{Ed}$ kN	P_f kN	$V_{f,Rd}$ kN	$\gamma_{Rd}V_{f,Rd}$ kN	$N_{Ed.k}$ kN	Diagonal	$N_{Rd.k}$ kN
1	179.16	50	180.95	289.52	221.88	CHS114.3x6.3	244.73
2	160.72	45	162.86	260.57	199.69	CHS114.3x5	200.54
3	123.83	35	126.67	202.67	155.32	CHS114.3x4	164.42
4	91.32	19	68.76	110.2	84.31	CHS88.9x5	96.20

Once the diagonals have been defined, so that the moment resisting frames contribute al least 25% to the total strength, the beam sections must be increased until this condition is met. Then to evaluate the flexural resistance of the single beams damper is considered the maximum moment acting on the beams of each storey, $M_{fb,Ed,max}$, between the ultimate limit state and seismic combination. From equation (2.4(2.4) the preloading force to be used in eq. (2.3) is calculated. A this point the local hierarchy criterion (2.5) must be satisfied. In Table 5.35 the final beam sections and the design and verification of FREEDAM beam-to-column joints are reported.

Table 5.35 – Design of FREEDAM joints for D-CBF nr.26

Storey	Beam	$M_{fb.Ed.max}$ kNm	P_f kN	$M_{f,Rd}$ kNm	$\gamma_{Rd} M_{f,Rd} l*$ kNm	$M_{b,Rd}$ kNm
1	IPE 360	72.36	29	74.17	97.64	361.75
2	IPE 360	70.39	28	71.61	94.27	361.75
3	IPE 330	52.24	22	53.08	69.98	285.53
4	IPE 330	34.40	15	36.19	47.72	285.53

where l* = (l - L)/l

The local hierarchy criterion is satisfied, otherwise the beam size must be further increased.

Now we design the columns following the 3-TPMC algorithm and what is reported in §3.4.

From the modal analysis performed with the software SAP2000 v.22 we obtain the first vibration period adopted for the preliminary design: T_1 = 0.77 s.

The seismic actions of storey are obtained from eq. (5.1) and with reference to the design spectrum in Figure 4.11 - Reduced horizontal elastic response spectrum for the MRFs (to design D-CBFs equipped with FREEDAM dampers reference was made to the spectrum of Moment

Resisting Frames). They are reported in Table 5.36Table 5.1, starting from a base shear action equal to 534.08 KN (obtained considering half of the structure).

Table 5.36 - Interstorey heights and design seismic horizontal forces at k-th storey for D-CBF nr.26

Storey	h_i m	F_k kN
1	3.5	54.99
2	3.5	109.97
3	3.5	164.96
4	3.5	204.16

In the following, the design procedure development is described.

a) Selection of the design displacement

See eq. (5.15)

b) Calculation of the mechanism equilibrium curves slopes, ${\gamma_{i}}_{m}^{(t)}$

The mechanism equilibrium curves slopes, ${\gamma_{i}}_{m}^{(t)}$, have been evaluated through Equations (3.8), (3.10), (3.12), (3.14) and the values are shown in Table 5.37 - Slopes of the mechanism equilibrium curves for D-CBF.

Table 5.37 - Slopes of the mechanism equilibrium curves for D-CBF nr.26

Storey	$\gamma_{im}^{(1)}$ m^{-1}	$\gamma_{im}^{(2)}$ m^{-1}	$\gamma_{im}^{(3)}$ m^{-1}
1	3.40	$\boxed{0.71}$	3.40
2	1.57	0.85	2.83
3	0.98	1.15	2.41
4	0.71	2.09	2.09

The value of the slope of global type mechanism equilibrium curve, $\gamma^{(g)}$, is the minimum between all the values of $\gamma_{i_m}{}^{(t)}$:

$$\gamma^{(g)} = 0.71 \tag{5.22}$$

c) *Design of first storey column sections*

The design of the columns at first storey occurs according to equations (3.18) and (3.30) with $W_{d.jk} = 2\gamma_{R_d} M_{fb.Rd.jk} \frac{L_j}{L^*_{j,k}} + \gamma_{R_d} V_{f.Rd.k} (h_k - h_{k-1})$

$$\sum_{i=1}^{n_c} M_{c.i.1} = \frac{\sum_{k=1}^{n_s} \sum_{j=1}^{n_b} W_{b.jk} + (\gamma_1^{(3)} - \gamma^{(g)}) \delta_u \sum_{k=1}^{n_s} F_k \, h_k}{2 \frac{\sum_{k=1}^{n_s} F_k \, h_k}{h_1 \sum_{k=1}^{n_s} F_k} - 1} = 2787.37 \; kNm \tag{5.23}$$

d) *Computation of the axial load acting in the columns at collapse state i.e., when the global mechanism is fully developed*

The axial loads acting on columns, as already seen, come from vertical loads distribution, the shear actions due to the flexural action that FREEDAMs are able to transmit and an additional value acting on the columns of braced bay due to shear resistance of device at the top of chevron braces. In particular:

$$N_{fbr} = \gamma_{R_d} V_{f.Rd.k} \sin \alpha \tag{5.24}$$

In the following Table 5.38 to Table 5.41, the four contributions and the total value N_{tot} are reported, with reference to each storey both for internal and external columns.

Table 5.38 - Axial forces acting on first storey columns at collapse state for D-CBF nr.26

STOREY 1

Column	N_q kN	N_F kN	$N_{f.b}$ kN	$N_{f.br}$ kN	N_{tot} kN
1	60.15	193.80	-125.36	0	128.59
2	120.30	314.10	0	217.63	652.03
3	120.30	314.10	0	217.63	652.03
4	120.30	314.10	125.36	0	559.76
5	60.15	193.80	0	0	253.95

Table 5.39 - Axial forces acting on storey 2 columns at collapse state for D-CBF nr.26

STOREY 2					
Column	N_q kN	N_F kN	$N_{f.b}$ kN	$N_{f.br}$ kN	N_{tot} kN
1	45.00	142.50	-85.80	0	101.70
2	90.00	232.50	0	118.71	441.21
3	90.00	232.50	0	118.71	441.21
4	90.00	232.50	85.80	0	408.30
5	45.00	142.50	0	0	187.50

Table 5.40 - Axial forces acting on storey 3 columns at collapse state for D-CBF nr.26

STOREY 3					
Column	N_q kN	N_F kN	$N_{f.b}$ kN	$N_{f.br}$ kN	N_{tot} kN
1	29.85	91.20	-47.61	0	73.44
2	59.70	150.90	0	41.77	252.37
3	59.70	150.90	0	41.77	252.37
4	59.70	150.90	47.61	0	258.21
5	29.85	91.20	0	0	121.05

Table 5.41 - Axial forces acting on storey 4 columns at collapse state for D-CBF nr.26

STOREY 4					
Column	N_q kN	N_F kN	$N_{f.b}$ kN	$N_{f.br}$ kN	N_{tot} kN

1	14.70	39.90	-19.30	0	35.30
2	29.40	69.30	0	0	98.70
3	29.40	69.30	0	0	98.70
4	29.40	69.30	19.30	0	118.00
5	14.70	39.90	0	0	54.60

e) The sum of the plastic moments required at first storey (Eq.(5.4)(3.18)) is spread among the columns

As already stated, the flexural resistance of the first storey columns, obtained in step c), $\sum_{i=1}^{n_c} M_{c,i,1}$, has to be distributed among the columns. So, the flexural resistance values required for each column, $M_{c,i,1,req}$, the required plastic modulus, $W_{pl,req}$, the obtained plastic modulus, $W_{pl,obt}$, the standard shapes and the flexural resistance achieved both for internal and external columns, $M_{pl,obt}$, are reported in Table 5.42Table 5.29. In this Table, also the standard sections of first storey columns are delivered.

Table 5.42 – Check of first storey columns to flexural resistance for D-CBF nr.26

STOREY 1						
Column	N_{tot} **kN**	$M^{(1)}_{reqc,i1}$ **kNm**	$W_{pl,req}$ **cm³**	**section**	$W_{pl,obt}$ **cm³**	$M_{pl,obt}$ **kNm**
1	128.59	621.84	1751.67	HE 300 B	1869.00	663.50
2	652.03	621.84	1751.67	HE 300 B	1869.00	663.50
3	652.03	621.84	1751.67	HE 300 B	1869.00	663.50
4	559.76	621.84	1751.67	HE 300 B	1869.00	663.50
5	253.95	300.00	845.07	HE 300 B	870.10	308.89

The sum of the first storey plastic moments, $\sum_{i=1}^{n_c} M^{*}_{c,i,1}$, coming from Table 5.42,is equal to:

$$\sum_{i=1}^{n_c} M^*_{c,i,1} = 2962.87\ kNm \tag{5.25}$$

Values are greater than the required one because the sections are chosen from standard shapes. At this stage, the value of ${\alpha_0}^{(g)}$ can be evaluate by replacing the values of $\sum_{i=1}^{n_c} M^*_{c,i,1}$ by $\sum_{i=1}^{n_c} M_{c,i,1}$ in Eq. (3.7).

$${\alpha_0}^{(g)} = \frac{\sum_{i=1}^{n_c} M_{c.1} + \sum_{k=1}^{n_s}\sum_{j=1}^{n_b} W_{d.jk}}{\sum_{k=1}^{n_s} F_k\, h_k} = \ 1.50 \tag{5.26}$$

the value of $\alpha^{(g)}$ can be evaluate by replacing both values of $\sum_{i=1}^{n_c} M^*_{c,i,1}$ by $\sum_{i=1}^{n_c} M_{c,i,1}$ in Eq. (3.5) with $\delta = \delta_u$ or simply from the following:

$$\alpha^{(g)} = \alpha_0^{(g)} - \gamma^{(g)}\delta_u = 1.50 - 0.71 \cdot 0.56 = 1.11 \tag{5.27}$$

f) - g) Calculation of the sum of the columns plastic moments reduced by a contemporary action of the axial load, $\sum_{i=1}^{n_c} M_{c,i,i_m}^{(t)}$, required at any storey in order to avoid the undesired mechanisms and selection of the maximum one

The sum of the columns plastic moments reduced by a contemporary action of the axial load, required at any storey in order to prevent the undesired mechanisms is obtained from Eqs. (3.19) - (3.21) properly modified for D-CBF, equipped with FREEDAM dampers, case. This values and the sum of the columns plastic moments which governs the design at each storey are reported in Table 5.43.

Table 5.43 – Required moments at each storey needed to avoid the undesired mechanism and maximum value of $\sum_{i=1}^{n_c} M_{c,i,i_m}^{(t)}$ for D-CBF nr.26

Storeys	$\sum_{i=1}^{n_c} M_{c,i,i_m}^{(1)}$ **kNm**	$\sum_{i=1}^{n_c} M_{c,i,i_m}^{(2)}$ **kNm**	$\sum_{i=1}^{n_c} M_{c,i,i_m}^{(3)}$ **kNm**	$\sum_{i=1}^{n_c} M_{c,i,i_m}^{(t)}$ **kNm**

1	2962.87	-	2962.87	2962.87
2	2311.53	2200.54	1800.04	2311.53
3	1652.87	1524.23	1233.88	1652.87
4	748.23	880.70	621.93	880.70

h) Design of the column sections at each storey

The sum of the columns required plastic moment, reduced for the simultaneous axial force, N_{tot}, $M_{c,i,1,req}$, the required plastic modulus, $W_{pl,req}$, and the obtained one, $W_{pl,obt}$, the columns sections chosen from standard shape and their corresponding obtained plastic moments, $M_{c,i,1,obt}$, are shown in the following Table 5.44 to Table 5.46.

Table 5.44 – Design of the column sections at storey 2 for D-CBF nr.26

STOREY 2						
Column	N_{tot} **kN**	$M_{reqc,i1}^{(2)}$ **kNm**	$W_{pl,req}$ **cm^3**	**section**	$W_{pl,obt}$ **cm^3**	$M_{pl,obt}$ **kNm**
1	101.70	502.88	1416.57	HE 300 B	1869.00	663.50
2	441.21	502.88	1416.57	HE 300 B	1869.00	663.50
3	441.21	502.88	1416.57	HE 300 B	1869.00	663.50
4	408.30	502.88	1416.57	HE 300 B	1869.00	663.50
5	187.50	300.00	845.07	HE 300 B	870.10	308.89

Table 5.45 – Design of the column sections at storey 3 for D-CBF nr.26

STOREY 3						
Column	N_{tot} **kN**	$M_{reqc,i1}^{(3)}$ **kNm**	$W_{pl,req}$ **cm^3**	**section**	$W_{pl,obt}$ **cm^3**	$M_{pl,obt}$ **kNm**
1	73.44	370.72	1044.28	HE 260 B	1283.00	455.47
2	252.37	370.72	1044.28	HE 260 B	1283.00	455.47
3	252.37	370.72	1044.28	HE 260 B	1283.00	455.47

4	258.21	370.72	1044.28	HE 260 B	1283.00	455.47
5	121.05	170.00	478.87	HE 260 B	602.20	213.78

Table 5.46 – Design of the column sections at storey 4 for D-CBF nr.26

STOREY 4						
Column	N_{tot} **kN**	$M^{(4)}_{reqc,i1}$ **kNm**	$W_{pl,req}$ **cm**^{3}	**section**	$W_{pl,obt}$ **cm**^{3}	$M_{pl,obt}$ **kNm**
1	35.30	177.68	500.50	HE 260 B	1283.00	455.47
2	98.70	177.68	500.50	HE 260 B	1283.00	455.47
3	98.70	177.68	500.50	HE 260 B	1283.00	455.47
4	118.00	177.68	500.50	HE 260 B	1283.00	455.47
5	54.60	170.00	478.87	HE 260 B	602.20	213.78

i) Control of technological condition

The Tables given in the previous steps show the definitive value, in which the technological condition has been already considered.

The adopted profiles are **HE 300 B** for storeys 1-2 and **HE 260 B** for storeys 3 and 4. The beam sections satisfy the interstorey drift set by Eurocode 8 [19] therefore they are not incremented. So the definitive values one are **IPE 360** for the first two storeys and **IPE 330** for the other two, instead IPE 220 for hinged bay.

The lateral horizontal displacements that structures can be exhibit have been avaluated in SAP2000. Lateral displacements, maximun interstorey drifts and modal informations in APPENDIX A are reported.

CHAPTER 6

VALIDATION OF THE PROCEDURE BY MEANS OF PUSH-OVER ANALYSIS

6.1 Introduction

In order to evaluate the seismic performances of the design structure, non-linear analyses have been carried out both for the structures designed by means of traditional and FREEDAM joints. Preliminarily, a static non-linear analysis, i.e. push-over, has been carried out by means of SAP 2000 [20] computer program. The primary aim of this analysis is the assessment of the collapse mechanism typology, aimed to confirm the accuracy of the proposed design methodology, based on the Theory of Plastic Mechanism Control.

It's about non-linear static method to study the structural behaviour of system under seismic action; in particular structures are considered under seismic combination, $G_k + \psi_2 Q_k$, and horizontal incremental actions.

The software apply incremental lateral load that is automatically increased until a predefined limit, or in some cases until collapse. Analysis are led in displacement control considering both geometrical and mechanical nonlinearities under two lateral load patterns:

1. A load distribution corresponding to the foundamental mode shape (First Mode of vibrate) according to lateral force method explained in EC8:

$$F_{i\_1°} = F_b \frac{W_{pi} U_{1i}}{\sum_i W_{pi} U_{1i}} \tag{6.1}$$

2. A uniform distribution proportional to seismic masses at each storey:

$$F_{i\_m} = F_b \frac{W_{pi}}{\sum_i W_{pi}} \tag{6.2}$$

Where $F_b = S_{ed}(T_1)W\lambda$ is the base shear seismic action with $\lambda = 1$, referred to half of the structure. W_{pi} is the weight of each storey and U_{1i} is the storey modal displacement obtained from an analysis with the Sap2000 software.

Pushover analyzes produce capacity curves, which expresses the relationship between the shear force and the displacements. The seismic performance of the sample frames has been assessed in terms of global parameters, as resistance (base shear, system overstrength), deformation (interstorey drifts and global ductility).

System **overstrength** has been quantified through structural redundancy:

$$q_R = \frac{V_u}{V_1} \tag{6.3}$$

Horizontal deflections are monitored through interstorey drift and **global ductility**:

$$\mu = \frac{\delta_{max}}{\delta_1} \tag{6.4}$$

6.2 Design assumptions for structures with traditional joints

Bams and columns have been modeled by means of beam-column elements, whose non linerities have been concentrated in plastic hinges ("Moment M3" elements). On the beams, hinges at the end of haunched connection that is at a distance s_h from the face of the column, are placed; while on the columns they are assigned with a relative distance of 0 and 1. Of foundamental importance are the demand for plastic rotation during the development of the kinematic mechanism and the capacity for plastic rotation. In the case of columns with dimensionless normal stress lower than 0.30 and beams in flexure, the plastic deformation capacity is expressed as a multiple of the chord rotation at yielding ϑ, defined as a property of the member itself.

In particular for columns arranged strong axis and for beams, the rotation of the member is:

$$\vartheta_y = \frac{\gamma_{rm} M_{pl.y} l_m}{6EI_m} \tag{6.5}$$

For columns arranged weak axis, the rotation of the member is:

$$\vartheta_z = \frac{\gamma_{rm} M_{pl.z} l_m}{6EI_m} \tag{6.6}$$

Where $M_{pl.y}$ and $M_{pl.z}$ are the plastic moment of the member for y and z axis respectively; l_m is the length of the member; I_m is the moment of inertia; E is the elastic modulus and γ_{rm} is the material overstrength coefficient place equal to 1.25.

Plastic rotation capacity at the end of beams or columns with dimensionless axial load ν not grater than 0.30 in Table B.1 of EC8-3 [21] are reported, as shown in the following figure.

	Limit State		
Class of cross section	DL	SD	NC
1	1,0 θ_y	6,0 θ_y	8,0 θ_y
2	0,25 θ_y	2,0 θ_y	3,0 θ_y

Figure 6.1 – Plastic rotation capacity at the end of beams or columns with ν not grater than 0.30 [21]

Taking into account the plastic rotation capacity, defined in Eurocode, and the calibration of the hinges, it is possible to model the hinges as follows.

Table 6.1 – Beams and column hinges model

Point	Moment/SF	Rotation/SF
E-	-0.67	$0.075/\vartheta$
D-	-1.2	$0.028/\vartheta$
C-	-1.2	$0.016/\vartheta$
B-	-1	0
A	0	0
B	1	0
C	1.2	$0.016/\vartheta$
D	1.2	$0.028/\vartheta$
E	0.67	$0.075/\vartheta$

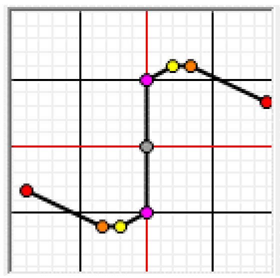

The hysteresis type is kinematic.

To model the plastic hinge of the bracing diagonals in Sap2000 we start from the Georgescu model generally used for cyclic analysis (Figure 6.2).

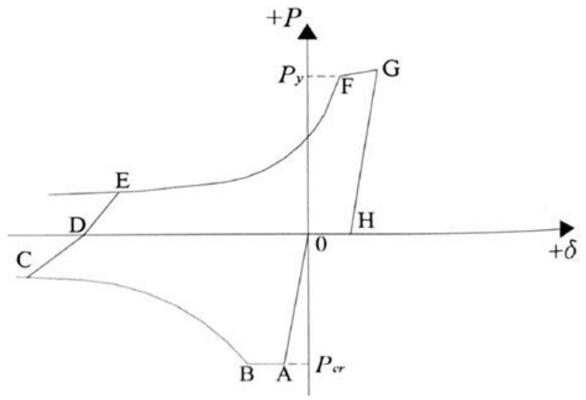

Figure 6.2 – Georgescu model for cyclic analysis

The model used for the pushover analyzes starts from a first simplification of the Georgescu model (Figure 6.3) that exploits the OA, AB and BC traits for compression. On the other hand, in traction the behavior is defined with a Perfectly Plastic Elastic bound (EPP).

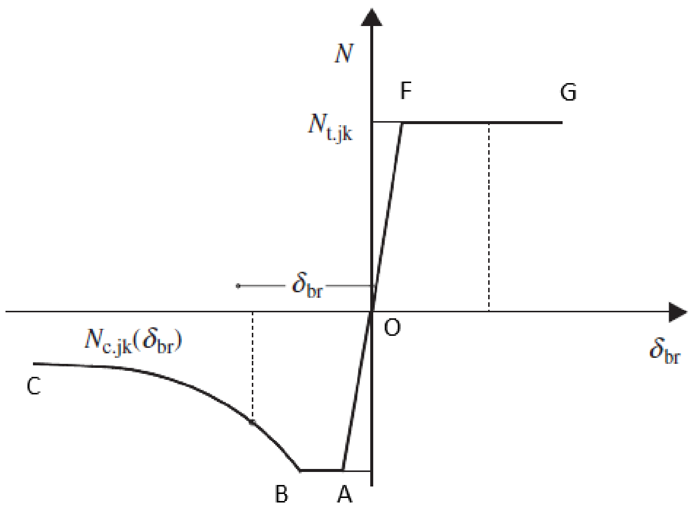

Figure 6.3 – First simplification of the Georgescu model for pushover analysis

The equations of the individual traits of the model are the follows:

- **Initial imperfection**

$$f_0 = \frac{W}{A}\alpha\left(\overline{\lambda^2} - 0.04\right) \quad with \;\; \alpha = 0.21\,, \bar{\lambda} = \frac{\lambda}{\lambda_y} \tag{6.7}$$

- **OA trait**

$$P = \frac{EA}{L}\delta_{OA} = K_d\delta_{OA} \quad with\; P\; limited\; to\; P_{crit}\,; \quad \delta_A = \frac{P_{crit}}{K_d} \tag{6.8}$$

- **AB trait**

$$\begin{gathered} P = P_{crit} \quad \forall\, \delta_{AB} \\ \delta_B = -\frac{P_{crit}L}{EA} + \frac{\pi^2}{4L}\left({f_{tB}}^2 - {f_0}^2\right) \\ f_{tB} = \frac{M_{pl}}{P_{crit}}\left(1 - \frac{P_{crit}}{P_y}\right) \end{gathered} \tag{6.9}$$

- **BC trait**

$$\begin{gathered} f_t = \frac{M_{pl}}{P}\left(1 - \frac{P}{P_y}\right) \; with\; P\; generic < \; P_{crit} \\ \delta_{BC} = -\frac{PL}{EA} + \frac{\pi^2}{4L}\left({f_t}^2 - {f_0}^2\right) \end{gathered} \tag{6.10}$$

- **OF trait**

$$P = \frac{EA}{L}\delta_{OF} = K_d\delta_{OF} \quad with\; P\; limited\; to\; P_y\,; \quad \delta_F = \frac{P_y}{K_d} \tag{6.11}$$

- **FG trait**

$$P = P_{crit} \quad \forall\, \delta_{FG} \tag{6.12}$$

A second simplification adopted in the Sap2000 model consist in considering the OA and OF sections as rigid, while the BC section is represented with bilinear approximation (Figure 6.4).

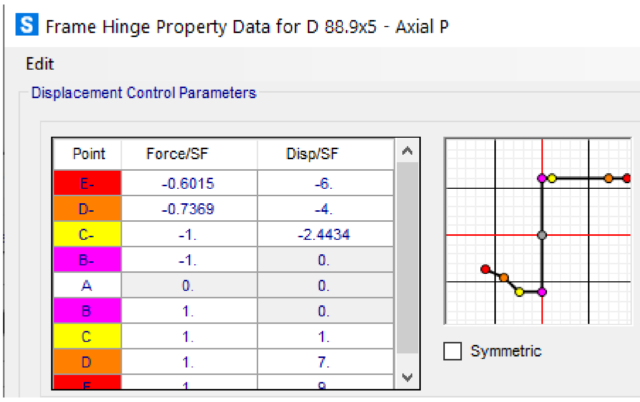

Figure 6.4 - Second simplification of the Georgescu model for pushover analysis, in Sap2000

The bilinear approximation of the BC section was obtained by considering two particular points of the curve, or those corresponding to the limit displacements provided by Eurocode for the compressed diagonals. These points were also identified in traction (on the horizontal branch) according to the limits given for taut diagonals.

For braces in compression the inelastic deformation capacity should be expressed in terms of the axial deformation of the brace, as a multiple of the axial deformation of the brace at buckling load, Δ_c. For braces in compression (except for braces of eccentric braced frames) the inelastic deformation capacities at the three LSs may be taken in accordance with Table B.2 of EC8-3 [21] (Figure 6.5).

	Limit State		
Class of cross section	DL	SD	NC
1	0,25 Δ_c	$\boxed{4{,}0\ \Delta_c}$	$\boxed{6{,}0\ \Delta_c}$
2	0,25 Δ_c	1,0 Δ_c	2,0 Δ_c

Figure 6.5 – Axial deformation capacity of braces in compression

For braces in tension the inelastic deformation capacity should be expressed in terms of the axial deformation of the brace, as a multiple of the axial deformation of the brace at tensile yielding load, Δ_t. For braces in tension (except for braces of eccentric braced frames) with cross section class 1 or 2, the inelastic deformation capacities at the three LSs may be taken in accordance with Table B.3 in EC8-3 [21], as shown in Figure 6.6.

Limit State		
DL	SD	NC
0,25 Δ_t	$\boxed{7{,}0\ \Delta_t}$	$\boxed{9{,}0\ \Delta_t}$

Figure 6.6 – Axial deformation capacity of braces in tension

The diagonals must have a knot in the middle. This node will be moved using the "move" command in the y direction (orthogonal to the visual plane) by a length equal to the initial imperfection f_0.

The hysteresis type is isotropic.

6.2.1 Push-over Analyses Results

The results obtained from the two pushover analyzes are reported below for the case studies: 4 St_DC3_ MRFs_X_TRADITIONAL and 4 St_DC3_ D-CBFs_X_TRADITIONAL. In particular Table 6.2 shows the modal dispacements obtained by Sap2000 software and the distributions of the horitontal seismic force corresponding to eqs. (6.1) and (6.2); in

Figure 6.7 the push-over curves are reported and in Table 6.7 – FREEDAM hinges "Shear V2" model the results of seismic performance. Finally Figure 6.8 represent the push-over hinge pattern from the Sap2000 Computer Program screenshot.

- **Structure code: 4 St_DC3_MRFs_X_TRADITIONAL**

Base shear seismic action: F_b = 238.88 kN

Table 6.2 – Modal displacements and seismic horizontal forces for 4 St_DC3_MRFs_X_TRADITIONAL

Storey	U_1 (m)	$F_{i\_1°}$ (kN)	F_{i_m} (kN)
1	0.011	18.89	60.81
2	0.029	48.60	60.81
3	0.047	78.05	60.81
4	0.061	93.33	56.45

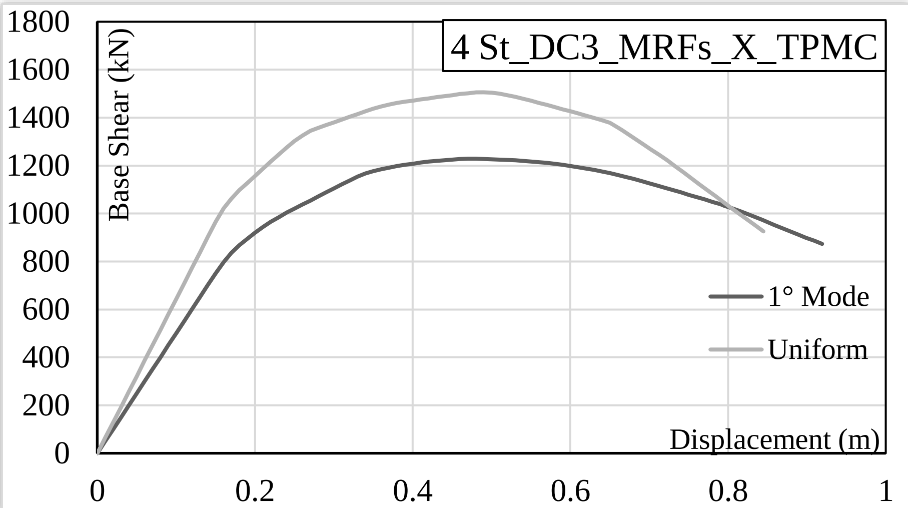

Figure 6.7 – Push-over curves for 4 St_DC3_MRFs_X_TRADITIONAL

Table 6.3 - Seismic performance for 4 St_DC3_MRFs_X_TRADITIONAL

CASE	d_1 (m)	V_1 (kN)	d_u (m)	V_u(kN)	μ (-)	q_R (-)

1° Mode	0.16	796.76	0.48	1228.71	3.00	1.54
Uniform	0.16	1021.06	0.49	1505.56	3.06	1.47

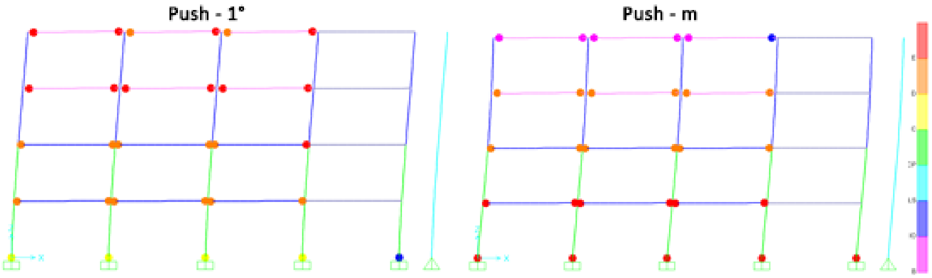

Figure 6.8 – Pushover hinge pattern for 4 St_DC3_MRFs_X_TRADITIONAL

❖ Structure code: 4 St_DC3_D-CBFs_X_TRADITIONAL

Base shear seismic action: F_b = 627.14 kN

Table 6.4 – Modal displacements and seismic horizontal forces for 4 St_DC3_D-CBFs_X_TRADITIONAL

Storey	U_1 (m)	$F_{i\_1°}$ (kN)	F_{i_m} (kN)
1	-0.013	55.46	159.65
2	-0.031	133.94	159.65
3	-0.048	203.91	159.65
4	-0.059	233.83	148.19

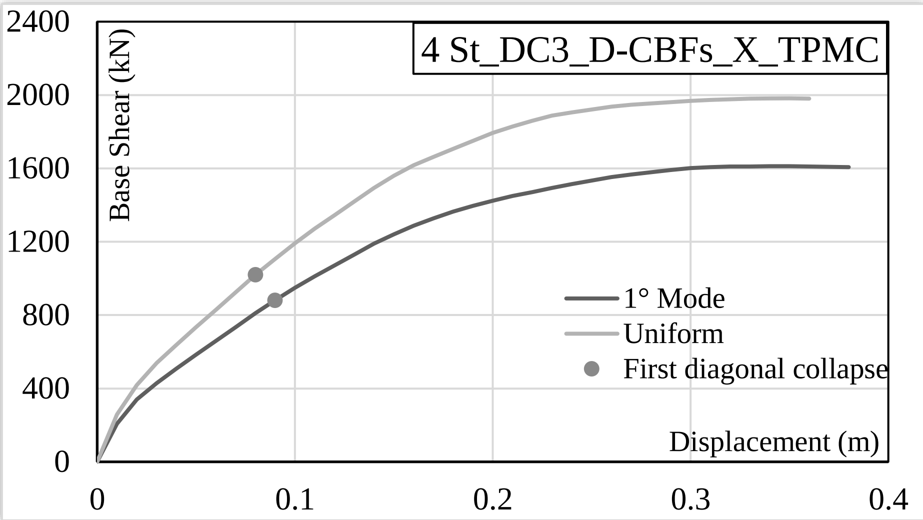

Figure 6.9 – Push-over curves for 4 St_DC3_D-CBFs_X_TRADITIONAL

Table 6.5 - Seismic performance data for 4 St_DC3_D-CBFs_X_TRADITIONAL

CASE	d_1 (m)	V_1 (kN)	d_u (m)	V_u(kN)	μ (-)	q_R (-)
1° Mode	0.09	880.75	0.35	1611.99	3.89	1.83
Uniform	0.08	1019.94	0.34	1981.44	4.25	1.94

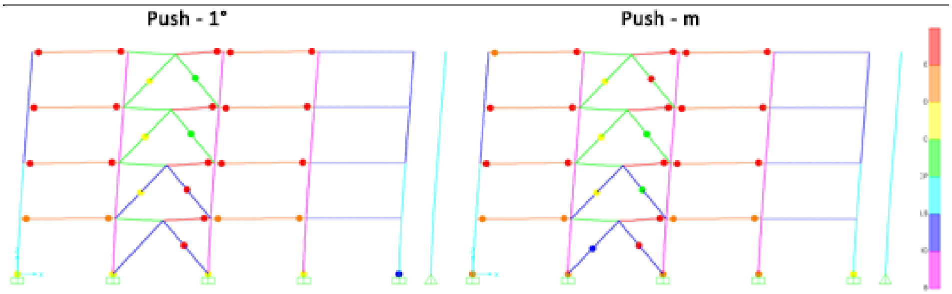

Figure 6.10 - Pushover hinge pattern for 4 St_DC3_D-CBFs_X_TRADITIONAL

The results of all the other analyzes on traditional structures are reported in appendix B.

6.3 Design assumptions for structures with FREEDAM joints

In this case the beams and columns will have plastic hinges as described in point 6.2 with the particularity that on the beams they are assigned a distance L, which represents the length of the FREEDAM joint. Furthermore, FREEDAM hinges modeled as rigid-plastic are inserted on the face of the column.

For FREEDAM hinges the rotation depends on the level arm of the device used. Under the bending action, the node is forced to rotate around the center of rotation, located at the base of the upper T-stub, and the dissipated energy is guaranteed by the alternating sliding of the bolts on the vertical stainless steel plate (Figure 6.11).

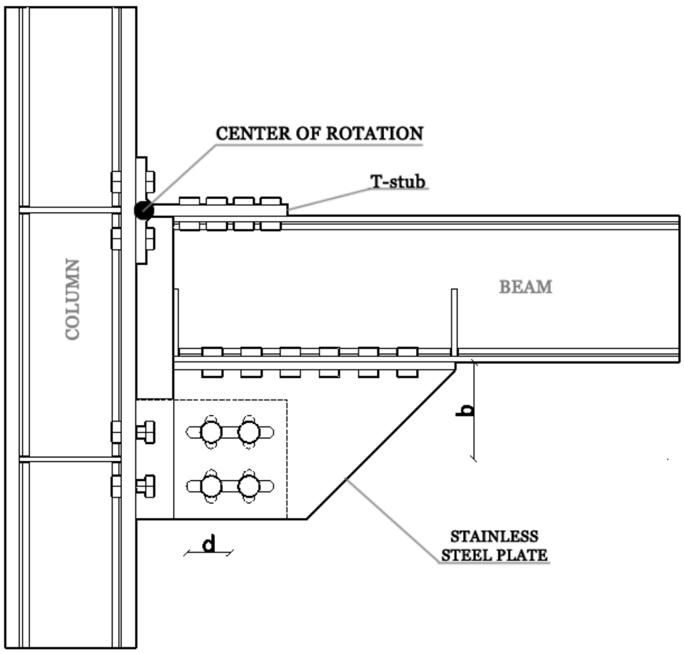

Figure 6.11 – Center of rotation of FREEDAM hinge

In particular, the FREEDAM rotation is:

$$\vartheta_y = \frac{d}{H} \qquad \text{with } H = h_b + b \tag{6.13}$$

Where:

- d is the distance between the bolt and the slot
- h_b is the beam height
- *b* is the distance between the center of gravity of the bolts and the lower flange of the beam.

Table 6.6 – FREEDAM hinges model

Point	Moment/SF	Rotation/SF
E-	-1	$-\vartheta_y$
D-	-1	-0.06
C-	-1	-0.04
B-	-1	0
A	0	0
B	1	0
C	1	0.04
D	1	0.06
E	1	ϑ_y

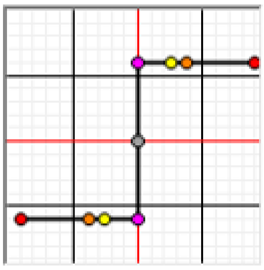

As already mentioned, the bracing diagonals of the D-CBFs structures equipped with FREEDAM dampers do not suffer any damage in the case of a seismic event as the energy dissipation occurs through the friction dampers plased at the top of chevron braces.

For the sole purpose of carring out pushover and IDA analyzes, this friction device was modeled as a "short link" with a cross-section equal to the diagonals it joins and a cross section axial area of zero. The length of the link is: $l_{link} = h_b/2 + 260$.

That is, it has been set equal to half the height of the beam plus the height of device D1.

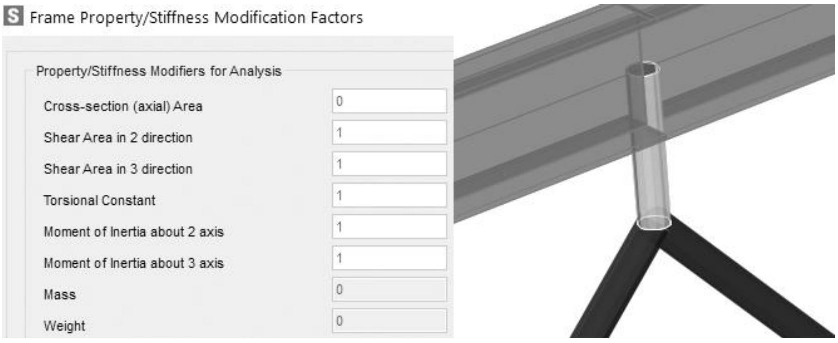

Figure 6.12 – Friction dampers model for pushover and IDA analysis

Rigid plastic frame hinge "Shear V2" to this link is assigned with a max displacement equal to: $d_{max} = 0.04 \cdot h_i = 0.04 \cdot 3.50 = 0.14$m; where h_i is the inter-storey height of the structure.

Table 6.7 – FREEDAM hinges "Shear V2" model

Point	Force/SF	Disp/SF
E-	-1	$-d_{max}$
D-	-1	-0.07
C-	-1	-0.04
B-	-1	0
A	0	0
B	1	0
C	1	0.04
D	1	0.07
E	1	d_{max}

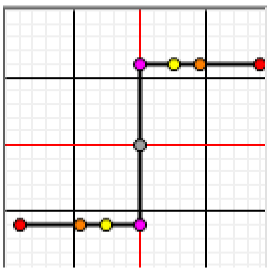

It is important to underline that, in the definition of FREEDAM hinges, the bending and shear strength of the beam-column and diagonal intersection devices respectively, was amplified with the coefficient γ_{rm} equal to 1.6.

6.3.1 Push-over Analyses Results

The results obtained from the two pushover analyzes are reported below for the case studies: 4 St_DC3_ MRFs_X_FREEDAM and 4 St_DC3_ D-CBFs_X_FREEDAM.

- **Structure code: 4 St_DC3_MRFs_X_FREEDAM**

Base shear seismic action: F_b = 238.88 kN

Table 6.8 – Modal displacements and seismic horizontal forces for 4 St_DC3_MRFs_X_FREEDAM

Storey	U_1 (m)	$F_{i\_1°}$ (kN)	F_{i_m} (kN)
1	0.012	20.21	60.81
2	0.030	49.06	60.81
3	0.048	78.38	60.81
4	0.060	91.23	56.45

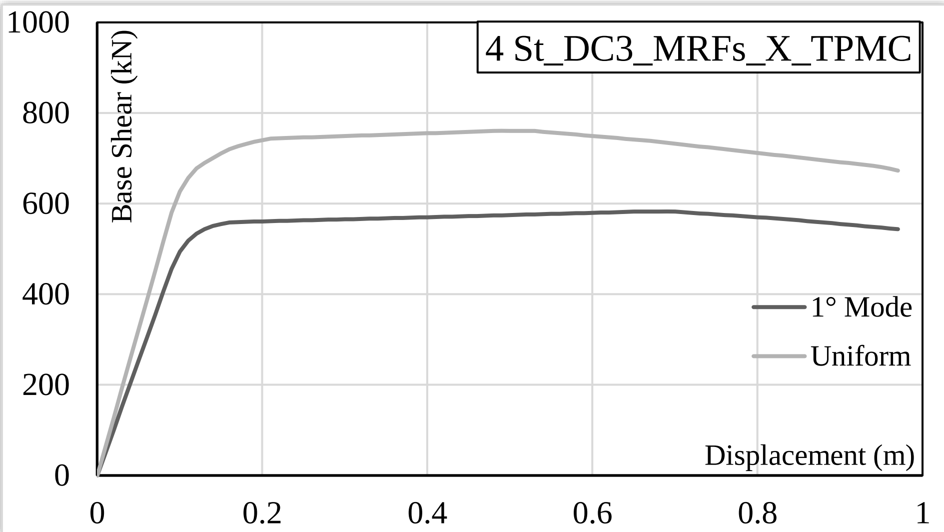

Figure 6.13 – Push-over curves for 4 St_DC3_MRFs_X_FREEDAM

Table 6.9 - Seismic performance for 4 St_DC3_MRFs_X_FREEDAM

CASE	d_1 (m)	V_1 (kN)	d_u (m)	V_u(kN)	μ (-)	q_R (-)
1° Mode	0.09	455.88	0.69	582.65	7.65	1.28
Uniform	0.09	580.20	0.49	760.74	5.43	1.31

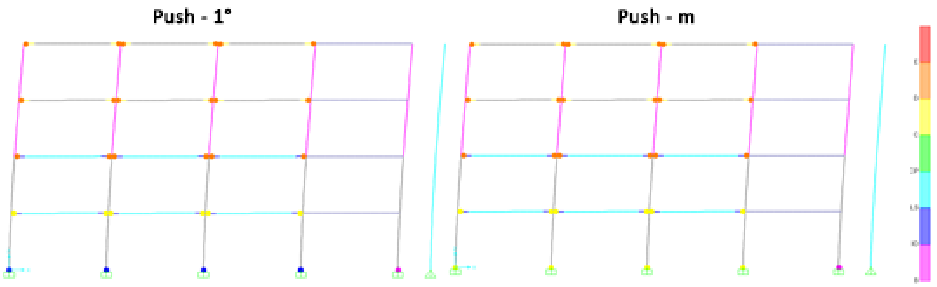

Figure 6.14 - Pushover hinge pattern for 4 St_DC3_MRFs_X_FREEDAM

❖ Structure code: 4 St_DC3_D-CBFs_X_FREEDAM

Base shear seismic action: F_b = 534.08 kN

Table 6.10 – Modal displacements and seismic horizontal forces for 4 St_DC3_D-CBFs_X_FREEDAM

Storey	U_1 (m)	$F_{i\_1°}$ (kN)	F_{i_m} (kN)
1	0.014	49.25	135.96
2	0.031	111.86	135.96
3	0.048	174.13	135.96
4	0.059	198.84	126.20

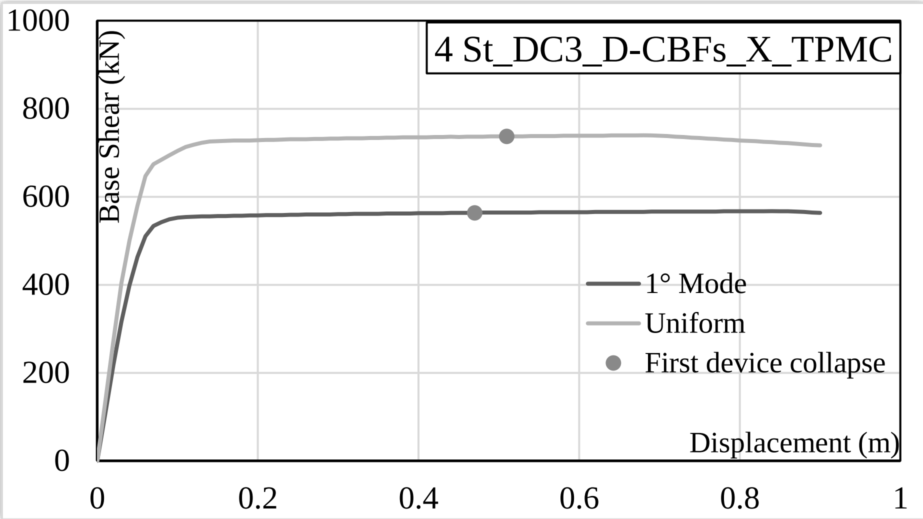

Figure 6.15 – Push-over curves for 4 St_DC3_D-CBFs_X_FREEDAM

Table 6.11 - Seismic performance data for 4 St_DC3_D-CBFs_X_FREEDAM

CASE	d_1 (m)	V_1 (kN)	d_u (m)	V_u(kN)	μ (-)	q_R (-)
1° Mode	0.03	316.10	0.13	555.18	4.32	1.76
Uniform	0.03	403.76	0.15	726.27	4.98	1.80

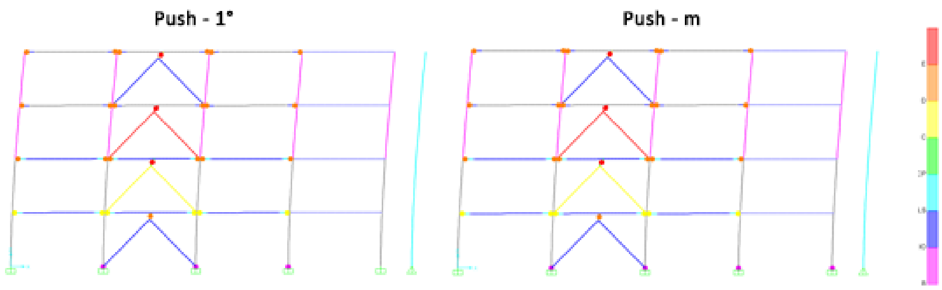

Figure 6.16 - Push-over curves for 4 St_DC3_D-CBFs_X_FREEDAM

CHAPTER 7

VALIDATION OF THE PROCEDURE BY MEANS OF INCREMENTAL DYNAMIC NON-LINEAR ANALYSIS (IDA)

7.1 Introduction

In this chapter, the investigation of the seismic response of the structures is reported. In particular, a further validation of the proposed design methodology called Theory of Plastic Mechanism Control (TPMC) has been gained by means of Incremental Dynamic Analyses (IDA) [22] which are aimed, on one hand, to confirm the pattern of yielding actually developed and, on the other hand, to compare the structural solutions in terms of local ductility demands, under seismic actions and energy dissipation capacity.

IDA analisis is a non linear analysis Type that continue from State at End of Nonlinear Case PUSH-V, with a solution type of direct integration and geometric parameters of P-Delta plus large Displacements.

The structure subjected to vertical loads is pushed horizontally with an acceleration at the base given by the time history corresponding to the earthquake considered.

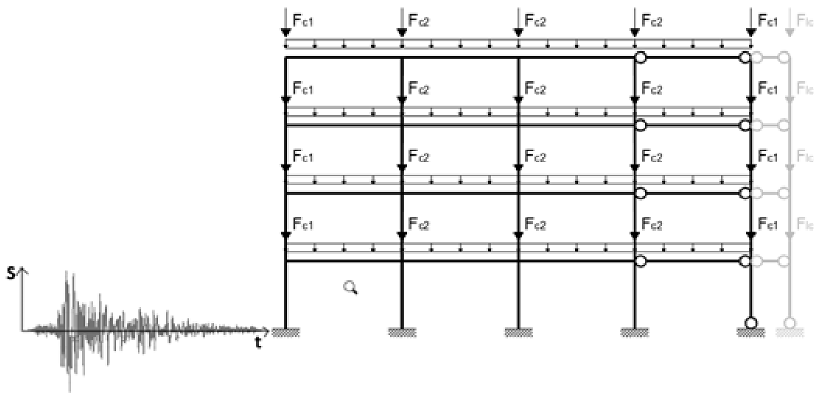

Figure 7.1 – Structure subjected to acceleration at the base

The structures designed according to TPMC have been subjected to IDA analyses carried out using the Sap2000 computer program. **Rayleigh formulation for a 5% damping** has been assumed with the proportional factors computed with reference to the first and second mode of vibration.

Record-to-record variability has been accounted for by considering 7 recorded accelerograms. In Table 7.1 the analysed records (name, date, station name, station code, network and magnitude) have been reported. These recorded accelerograms have been selected to approximately match the linear elastic design response spectrum of Eurocode 8, for soil type B and reference spectral acceleration of 5.28 m/s^2 and 7.03 m/s^2 for DC2 and DC3 respectively. In addition, each earthquake record has been increased of 10s at the end to simulate by means of IDA analyses the achievement of the state of rest.

Table 7.1 – Analized ground motion records

Station Code	Station Name	Earthquake name	Date	Network	Mw
BAR	Bar-Skupstina	NW_Balkan_Peninsula	15.04.1979	EU	6.9
CSO1	CARSOLI1	L'Aquila	06.04.2009	IT	6.1
KAL1	KAL1	Southern_Greece	13.09.1986	HI	5.9
MCT	Macerata	Central_Italy	26.10.2016	IT	5.9
MZ12	Amatrice	Central_Italy	26.10.2016	3A	5.9
MZ102	Accumoli	Central_Italy	30.10.2016	3A	6.5
PZI1	Pizzoli	Central_Italy	24.08.2016	IT	6.0

These recorded accelerograms have been selected to approximately match the linear elastic response spectrum defined in Figure 4.10. Accelerogram multipliers for different Ductility Class have been considered.

In FiguresFigure 7.2 – Selected earthquake spectra for DC2 ductility class and Figure 7.3 – Selected earthquake spectra for DC3 ductility class the reduced spectra of the seven recorded accelerograms are reported. They have been properly scaled to let their average value to be compatible with the design EC8 spectrum for a soil type B. The Incremental Dynamic Analyses have been carried out by increasing the spectral acceleration values until the occurrence of structural collapse. Finally, the scale factors assumed to assure that the average spectrum is compatible with the design one are reported in Table 7.2.

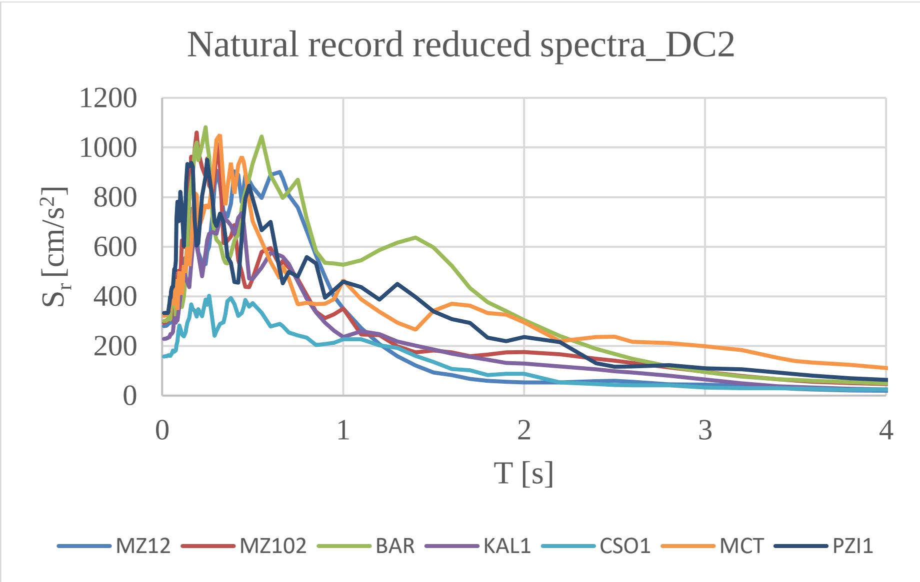

Figure 7.2 – Selected earthquake spectra for DC2 ductility class

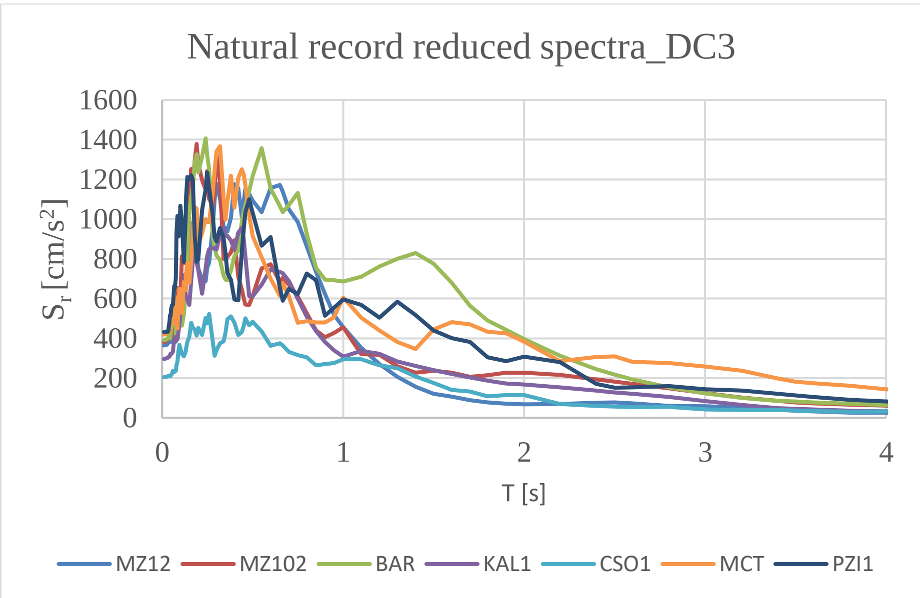

Figure 7.3 – Selected earthquake spectra for DC3 ductility class

The spectrum corresponding to the average value of the seven natural signals follows the trend of the design spectrum defined according to the Eurocode, moreover it is included between a defined range which has as a minimum value the EC8 design spectrum reduced by 10% and as a maximum value the EC8 design spectrum increased by 15%. This is shown in Figures Figure 7.4 – Comparison between EC8 design spectrum and mean natural spectra for DC2and Figure 7.5 for the ductility class DC2 and DC3 respectively.

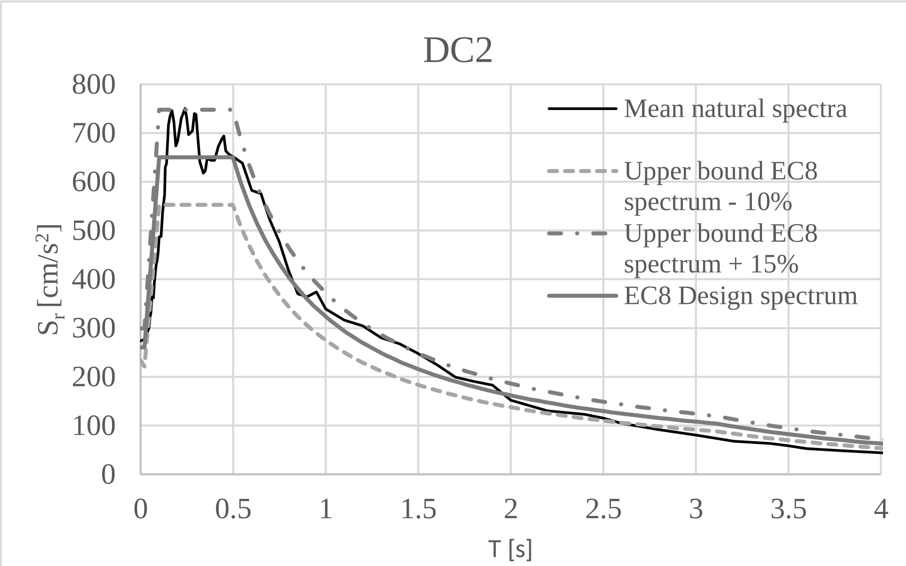

Figure 7.4 – Comparison between EC8 design spectrum and mean natural spectra for DC2

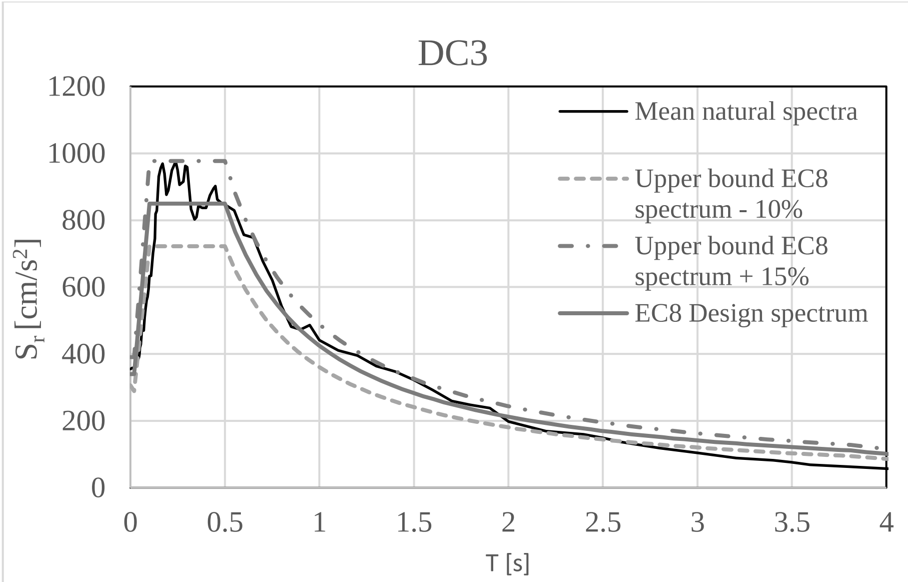

Figure 7.5 – Comparison between EC8 design spectrum and mean natural spectra for DC3

Table 7.2 – Length and scale factor for each earthquake

Station Code	Length (s)	Step recording (s)	Scale Factor DC2	Scale Factor DC3
BAR	47.83	0.01	0.85	1.11
CSO1	99.80	0.01	9	11.7
KAL1	30.02	0.01	1	1.3
MCT	96.38	0.01	4.5	5.85
MZ12	82.67	0.01	2.8	3.64
MZ102	77.15	0.01	0.8	1.04
PZI1	63.45	0.01	7.5	9.75

The seismic performance of a structure shall be measured by its state of damage under given seismic action. The state of damage shall be referred to the four limit states [11]:

- **Fully Operational LS (OP)** shall be defined as one in which the structure is only slightly damaged and economic to repair, allowing continuous operation of systems hosted by the structure remain in continuous operation.
- LS of **Damage Limitation (DL)** shall be defined as one in which the structures is only slightly damaged and economic to repair, with negligible permanent drifts, undiminished ability to withstand future earthquakes and structural members retaining their full strength with a limited decrease in stiffness; ancillary components, where present, exhibit only minor damage that can be economically repaired (e.g. partitions and infills may show distributed cracking).
- LS of **Significant Damage (SD)** shall be defined as one in which the structure is significantly damaged, possibly with moderate permanent drifts, but retains its vertical-load bearing capacity; ancillary components, where present, are damaged (e.g., partitions and infills have not yet failed out-of-plane). The structure is expected to be repairable, but, in some cases, it may be uneconomic to repair.
- LS of **Near Collapse (NC)** shall be defined as one in which the structure is heavily damaged, with large permanent drifts, but retains its vertical load bearing capacity; most ancillary components, where present, have collapsed.

SD and NC limits states should be considered as Ultimate Limit States. DL and OP limit states should be considered as Serviceability Limit States.

For each earthquake IDA analyzes have been were carried out for three increasing values of spectral acceleration corresponding to 0.5, 1 and 1.5. These could be the values corresponding to the limit states of Damage limitation (DL), Significant Damage (SD) and Near Collapse (NC) that will be provided in the new EC8. Currently this values of the multiplier of accelerograms are assumed equal to 0.69, 1 and 1.73 for DL, SD and NC, respectively.

7.2 Incremental Dynamic Analyses Results

Dynamic Analyzes were performed for all structures in X direction and only two structures in the Y direction (nr. 4 and 20).

The aim is to compare the seismic performances of traditional structures and FREEDAM structures. In particular, in this chapter only the case strudies (numbers 2-10-18-26) are analysed. The results for others analysed structures are reported in Appendix C.

The results of non-linear dynamic analyses have been reported with reference to the peak interstorey drift.

After carrying out the analyzes for each structure, the maximun and minimum intersorey displacements due to each earthquake were extracted, after which the average of these displacements was considered. The graphs obtained show the average maximum, average minimum and average absolute interstorey drift ratio.

Finally, it important to observe that, for FREEDAM structures at 0.04 rad, the dissipative devices have only achieved the device stroke and are even able to resort to other ductility resources such as the yielding of bolt in shear.

- **Structure code: 4 St_DC3_MRFs_X_TRADITIONAL**

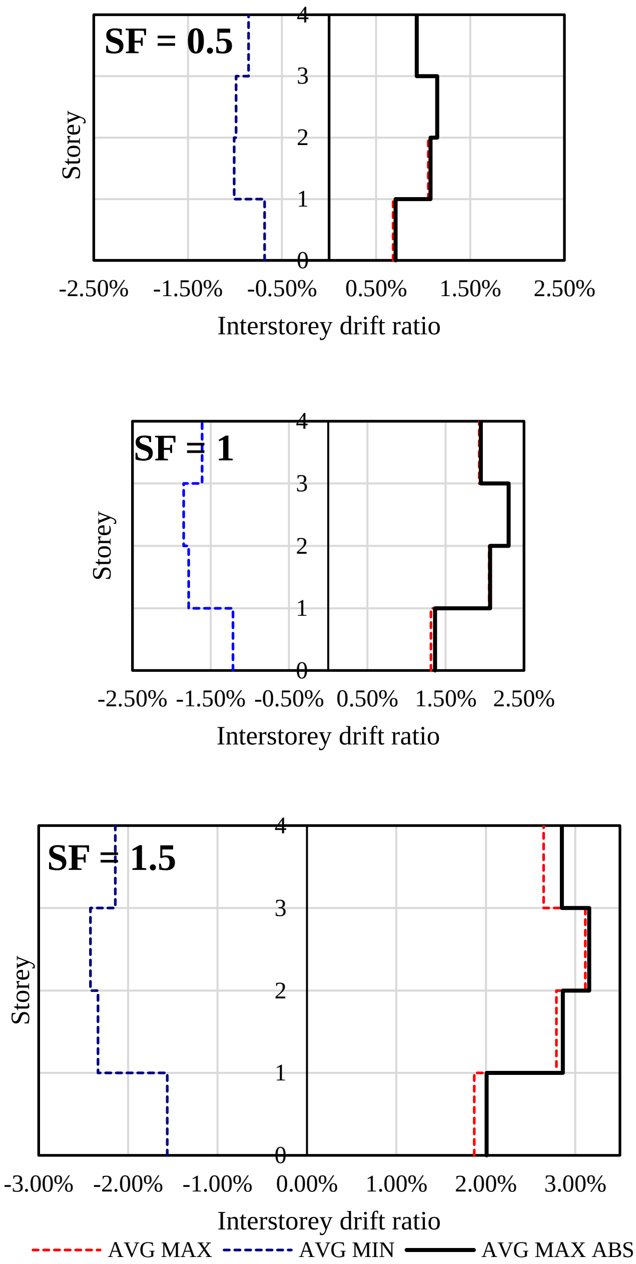

Figure 7.6 – Interstorey drift ratio for 4 St_DC3_MRFs_X_TRADITIONAL

- **Structure code: 4 St_DC3_D-CBFs_X_TRADITIONAL**

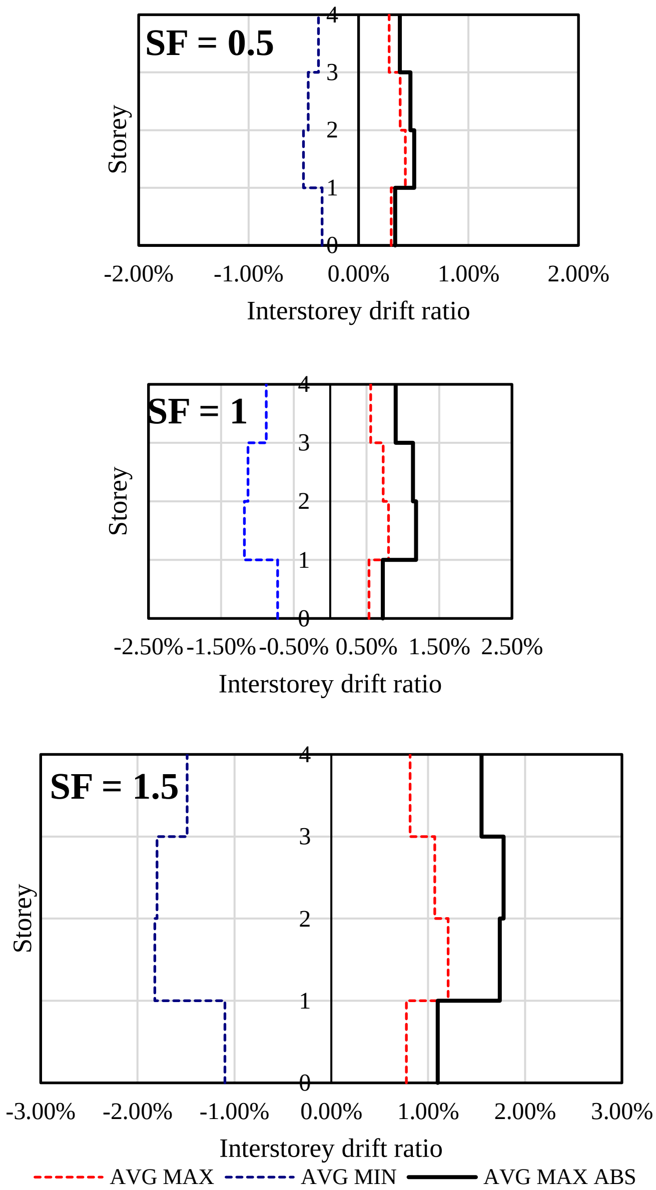

Figure 7.7 – Interstorey drift ratio for 4 St_DC3_D-CBFs_X_TRADITIONAL

❖ Structure code: 4 St_DC3_MRFs_X_FREEDAM

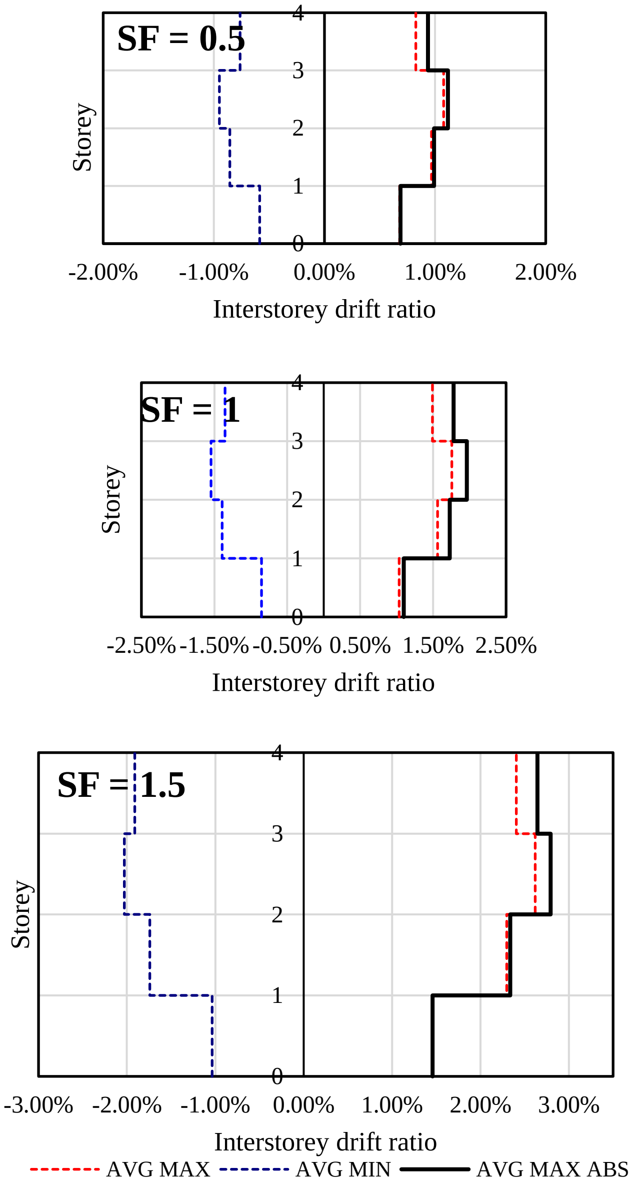

Figure 7.8 – Interstorey drift ratio for 4 St_DC3_MRFs_X_FREEDAM

- **Structure code: 4 St_DC3_D-CBFs_X_FREEDAM**

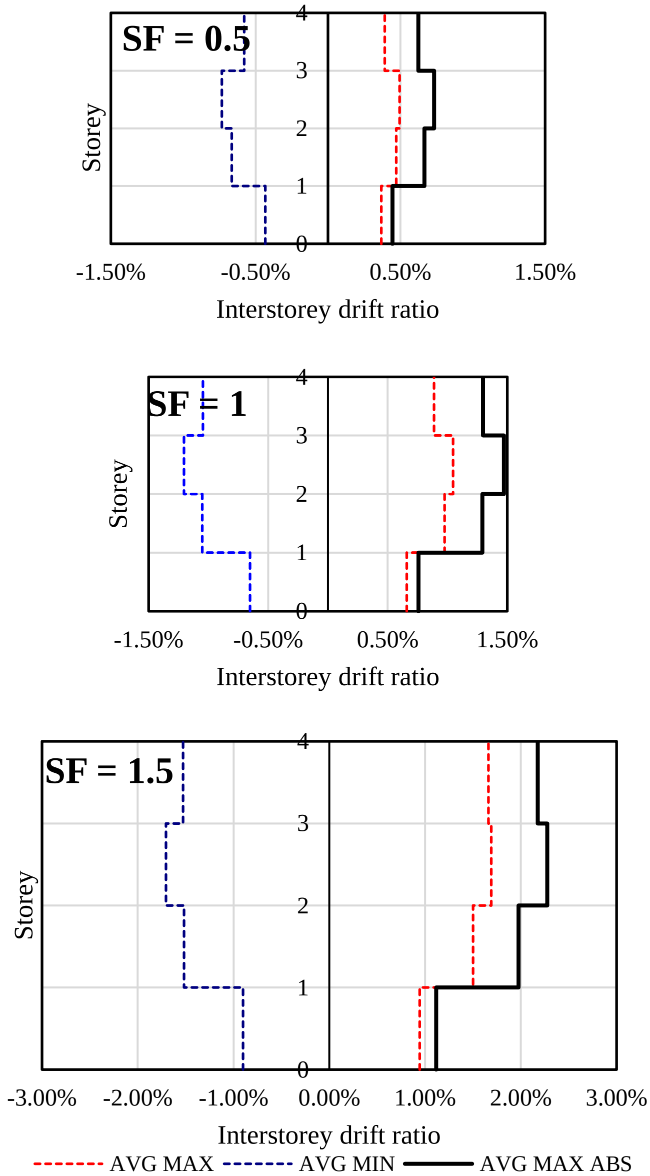

Figure 7.9 – Interstorey drift ratio for 4 St_DC3_D-CBFs_X_FREEDAM

CONCLUSIONS

This thesis work was carried out within the European research project FREEDAM Plus, in particular it concerns the Task 3 of WP3. The selected structural typologies are Moment Resisting Frames (MRFs) and Dual Concentrically Braced Frames (D-CBFs) with chevron braces. Concentrically Braced Frames exhibit both adequate lateral stiffness, due to the high contribution coming from the diagonal braces, and ductile behaviour. Moreover, low-rise (4 storey) and medium-rise structures (8-storey) are designed. In particular, the structures were designed by adopting the Theory of Plastic Mechanism Control, an advanced seismic design strategy, which allows a development of the collapse mechanism of global type. Design guidelines have been developed regarding the TPMC that has been specialized to be used for the two ductility classes that allow energy dissipation, namely DC2 and DC3 as reported in the new Eurocode 8 draft.

At first, 16 structures with traditional haunched connections prequalified in the framework of EQUALJOINTS RFCS Project (RFSR-CT-2013-00021) are designed through TPMC. Consequently, the same structures are designed considering FREEDAM connections, for a total number of 32 examined structures. In particular, FREEDAM devices are located at the beam-to-column connections for MRFs and dual systems, while an additional device located at the brace intersection is also introduced in the case of dual frames. It is important observing that, while for traditional dual systems, diagonal braces are involved in the dissipative behaviour both in tension and compression, in case of FREEDAM structures, diagonals are designed to remain in elastic range. Beams and diagonals are also checked against local hierarchy criterion.

The design of the structures with traditional connections helped clarifying the role of FREEDAM connections on the design and performance of seismic resistant structures. The accuracy of the proposed guidelines has been carried out, for all the structures, by means of push-over analyses to check the development of a collapse mechanism of global type, that is the design goal. In addition, non-linear dynamic analyses on a sample of 18 considered structures have been carried out by means of Sap2000. The scope of this analyses is the comparison between the seismic performance of the structures with traditional haunched connections and the same structures equipped with FREEDAM connections at beam-to-column joint. The design results have been reported and compared in terms of sections, structural weight, dynamic characteristics and seismic performance.

The comparison can be made on different points. First of all, from the following histograms, it should be noted that MRFs equipped with FREEDAM connections are lighter, in terms of **weight**, than those equipped with traditional joints for both ductility classes in low-rise structure; only in DC3 medium-rise structures have the same weight. As regards the Dual structures, for the ductility class DC2 the weight is almost the same; while for the DC3 ductility class the FREEDAM structures are also here lighter than the traditional ones This latter observation is of paramount importance and belongs to the characteristics of the FREEDAM connections which configures themselves as partial strength connections whose resistance threshold can be opportunely calibrated against the internal actions arising from the design load combination. Therefore, the application of the hierarchy criterion can be fulfilled with lighter column sections being always respected the drift limitation at serviceability limit state.

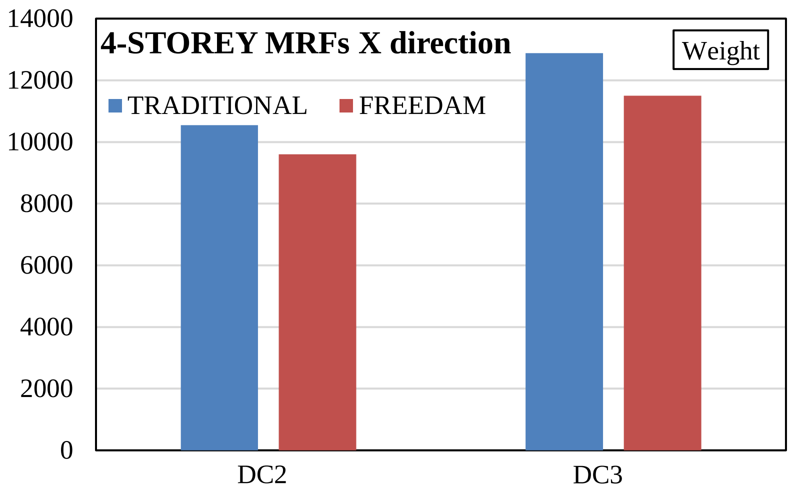
4-STOREY MRFs X direction
Weight
TRADITIONAL
FREEDAM
14000
12000
10000
8000
6000
4000
2000
0
DC2
DC3

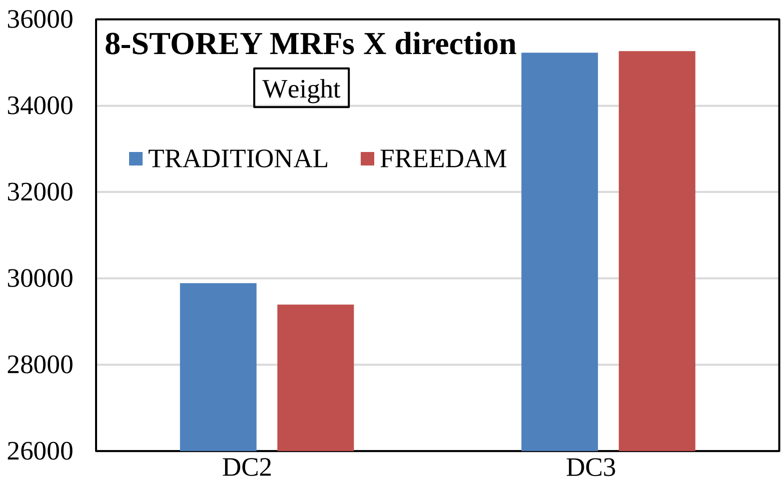
8-STOREY MRFs X direction
Weight
TRADITIONAL
FREEDAM
36000
34000
32000
30000
28000
26000
DC2
DC3

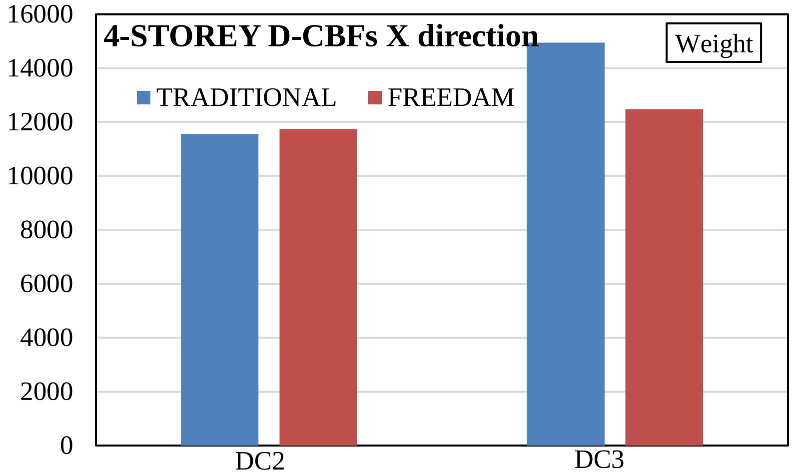

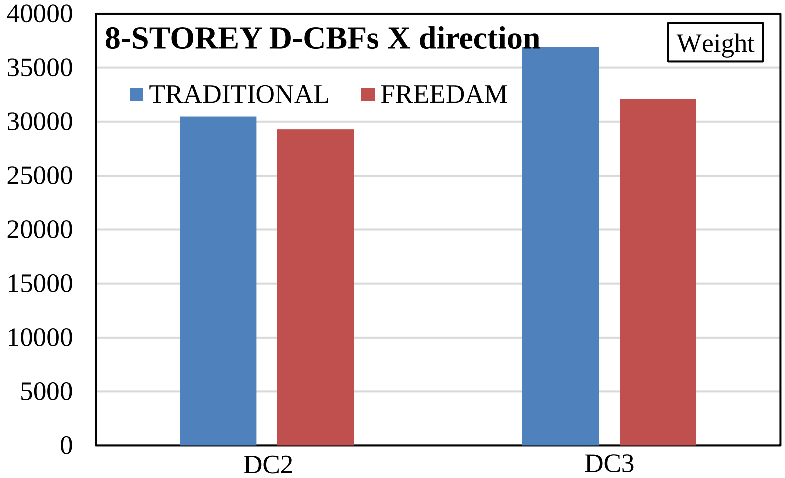

It can be concluded that FREEDAM structures are cheaper than traditional ones.

About **global ductility** it can be noted that the MRFs_FREEDAM have a higher ductility which is more evident in the DC3 ductility class. In DC2 instead it remains constant on the average value of 2.5 (for low-rise structures). D-CBFs_FREEDAM have higher ductility than traditional ones in low-rise structures, while in medium-rise the ductility is lower, this does not mean that the joint has a lower dissipative capacity but that being the hinges FREEDAM plastics calibrated directly in the basis of the seismic action of project, tend to form simultaneously. A single example graph is shown below referring to the 4-storey MRFs in X direction.

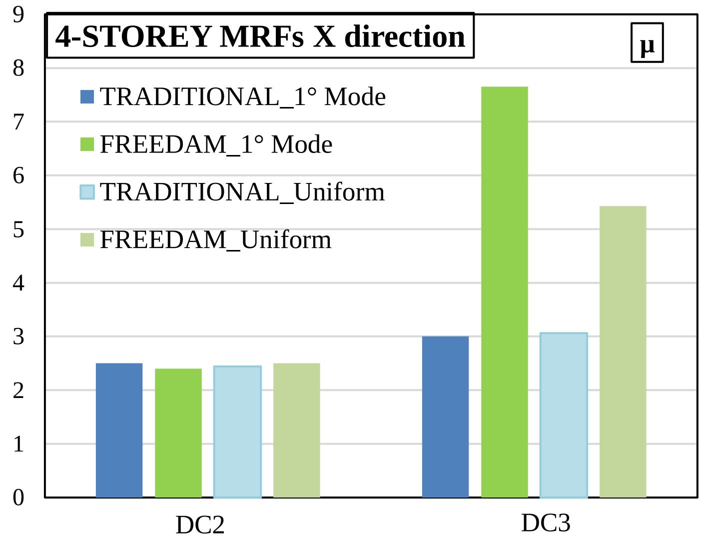

About the **System overstrength,** it can be observed that in traditional structures is greater than the FREEDAM ones. However, it is higher than that suggested by the Eurocode (see Table 4.20). A single graph is shown below referring to the 4-storey D-CBFs in X direction.

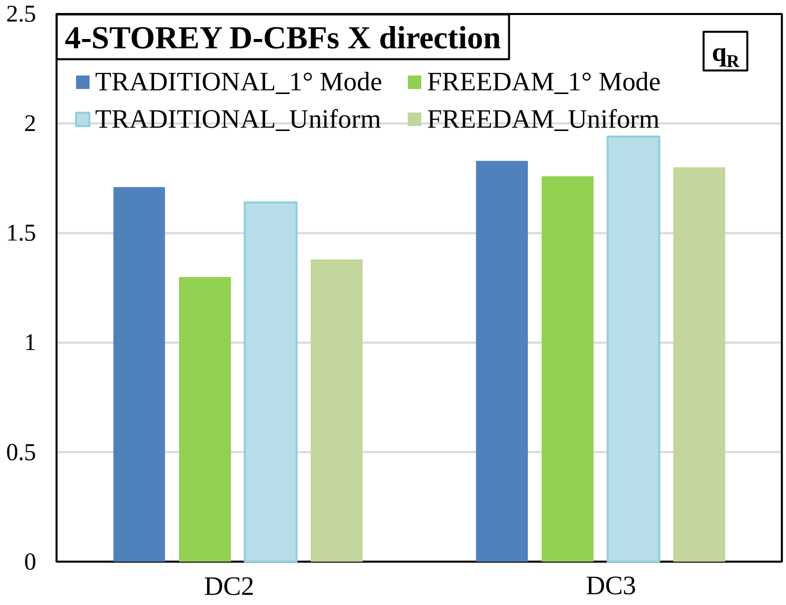

From **dynamic analyses** it can be observed that the soft-storey mechanism do not develop, but the collapse mechanism is almost global both in DC2 and DC3. In the analyzes conducted on DC2_MRFs_FREEDAM it is noted that, for some earthquake, with a PGA scale factor of 1 and 1.5, plastic hinges are also activated on the beams at a distance L from the face of the column. This is due to the fact that in DC2 the local hierarchy criterion was not respected with an adequate level reliabilty in the joint design. In DC3_MRFs_FREEDAM this phenomenon rarely occurs, and it happens only for spectral acceleration scale factor of 1.5, neamely for Near Collapse limit state In D-CBFs_FREEDAM, on beams, only FREEDAM hinges are activated; in fact the beams have already been designed, together with the columns, to withstand 25% of the seismic action at least, so the collapse of the beam never occurs.

From a comparison between the seismic performance of the structures with traditional connections and the same structures equipped with FREEDAM connections given in terms of **Maximum Interstorey Drift**, it is possible to observe that the structure equipped with FREEDAM connections at beam-to-column joint show, on average, better performances if compared with full strength joint ones. It is due to the high dissipative capacity of FREEDAM connections which do not present relevant degradation under cyclic loading. In addition, it is important obsereving that the performances of the structures equipped with FREEDAM connections can be higher if the involvement of bolt in shear is considered after the achievement of the ultimate stoke of dampers. However, the maximum stroke is never achieved even at Near Collapse limit state. The average maximum absolute peak interstorey drift of FREEDAM structures is lower than the structures with traditional full strength joints for MRFs.In particular this happens for increasing values of PGA correspondging to the multipliers 1 and 1.5. Conversley, for the D-CBFs structures the opposite occurs, this is probably due to the insertion of the friction device at the top of chevron braces which guarantees a maximum displacement that can be reached of 14 cm. Below the comparison beteween MRFs and D-CBFs in terms of peak interstorey drift for each limit state is reported.

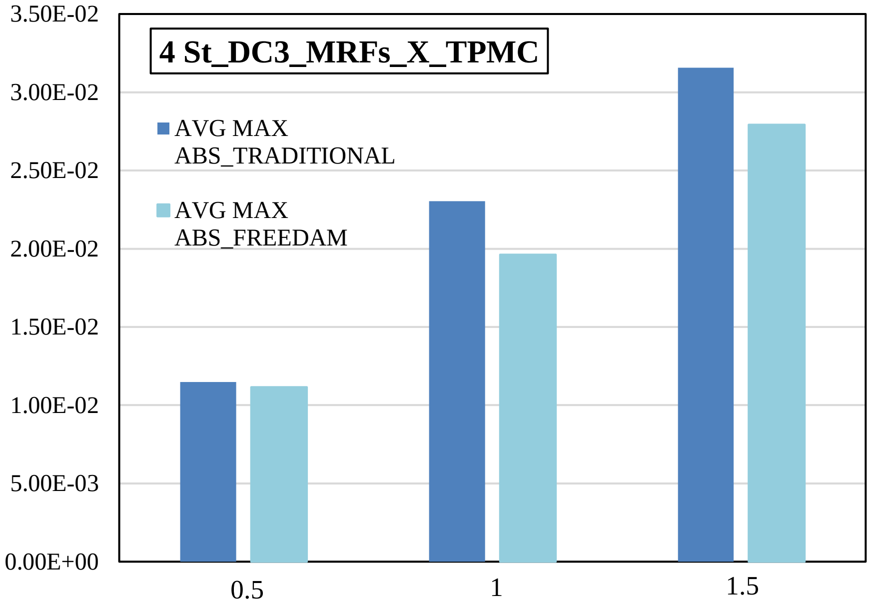
3.50E-02
3.00E-02
2.50E-02
2.00E-02
1.50E-02
1.00E-02
5.00E-03
0.00E+00
4 St_DC3_MRFs_X_TPMC
AVG MAX ABS_TRADITIONAL
AVG MAX ABS_FREEDAM
0.5
1
1.5

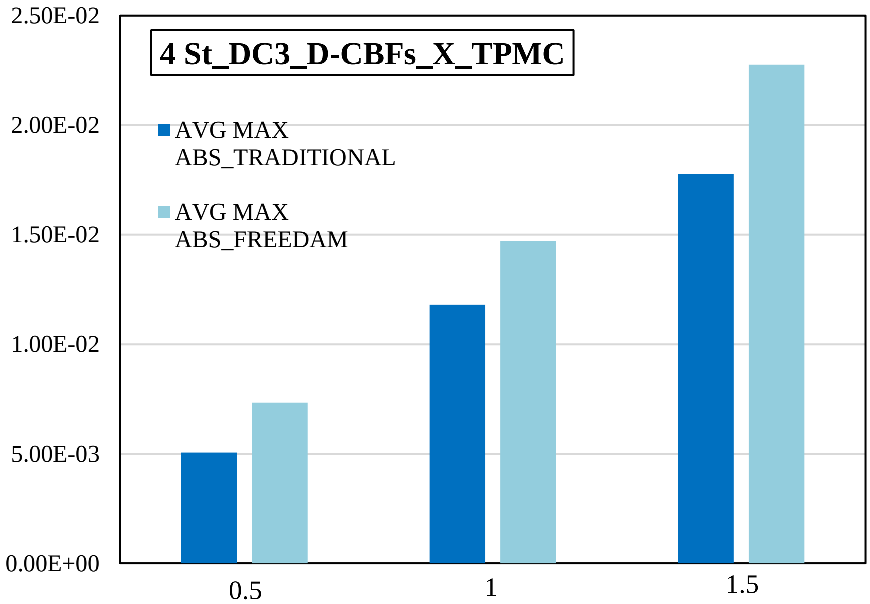
2.50E-02
2.00E-02
1.50E-02
1.00E-02
5.00E-03
0.00E+00
4 St_DC3_D-CBFs_X_TPMC
AVG MAX ABS_TRADITIONAL
AVG MAX ABS_FREEDAM
0.5
1
1.5

Finally, it is possible to observe that structures equipped with FREEDAM connections have better seismic performance than structures equipped with traditional connections, they own additional resources of ductility given by bolt in shear. In addition, they assure that non-dissipative zones, such as beams and columns, are prevented from damage. Furthermore, the TPMC has proved to be an excellent design tool for both traditional and FREEDAM structures and in both ductility classes assuring that columns sections are not involved in plastic range.

REFERENCES

[1] F. Mazzolani and V. Piluso, "Theory and Design of Seismic Resistant Steel Frames", London: E & FN Spoon, an Imprint of Chapman & Hall, 1996.

[2] CEN, Eurocode 8: "Design of structures for earthquake resistance - Part 1: General rules, seismic actions and rules for buildings", 2005a.

[3] F. Mazzolani, "Moment Resistant Connections of Steel Frames in Seismic Areas, Design and Reliability", E&FN Spoon, 2000.

[4] G. De Matteis, F. Mazzolani, R. Landolfo and J. Milev, "Q-factor evaluation of moment resisting steel frames with semi-rigid connections by applying different approaches," *Acta Polytechnica, Journal of Czech Technical University,* vol. 39, no. 5, pp. 183-194, 1999.

[5] C. Faella, V. Piluso and G. Rizzano, "Structural Steel Semi-Rigid Connections", Boca Raton: CRC Press, 2000.

[6] V. Piluso and G. Rizzano, "Random Material Variability effects on Full-strength end-plate Beam-to-Column Joints," *Journal of Constructional Steel Research,* vol. 63, no. 5, pp. 658-666, 2007.

[7] A. Y. Elghazouli, "Seismic Design of Steel Frames with Bolted Beam-to-Column Connections", Elnashai, S. and Dowling, P. J., 2000.

[8] I. Aiken, P. Clark and J. Kelly, "Design and Ultimate-Level Earthquake Tests of a 1/2.5 Scale Base-Isolated Reinforced-Concrete Building," in *Proceedings of ATC-17-1 Seminar on seismic Isolation, Passive Energy Dissipation and Active Control*, San Francisco. California, 1993.

[9] J. Kelly, "Aseismic Base Isolation: A review. Proceedings, 2nd U.S.," in *National Conference on Earthquake Engineering, 823-837*, Stanford, CA, 1979.

[10] A. Longo, R. Montuori and V. Piluso, "Plastic design of seismic resistant V-Braced frames," *Journal of Earthquake Engineering,* vol. 12, pp. 1246-66, 2008.

[11] CEN, Eurocode 8, draft. "Design of structures for earthquake resistance - Part 1-1: General rules and seismic action", 2020a.

[12] "EQUALJOINTS RFCS Project (RFSR-CT-2013-00021), final report," 2015.

[13] V. Piluso, R. Montuori, E. Nastri and A. Paciello, "Seismic response of MRF-CBF dual systems equipped with low damage friction connections," *Journal of Constructional Steel Research,* no. 154, pp. 263-277, 2018.

[14] F. Mazzolani and V. Piluso, "Plastic Design of Seismic Resistant Steel Frames," *Earthquake Engineering and Structural Dynamics,* pp. Vol. 26, pp. 167-191, 1997.

[15] R. Montuori, E. Nastri and V. Piluso, "Advances in theory of plastic mechanism control: Closed form solution for MR-Frames," *Earthquake Engineering and Structural Dynamics,* vol. 44, no. 7, pp. 1035-1054, 2015.

[16] M. Giugliano, A. Longo, R. Montuori and V. Piluso, "Failure Mode and Drift Control of MR-CBF Dual Systems," *The Open Journal of Construction and Building Technology,* vol. 4, pp. 121-133, 2010.

[17] CEN, Eurocode 1: "Actions on structure Part 1-1: General actions-Densities, self-weight, imposed loads for buildings", 2004.

[18] CEN, Eurocode 3: "Design of steel structures - Part 1-1: General rules and rules for buildings", 2005b.

[19] CEN, Eurocode 8 draft:"Design of structures for earthquake resistance - Part 1-2: Rules for new buildings", 2020.

[20] CSI 2007. SAP 2000, "Integrated Finite Element Analysis and Design of Structures. Analysis Reference.," Computer and Structure Inc. University of California, Bekerley..

[21] UNI EN, 1998-3, "Design of structures for earthquake resistance - Assessment and retrofitting of buildings", 2005.

[22] D. Vamvatsikos and C. Cornell, "Incremental dynamic analysis," *Earthquake Engineering and Structural Dynamics*, 2002.

APPENDIX A

DESIGNED STRUCTURES

In this section the designed structures, specifying the design sctions, the modal informations, interstorey-drift and weight of structural elements for study cases described in CHAPTER 4 are reported.

Low Rise Moment Resisting Frames (LR-MRFs)

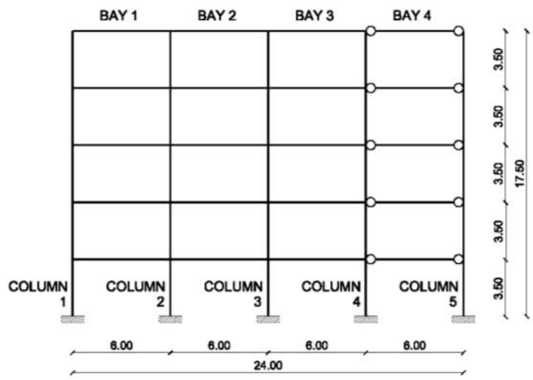

Figure A.1 – Reference image for structures LR-MRFs

❖ Structure code: 4 St_DC2_MRFs_X_TRADITIONAL

Table A.1 – Beam and column sections for 4 St_DC2_MRFs_X_TRADITIONAL

Storey	Bay 1	Bay 2	Bay 3	Bay 4 (pinned)
1-4	IPE 300 haunched	IPE 300 haunched	IPE 300 haunched	IPE 220
Storey	**Column 1-5**	**Column 2**	**Column 3**	**Column 4**
1-2	HE 300 B	HE 300 B	HE 300 B	HE 300 B
3-4	HE 240 B	HE 240 B	HE 240 B	HE 240 B

Weight of structural elements: 10541 kg

Buckling multiplier and amplification coefficient for the fundamental load combination: $\begin{cases} \alpha_{cr} = 4.85 \\ \frac{1}{1-\frac{1}{\alpha_{cr}}} = 1.26 \end{cases}$

Table A.2 – Modal information for 4 St_DC2_MRFs_X_TRADITIONAL

Mode	Vibration period (s)	Sum of effective modal masses on X direction
1	1.93	0.803
2	0.59	0.926
3	0.30	0.972
4	0.18	1.000

Table A.3 – Drift limitation at SD limit state for 4 St_DC2_MRFs_X_TRADITIONAL

Storey	$d_{r,SD}$ (m)	h_s (m)	$d_{r,SD}$ (rad)	$d_{r,SDadm}$ (rad)
1	0.043	3.5	0.01	0.02
2	0.065	3.5	0.02	0.02
3	0.067	3.5	0.02	0.02
4	0.048	3.5	0.01	0.02

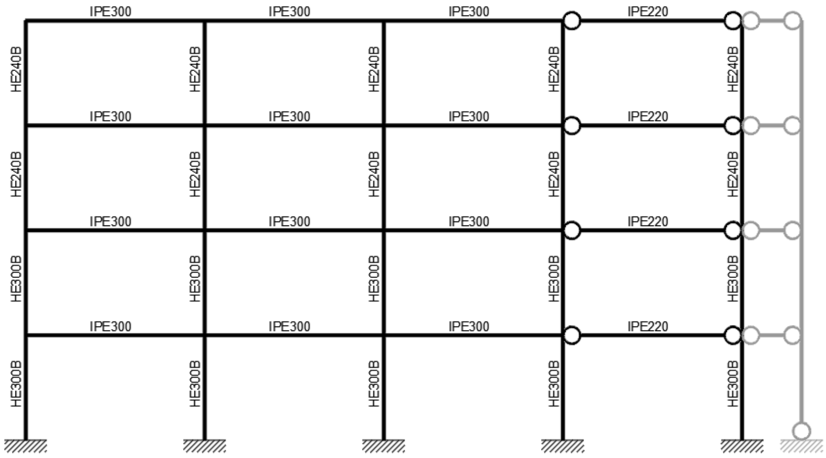

Figure A.2 – Designed structure 4 St_DC2_MRFs_X_TRADITIONAL

❖ Structure code: 4 St_DC3_MRFs_X_TRADITIONAL

Table A.4 – Beam and column sections for 4 St_DC3_MRFs_X_TRADITIONAL

Storey	Bay 1	Bay 2	Bay 3	Bay 4 (pinned)
1-2	IPE 330 haunched	IPE 330 haunched	IPE 330 haunched	IPE 220
3-4	IPE 300 haunched	IPE 300 haunched	IPE 300 haunched	IPE 220
Storey	**Column 1-5**	**Column 2**	**Column 3**	**Column 4**
1-2	HE 340 B	HE 340 B	HE 340 B	HE 340 B
3-4	HE 320 B	HE 320 B	HE 320 B	HE 320 B

Weight of structural elements: 12876 kg

Buckling multiplier and amplification coefficient for the fundamental load combination: $\begin{cases} \alpha_{cr} = 7.02 \\ \frac{1}{1-\frac{1}{\alpha_{cr}}} = 1.17 \end{cases}$

Table A.5 – Modal information for 4 St_DC3_MRFs_X_TRADITIONAL

Mode	Vibration period (s)	Sum of effective modal masses on X direction

1	1.62	0.798
2	0.48	0.934
3	0.23	0.983
4	0.14	1.000

Table A.6 – Drift limitation at SD limit state for 4 St_DC3_MRFs_X_TRADITIONAL

Storey	$d_{r,SD}$ (m)	h_s (m)	$d_{r,SD}$ (rad)	$d_{r,SDadm}$ (rad)
1	0.047	3.5	0.01	0.02
2	0.069	3.5	0.02	0.02
3	0.070	3.5	0.02	0.02
4	0.060	3.5	0.02	0.02

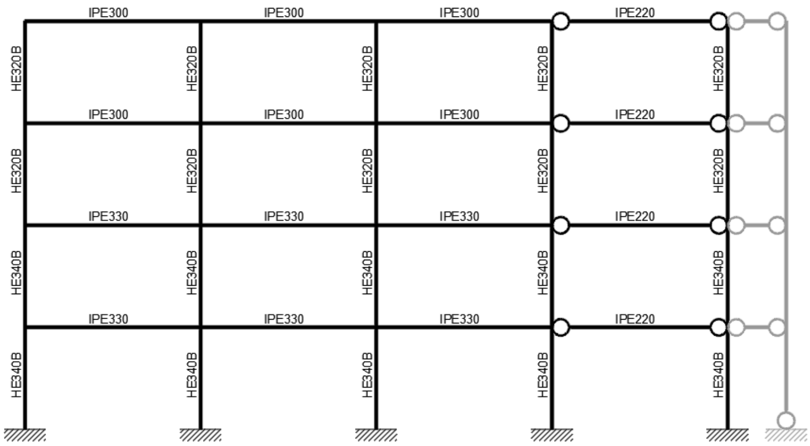

Figure A.3 – Designed structure 4 St_DC3_MRFs_X_TRADITIONAL

❖ Structure code: 4 St_DC2_MRFs_Y_TRADITIONAL

Table A.7 – Beam and column sections for 4 St_DC2_MRFs_Y_TRADITIONAL

Storey	Bay 1	Bay 2	Bay 3	Bay 4 (pinned)
1-4	IPE 300 haunched	IPE 300 haunched	IPE 300 haunched	IPE 270
Storey	**Column 1-5**	**Column 2**	**Column 3**	**Column 4**
1-2	HE 300 B	HE 300 B	HE 300 B	HE 300 B
3-4	HE 240 B	HE 240 B	HE 240 B	HE 240 B

Weight of structural elements: 10771 kg

Buckling multiplier and amplification coefficient for the fundamental load combination: $\begin{cases} \alpha_{cr} = 4.84 \\ \frac{1}{1-\frac{1}{\alpha_{cr}}} = 1.26 \end{cases}$

Table A.8 – Modal information for 4 St_DC2_MRFs_Y_TRADITIONAL

Mode	Vibration period (s)	Sum of effective modal masses on X direction
1	1.92	0.803
2	0.59	0.926
3	0.30	0.972
4	0.25	0.972

Table A.9 – Drift limitation at SD limit state for 4 St_DC2_MRFs_Y_TRADITIONAL

Storey	$d_{r,SD}$ (m)	h_s (m)	$d_{r,SD}$ (rad)	$d_{r,SD\ adm}$ (rad)
1	0.043	3.5	0.01	0.02
2	0.065	3.5	0.02	0.02
3	0.067	3.5	0.02	0.02
4	0.050	3.5	0.01	0.02

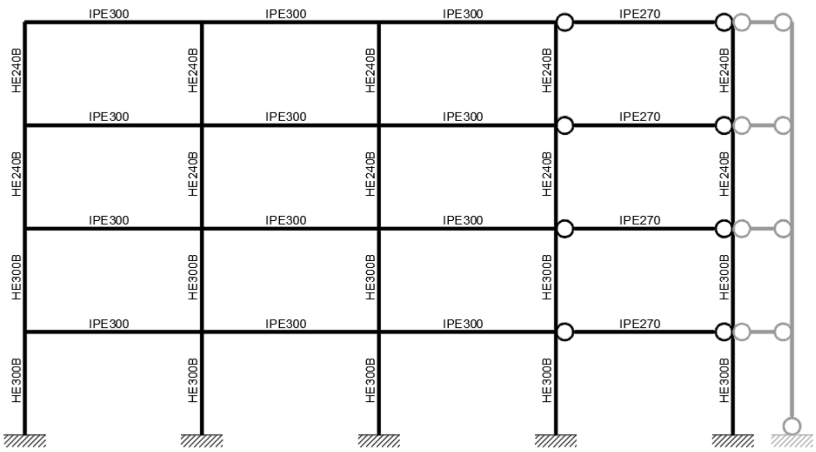

Figure A.4 – Designed structure 4 St_DC2_MRFs_Y_TRADITIONAL

❖ Structure code: 4 St_DC3_MRFs_Y_TRADITIONAL

Table A.10 – Beam and column sections for 4 St_DC3_MRFs_Y_TRADITIONAL

Storey	Bay 1	Bay 2	Bay 3	Bay 4 (pinned)
1-4	IPE 330 haunched	IPE 330 haunched	IPE 330 haunched	IPE 270
Storey	**Column 1-5**	**Column 2**	**Column 3**	**Column 4**
1-2	HE 340 B	HE 340 B	HE 340 B	HE 340 B
3-4	HE 320 B	HE 320 B	HE 320 B	HE 320 B

Weight of structural elements: 13106 kg

Buckling multiplier and amplification coefficient for the fundamental load combination: $\begin{cases} \alpha_{cr} = 7.01 \\ \frac{1}{1-\frac{1}{\alpha_{cr}}} = 1.17 \end{cases}$

Table A.11 – Modal information for 4 St_DC3_MRFs_Y_TRADITIONAL

Mode	Vibration period (s)	Sum of effective modal masses on X direction
1	1.62	0.798
2	0.48	0.934
3	0.23	0.934
4	0.25	0.934

Table A.12 – Drift limitation at SD limit state for 4 St_DC3_MRFs_Y_TRADITIONAL

Storey	$d_{r,SD}$ (m)	h_s (m)	$d_{r,SD}$ (rad)	$d_{r,SDadm}$ (rad)
1	0.047	3.5	0.01	0.02
2	0.069	3.5	0.02	0.02
3	0.070	3.5	0.02	0.02
4	0.060	3.5	0.02	0.02

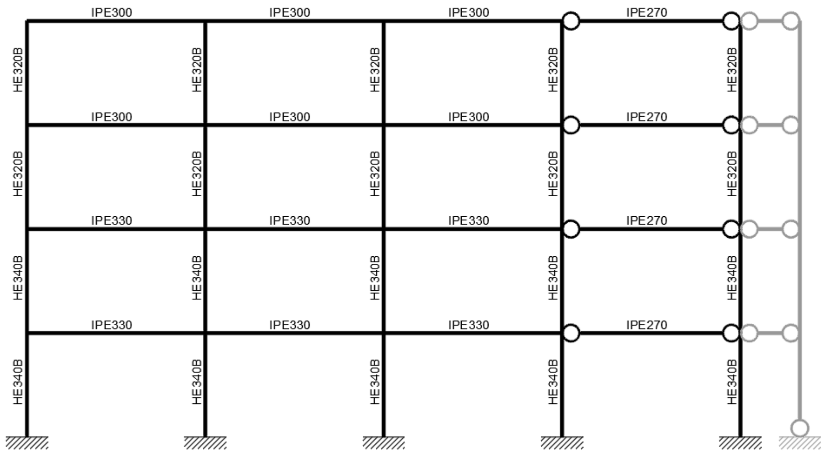

Figure A.5 – Designed structure 4 St_DC3_MRFs_Y_TRADITIONAL

❖ Structure code: 4 St_DC2_MRFs_X_FREEDAM

Table A.13 – Beam and column sections for 4 St_DC2_MRFs_ X_FREEDAM

Storey	Bay 1	Bay 2	Bay 3	Bay 4 (pinned)
1-4	IPE 270 FREEDAM	IPE 270 FREEDAM	IPE 270 FREEDAM	IPE 220
Storey	**Column 1-5**	**Column 2**	**Column 3**	**Column 4**
1-2	HE 280 B	HE 280 B	HE 280 B	HE 280 B
3-4	HE 220 B	HE 220 B	HE 220 B	HE 220 B

Weight of structural elements: 9596 kg

Buckling multiplier and amplification coefficient for the fundamental load combination: $\begin{cases} \alpha_{cr} = 4.14 \\ \frac{1}{1-\frac{1}{\alpha_{cr}}} = 1.32 \end{cases}$

Table A.14 – Modal information for 4 St_DC2_MRFs_X_ FREEDAM

Mode	Vibration period (s)	Sum of effective modal masses on X direction
1	2.08	0.804
2	0.65	0.928

3	0.34	0.971
4	0.21	1.000

Table A.15 – Drift limitation at SD limit state for 4 St_DC2_MRFs_X_ FREEDAM

Storey	$d_{r,SD}$ (m)	h_s (m)	$d_{r,SD}$ (rad)	$d_{r,SDadm}$ (rad)
1	0.047	3.5	0.01	0.02
2	0.070	3.5	0.02	0.02
3	0.073	3.5	0.02	0.02
4	0.054	3.5	0.02	0.02

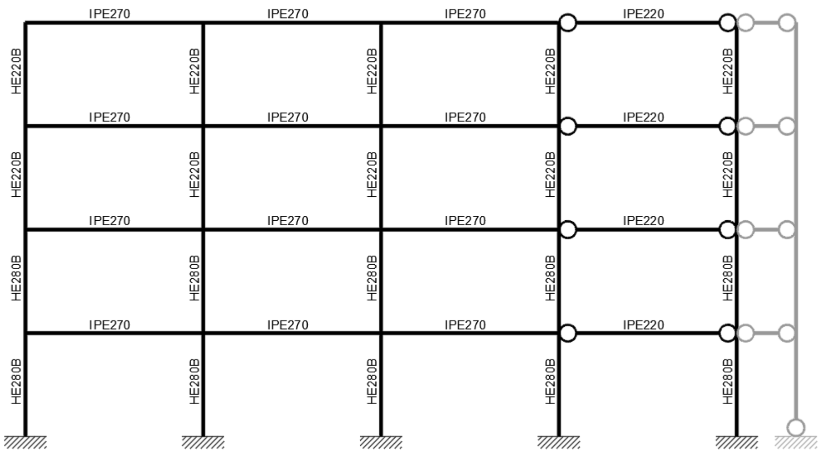

Figure A.6 – Designed structure 4 St_DC2_MRFs_X_ FREEDAM

❖ Structure code: 4 St_DC3_MRFs_X_FREEDAM

Table A.16 – Beam and column sections for 4 St_DC3_MRFs_X_ FREEDAM

Storey	Bay 1	Bay 2	Bay 3	Bay 4 (pinned)
1-2	IPE 330 FREEDAM	IPE 330 FREEDAM	IPE 330 FREEDAM	IPE 220
3-4	IPE 300 FREEDAM	IPE 300 FREEDAM	IPE 300 FREEDAM	IPE 220
Storey	**Column 1-5**	**Column 2**	**Column 3**	**Column 4**
1-2	HE 300 B	HE 300 B	HE 300 B	HE 300 B

3-4	HE 260 B	HE 260 B	HE 260 B	HE 260 B

Weight of structural elements: 11500 kg

Buckling multiplier and amplification coefficient for the fundamental load combination: $\begin{cases} \alpha_{cr} = 6.85 \\ \frac{1}{1-\frac{1}{\alpha_{cr}}} = 1.17 \end{cases}$

Table A.17 – Modal information for 4 St_DC3_MRFs_X_ FREEDAM

Mode	Vibration period (s)	Sum of effective modal masses on X direction
1	1.63	0.810
2	0.52	0.938
3	0.27	0.979
4	0.17	1.000

Table A.18 – Drift limitation at SD limit state for 4 St_DC3_MRFs_X_ FREEDAM

Storey	$d_{r,SD}$ (m)	h_s (m)	$d_{r,SD}$ (rad)	$d_{r,SDadm}$ (rad)
1	0.051	3.5	0.01	0.02
2	0.069	3.5	0.02	0.02
3	0.072	3.5	0.02	0.02
4	0.057	3.5	0.02	0.02

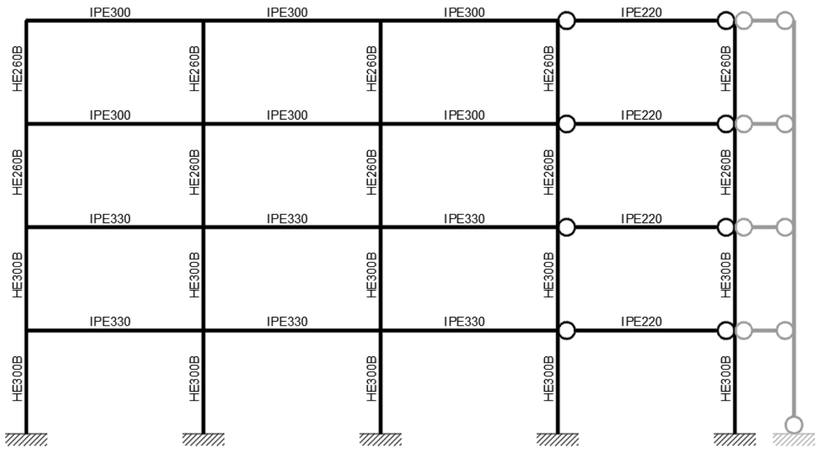

Figure A.7 – Designed structure 4 St_DC3_MRFs_X_ FREEDAM

❖ Structure code: 4 St_DC2_MRFs_Y_FREEDAM

Table A.19 – Beam and column sections for 4 St_DC2_MRFs_Y_ FREEDAM

Storey	Bay 1	Bay 2	Bay 3	Bay 4 (pinned)
1-2	IPE 300 FREEDAM	IPE 300 FREEDAM	IPE 300 FREEDAM	IPE 270
3-4	IPE 270 FREEDAM	IPE 270 FREEDAM	IPE 270 FREEDAM	IPE 270
Storey	**Column 1-5**	**Column 2**	**Column 3**	**Column 4**
1-2	HE 300 B	HE 300 B	HE 300 B	HE 300 B
3-4	HE 240 B	HE 240 B	HE 240 B	HE 240 B

Weight of structural elements: 10942 kg

Buckling multiplier and amplification coefficient for the fundamental load combination: $\begin{cases} \alpha_{cr} = 5.52 \\ \frac{1}{1-\frac{1}{\alpha_{cr}}} = 1.22 \end{cases}$

Table A.20 – Modal information for 4 St_DC2_MRFs_Y_ FREEDAM

Mode	Vibration period (s)	Sum of effective modal masses on X direction
1	1.83	0.792
2	0.59	0.927
3	0.30	0.972
4	0.25	0.972

Table A.21 – Drift limitation at SD limit state for 4 St_DC2_MRFs_Y_ FREEDAM

Storey	$d_{r,SD}$ (m)	h_s (m)	$d_{r,SD}$ (rad)	$d_{r,SDadm}$ (rad)
1	0.040	3.5	0.01	0.02
2	0.058	3.5	0.02	0.02
3	0.065	3.5	0.02	0.02
4	0.053	3.5	0.02	0.02

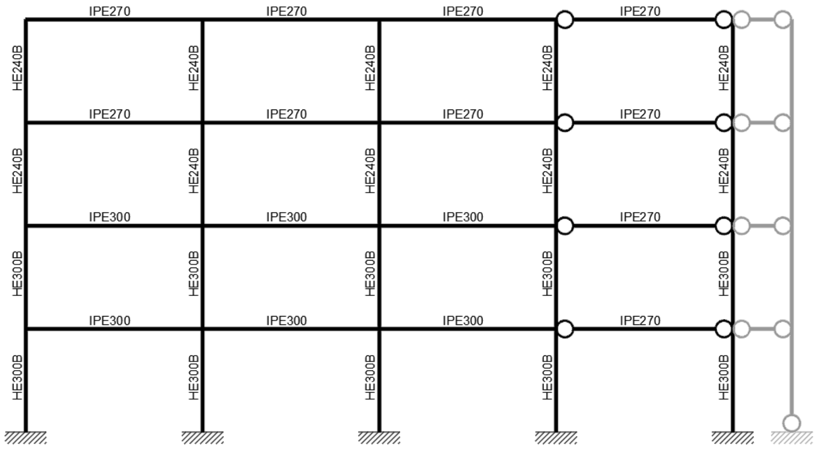

Figure A.8 – Designed structure 4 St_DC2_MRFs_Y_ FREEDAM

❖ Structure code: 4 St_DC3_MRFs_Y_FREEDAM

Table A.22 – Beam and column sections for 4 St_DC3_MRFs_Y_ FREEDAM

Storey	Bay 1	Bay 2	Bay 3	Bay 4 (pinned)
1-2	IPE 330 FREEDAM	IPE 330 FREEDAM	IPE 330 FREEDAM	IPE 270
3-4	IPE 300 FREEDAM	IPE 300 FREEDAM	IPE 300 FREEDAM	IPE 270
Storey	**Column 1-5**	**Column 2**	**Column 3**	**Column 4**
1-2	HE 300 B	HE 300 B	HE 300 B	HE 300 B
3-4	HE 260 B	HE 260 B	HE 260 B	HE 260 B

Weight of structural elements: 11731 kg

Buckling multiplier and amplification coefficient for the fundamental load combination: $\begin{cases} \alpha_{cr} = 6.85 \\ \frac{1}{1-\frac{1}{\alpha_{cr}}} = 1.17 \end{cases}$

Table A.23 – Modal information for 4 St_DC3_MRFs_Y_ FREEDAM

Mode	Vibration period (s)	Sum of effective modal masses on X direction

1	1.63	0.810
2	0.52	0.937
3	0.27	0.979
4	0.25	0.979

Table A.24 – Drift limitation at SD limit state for 4 St_DC3_MRFs_Y_ FREEDAM

Storey	$d_{r,SD}$ **(m)**	h_s **(m)**	$d_{r,SD}$ **(rad)**	$d_{r,SDadm}$ **(rad)**
1	0.051	3.5	0.01	0.02
2	0.069	3.5	0.02	0.02
3	0.072	3.5	0.02	0.02
4	0.057	3.5	0.02	0.02

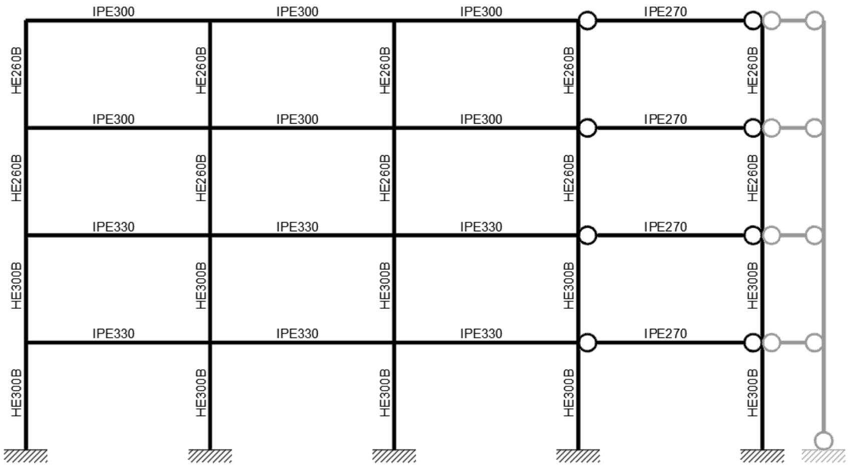

Figure A.9 – Designed structure 4 St_DC3_MRFs_Y_ FREEDAM

Medium Rise Moment Resisting Frames (MR-MRFs)

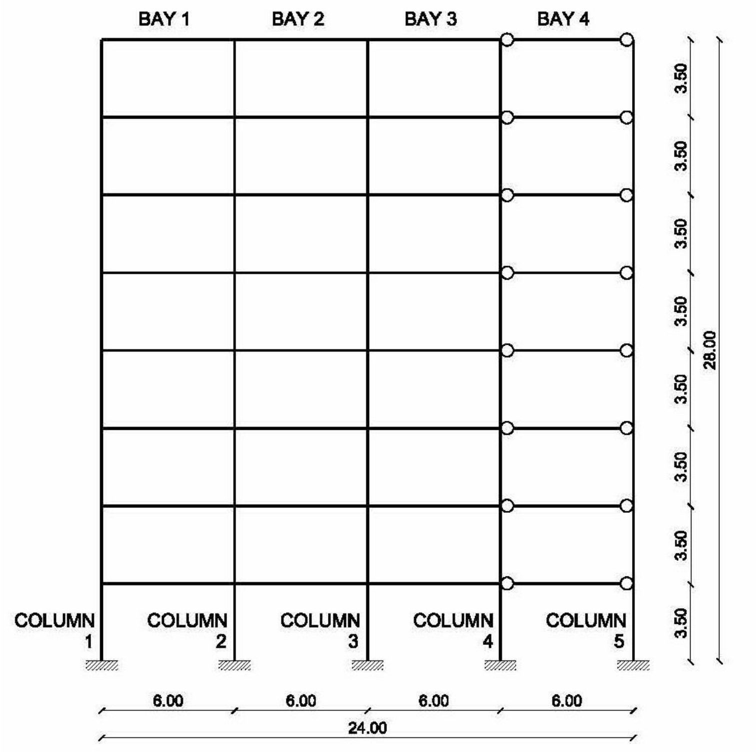

Figure A.10 – Reference image for structures MR-MRFs

❖ Structure code: 8 St_DC2_MRFs_X_TRADITIONAL

Table A.25 – Beam and column sections for 8 St_DC2_MRFs_X_TRADITIONAL

Storey	**Bay 1**	**Bay 2**	**Bay 3**	**Bay 4 (pinned)**
1-4	IPE 300 haunched	IPE 300 haunched	IPE 300 haunched	IPE 220
5-8	IPE 270 haunched	IPE 270 haunched	IPE 270 haunched	IPE 220
Storey	**Column 1-5**	**Column 2**	**Column 3**	**Column 4**
1-2	HE 550 B	HE 550 B	HE 550 B	HE 550 B
3-4	HE 500 B	HE 500 B	HE 500 B	HE 500 B

5-6	HE 400 B	HE 400 B	HE 400 B	HE 400 B
7-8	HE 320 B	HE 320 B	HE 320 B	HE 320 B

Weight of structural elements: 29893 kg

Buckling multiplier and amplification coefficient for the fundamental load combination: $\begin{cases} \alpha_{cr} = 3.02 \\ \frac{1}{1-\frac{1}{\alpha_{cr}}} = 1.50 \end{cases}$

Table A.26 – Modal information for 8 St_DC2_MRFs_X_TRADITIONAL

Mode	Vibration period (s)	Sum of effective modal masses on X direction
1	3.37	0.725
2	1.06	0.859
3	0.52	0.916
4	0.31	0.950
5	0.20	0.970
6	0.14	0.983
7	0.11	0.993
8	0.09	0.999

Table A.27 – Drift limitation at SD limit state for 8 St_DC2_MRFs_X_TRADITIONAL

Storey	$d_{r,SD}$ (m)	h_s (m)	$d_{r,SD}$ (rad)	$d_{r,SDadm}$ (rad)
1	0.022	3.5	0.01	0.02
2	0.043	3.5	0.01	0.02
3	0.053	3.5	0.02	0.02
4	0.057	3.5	0.02	0.02
5	0.061	3.5	0.02	0.02
6	0.063	3.5	0.02	0.02
7	0.059	3.5	0.02	0.02
8	0.050	3.5	0.01	0.02

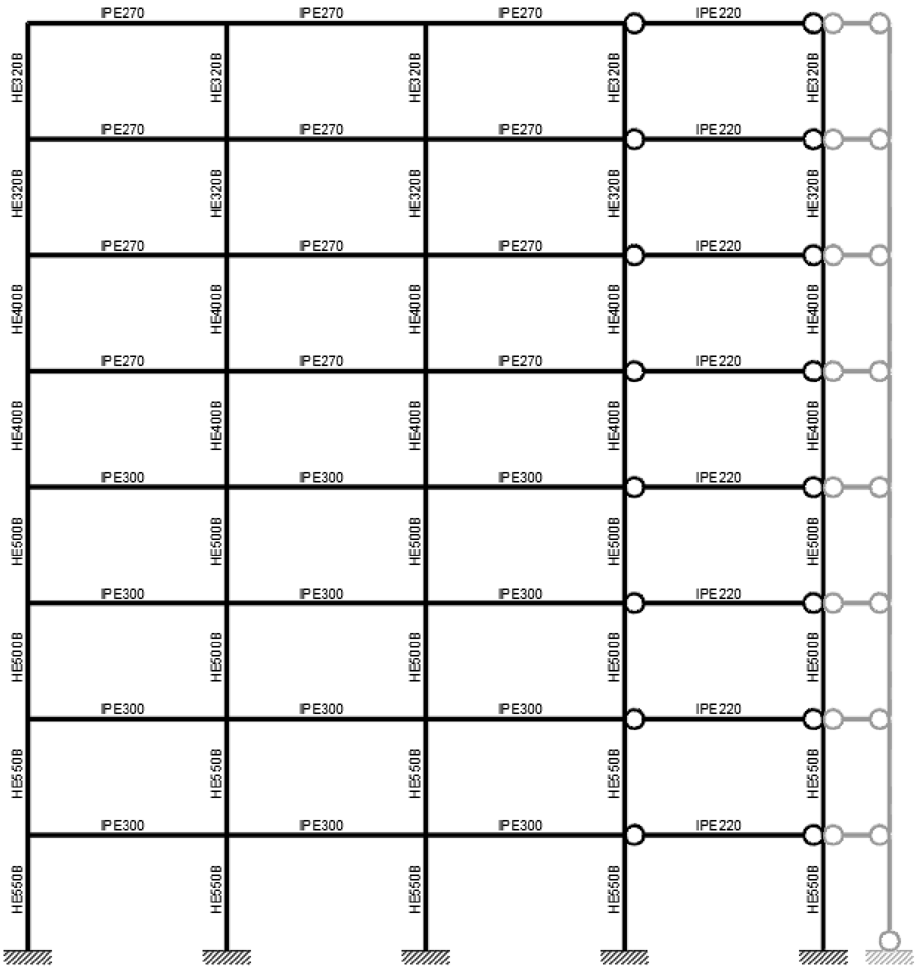

Figure A.11 – Designed structure 8 St_DC2_MRFs_X_TRADITIONAL

❖ Structure code: 8 St_DC3_MRFs_X_TRADITIONAL

Table A.28 – Beam and column sections for 8 St_DC3_MRFs_X_TRADITIONAL

Storey	**Bay 1**	**Bay 2**	**Bay 3**	**Bay 4 (pinned)**
1-4	IPE 330 haunched	IPE 330 haunched	IPE 330 haunched	IPE 220

5-8	IPE 300 haunched	IPE 300 haunched	IPE 300 haunched	IPE 220
Storey	**Column 1-5**	**Column 2**	**Column 3**	**Column 4**
1-2	HE 700 B	HE 700 B	HE 700 B	HE 700 B
3-4	HE 600 B	HE 600 B	HE 600 B	HE 600 B
5-6	HE 500 B	HE 500 B	HE 500 B	HE 500 B
7-8	HE 400 B	HE 400 B	HE 400 B	HE 400 B

Weight of structural elements: 35228 kg

Buckling multiplier and amplification coefficient for the fundamental load combination: $\begin{cases} \alpha_{cr} = 4.76 \\ \frac{1}{1-\frac{1}{\alpha_{cr}}} = 1.27 \end{cases}$

Table A.29 – Modal information for 8 St_DC3_MRFs_X_TRADITIONAL

Mode	Vibration period (s)	Sum of effective modal masses on X direction
1	2.68	0.718
2	0.83	0.857
3	0.41	0.915
4	0.24	0.949
5	0.15	0.969
6	0.11	0.983
7	0.08	0.983
8	0.08	0.999

Table A.30 – Drift limitation at SD limit state for 8 St_DC3_MRFs_X_TRADITIONAL

Storey	$d_{r,SD}$ (m)	h_s (m)	$d_{r,SD}$ (rad)	$d_{r,SDadm}$ (rad)
1	0.023	3.5	0.01	0.02
2	0.045	3.5	0.01	0.02
3	0.057	3.5	0.02	0.02
4	0.063	3.5	0.02	0.02
5	0.068	3.5	0.02	0.02
6	0.069	3.5	0.02	0.02
7	0.065	3.5	0.02	0.02
8	0.054	3.5	0.02	0.02

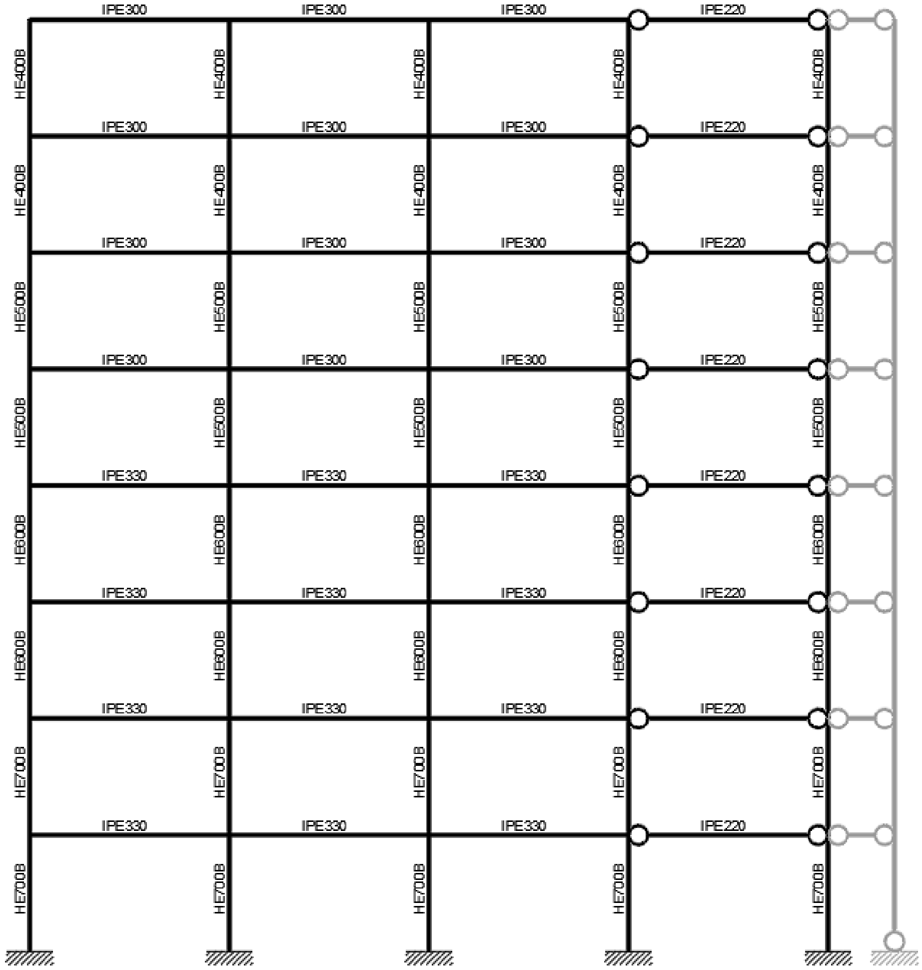

Figure A.12 – Designed structure 8 St_DC3_MRFs_X_TRADITIONAL

❖ Structure code: 8 St_DC2_MRFs_Y_TRADITIONAL

Table A.31 – Beam and column sections for 8 St_DC2_MRFs_Y_TRADITIONAL

Storey	Bay 1	Bay 2	Bay 3	Bay 4 (pinned)
1-4	IPE 300 haunched	IPE 300 haunched	IPE 300 haunched	IPE 270

5-8	IPE 270 haunched	IPE 270 haunched	IPE 270 haunched	IPE 270
Storey	**Column 1-5**	**Column 2**	**Column 3**	**Column 4**
1-2	HE 550 B	HE 550 B	HE 550 B	HE 550 B
3-4	HE 500 B	HE 500 B	HE 500 B	HE 500 B
5-6	HE 400 B	HE 400 B	HE 400 B	HE 400 B
7-8	HE 320 B	HE 320 B	HE 320 B	HE 320 B

Weight of structural elements: 30353 kg

Buckling multiplier and amplification coefficient for the fundamental load combination: $\begin{cases} \alpha_{cr} = 3.01 \\ \frac{1}{1-\frac{1}{\alpha_{cr}}} = 1.50 \end{cases}$

Table A.32 – Modal information for 8 St_DC2_MRFs_Y_TRADITIONAL

Mode	Vibration period (s)	Sum of effective modal masses on X direction
1	3.37	0.725
2	1.06	0.859
3	0.52	0.915
4	0.31	0.950
5	0.25	0.950
6	0.25	0.950
7	0.25	0.950
8	0.25	0.950

Table A.33 – Drift limitation at SD limit state for 8 St_DC2_MRFs_Y_TRADITIONAL

Storey	$d_{r,SD}$ (m)	h_s (m)	$d_{r,SD}$ (rad)	$d_{r,SDadm}$ (rad)
1	0.022	3.5	0.01	0.02
2	0.043	3.5	0.01	0.02
3	0.052	3.5	0.01	0.02
4	0.056	3.5	0.02	0.02
5	0.061	3.5	0.02	0.02
6	0.063	3.5	0.02	0.02
7	0.059	3.5	0.02	0.02
8	0.050	3.5	0.01	0.02

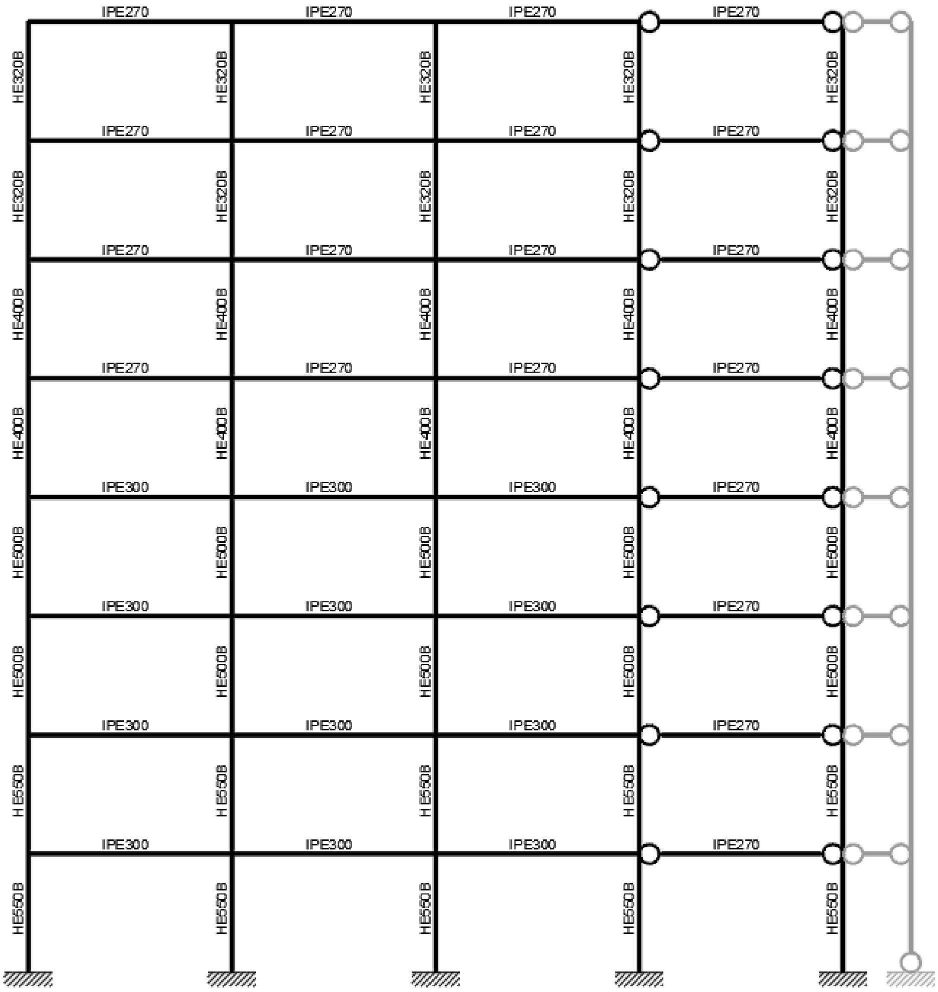

Figure A.13 – Designed structure 8 St_DC2_MRFs_Y_TRADITIONAL

❖ Structure code: 8 St_DC3_MRFs_Y_TRADITIONAL

Table A.34 – Beam and column sections for 8 St_DC3_MRFs_Y_TRADITIONAL

Storey	Bay 1	Bay 2	Bay 3	Bay 4 (pinned)
1-4	IPE 330 haunched	IPE 330 haunched	IPE 330 haunched	IPE 270

5-8	IPE 300 haunched	IPE 300 haunched	IPE 300 haunched	IPE 270
Storey	**Column 1-5**	**Column 2**	**Column 3**	**Column 4**
1-2	HE 700 B	HE 700 B	HE 700 B	HE 700 B
3-4	HE 600 B	HE 600 B	HE 600 B	HE 600 B
5-6	HE 500 B	HE 500 B	HE 500 B	HE 500 B
7-8	HE 400 B	HE 400 B	HE 400 B	HE 400 B

Weight of structural elements: 35686 kg

Buckling multiplier and amplification coefficient for the fundamental load combination: $\begin{cases} \alpha_{cr} = 4.74 \\ \frac{1}{1-\frac{1}{\alpha_{cr}}} = 1.27 \end{cases}$

Table A.35 – Modal information for 8 St_DC3_MRFs_Y_TRADITIONAL

Mode	Vibration period (s)	Sum of effective modal masses on X direction
1	2.68	0.718
2	0.83	0.857
3	0.41	0.914
4	0.25	0.914
5	0.25	0.914
6	0.25	0.914
7	0.25	0.914
8	0.25	0.914

Table A.36 – Drift limitation at SD limit state for 8 St_DC3_MRFs_Y_TRADITIONAL

Storey	d_{rSD} (m)	h_s (m)	d_{rSD} (rad)	$d_{r,SDadm}$ (rad)
1	0.023	3.5	0.01	0.02
2	0.045	3.5	0.01	0.02
3	0.057	3.5	0.02	0.02
4	0.063	3.5	0.02	0.02
5	0.068	3.5	0.02	0.02
6	0.069	3.5	0.02	0.02
7	0.065	3.5	0.02	0.02
8	0.054	3.5	0.02	0.02

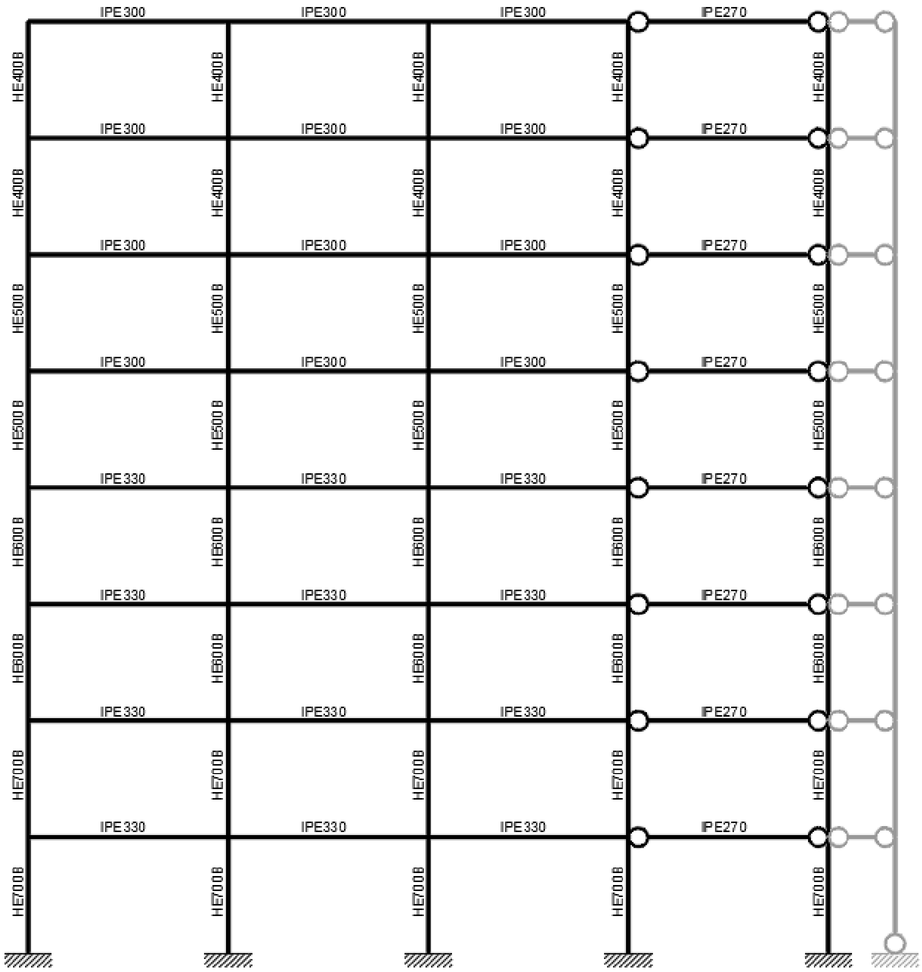

Figure A.14 – Designed structure 8 St_DC3_MRFs_Y_TRADITIONAL

❖ Structure code: 8 St_DC2_MRFs_X_FREEDAM

Table A.37 – Beam and column sections for 8 St_DC2_MRFs_X_FREEDAM

Storey	Bay 1	Bay 2	Bay 3	Bay 4 (pinned)
1-4	IPE 300 haunched	IPE 300 haunched	IPE 300 haunched	IPE 220

5-8	IPE 270 haunched	IPE 270 haunched	IPE 270 haunched	IPE 220
Storey	**Column 1-5**	**Column 2**	**Column 3**	**Column 4**
1-2	HE 550 B	HE 550 B	HE 550 B	HE 550 B
3-4	HE 450 B	HE 450 B	HE 450 B	HE 450 B
5-6	HE 360 B	HE 360 B	HE 360 B	HE 360 B
7-8	HE 300 B	HE 300 B	HE 300 B	HE 300 B

Weight of structural elements: 29392 kg

Buckling multiplier and amplification coefficient for the fundamental load combination: $\begin{cases} \alpha_{cr} = 3.58 \\ \frac{1}{1-\frac{1}{\alpha_{cr}}} = 1.39 \end{cases}$

Table A.38 – Modal information for 8 St_DC2_MRFs_X_FREEDAM

Mode	Vibration period (s)	Sum of effective modal masses on X direction
1	3.07	0.730
2	1.01	0.862
3	0.52	0.915
4	0.32	0.947
5	0.21	0.966
6	0.15	0.979
7	0.12	0.990
8	0.09	0.990

Table A.39 – Drift limitation at SD limit state for 8 St_DC2_MRFs_X_FREEDAM

Storey	$d_{r,SD}$ (m)	h_s (m)	$d_{r,SD}$ (rad)	$d_{r,SDadm}$ (rad)
1	0.022	3.5	0.01	0.02
2	0.042	3.5	0.01	0.02
3	0.052	3.5	0.01	0.02
4	0.056	3.5	0.02	0.02
5	0.061	3.5	0.02	0.02
6	0.061	3.5	0.02	0.02
7	0.056	3.5	0.02	0.02
8	0.043	3.5	0.01	0.02

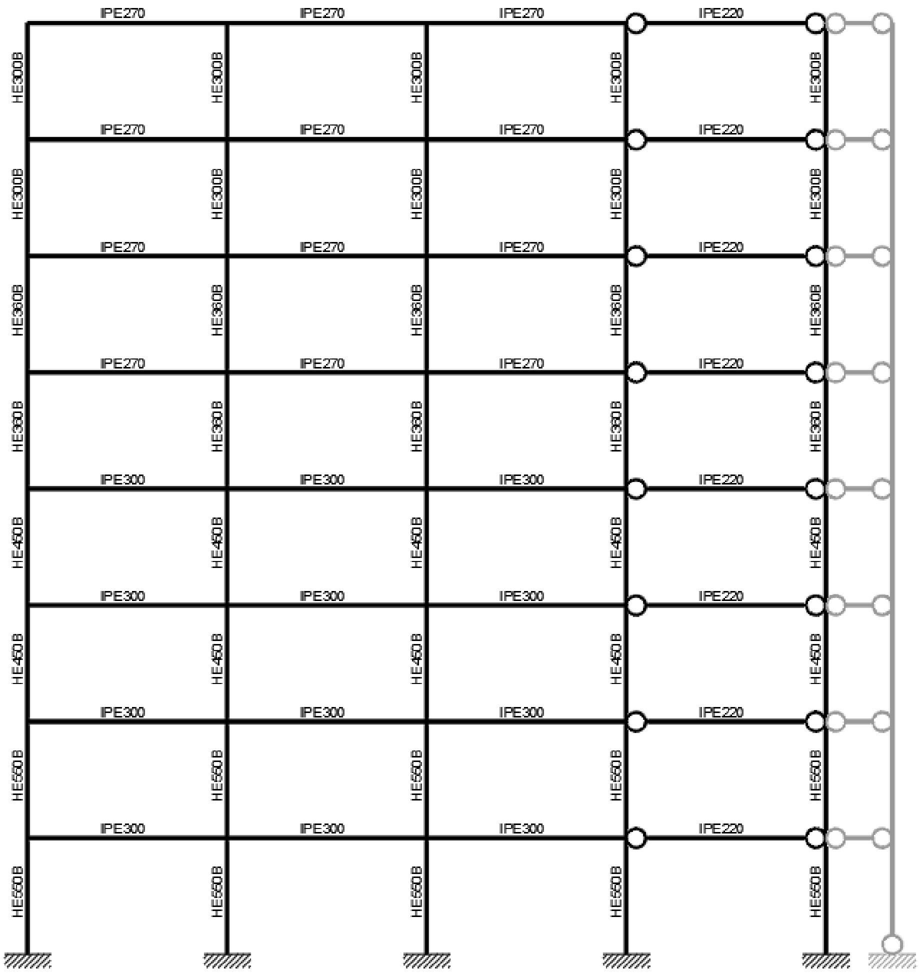

Figure A.15 – Designed structure 8 St_DC2_MRFs_X_FREEDAM

❖ Structure code: 8 St_DC3_MRFs_X_FREEDAM

Table A.40 – Beam and column sections for 8 St_DC3_MRFs_X_ FREEDAM

Storey	Bay 1	Bay 2	Bay 3	Bay 4 (pinned)
1-4	IPE 400 FREEDAM	IPE 400 FREEDAM	IPE 400 FREEDAM	IPE 220

5-6	IPE 360 FREEDAM	IPE 360 FREEDAM	IPE 360 FREEDAM	IPE 220
7-8	IPE 300 FREEDAM	IPE 300 FREEDAM	IPE 300 FREEDAM	IPE 220
Storey	**Column 1-5**	**Column 2**	**Column 3**	**Column 4**
1-2	HE 650 B	HE 650 B	HE 650 B	HE 650 B
3-4	HE 550 B	HE 550 B	HE 550 B	HE 550 B
5-6	HE 450 B	HE 450 B	HE 450 B	HE 450 B
7-8	HE 320 B	HE 320 B	HE 320 B	HE 320 B

Weight of structural elements: 35263 kg

Buckling multiplier and amplification coefficient for the fundamental load combination: $\begin{cases} \alpha_{cr} = 8.18 \\ \frac{1}{1-\frac{1}{\alpha_{cr}}} = 1.14 \end{cases}$

Table A.41 – Modal information for 8 St_DC3_MRFs_X_ FREEDAM

Mode	Vibration period (s)	Sum of effective modal masses on X direction
1	2.07	0.731
2	0.75	0.862
3	0.40	0.918
4	0.24	0.950
5	0.17	0.968
6	0.12	0.982
7	0.09	0.992
8	0.09	0.993

Table A.42 – Drift limitation at SD limit state for 8 St_DC3_MRFs_X_ FREEDAM

Storey	$d_{r,SD}$ (m)	h_s (m)	$d_{r,SD}$ (rad)	$d_{r,SDadm}$ (rad)
1	0.021	3.5	0.01	0.02
2	0.038	3.5	0.01	0.02
3	0.044	3.5	0.01	0.02
4	0.045	3.5	0.01	0.02
5	0.049	3.5	0.01	0.02
6	0.050	3.5	0.01	0.02

7	0.057	3.5	0.02	0.02
8	0.051	3.5	0.01	0.02

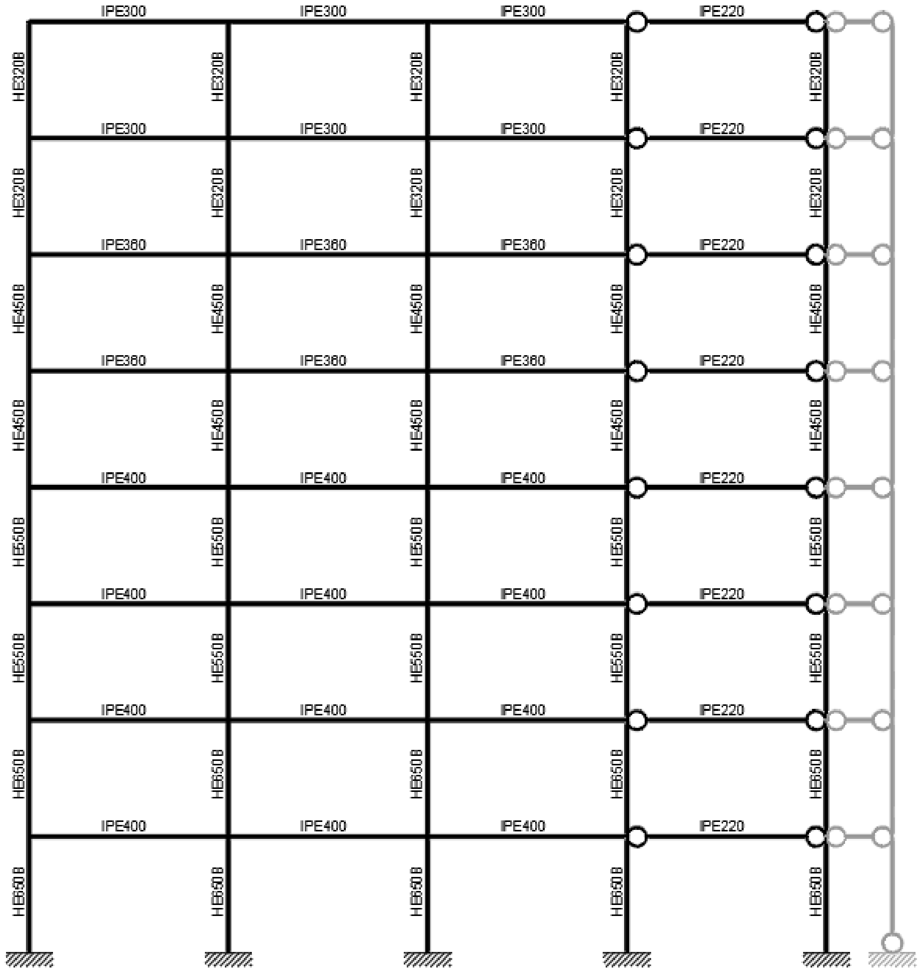

Figure A.16 – Designed structure 8 St_DC3_MRFs_X_ FREEDAM

❖ Structure code: 8 St_DC2_MRFs_Y_FREEDAM

Table A.43 – Beam and column sections for 8 St_DC2_MRFs_Y_FREEDAM

Storey	Bay 1	Bay 2	Bay 3	Bay 4

				(pinned)
1-4	IPE 330 FREEDAM	IPE 330 FREEDAM	IPE 330 FREEDAM	IPE 270
5-6	IPE 300 FREEDAM	IPE 300 FREEDAM	IPE 300 FREEDAM	IPE 270
7-8	IPE 270 FREEDAM	IPE 270 FREEDAM	IPE 270 FREEDAM	IPE 270
Storey	**Column 1-5**	**Column 2**	**Column 3**	**Column 4**
1-2	HE 550 B	HE 550 B	HE 550 B	HE 550 B
3-4	HE 450 B	HE 450 B	HE 450 B	HE 450 B
5-6	HE 360 B	HE 360 B	HE 360 B	HE 360 B
7-8	HE 300 B	HE 300 B	HE 300 B	HE 300 B

Weight of structural elements: 30577 kg

Buckling multiplier and amplification coefficient for the fundamental load combination: $\begin{cases} \alpha_{cr} = 4.54 \\ \frac{1}{1-\frac{1}{\alpha_{cr}}} = 1.28 \end{cases}$

Table A.44 – Modal information for 8 St_DC2_MRFs_Y_FREEDAM

Mode	Vibration period (s)	Sum of effective modal masses on X direction
1	2.74	0.734
2	0.95	0.863
3	0.50	0.916
4	0.31	0.948
5	0.25	0.948
6	0.25	0.948
7	0.25	0.948
8	0.25	0.948

Table A.45 – Drift limitation at SD limit state for 8 St_DC2_MRFs_Y_FREEDAM

Storey	$d_{r,SD}$ (m)	h_s (m)	$d_{r,SD}$ (rad)	$d_{r,SDadm}$ (rad)
1	0.021	3.5	0.01	0.02
2	0.038	3.5	0.01	0.02
3	0.046	3.5	0.01	0.02
4	0.048	3.5	0.01	0.02

5	0.052	3.5	0.01	0.02
6	0.052	3.5	0.01	0.02
7	0.052	3.5	0.01	0.02
8	0.044	3.5	0.01	0.02

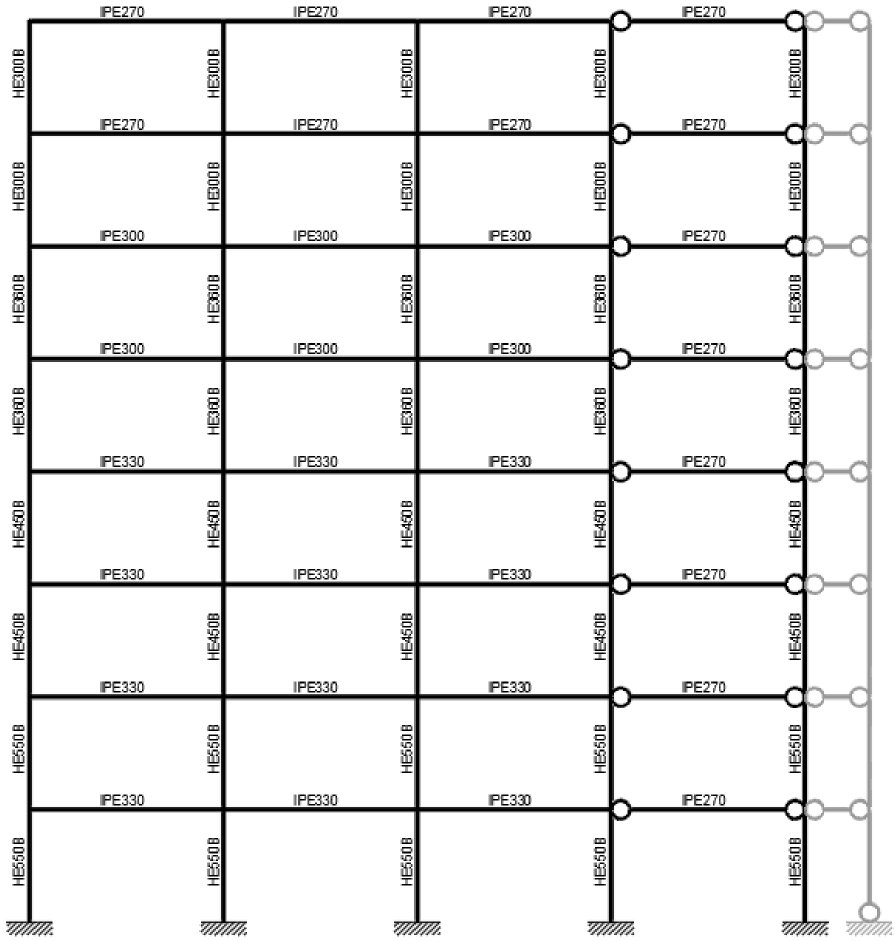

Figure A.17 – Designed structure 8 St_DC2_MRFs_Y_FREEDAM

❖ Structure code: 8 St_DC3_MRFs_Y_FREEDAM

Table A.46 – Beam and column sections for 8 St_DC3_MRFs_Y_ FREEDAM

Storey	Bay 1	Bay 2	Bay 3	Bay 4 (pinned)
1-4	IPE 400 FREEDAM	IPE 400 FREEDAM	IPE 400 FREEDAM	IPE 270
5-6	IPE 360 FREEDAM	IPE 360 FREEDAM	IPE 360 FREEDAM	IPE 270
7-8	IPE 300 FREEDAM	IPE 300 FREEDAM	IPE 300 FREEDAM	IPE 270
Storey	**Column 1-5**	**Column 2**	**Column 3**	**Column 4**
1-2	HE 700 B	HE 700 B	HE 700 B	HE 700 B
3-4	HE 600 B	HE 600 B	HE 600 B	HE 600 B
5-6	HE 500 B	HE 500 B	HE 500 B	HE 500 B
7-8	HE 400 B	HE 400 B	HE 400 B	HE 400 B

Weight of structural elements: 38299 kg

Buckling multiplier and amplification coefficient for the fundamental load combination: $\begin{cases} \alpha_{cr} = 8.80 \\ \frac{1}{1-\frac{1}{\alpha_{cr}}} = 1.13 \end{cases}$

Table A.47 – Modal information for 8 St_DC3_MRFs_Y_ FREEDAM

Mode	Vibration period (s)	Sum of effective modal masses on X direction
1	1.99	0.730
2	0.69	0.863
3	0.36	0.919
4	0.25	0.919
5	0.25	0.919
6	0.25	0.919
7	0.25	0.919
8	0.25	0.919

Table A.48 – Drift limitation at SD limit state for 8 St_DC3_MRFs_Y_ FREEDAM

Storey	$d_{r,SD}$ (m)	h_s (m)	$d_{r,SD}$ (rad)	$d_{r,SDadm}$ (rad)
1	0.020	3.5	0.01	0.02
2	0.036	3.5	0.01	0.02

3	0.043	3.5	0.01	0.02
4	0.044	3.5	0.01	0.02
5	0.048	3.5	0.01	0.02
6	0.049	3.5	0.01	0.02
7	0.052	3.5	0.01	0.02
8	0.047	3.5	0.01	0.02

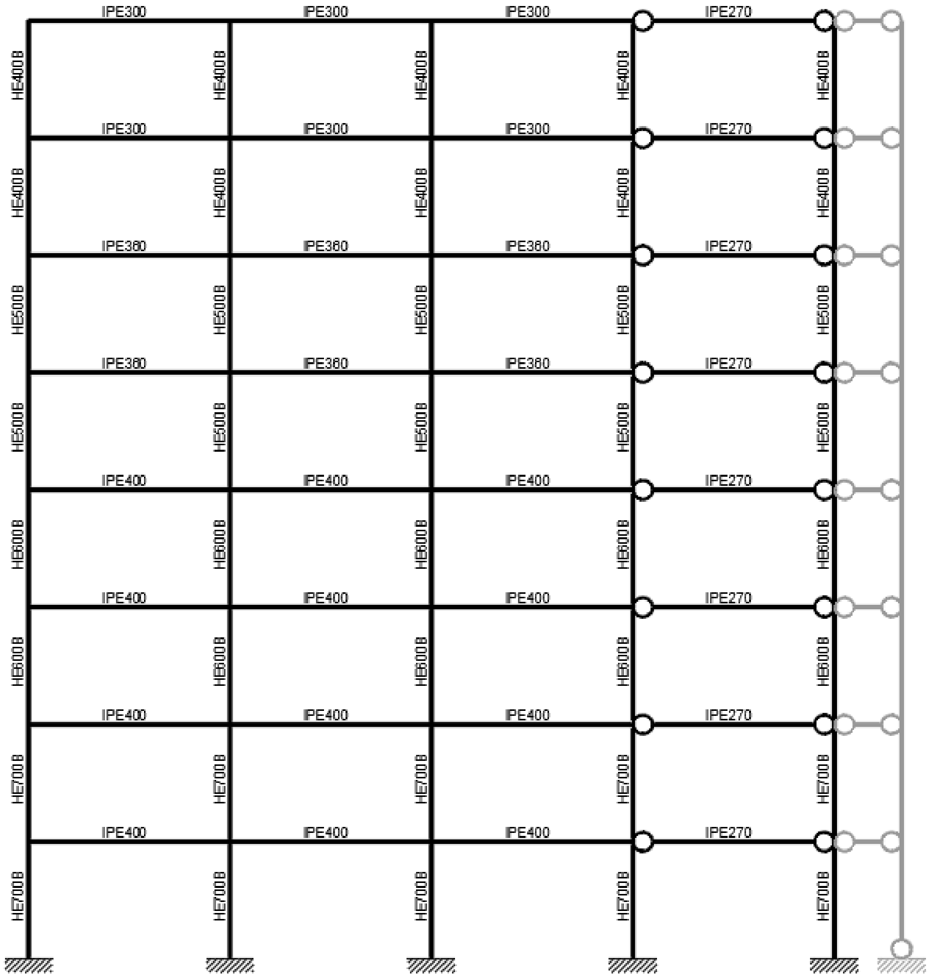

Figure A.18 – Designed structure 8 St_DC3_MRFs_Y_ FREEDAM

Low Rise Dual Concentrically Braced Frames (LR-D-CBFs)

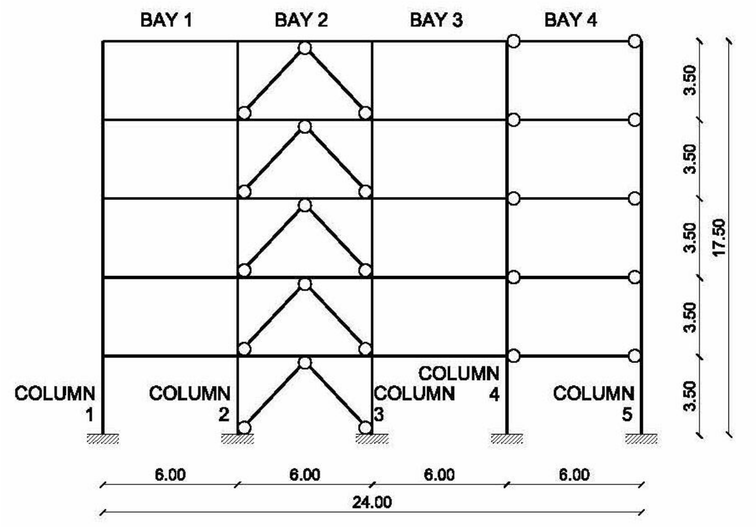

Figure A.19 – Reference image for structures LR-D-CBFs

❖ Structure code: 4 St_DC2_D-CBFs_X_TRADITIONAL

Table A.49 – Beam, diagonal and column sections for 4 St_DC2_D-CBFs_X_TRADITIONAL

Storey	Bay 1	Bay 2	Bay 3	Bay 4 (pinned)
1-2	IPE 300 haunched	IPE 300 haunched	IPE 300 haunched	IPE 220
3-4	IPE 270 haunched	IPE 270 haunched	IPE 270 haunched	IPE 220
Storey	**Column 1-5**	**Column 2**	**Column 3**	**Column 4**
1-2	HE 320 B	HE 320 B	HE 320 B	HE 320 B
3-4	HE 280 B	HE 280 B	HE 280 B	HE 280 B
Storey	**Diagonals**			
1	CHS 88.9x4			
2	CHS 88.9x3.2			
3	CHS 76.1x3.2			

4	CHS 76.1x2.9

Weight of structural elements: 11552 kg

Buckling multiplier and amplification coefficient for the fundamental load combination: $\begin{cases} \alpha_{cr} = 16.77 \\ \frac{1}{1-\frac{1}{\alpha_{cr}}} = 1.00 \end{cases}$

Table A.50 – Modal information for 4 St_DC2_D-CBFs_X_TRADITIONAL

Mode	Vibration period (s)	Sum of effective modal masses on X direction
1	1.02	0.818
2	0.35	0.938
3	0.20	0.980
4	0.13	1.000

Table A.51 – Drift limitation at SD limit state for 4 St_DC2_D-CBFs_X_TRADITIONAL

Storey	$d_{r,SD}$ (m)	h_s (m)	$d_{r,SD}$ (rad)	$d_{r,SDadm}$ (rad)
1	0.025	3.5	0.01	0.02
2	0.034	3.5	0.01	0.02
3	0.032	3.5	0.01	0.02
4	0.025	3.5	0.01	0.02

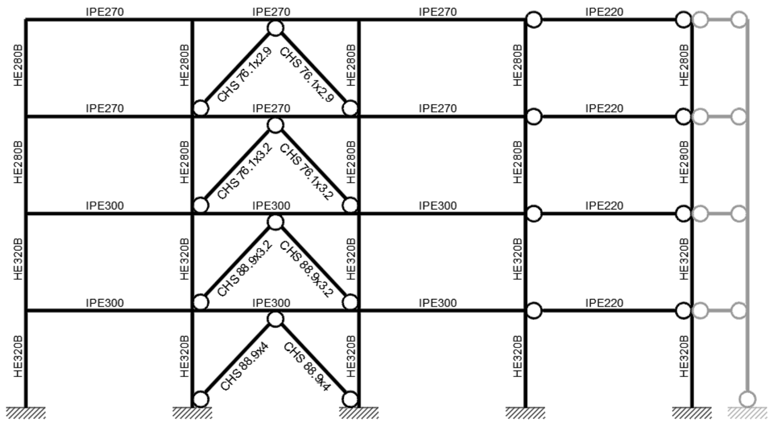

Figure A.20 – Designed structure 4 St_X-DC2_D-CBF with haunched connections

❖ Structure code: 4 St_DC3_D-CBFs_X_TRADITIONAL

Table A.52 – Beam,diagonal and column sections for 4 St_DC3_D-CBFs_X_TRADITIONAL

Storey	Bay 1	Bay 2	Bay 3	Bay 4 (pinned)
1-4	IPE 330 haunched	IPE 270 haunched	IPE 330 haunched	IPE 220
Storey	**Column 1-5**	**Column 2**	**Column 3**	**Column 4**
1-2	HE 360 B	HE 450 B	HE 450 B	HE 450 B
3-4	HE 320 B	HE 450 B	HE 450 B	HE 450 B
Storey	**Diagonal**			
1-2	CHS 88.9x5			
3-4	CHS 88.9x4			

Weight of structural elements: 14951.8 kg

Buckling multiplier and amplification coefficient for the fundamental load combination: $\begin{cases} \alpha_{cr} = 25.11 \\ \frac{1}{1-\frac{1}{\alpha_{cr}}} = 1.00 \end{cases}$

Table A.53 – Modal information for 4 St_DC3_D-CBFs_X_TRADITIONAL

Mode	Vibration period (s)	Sum of effective modal masses on X direction
1	0.84	0.824
2	0.27	0.944
3	0.14	0.986
4	0.09	1.000

Table A.54 – Drift limitation at SD limit state for 4 St_DC3_D-CBFs_X_TRADITIONAL

Storey	$d_{r,SD}$ (m)	h_s (m)	$d_{r,SD}$ (rad)	$d_{r,SDadm}$ (rad)
1	0.026	3.5	0.01	0.02
2	0.037	3.5	0.01	0.02
3	0.033	3.5	0.01	0.02
4	0.024	3.5	0.01	0.02

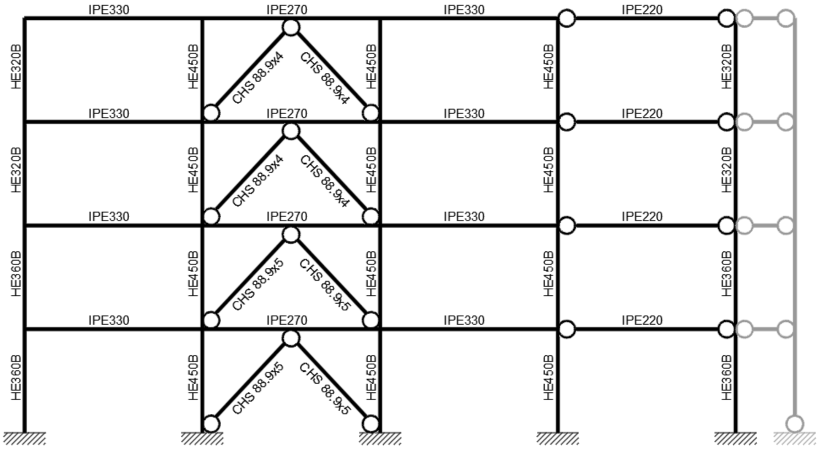

Figure A.21 – Designed structure 4 St_DC3_D-CBFs_X_TRADITIONAL

❖ Structure code: 4 St_DC2_D-CBFs_Y_TRADITIONAL

Table A.55 – Beam, diagonal and column sections for 4 St_DC2_D-CBFs_Y_TRADITIONAL

Storey	**Bay 1**	**Bay 2**	**Bay 3**	**Bay 4 (pinned)**
1-4	IPE 300 haunched	IPE 270 haunched	IPE 300 haunched	IPE 270
Storey	**Column 1-5**	**Column 2**	**Column 3**	**Column 4**
1-2	HE 320 B	HE 340 B	HE 340 B	HE 320 B
3-4	HE 280 B	HE 300 B	HE 300 B	HE 280 B

Storey	**Diagonal**
1	CHS 88.9x4
2	CHS 88.9x3.2
3	CHS 76.1x3.2
4	CHS 76.1x2.9

Weight of structural elements: 12161 kg

Buckling multiplier and amplification coefficient for the fundamental load combination: $\begin{cases} \alpha_{cr} = 17.16 \\ \frac{1}{1-\frac{1}{\alpha_{cr}}} = 1.00 \end{cases}$

Table A.56 – Modal information for 4 St_DC2_D-CBFs_Y_TRADITIONAL

Mode	Vibration period (s)	Sum of effective modal masses on X direction
1	1.01	0.822
2	0.34	0.938
3	0.25	0.938
4	0.25	0.938

Table A.57 – Drift limitation at SD limit state for 4 St_DC2_D-CBFs_Y_TRADITIONAL

Storey	$d_{r,\,SD}$ (m)	h_s (m)	$d_{r,\,SD}$ (rad)	$d_{r,\,SD\ adm}$ (rad)
1	0.024	3.5	0.01	0.02
2	0.034	3.5	0.01	0.02
3	0.031	3.5	0.01	0.02
4	0.022	3.5	0.01	0.02

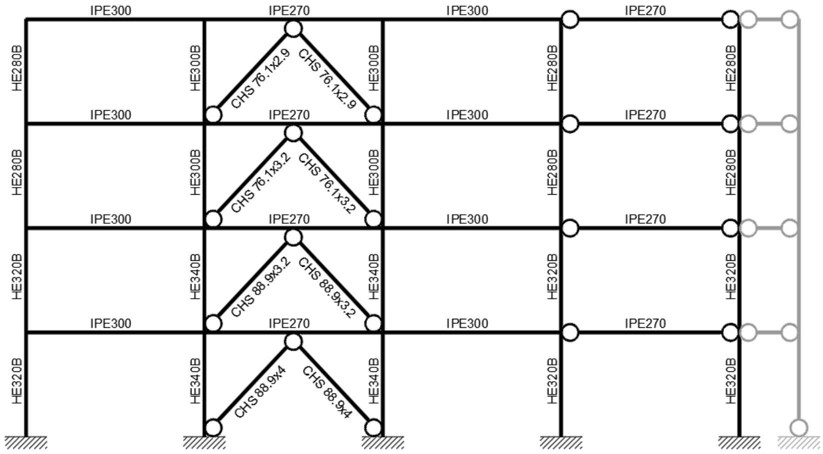

Figure A.22 – Designed structure 4 St_DC2_D-CBFs_Y_TRADITIONAL

❖ Structure code: 4 St_DC3_D-CBFs_Y_TRADITIONAL

Table A.58 – Beam, diagonal and column sections for 4 St_DC3_D-CBFs_Y_TRADITIONAL

Storey	Bay 1	Bay 2	Bay 3	Bay 4 (pinned)
1-4	IPE 330	IPE 270	IPE 330	IPE 270

Storey	haunched Column 1-5	haunched Column 2	haunched Column 3	Column 4
1-2	HE 360 B	HE 450 B	HE 450 B	HE 450 B
3-4	HE 320 B	HE 450 B	HE 450 B	HE 450 B

Storey	Diagonal
1-2	CHS 88.9x5
3-4	CHS 88.9x4

Weight of structural elements: 15179 kg

Buckling multiplier and amplification coefficient for the fundamental load combination: $\begin{cases} \alpha_{cr} = 25.27 \\ \frac{1}{1-\frac{1}{\alpha_{cr}}} = 1.00 \end{cases}$

Table A.59 – Modal information for 4 St_DC3_D-CBFs_Y_TRADITIONAL

Mode	Vibration period (s)	Sum of effective modal masses on X direction
1	0.84	0.823
2	0.27	0.943
3	0.25	0.943
4	0.25	0.943

Table A.60 – Drift limitation at SD limit state for 4 St_DC3_D-CBFs_Y_TRADITIONAL

Storey	$d_{r,SD}$ (m)	h_s (m)	$d_{r,SD}$ (rad)	$d_{r,SDadm}$ (rad)
1	0.026	3.5	0.01	0.02
2	0.037	3.5	0.01	0.02
3	0.033	3.5	0.01	0.02
4	0.024	3.5	0.01	0.02

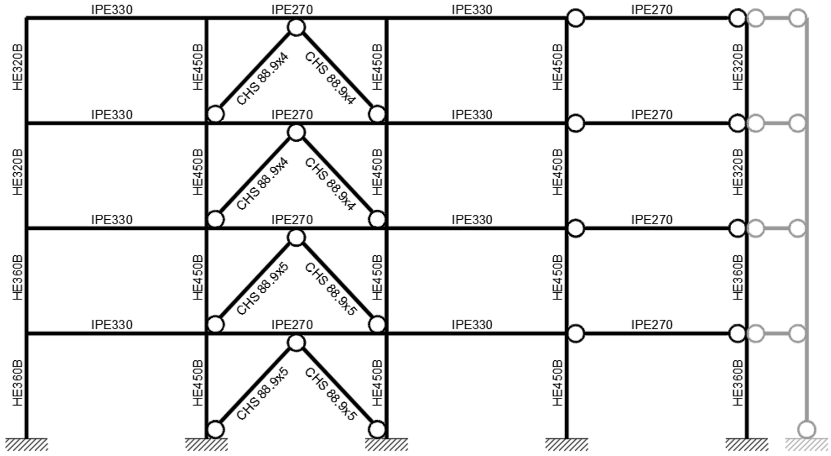

Figure A.23 – Designed structure 4 St_DC3_D-CBFs_Y_TRADITIONAL

❖ Structure code: 4 St_DC2_D-CBFs_X_FREEDAM

Table A.61 – Beam, diagonal and column sections for 4 St_DC2_D-CBFs_X_FREEDAM

Storey	**Bay 1**	**Bay 2**	**Bay 3**	**Bay 4 (pinned)**
1-4	IPE 330 FREEDAM	IPE 330 FREEDAM	IPE 330 FREEDAM	IPE 220
Storey	**Column 1-5**	**Column 2**	**Column 3**	**Column 4**
1-2	HE 300 B	HE 300 B	HE 300 B	HE 300 B
3-4	HE 240 B	HE 240 B	HE 240 B	HE 240 B
Storey	**Diagonals**			
1	CHS 114.3x4			
2	CHS 114.3x3.6			
3	CHS 114.3x3.2			
4	CHS 88.9x3.2			

Weight of structural elements: 11745 kg

Buckling multiplier and amplification coefficient for the fundamental load combination: $\begin{cases} \alpha_{cr} = 21.98 \\ \frac{1}{1-\frac{1}{\alpha_{cr}}} = 1.00 \end{cases}$

Table A.62 – Modal information for 4 St_DC2_D-CBFs_X_FREEDAM

Mode	Vibration period (s)	Sum of effective modal masses on X direction
1	0.88	0.836
2	0.31	0.949
3	0.19	0.982
4	0.13	1.000

Table A.63 – Drift limitation at SD limit state for 4 St_DC2_D-CBFs_X_FREEDAM

Storey	$d_{r,SD}$ (m)	h_s (m)	$d_{r,SD}$ (rad)	$d_{r,SDadm}$ (rad)
1	0.024	3.5	0.01	0.02
2	0.028	3.5	0.01	0.02
3	0.027	3.5	0.01	0.02
4	0.019	3.5	0.01	0.02

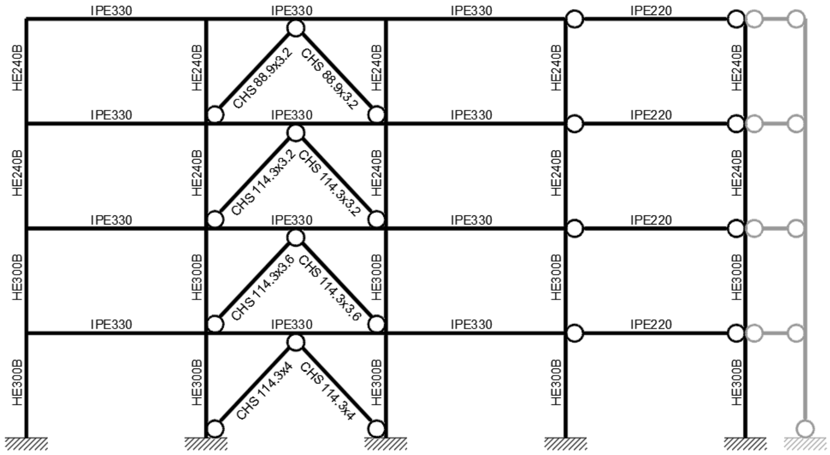

Figure A.24 – Designed structure 4 St_DC2_D-CBFs_X_FREEDAM

❖ Structure code: 4 St_DC3_D-CBFs_X_FREEDAM

Table A.64 – Beam, diagonal and column sections for 4 St_DC3_D-CBFs_X_FREEDAM

Storey	Bay 1	Bay 2	Bay 3	Bay 4 (pinned)
1-2	IPE 360	IPE 360	IPE 360	IPE 220

	FREEDAM	FREEDAM	FREEDAM	
3-4	IPE 330 FREEDAM	IPE 330 FREEDAM	IPE 330 FREEDAM	IPE 220
Storey	**Column 1-5**	**Column 2**	**Column 3**	**Column 4**
1-2	HE 300 B	HE 300 B	HE 300 B	HE 300 B
3-4	HE 260 B	HE 260 B	HE 260 B	HE 260 B

Storey	**Diagonal**
1	CHS 114.3x6.3
2	CHS 114.3x5
3	CHS 114.3x4
4	CHS 88.9x5

Weight of structural elements: 12486 kg

Buckling multiplier and amplification coefficient for the fundamental load combination: $\begin{cases} \alpha_{cr} = 29.24 \\ \frac{1}{1-\frac{1}{\alpha_{cr}}} = 1.00 \end{cases}$

Table A.65 – Modal information for 4 St_DC3_D-CBFs_X_FREEDAM

Mode	Vibration period (s)	Sum of effective modal masses on X direction
1	0.77	0.826
2	0.27	0.950
3	0.16	0.983
4	0.12	1.000

Table A.66 – Drift limitation at SD limit state for 4 St_DC3_D-CBFs_X_FREEDAM

Storey	$d_{r,SD}$ (m)	h_s (m)	$d_{r,SD}$ (rad)	$d_{r,SDadm}$ (rad)
1	0.026	3.5	0.01	0.02
2	0.032	3.5	0.01	0.02
3	0.032	3.5	0.01	0.02
4	0.022	3.5	0.01	0.02

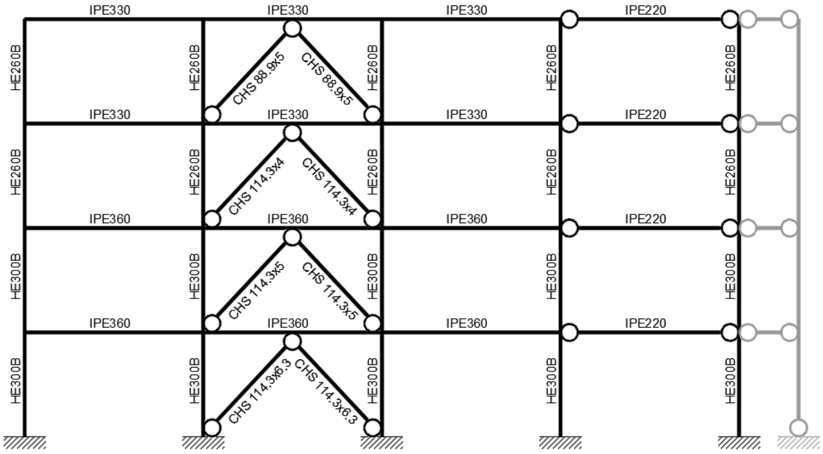

Figure A.25 – Designed structure 4 St_DC3_D-CBFs_X_FREEDAM

❖ Structure code: 4 St_DC2_D-CBFs_Y_FREEDAM

Table A.67 – Beam, diagonal and column sections for 4 St_DC2_D-CBFs_Y_FREEDAM

Storey	**Bay 1**	**Bay 2**	**Bay 3**	**Bay 4 (pinned)**
1-4	IPE 330 FREEDAM	IPE 330 FREEDAM	IPE 330 FREEDAM	IPE 270
Storey	**Column 1-5**	**Column 2**	**Column 3**	**Column 4**
1-2	HE 300 B	HE 300 B	HE 300 B	HE 300 B
3-4	HE 240 B	HE 240 B	HE 240 B	HE 240 B
Storey	**Diagonal**			
1	CHS 114.3x4			
2	CHS 114.3x3.6			
3	CHS 114.3x3.2			
4	CHS 88.9x3.2			

Weight of structural elements: 11976 kg

Buckling multiplier and amplification coefficient for the fundamental load combination: $\begin{cases} \alpha_{cr} = 22.48 \\ \frac{1}{1-\frac{1}{\alpha_{cr}}} = 1.00 \end{cases}$

Table A.68 – Modal information for 4 St_DC2_D-CBFs_Y_FREEDAM

Mode	Vibration period (s)	Sum of effective modal masses on X direction
1	0.87	0.836
2	0.31	0.948
3	0.25	0.948
4	0.25	0.948

Table A.69 – Drift limitation at SD limit state for 4 St_DC2_D-CBFs_Y_FREEDAM

Storey	$d_{r,SD}$ (m)	h_s (m)	$d_{r,SD}$ (rad)	$d_{r,SDadm}$ (rad)
1	0.023	3.5	0.01	0.02
2	0.028	3.5	0.01	0.02
3	0.026	3.5	0.01	0.02
4	0.019	3.5	0.01	0.02

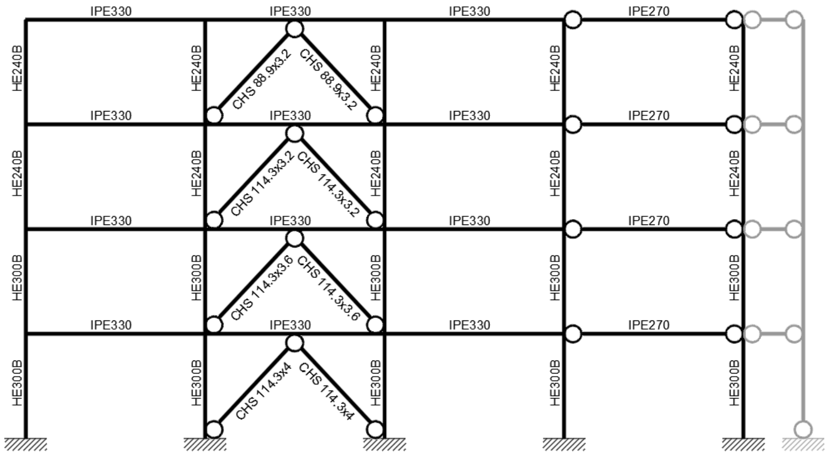

Figure A.26 – Designed structure 4 St_DC2_D-CBFs_Y_FREEDAM

❖ Structure code: 4 St_DC3_D-CBFs_Y_FREEDAM

Table A.70 – Beam, diagonal and column sections for 4 St_DC3_D-CBFs_Y_ FREEDAM

Storey	Bay 1	Bay 2	Bay 3	Bay 4 (pinned)
1-2	IPE 360	IPE 360	IPE 360	IPE 270

	FREEDAM	FREEDAM	FREEDAM	
3-4	IPE 330 FREEDAM	IPE 330 FREEDAM	IPE 330 FREEDAM	IPE 270
Storey	**Column 1-5**	**Column 2**	**Column 3**	**Column 4**
1-2	HE 320 B	HE 320 B	HE 320 B	HE 320 B
3-4	HE 280 B	HE 280 B	HE 280 B	HE 280 B

Storey	**Diagonal**
1	CHS 114.3x6.3
2	CHS 114.3x5
3	CHS 114.3x4
4	CHS 88.9x5

Weight of structural elements: 13401 kg

Buckling multiplier and amplification coefficient for the fundamental load combination: $\begin{cases} \alpha_{cr} = 31.20 \\ \frac{1}{1-\frac{1}{\alpha_{cr}}} = 1.00 \end{cases}$

Table A.71 – Modal information for 4 St_DC3_D-CBFs_Y_ FREEDAM

Mode	**Vibration period (s)**	**Sum of effective modal masses on X direction**
1	0.75	0.824
2	0.26	0.948
3	0.25	0.948
4	0.25	0.948

Table A.72 – Drift limitation at SD limit state for 4 St_DC3_D-CBFs_Y_ FREEDAM

Storey	**$d_{r,SD}$ (m)**	**h_s (m)**	**$d_{r,SD}$ (rad)**	**$d_{r,SDadm}$ (rad)**
1	0.025	3.5	0.01	0.02
2	0.031	3.5	0.01	0.02
3	0.031	3.5	0.01	0.02
4	0.022	3.5	0.01	0.02

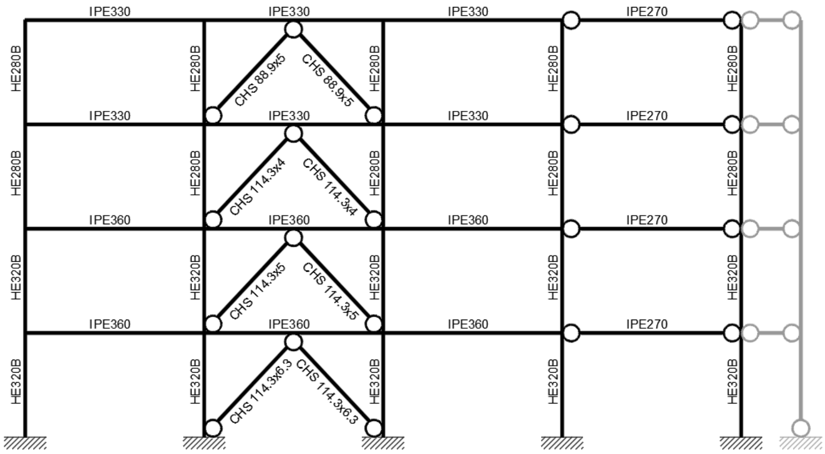

Figure A.27 – Designed structure 4 St_DC3_D-CBFs_Y_ FREEDAM

Medium Rise Dual Concentrically Braced Frames (MR-D-CBFs)

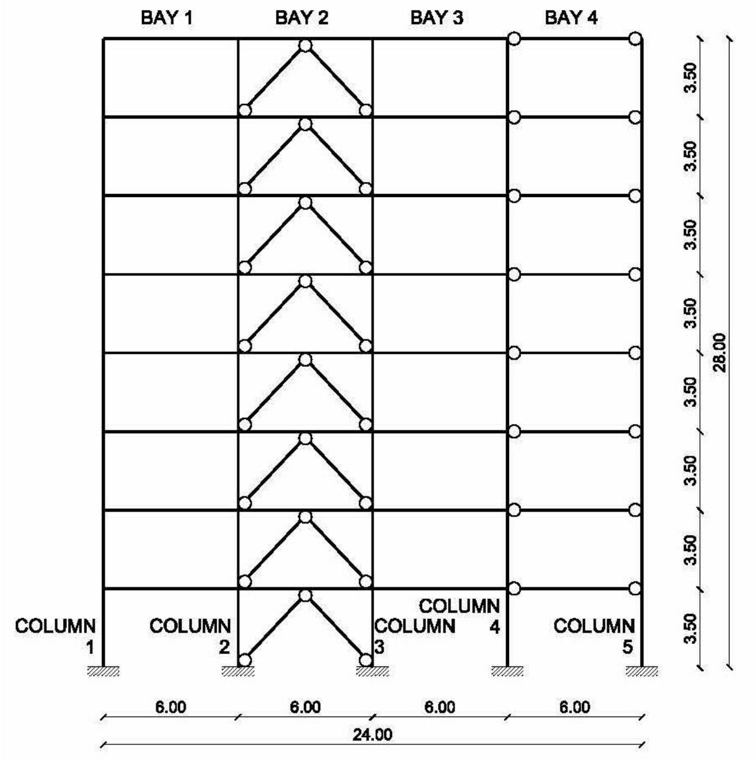

Figure A.28 – Reference image for structures MR-D-CBFs

❖ Structure code: 8 St_DC2_D-CBFs_X_TRADITIONAL

Table A.73 – Beam, diagonal and column sections for 8 St_DC2_D-CBFs_X_TRADITIONAL

Storey	**Bay 1**	**Bay 2**	**Bay 3**	**Bay 4 (pinned)**
1-4	IPE 300 haunched	IPE 300 haunched	IPE 300 haunched	IPE 220
5-8	IPE 270 haunched	IPE 270 haunched	IPE 270 haunched	IPE 220
Storey	**Column 1-5**	**Column 2**	**Column 3**	**Column 4**

1-2	HE 600 B	HE 600 B	HE 600 B	HE 600 B
3-4	HE 500 B	HE 500 B	HE 500 B	HE 500 B
5-6	HE 400 B	HE 400 B	HE 400 B	HE 400 B
7-8	HE 300 B	HE 300 B	HE 300 B	HE 300 B

Storey	Diagonals
1-2	CHS 88.9x4
3-4	CHS 76.1x4
5-8	CHS 76.1x3.2

Weight of structural elements: 30492 kg

Buckling multiplier and amplification coefficient for the fundamental load combination: $\begin{cases} \alpha_{cr} = 9.23 \\ \frac{1}{1-\frac{1}{\alpha_{cr}}} = 1.12 \end{cases}$

Table A.74 – Modal information for 8 St_DC2_D-CBFs_X_TRADITIONAL

Mode	Vibration period (s)	Sum of effective modal masses on X direction
1	1.91	0.751
2	0.64	0.881
3	0.35	0.925
4	0.24	0.953
5	0.17	0.969
6	0.13	0.981
7	0.10	0.991
8	0.09	0.991

Table A.75 – Drift limitation at SD limit state for 8 St_DC2_D-CBFs_X_TRADITIONAL

Storey	$d_{r,SD}$ (m)	h_s (m)	$d_{r,SD}$ (rad)	$d_{r,SDadm}$ (rad)
1	0.016	3.5	0.00	0.02
2	0.029	3.5	0.01	0.02
3	0.033	3.5	0.01	0.02
4	0.034	3.5	0.01	0.02
5	0.036	3.5	0.01	0.02
6	0.035	3.5	0.01	0.02
7	0.031	3.5	0.01	0.02

8	0.023	3.5	0.01	0.02

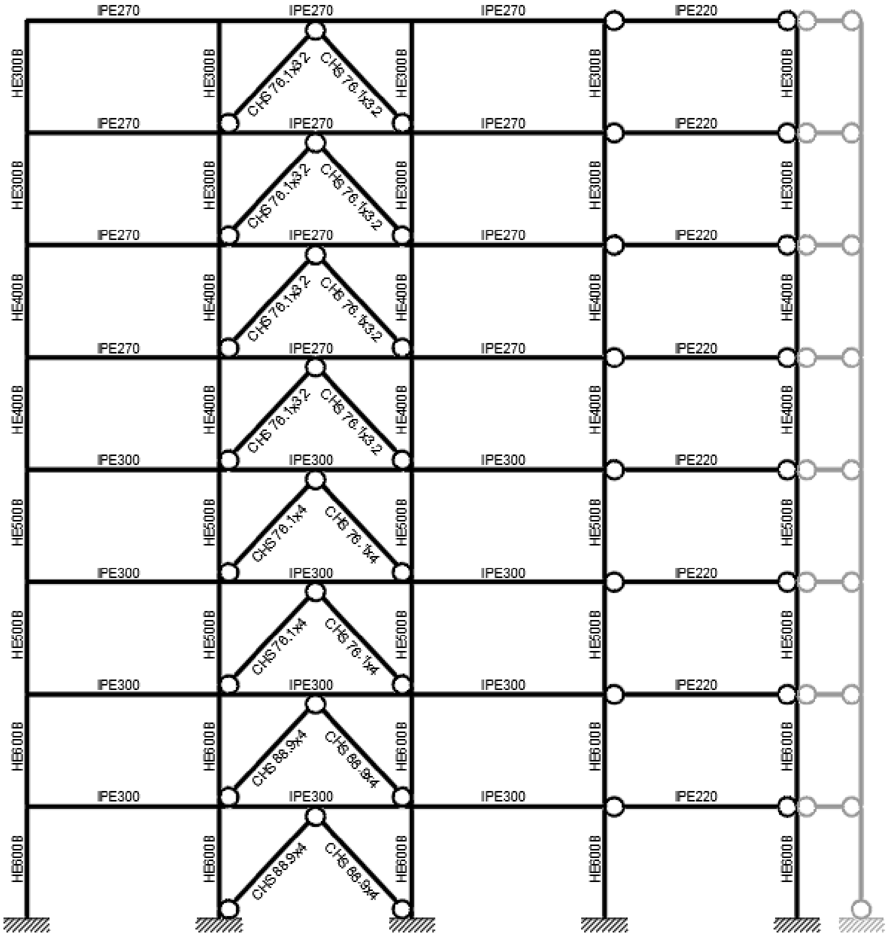

Figure A.29 – Designed structure 8 St_DC2_D-CBFs_X_TRADITIONAL

❖ Structure code: 8 St_DC3_D-CBFs_X_TRADITIONAL

Table A.76 – Beam, diagonal and column sections for 8 St_DC3_D-CBFs_X_TRADITIONAL

Storey	Bay 1	Bay 2	Bay 3	Bay 4 (pinned)
1-8	IPE 300 haunched	IPE 270 haunched	IPE 300 haunched	IPE 220

Storey	Column 1-5	Column 2	Column 3	Column 4
1-4	HE 650 B	HE 650 B	HE 650 B	HE 650 B
5-6	HE 600 B	HE 600 B	HE 600 B	HE 600 B
7-8	HE 500 B	HE 500 B	HE 500 B	HE 500 B

Storey	Diagonals
1-4	CHS 88.9x5
5-8	CHS 88.9x4

Weight of structural elements: 36936 kg

Buckling multiplier and amplification coefficient for the fundamental load combination: $\begin{cases} \alpha_{cr} = 11.73 \\ \frac{1}{1-\frac{1}{\alpha_{cr}}} = 1.09 \end{cases}$

Table A.77 – Modal information for 8 St_DC3_D-CBFs_X_TRADITIONAL

Mode	Vibration period (s)	Sum of effective modal masses on X direction
1	1.77	0.767
2	0.56	0.893
3	0.29	0.938
4	0.19	0.965
5	0.13	0.981
6	0.09	0.991
7	0.09	0.991
8	0.08	0.991

Table A.78 – Drift limitation at SD limit state for 8 St_DC3_D-CBFs_X_TRADITIONAL

Storey	$d_{r,SD}$ (m)	h_s (m)	$d_{r,SD}$ (rad)	$d_{r,SDadm}$ (rad)
1	0.022	3.5	0.01	0.02
2	0.038	3.5	0.01	0.02
3	0.041	3.5	0.01	0.02
4	0.041	3.5	0.01	0.02
5	0.041	3.5	0.01	0.02
6	0.039	3.5	0.01	0.02
7	0.034	3.5	0.01	0.02
8	0.027	3.5	0.01	0.02

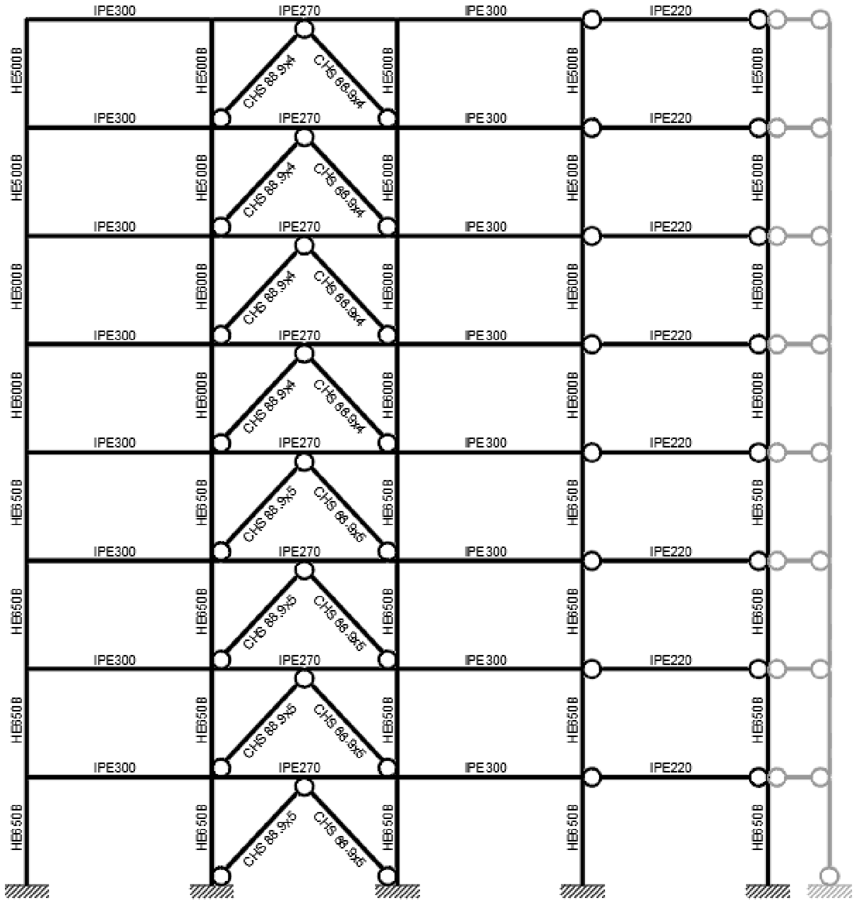

Figure A.30 – Designed structure 8 St_DC3_D-CBFs_X_TRADITIONAL

❖ Structure code: 8 St_DC2_D-CBFs_Y_TRADITIONAL

Table A.79 – Beam, diagonal and column sections for 8 St_DC2_D-CBFs_Y_TRADITIONAL

Storey	Bay 1	Bay 2	Bay 3	Bay 4 (pinned)
1-4	IPE 300 haunched	IPE 300 haunched	IPE 300 haunched	IPE 270
5-8	IPE 270 haunched	IPE 270 haunched	IPE 270 haunched	IPE 270

Storey	Column 1-5	Column 2	Column 3	Column 4
1-2	HE 600 B	HE 600 B	HE 600 B	HE 600 B
3-4	HE 500 B	HE 500 B	HE 500 B	HE 500 B
5-6	HE 400 B	HE 400 B	HE 400 B	HE 400 B
7-8	HE 300 B	HE 300 B	HE 300 B	HE 300 B

Storey	Diagonals
1-2	CHS 88.9x4
3-4	CHS 76.1x4
5-8	CHS 76.1x3.2

Weight of structural elements: 30952 kg

Buckling multiplier and amplification coefficient for the fundamental load combination: $\begin{cases} \alpha_{cr} = 9.39 \\ \frac{1}{1-\frac{1}{\alpha_{cr}}} = 1.12 \end{cases}$

Table A.80 – Modal information for 8 St_DC2_D-CBFs_Y_TRADITIONAL

Mode	Vibration period (s)	Sum of effective modal masses on X direction
1	1.89	0.751
2	0.63	0.881
3	0.35	0.926
4	0.25	0.926
5	0.25	0.926
6	0.25	0.926
7	0.25	0.926
8	0.25	0.926

Table A.81 – Drift limitation at SD limit state for 8 St_DC2_D-CBFs_Y_TRADITIONAL

Storey	$d_{r,SD}$ (m)	h_s (m)	$d_{r,SD}$ (rad)	$d_{r,SDadm}$ (rad)
1	0.016	3.5	0.00	0.02
2	0.028	3.5	0.01	0.02
3	0.033	3.5	0.01	0.02
4	0.033	3.5	0.01	0.02
5	0.036	3.5	0.01	0.02
6	0.035	3.5	0.01	0.02

7	0.031	3.5	0.01	0.02
8	0.023	3.5	0.01	0.02

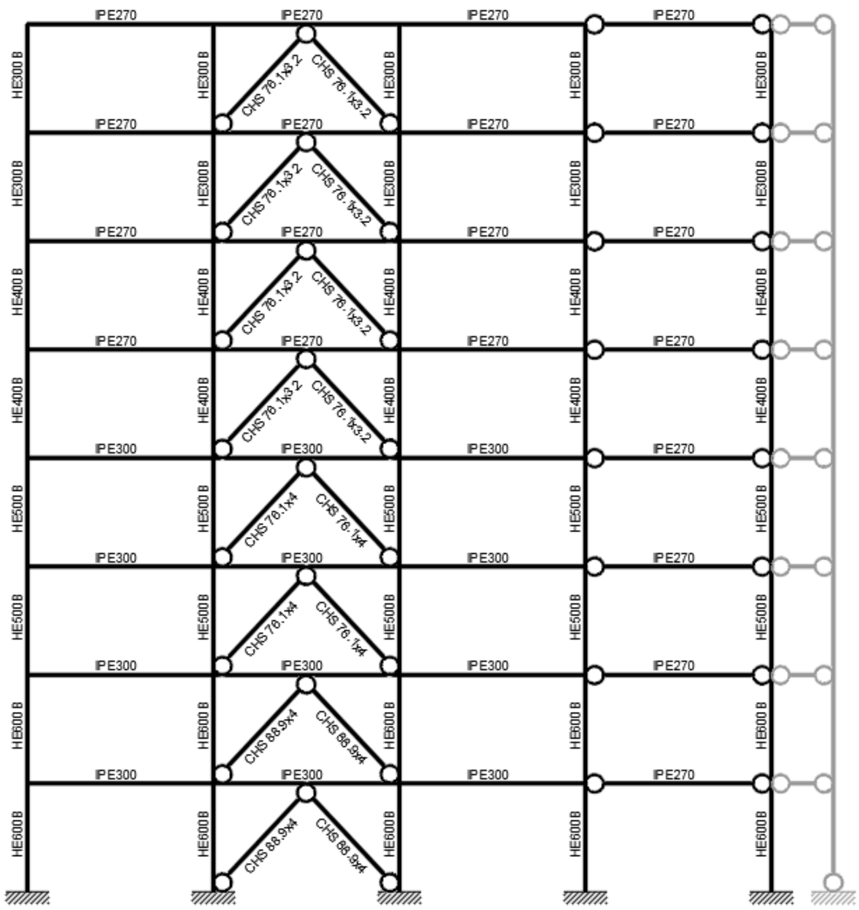

Figure A.31 – Designed structure 8 St_DC2_D-CBFs_Y_TRADITIONAL

❖ Structure code: 8 St_DC3_D-CBFs_Y_TRADITIONAL

Table A.82 – Beam, diagonal and column sections for 8 St_DC3_D-CBFs_Y_TRADITIONAL

Storey	**Bay 1**	**Bay 2**	**Bay 3**	**Bay 4 (pinned)**
1-8	IPE 300 haunched	IPE 300 haunched	IPE 300 haunched	IPE 270

Storey	Column 1-5	Column 2	Column 3	Column 4
1-5	HE 650 B	HE 650 B	HE 650 B	HE 650 B
6	HE 600 B	HE 600 B	HE 600 B	HE 600 B
7-8	HE 500 B	HE 500 B	HE 500 B	HE 500 B

Storey	Diagonals
1-4	CHS 88.9x5
5-8	CHS 88.9x4

Weight of structural elements: 37920 kg

Buckling multiplier and amplification coefficient for the fundamental load combination: $\begin{cases} \alpha_{cr} = 12.27 \\ \frac{1}{1-\frac{1}{\alpha_{cr}}} = 1.09 \end{cases}$

Table A.83 – Modal information for 8 St_DC3_D-CBFs_Y_TRADITIONAL

Mode	Vibration period (s)	Sum of effective modal masses on X direction
1	1.65	0.767
2	0.52	0.895
3	0.27	0.939
4	0.25	0.939
5	0.25	0.939
6	0.25	0.939
7	0.25	0.939
8	0.25	0.939

Table A.84 – Drift limitation at SD limit state for 8 St_DC3_D-CBFs_Y_TRADITIONAL

Storey	$d_{r,SD}$ (m)	h_s (m)	$d_{r,SD}$ (rad)	$d_{r,SDadm}$ (rad)
1	0.020	3.5	0.01	0.02
2	0.035	3.5	0.01	0.02
3	0.038	3.5	0.01	0.02
4	0.038	3.5	0.01	0.02
5	0.038	3.5	0.01	0.02
6	0.036	3.5	0.01	0.02
7	0.032	3.5	0.01	0.02
8	0.025	3.5	0.01	0.02

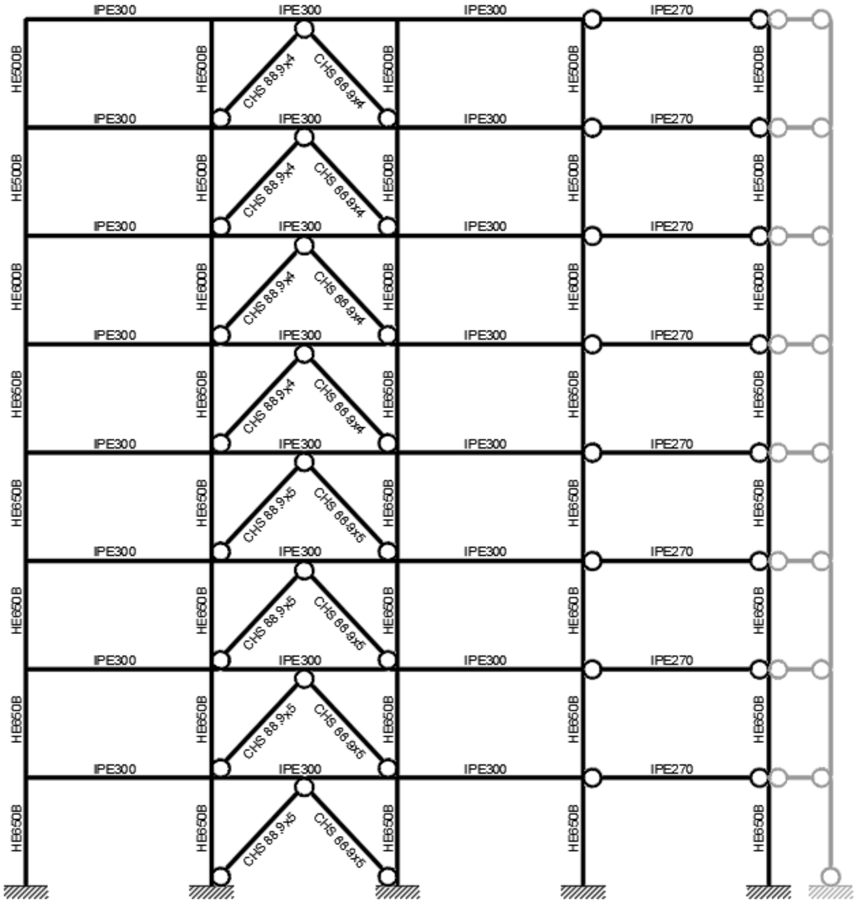

Figure A.32 – Designed structure 8 St_DC3_D-CBFs_Y_TRADITIONAL

❖ Structure code: 8 St_DC2_D-CBFs_X_FREEDAM

Table A.85 – Beam, diagonal and column sections for 8 St_DC2_D-CBFs_X_ FREEDAM

Storey	Bay 1	Bay 2	Bay 3	Bay 4 (pinned)
1-4	IPE 300 FREEDAM	IPE 300 FREEDAM	IPE 300 FREEDAM	IPE 220
5-8	IPE 270 FREEDAM	IPE 270 FREEDAM	IPE 270 FREEDAM	IPE 220

Storey	Column 1-5	Column 2	Column 3	Column 4
1-2	HE 550 B	HE 550 B	HE 550 B	HE 550 B
3-4	HE 450 B	HE 450 B	HE 450 B	HE 450 B
5-6	HE 360 B	HE 360 B	HE 360 B	HE 360 B
7-8	HE 260 B	HE 260 B	HE 260 B	HE 260 B

Storey	Diagonals
1-2	CHS 114.3x5
3-4	CHS 114.3x4
5-6	CHS 114.3x3.2
7-8	CHS 88.9x4

Weight of structural elements: 29300 kg

Buckling multiplier and amplification coefficient for the fundamental load combination: $\begin{cases} \alpha_{cr} = 12.07 \\ \frac{1}{1-\frac{1}{\alpha_{cr}}} = 1.09 \end{cases}$

Table A.86 – Modal information for 8 St_DC2_D-CBFs_X_ FREEDAM

Mode	Vibration period (s)	Sum of effective modal masses on X direction
1	1.68	0.752
2	0.57	0.889
3	0.32	0.932
4	0.22	0.957
5	0.17	0.970
6	0.13	0.982
7	0.10	0.992
8	0.09	0.992

Table A.87 – Drift limitation at SD limit state for 8 St_DC2_D-CBFs_X_ FREEDAM

Storey	$d_{r,SD}$ (m)	h_s (m)	$d_{r,SD}$ (rad)	$d_{r,SDadm}$ (rad)
1	0.015	3.5	0.00	0.02
2	0.025	3.5	0.01	0.02
3	0.028	3.5	0.01	0.02
4	0.029	3.5	0.01	0.02
5	0.031	3.5	0.01	0.02

6	0.031	3.5	0.01	0.02
7	0.029	3.5	0.01	0.02
8	0.020	3.5	0.01	0.02

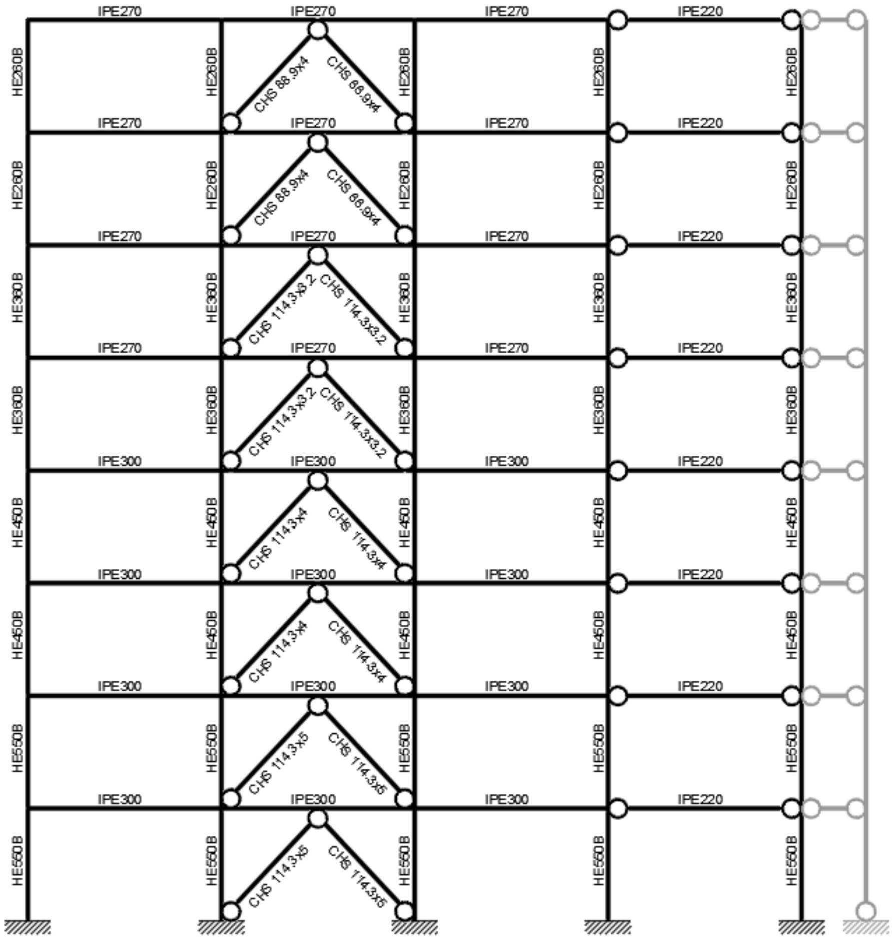

Figure A.33 – Designed structure 8 St_DC2_D-CBFs_X_ FREEDAM

❖ Structure code: 8 St_DC3_D-CBFs_X_FREEDAM

Table A.88 – Beam, diagonal and column sections for 8 St_DC3_D-CBFs_X_ FREEDAM

Storey	Bay 1	Bay 2	Bay 3	Bay 4

				(pinned)
1-4	IPE 330 FREEDAM	IPE 330 FREEDAM	IPE 330 FREEDAM	IPE 220
5-8	IPE 270 FREEDAM	IPE 270 FREEDAM	IPE 270 FREEDAM	IPE 220
Storey	**Column 1-5**	**Column 2**	**Column 3**	**Column 4**
1-2	HE 550 B	HE 600 B	HE 600 B	HE 550 B
3-4	HE 500 B	HE 500 B	HE 500 B	HE 500 B
5-6	HE 400 B	HE 400 B	HE 400 B	HE 400 B
7-8	HE 300 B	HE 300 B	HE 300 B	HE 300 B

Storey	**Diagonals**
1-2	CHS 114.3x7.1
3-4	CHS 114.3x6.3
5	CHS 114.3x5
6	CHS 114.3x4
7-8	CHS 114.3x3.2

Weight of structural elements: 32073 kg

Buckling multiplier and amplification coefficient for the fundamental load combination: $\begin{cases} \alpha_{cr} = 16.06 \\ \frac{1}{1-\frac{1}{\alpha_{cr}}} = 1.00 \end{cases}$

Table A.89 – Modal information for 8 St_DC3_D-CBFs_X_ FREEDAM

Mode	Vibration period (s)	Sum of effective modal masses on X direction
1	1.55	0.738
2	0.54	0.889
3	0.30	0.933
4	0.21	0.959
5	0.15	0.973
6	0.12	0.984
7	0.10	0.984
8	0.09	0.991

Table A.90 – Drift limitation at SD limit state for 8 St_DC3_D-CBFs_X_ FREEDAM

Storey	$d_{r,SD}$ (m)	h_s (m)	$d_{r,SD}$ (rad)	$d_{r,SDadm}$ (rad)
1	0.019	3.5	0.01	0.02
2	0.029	3.5	0.01	0.02
3	0.032	3.5	0.01	0.02
4	0.032	3.5	0.01	0.02
5	0.037	3.5	0.01	0.02
6	0.040	3.5	0.01	0.02
7	0.040	3.5	0.01	0.02
8	0.030	3.5	0.01	0.02

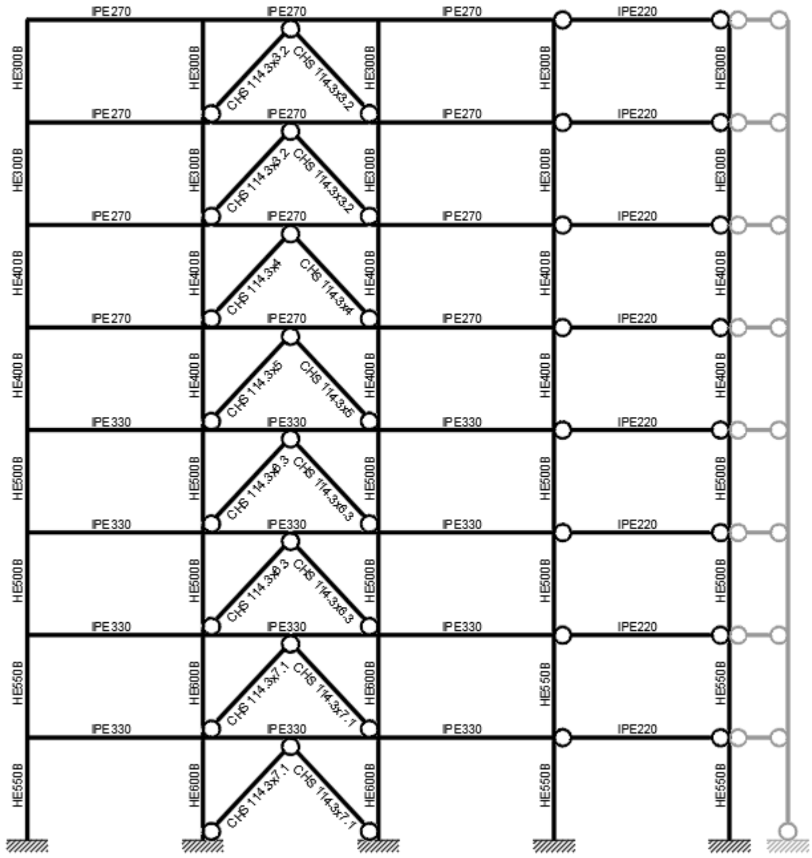

Figure A.34 – Designed structure 8 St_DC3_D-CBFs_X_ FREEDAM

❖ Structure code: 8 St_DC2_D-CBFs_Y_FREEDAM

Table A.91 – Beam, diagonal and column sections for 8 St_DC2_D-CBFs_Y_ FREEDAM

Storey	Bay 1	Bay 2	Bay 3	Bay 4 (pinned)
1-6	IPE 300 FREEDAM	IPE 300 FREEDAM	IPE 300 FREEDAM	IPE 270
7-8	IPE 270 FREEDAM	IPE 270 FREEDAM	IPE 270 FREEDAM	IPE 270
Storey	**Column 1-5**	**Column 2**	**Column 3**	**Column 4**
1-2	HE 550 B	HE 550 B	HE 550 B	HE 550 B
3-4	HE 450 B	HE 450 B	HE 450 B	HE 450 B
5-6	HE 360 B	HE 360 B	HE 360 B	HE 360 B
7-8	HE 260 B	HE 260 B	HE 260 B	HE 260 B

Storey	Diagonals
1-2	CHS 114.3x5
3-4	CHS 114.3x4
5-6	CHS 114.3x3.2
7-8	CHS 88.9x4

Weight of structural elements: 29981 kg

Buckling multiplier and amplification coefficient for the fundamental load combination: $\begin{cases} \alpha_{cr} = 12.50 \\ \frac{1}{1-\frac{1}{\alpha_{cr}}} = 1.09 \end{cases}$

Table A.92 – Modal information for 8 St_DC2_D-CBFs_Y_ FREEDAM

Mode	Vibration period (s)	Sum of effective modal masses on X direction
1	1.64	0.756
2	0.55	0.889
3	0.32	0.933
4	0.25	0.933
5	0.25	0.933
6	0.25	0.933
7	0.25	0.933

8	0.25	0.933

Table A.93 – Drift limitation at SD limit state for 8 St_DC2_D-CBFs_Y_ FREEDAM

Storey	$d_{r,SD}$ (m)	h_s (m)	$d_{r,SD}$ (rad)	$d_{r,SDadm}$ (rad)
1	0.015	3.5	0.00	0.02
2	0.025	3.5	0.01	0.02
3	0.028	3.5	0.01	0.02
4	0.029	3.5	0.01	0.02
5	0.030	3.5	0.01	0.02
6	0.029	3.5	0.01	0.02
7	0.028	3.5	0.01	0.02
8	0.020	3.5	0.01	0.02

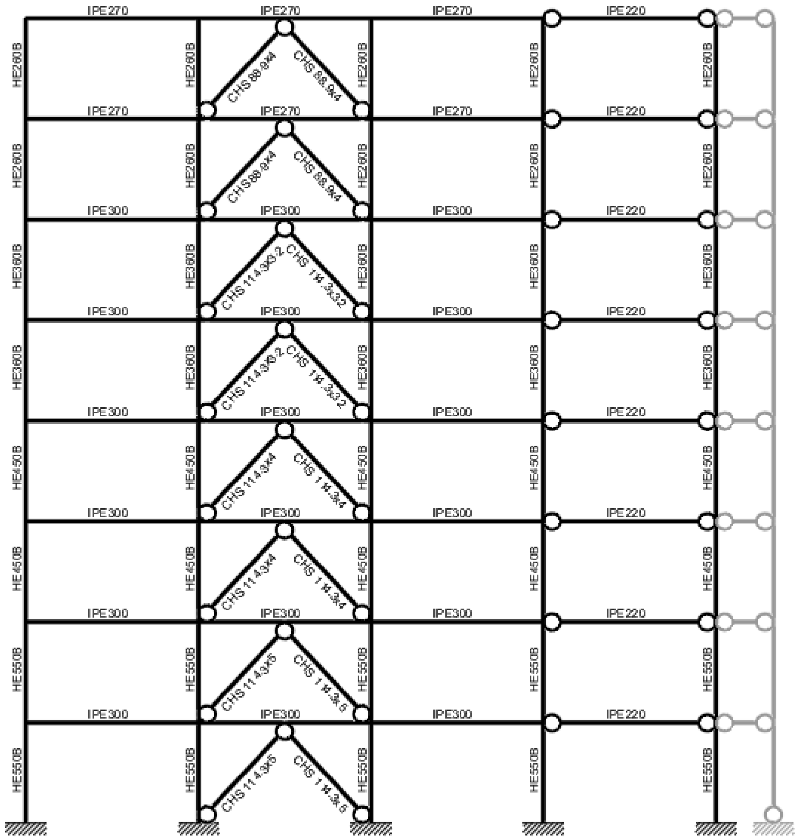

Figure A.35 – Designed structure 8 St_DC2_D-CBFs_Y_ FREEDAM

❖ Structure code: 8 St_DC3_D-CBFs_Y_FREEDAM

Table A.94 – Beam, diagonal and column sections for 8 St_DC3_D-CBFs_Y_FREEDAM

Storey	Bay 1	Bay 2	Bay 3	Bay 4 (pinned)
1-4	IPE 360 FREEDAM	IPE 300 FREEDAM	IPE 360 FREEDAM	IPE 270
5-8	IPE 300 FREEDAM	IPE 270 FREEDAM	IPE 300 FREEDAM	IPE 270
Storey	**Column 1-5**	**Column 2**	**Column 3**	**Column 4**
1-2	HE 550 B	HE 600 B	HE 600 B	HE 550 B
3-4	HE 500 B	HE 550 B	HE 550 B	HE 500 B
5-6	HE 400 B	HE 450 B	HE 450 B	HE 400 B
7-8	HE 300 B	HE 340 B	HE 340 B	HE 300 B
Storey	**Diagonals**			
1-2	CHS 114.3x7.1			
3-4	CHS 114.3x6.3			
5	CHS 114.3x5			
6	CHS 114.3x4			
7-8	CHS 114.3x3.2			

Weight of structural elements: 33709 kg

Buckling multiplier and amplification coefficient for the fundamental load combination: $\begin{cases} \alpha_{cr} = 17.59 \\ \frac{1}{1-\frac{1}{\alpha_{cr}}} = 1.00 \end{cases}$

Table A.95 – Modal information for 8 St_DC3_D-CBFs_Y_FREEDAM

Mode	Vibration period (s)	Sum of effective modal masses on X direction
1	1.41	0.745
2	0.49	0.892
3	0.27	0.936
4	0.25	0.936
5	0.25	0.936
6	0.25	0.936

7	0.25	0.936
8	0.25	0.936

Table A.96 – Drift limitation at SD limit state for 8 St_DC3_D-CBFs_Y_FREEDAM

Storey	$d_{r,SD}$ (m)	h_s (m)	$d_{r,SD}$ (rad)	$d_{r,SDadm}$ (rad)
1	0.018	3.5	0.01	0.02
2	0.027	3.5	0.01	0.02
3	0.029	3.5	0.01	0.02
4	0.029	3.5	0.01	0.02
5	0.033	3.5	0.01	0.02
6	0.036	3.5	0.01	0.02
7	0.036	3.5	0.01	0.02
8	0.026	3.5	0.01	0.02

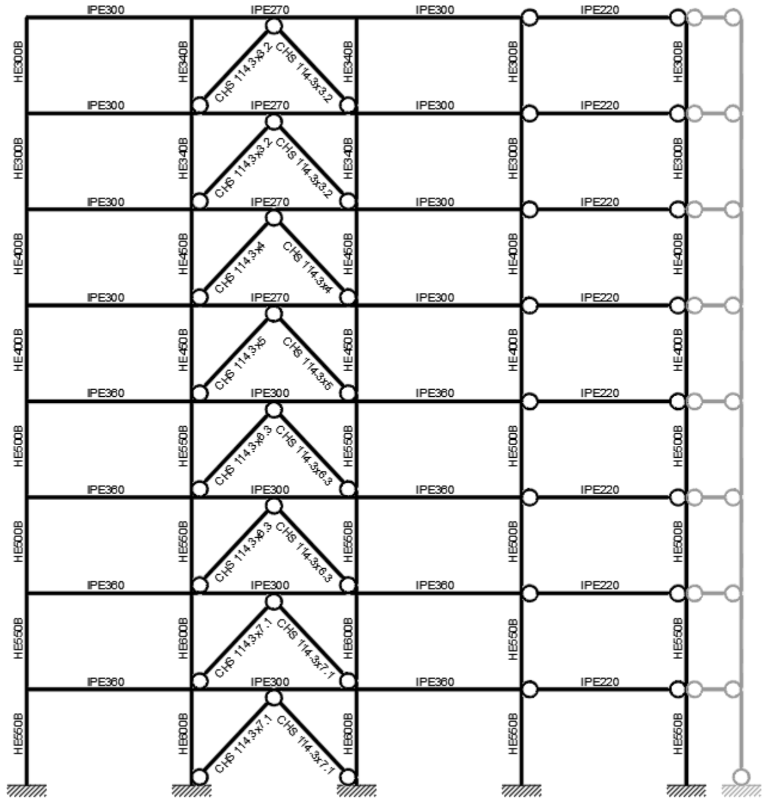

Figure A.36 – Designed structure 8 St_DC3_D-CBFs_Y_FREEDAM

APPENDIX B

PUSH-OVER ANALYSIS RESULTS

In this section the plastic hinge distribution for the study cases described in CHAPTER 4 are reported. A total number of 32 structures have been considered. These structures have been analysed by means of push-over analyses carried out by SAP2000 computer program.

For each structure, the design base shear seismic action (calculated for half the structure), the modal displacements and the static forces corresponding to the two distributions given by eqs. (6.1) and (6.2) are reported.

Low Rise Moment Resisting Frames (LR-MRFs)

- **Structure code: 4 St_DC2_MRFs_X_TRADITIONAL**

Base shear seismic action: F_b = 282.45 kN

Table B.1 – Modal displacements and seismic horizontal forces for 4

St_DC2_MRFs_X_TRADITIONAL

Storey	U_1 (m)	$F_{i\_1°}$ (kN)	F_{i_m} (kN)
1	0.012	22.41	71.90
2	0.030	57.91	71.90
3	0.048	93.91	71.90
4	0.060	108.21	66.74

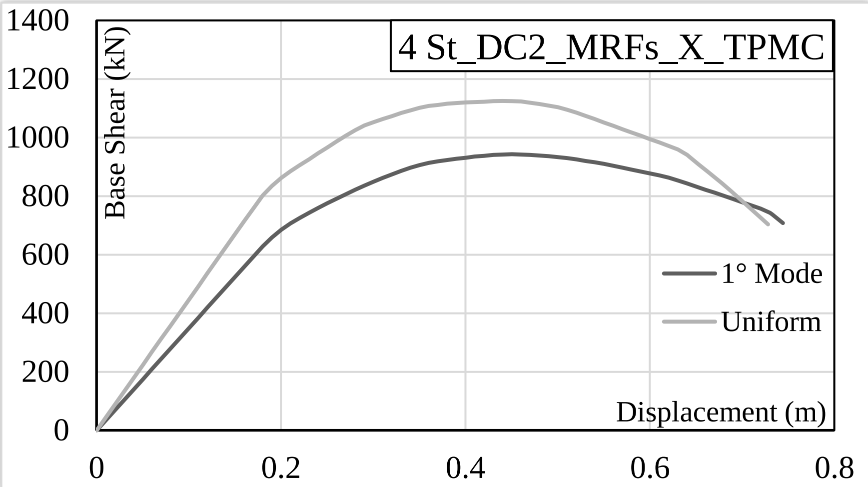

Figure B.1 – Push-over curves for 4 St_DC2_MRFs_X_TRADITIONAL

Table B.2 - Seismic performance for 4 St_DC2_MRFs_X_TRADITIONAL

CASE	d_1 (m)	V_1 (kN)	d_u (m)	V_u(kN)	μ (-)	q_R (-)
1° Mode	0.18	628.30	0.45	943.02	2.50	1.50
Uniform	0.18	801.93	0.44	1124.84	2.44	1.40

❖ Structure code: 4 St_DC3_MRFs_X_TRADITIONAL

Base shear seismic action: F_b = 238.88 kN

Table B.3 – Modal displacements and seismic horizontal forces for 4 St_DC3_MRFs_X_TRADITIONAL

Storey	U_1 (m)	$F_{i\_1°}$ (kN)	F_{i_m} (kN)

1	0.011	18.89	60.81
2	0.029	48.60	60.81
3	0.047	78.05	60.81
4	0.061	93.33	56.45

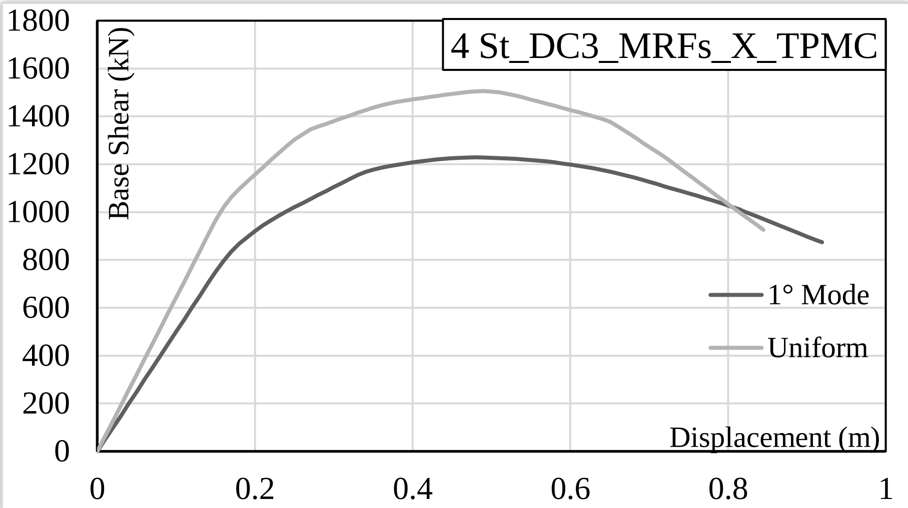

Figure B.2 – Push-over curves for 4 St_DC3_MRFs_X_TRADITIONAL

Table B.4 - Seismic performance for 4 St_DC3_MRFs_X_TRADITIONAL

CASE	d_1 (m)	V_1 (kN)	d_u (m)	V_u(kN)	μ (-)	q_R (-)
1° mode	0.16	796.76	0.48	1228.71	3.00	1.54
Uniform	0.16	1021.06	0.49	1505.56	3.06	1.47

❖ Structure code: 4 St_DC2_MRFs_Y_TRADITIONAL

Base shear seismic action: F_b = 282.45 kN

Table B.5 – Modal displacements and seismic horizontal forces for 4 St_DC2_MRFs_Y_TRADITIONAL

Storey	U_1 (m)	$F_{i\_1°}$ (kN)	F_{i_m} (kN)
1	0.012	22.41	71.90

2	0.030	57.92	71.90
3	0.048	93.92	71.90
4	0.060	108.21	66.74

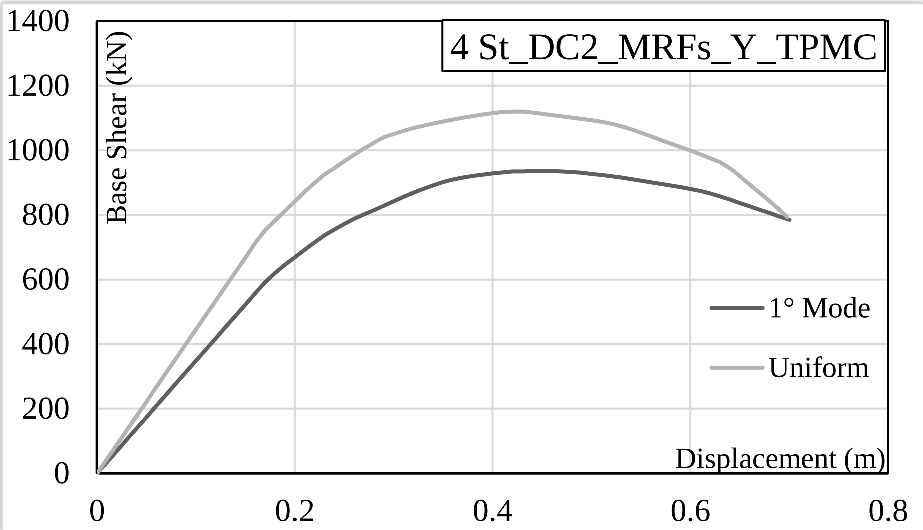

Figure B.3 – Push-over curves for 4 St_DC2_MRFs_Y_TRADITIONAL

Table B.6 - Seismic performance for 4 St_DC2_MRFs_Y_TRADITIONAL

CASE	d_1 (m)	V_1 (kN)	d_u (m)	V_u(kN)	μ (-)	q_R (-)
1° mode	0.17	591.26	0.45	935.60	2.64	1.58
Uniform	0.17	752.85	0.42	1119.66	2.47	1.49

❖ Structure code: 4 St_DC3_MRFs_Y_TRADITIONAL

Base shear seismic action: F_b = 238.88 kN

Table B.7 – Modal displacements and seismic horizontal forces for 4 St_DC3_MRFs_Y_TRADITIONAL

Storey	U_1 (m)	$F_{i\_1°}$ (kN)	F_{i_m} (kN)
1	0.011	18.89	60.81
2	0.029	48.59	60.81

3	0.047	78.06	60.81
4	0.061	93.34	56.45

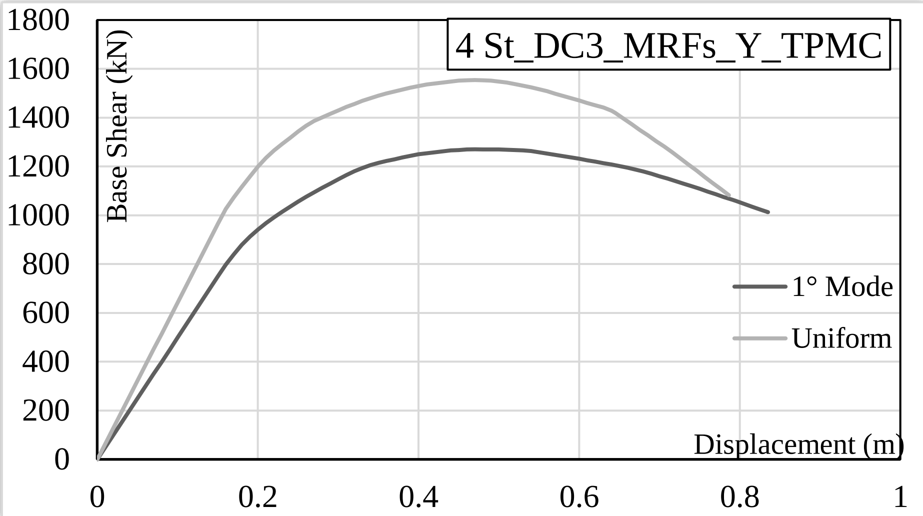

Figure B.4 – Push-over curves for 4 St_DC3_MRFs_Y_TRADITIONAL

Table B.8 - Seismic performance for 4 St_DC3_MRFs_Y_TRADITIONAL

CASE	d_1 (m)	V_1 (kN)	d_u (m)	V_u(kN)	μ (-)	q_R (-)
1° mode	0.16	798.26	0.47	1270.32	2.93	1.59
Uniform	0.16	1025.61	0.47	1553.98	2.93	1.52

❖ Structure code: 4 St_DC2_MRFs_X_FREEDAM

Base shear seismic action: F_b = 258.63 kN

Table B.9 – Modal displacements and seismic horizontal forces for 4 St_DC2_MRFs_X_FREEDAM

Storey	U_1 (m)	$F_{i\_1°}$ (kN)	F_{i_m} (kN)
1	-0.012	20.77	65.84
2	-0.030	52.90	65.84
3	-0.048	86.12	65.84

4	-0.060	98.83	61.11

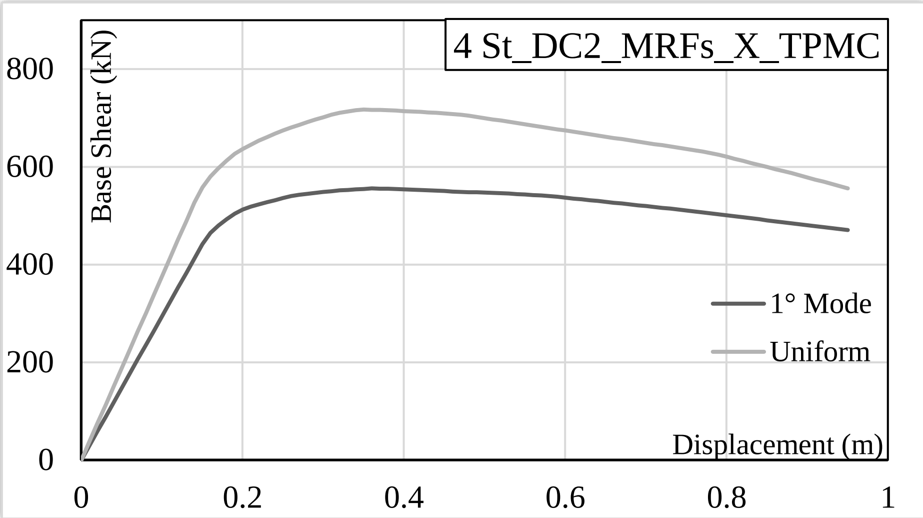

Figure B.5 – Push-over curves for 4 St_DC2_MRFs_X_FREEDAM

Table B.10 - Seismic performance for 4 St_DC2_MRFs_X_FREEDAM

CASE	d_1 (m)	V_1 (kN)	d_u (m)	V_u(kN)	μ (-)	q_R (-)
1° mode	0.15	441.49	0.36	555.84	2.40	1.26
Uniform	0.14	526.62	0.35	717.18	2.50	1.36

❖ Structure code: 4 St_DC3_MRFs_X_FREEDAM

Base shear seismic action: F_b = 238.88 kN

Table B.11 – Modal displacements and seismic horizontal forces for 4 St_DC3_MRFs_X_FREEDAM

Storey	U_1 (m)	$F_{i\_1°}$ (kN)	F_{i_m} (kN)
1	0.012	20.21	60.81
2	0.030	49.06	60.81
3	0.048	78.38	60.81
4	0.060	91.23	56.45

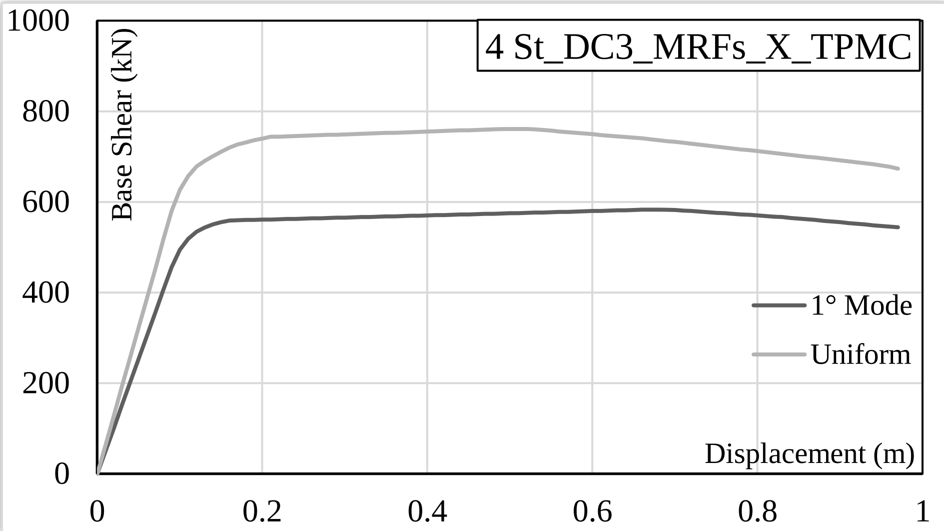

Figure B.6 – Push-over curves for 4 St_DC3_MRFs_X_FREEDAM

Table B.12 - Seismic performance for 4 St_DC3_MRFs_X_FREEDAM

CASE	d_1 (m)	V_1 (kN)	d_u (m)	V_u(kN)	μ (-)	q_R (-)
1° mode	0.09	455.88	0.69	582.65	7.65	1.28
Uniform	0.09	580.20	0.49	760.74	5.43	1.31

❖ Structure code: 4 St_DC2_MRFs_Y_FREEDAM

Base shear seismic action: F_b = 296.09 kN

Table B.13 – Modal displacements and seismic horizontal forces for 4 St_DC2_MRFs_Y_FREEDAM

Storey	U_1 (m)	$F_{i\_1°}$ (kN)	F_{i_m} (kN)
1	-0.011	23.11	75.37
2	-0.028	58.56	75.37
3	-0.048	97.93	75.37
4	-0.061	116.48	69.96

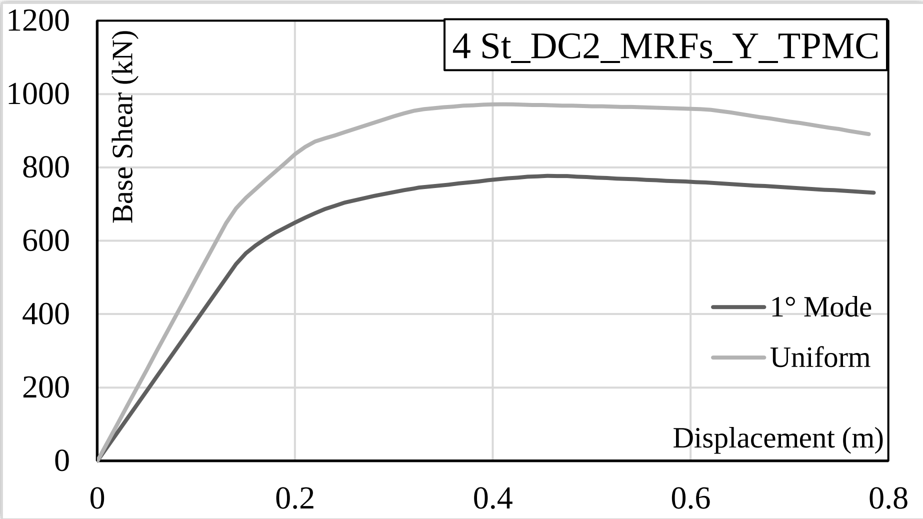

Figure B.7 – Push-over curves for 4 St_DC2_MRFs_Y_FREEDAM

Table B.14 - Seismic performance for 4 St_DC2_MRFs_Y_FREEDAM

CASE	d_1 (m)	V_1 (kN)	d_u (m)	V_u(kN)	μ (-)	q_R (-)
1° mode	0.14	536.07	0.46	776.89	3.25	1.45
Uniform	0.13	647.72	0.41	971.99	3.15	1.50

❖ Structure code: 4 St_DC3_MRFs_Y_FREEDAM

Base shear seismic action: F_b = 238.88 kN

Table B.15 – Modal displacements and seismic horizontal forces for 4 St_DC3_MRFs_Y_FREEDAM

Storey	U_1 (m)	$F_{i\_1°}$ (kN)	F_{i_m} (kN)
1	0.012	20.21	60.81
2	0.030	49.06	60.81
3	0.048	78.38	60.81
4	0.060	91.24	56.45

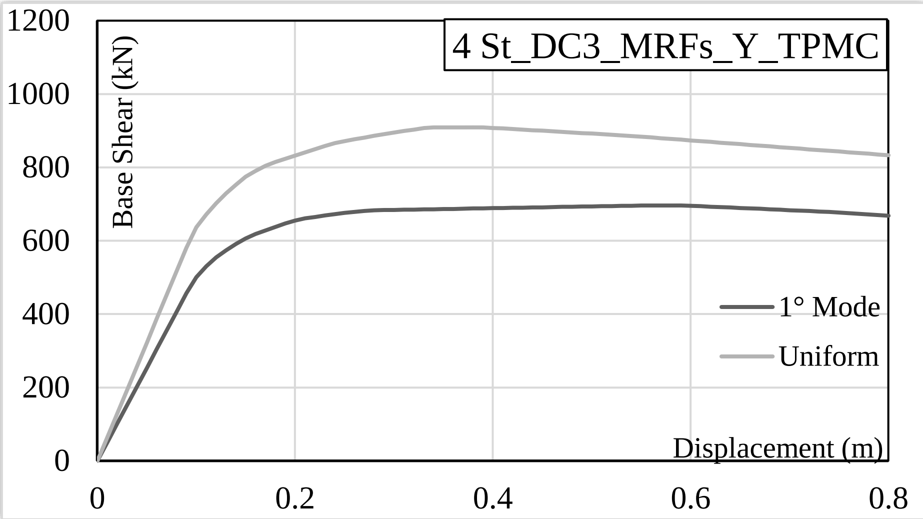

Figure B.8 – Push-over curves for 4 St_DC3_MRFs_Y_FREEDAM

Table B.16 - Seismic performance for 4 St_DC3_MRFs_Y_FREEDAM

CASE	d_1 (m)	V_1 (kN)	d_u (m)	V_u(kN)	μ (-)	q_R (-)
1° mode	0.10	500.20	0.59	696.17	5.89	1.39
Uniform	0.10	636.77	0.38	909.02	3.79	1.43

Medium Rise Moment Resisting Frames (MR-MRFs)

❖ Structure code: 8 St_DC2_MRFs_X_TRADITIONAL

Base shear seismic action: F_b = 300.34 kN

Table B.17 – Modal displacements and seismic horizontal forces for 8 St_DC2_MRFs_X_TRADITIONAL

Storey	U_1 (m)	$F_{i\_1°}$ (kN)	F_{i_m} (kN)
1	-0.002	3.78	37.88
2	-0.008	11.53	37.88
3	-0.014	21.46	37.88

4	-0.021	32.37	37.88
5	-0.029	44.10	37.88
6	-0.036	55.46	37.88
7	-0.042	65.06	37.88
8	-0.047	66.58	35.16

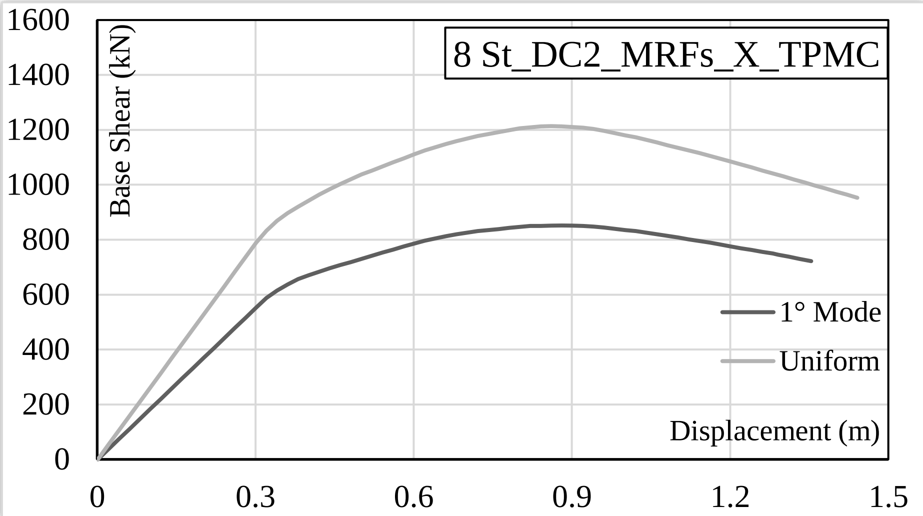

Figure B.9 – Push-over curves for 8 St_DC2_MRFs_X_TRADITIONAL

Table B.18 - Seismic performance for 8 St_DC2_MRFs_X_TRADITIONAL

CASE	d_1 (m)	V_1 (kN)	d_u (m)	V_u(kN)	μ (-)	q_R (-)
1° mode	0.34	614.56	0.88	851.72	2.58	1.39
Uniform	0.30	789.45	0.86	1213.66	2.86	1.54

❖ Structure code: 8 St_DC3_MRFs_X_TRADITIONAL

Base shear seismic action: F_b = 287.24 kN

Table B.19 – Modal displacements and seismic horizontal forces for 8 St_DC3_MRFs_X_TRADITIONAL

Storey	U_1 (m)	$F_{i\_1°}$ (kN)	F_{i_m} (kN)

1	0.002	3.45	36.23
2	0.007	10.57	36.23
3	0.014	20.01	36.23
4	0.021	30.68	36.23
5	0.029	42.11	36.23
6	0.036	53.20	36.23
7	0.043	62.68	36.23
8	0.047	64.54	33.63

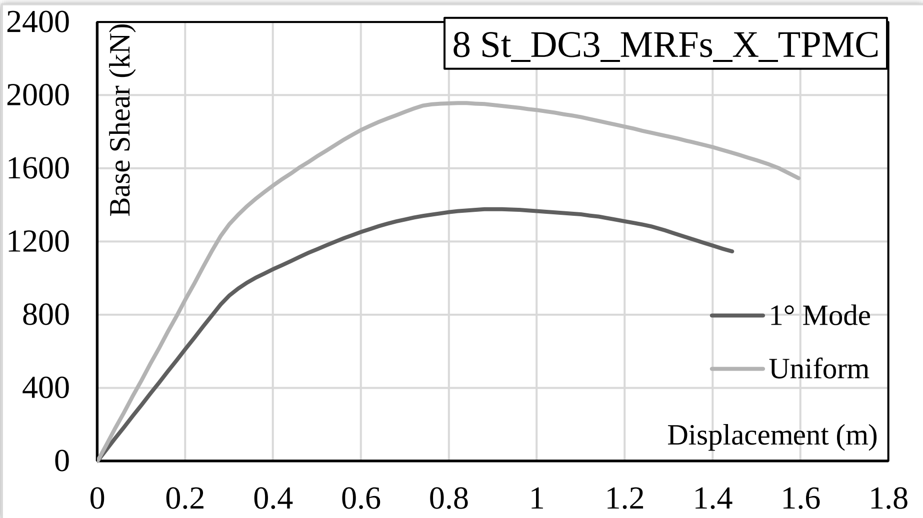

Figure B.10 – Push-over curves for 8 St_DC3_MRFs_X_TRADITIONAL

Table B.20 - Seismic performance for 8 St_DC3_MRFs_X_TRADITIONAL

CASE	d_1 (m)	V_1 (kN)	d_u (m)	V_u(kN)	μ (-)	q_R (-)
1° mode	0.28	855.66	0.90	1376.45	3.21	1.61
Uniform	0.28	1229.29	0.82	1956.94	2.92	1.59

❖ Structure code: 8 St_DC2_MRFs_Y_TRADITIONAL

Base shear seismic action: F_b = 300.34 kN

Table B.21 – Modal displacements and seismic horizontal forces for 8 St_DC2_MRFs_Y_TRADITIONAL

Storey	U_1 (m)	$F_{i\_1°}$ (kN)	F_{i_m} (kN)
1	-0.002	3.77	37.88
2	-0.008	11.53	37.88
3	-0.014	21.46	37.88
4	-0.021	32.38	37.88
5	-0.029	44.10	37.88
6	-0.036	55.46	37.88
7	-0.042	65.06	37.88
8	-0.047	66.58	35.16

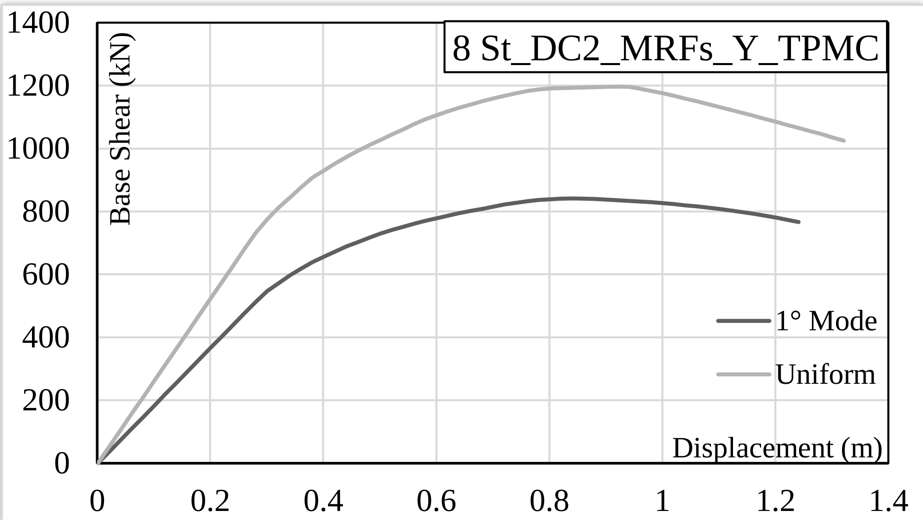

Figure B.11 – Push-over curves for 8 St_DC2_MRFs_Y_TRADITIONAL

Table B.22 - Seismic performance for 8 St_DC2_MRFs_Y_TRADITIONAL

CASE	d_1 (m)	V_1 (kN)	d_u (m)	V_u(kN)	μ (-)	q_R (-)
1° mode	0.30	547.05	0.84	841.38	2.79	1.54
Uniform	0.28	734.14	0.92	1196.66	3.28	1.63

- **Structure code: 8 St_DC3_MRFs_Y_TRADITIONAL**

Base shear seismic action: F_b = 287.24 kN

Table B.23 – Modal displacements and seismic horizontal forces for 8 St_DC3_MRFs_Y_TRADITIONAL

Storey	U_1 (m)	$F_{i\_1°}$ (kN)	F_{i_m} (kN)
1	-0.002	3.45	36.23
2	-0.007	10.56	36.23
3	-0.014	20.01	36.23
4	-0.021	30.69	36.23
5	-0.029	42.11	36.23
6	-0.036	53.20	36.23
7	-0.043	62.69	36.23
8	-0.047	64.54	33.63

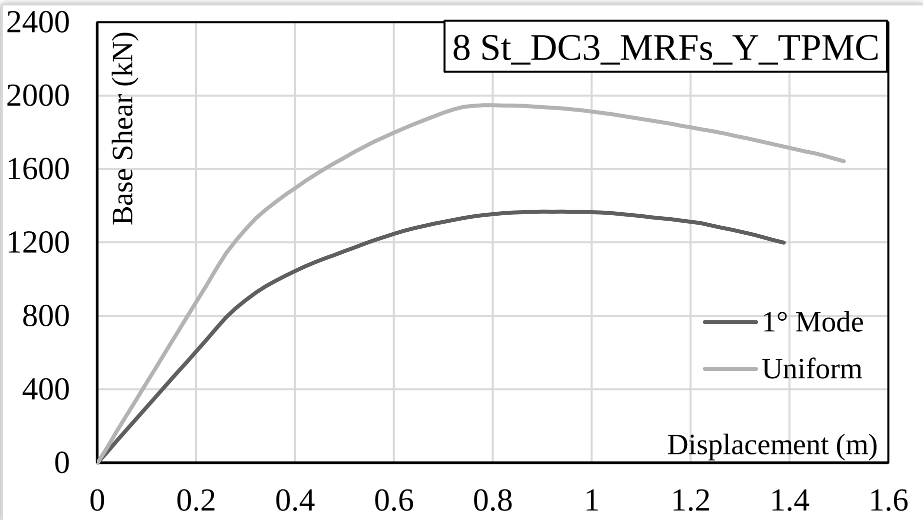

Figure B.12 – Push-over curves for 8 St_DC3_MRFs_Y_TRADITIONAL

Table B.24 - Seismic performance for 8 St_DC3_MRFs_Y_TRADITIONAL

CASE	d_1 (m)	V_1 (kN)	d_u (m)	V_u(kN)	μ (-)	q_R (-)
1° mode	0.26	792.67	0.92	1367.60	3.53	1.73
Uniform	0.26	1141.27	0.80	1947.65	3.07	1.71

❖ Structure code: 8 St_DC2_MRFs_X_FREEDAM

Base shear seismic action: F_b = 351.51 kN

Table B.25 – Modal displacements and seismic horizontal forces for 8 St_DC2_MRFs_X_FREEDAM

Storey	U_1 (m)	$F_{i\_1°}$ (kN)	F_{i_m} (kN)
1	0.003	4.57	44.34
2	0.008	13.65	44.34
3	0.014	25.40	44.34
4	0.021	38.22	44.34
5	0.029	52.02	44.34
6	0.036	65.10	44.34
7	0.042	75.80	44.34
8	0.046	76.75	41.15

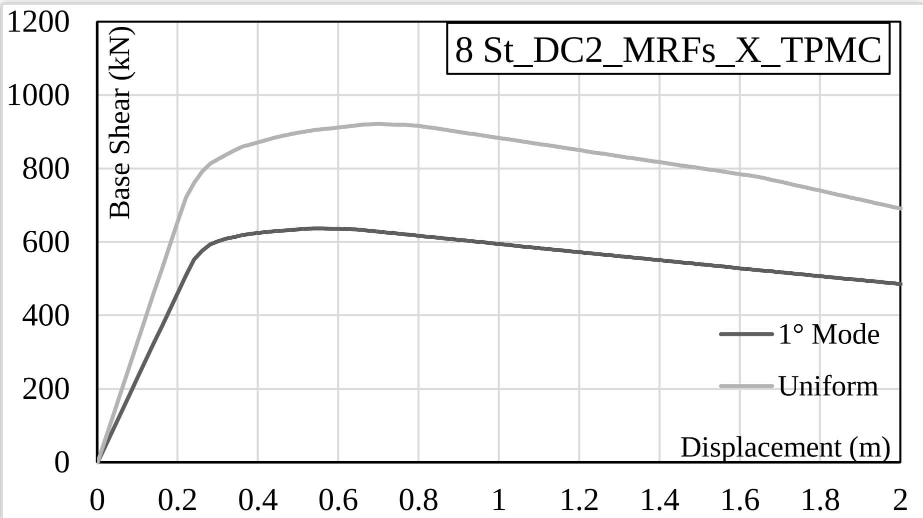

Figure B.13 – Push-over curves for 8 St_DC2_MRFs_X_FREEDAM

Table B.26 - Seismic performance for 8 St_DC2_MRFs_X_FREEDAM

CASE	d_1 (m)	V_1 (kN)	d_u (m)	V_u(kN)	μ (-)	q_R (-)
1° mode	0.24	552.34	0.54	636.87	2.24	1.15

Uniform	0.22	721.53	0.70	921.23	3.17	1.28

❖ Structure code: 8 St_DC3_MRFs_X_FREEDAM

Base shear seismic action: F_b = 372.51 kN

Table B.27 – Modal displacements and seismic horizontal forces for 8 St_DC3_MRFs_X_FREEDAM

Storey	U_1 (m)	$F_{i\_1°}$ (kN)	F_{i_m} (kN)
1	-0.003	5.42	46.99
2	-0.008	15.28	46.99
3	-0.014	27.35	46.99
4	-0.021	40.00	46.99
5	-0.028	53.58	46.99
6	-0.035	66.78	46.99
7	-0.042	80.20	46.99
8	-0.048	83.91	43.61

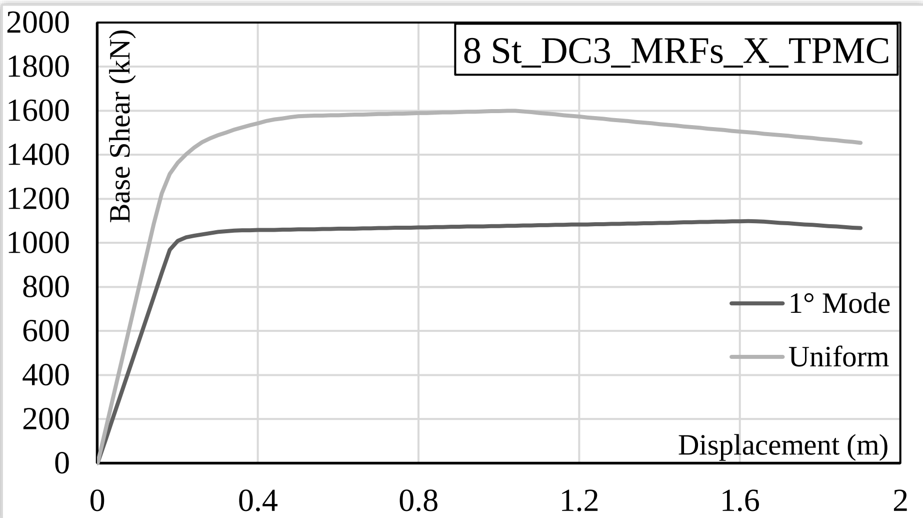

Figure B.14 – Push-over curves for 8 St_DC3_MRFs_X_FREEDAM

Table B.28 - Seismic performance for 8 St_DC3_MRFs_X_FREEDAM

CASE	d_1 (m)	V_1 (kN)	d_u (m)	V_u(kN)	μ (-)	q_R (-)
1° Mode	0.18	967.52	1.62	1098.63	8.95	1.14
Uniform	0.16	1224.43	1.02	1599.25	6.34	1.31

❖ Structure code: 8 St_DC2_MRFs_Y_FREEDAM

Base shear seismic action: F_b = 356.57 kN

Table B.29 – Modal displacements and seismic horizontal forces for 8 St_DC2_MRFs_Y_FREEDAM

Storey	U_1 (m)	$F_{i\_1°}$ (kN)	F_{i_m} (kN)
1	-0.003	4.66	44.97
2	-0.008	13.92	44.97
3	-0.014	25.84	44.97
4	-0.021	38.80	44.97
5	-0.029	52.75	44.97
6	-0.036	65.97	44.97
7	-0.042	76.82	44.97
8	-0.046	77.81	41.75

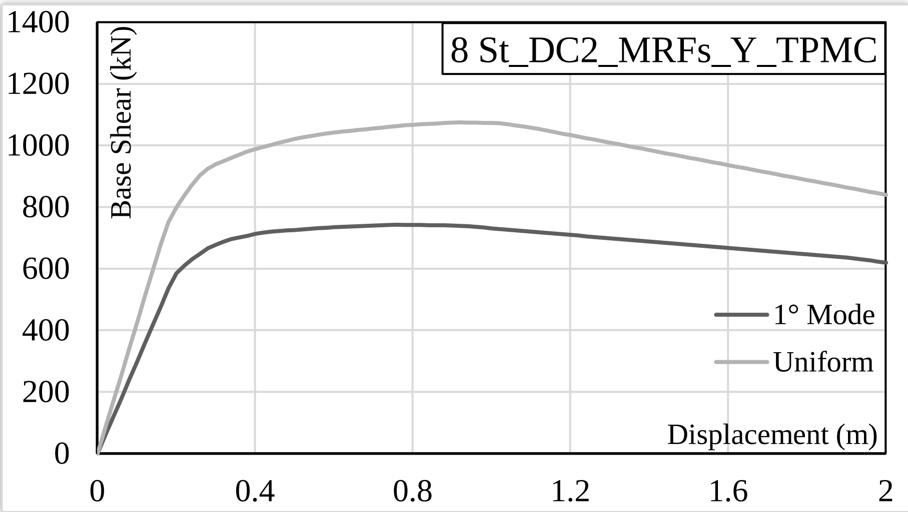

Figure B.15 – Push-over curves for 8 St_DC2_MRFs_Y_FREEDAM

Table B.30 - Seismic performance for 8 St_DC2_MRFs_Y_FREEDAM

CASE	d_1 (m)	V_1 (kN)	d_u (m)	V_u(kN)	μ (-)	q_R (-)
1° Mode	0.20	585.43	0.76	742.54	3.78	1.27
Uniform	0.18	750.72	0.92	1074.88	5.08	1.43

❖ Structure code: 8 St_DC3_MRFs_Y_FREEDAM

Base shear seismic action: F_b = 393.76 kN

Table B.31 – Modal displacements and seismic horizontal forces for 8 St_DC3_MRFs_Y_FREEDAM

Storey	U_1 (m)	$F_{i\_1°}$ (kN)	F_{i_m} (kN)
1	-0.003	5.59	49.67
2	-0.008	15.97	49.67
3	-0.014	28.83	49.67
4	-0.021	42.48	49.67
5	-0.028	56.98	49.67
6	-0.035	71.07	49.67
7	-0.042	84.50	49.67
8	-0.047	88.36	46.10

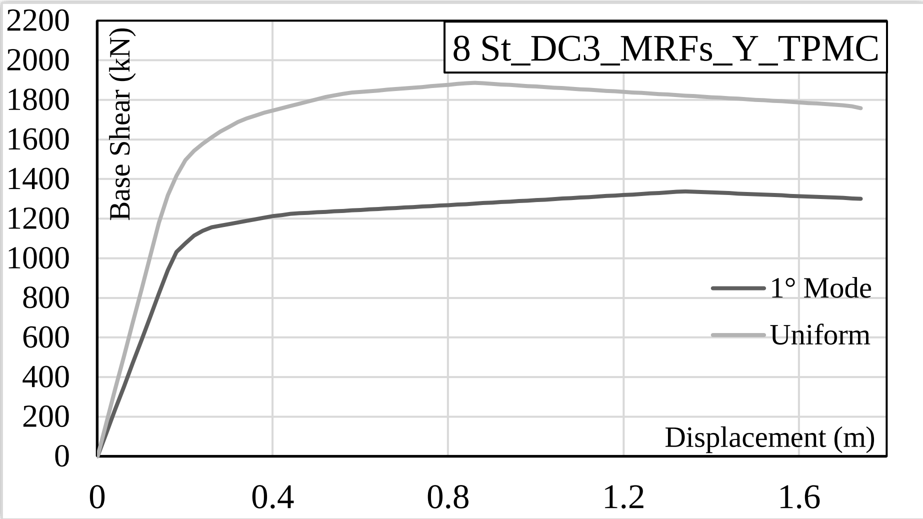

Figure B.16 – Push-over curves for 8 St_DC3_MRFs_Y_FREEDAM

Table B.32 - Seismic performance for 8 St_DC3_MRFs_Y_FREEDAM

CASE	d_1 (m)	V_1 (kN)	d_u (m)	V_u(kN)	μ (-)	q_R (-)
1° Mode	0.18	1032.16	1.34	1337.51	7.41	1.30
Uniform	0.16	1318.03	0.86	1886.14	5.35	1.43

Low Rise Dual Concentrically Braced Frames (LR-D-CBFs)

❖ Structure code: 4 St_DC2_D-CBFs_X_TRADITIONAL

Base shear seismic action: F_b = 650.46 kN

Table B.33 – Modal displacements and seismic horizontal forces for 4 St_DC2_D-CBFs_X_TRADITIONAL

Storey	U_1 (m)	$F_{i\_1°}$ (kN)	F_{i_m} (kN)
1	0.013	56.50	165.59
2	0.031	136.64	165.59
3	0.048	212.33	165.59

4	0.059	245.00	153.70

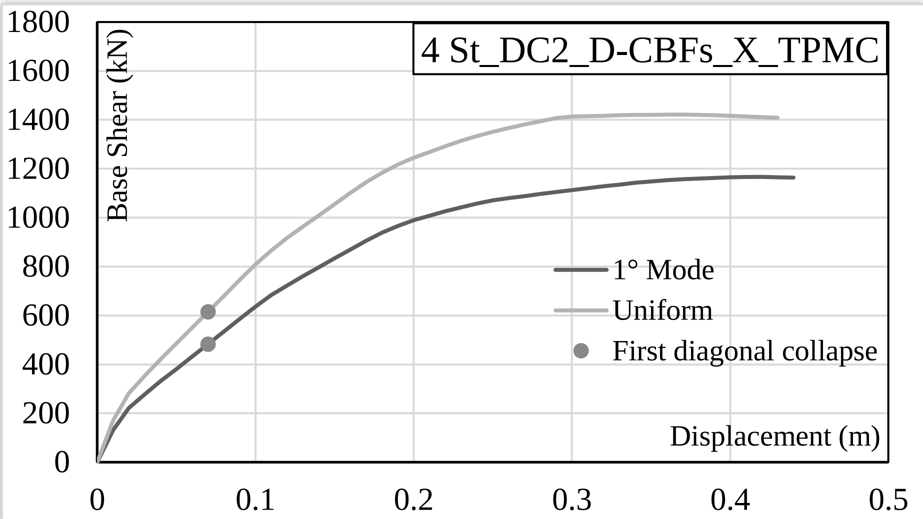

Figure B.17 – Push-over curves for 4 St_DC2_D-CBFs_X_TRADITIONAL

Table B.34 - Seismic performance data for 4 St_DC2_D-CBFs_X_TRADITIONAL

CASE	d_1 (m)	V_1 (kN)	d_u (m)	V_u(kN)	μ (-)	q_R (-)
1° Mode	0.11	683.10	0.42	1166.81	3.82	1.71
Uniform	0.11	865.90	0.36	1421.24	3.27	1.64

❖ Structure code: 4 St_DC3_D-CBFs_X_TRADITIONAL

Base shear seismic action: F_b = 627.14 kN

Table B.35 – Modal displacements and seismic horizontal forces for 4 St_DC3_D-CBFs_X_TRADITIONAL

Storey	U_1 (m)	$F_{i\_1°}$ (kN)	F_{i_m} (kN)
1	-0.013	55.46	159.65
2	-0.031	133.94	159.65
3	-0.048	203.91	159.65

4	-0.059	233.83	148.19

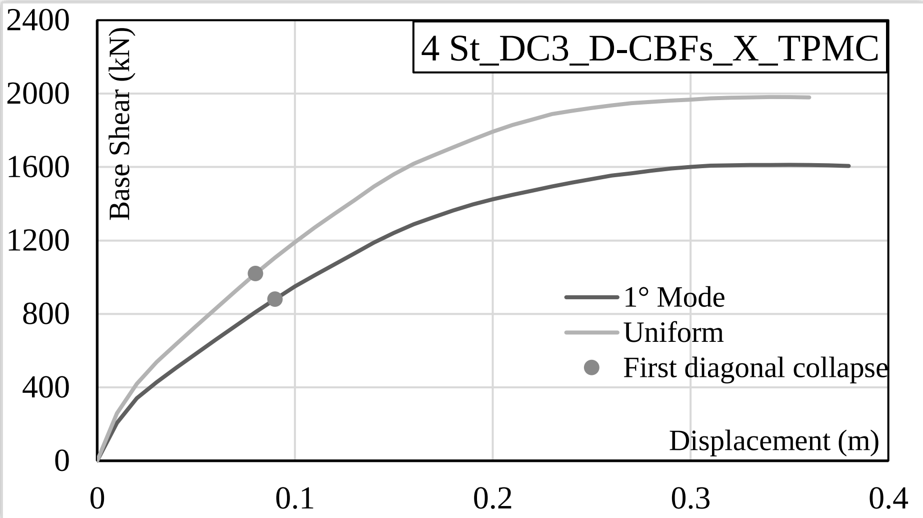

Figure B.18 – Push-over curves for 4 St_DC3_D-CBFs_X_TRADITIONAL

Table B.36 - Seismic performance data for 4 St_DC3_D-CBFs_X_TRADITIONAL

CASE	d_1 (m)	V_1 (kN)	d_u (m)	V_u(kN)	μ (-)	q_R (-)
1° Mode	0.09	880.75	0.35	1611.99	3.89	1.83
Uniform	0.08	1019.94	0.34	1981.44	4.25	1.94

❖ Structure code: 4 St_DC2_D-CBFs_Y_TRADITIONAL

Base shear seismic action: F_b = 650.46 kN

Table B.37 – Modal displacements and seismic horizontal forces for 4 St_DC2_D-CBFs_Y_TRADITIONAL

Storey	U_1 (m)	$F_{i\_1°}$ (kN)	F_{i_m} (kN)
1	0.013	56.85	165.59
2	0.031	138.68	165.59
3	0.048	212.81	165.59
4	0.059	242.12	153.70

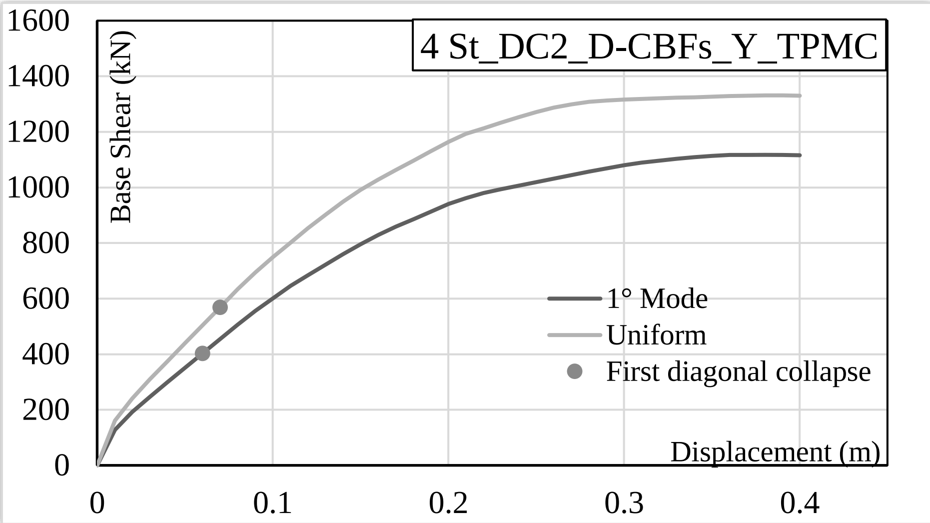

Figure B.19 – Push-over curves for 4 St_DC2_D-CBFs_Y_TRADITIONAL

Table B.38 - Seismic performance data for 4 St_DC2_D-CBFs_Y_TRADITIONAL

CASE	d_1 (m)	V_1 (kN)	d_u (m)	V_u(kN)	μ (-)	q_R (-)
1° Mode	0.09	555.56	0.38	1117.20	4.22	2.01
Uniform	0.09	694.04	0.39	1331.19	4.33	1.92

❖ Structure code: 4 St_DC3_D-CBFs_Y_TRADITIONAL

Base shear seismic action: F_b = 627.14 kN

Table B.39 – Modal displacements and seismic horizontal forces for 4 St_DC3_D-CBFs_Y_TRADITIONAL

Storey	U_1 (m)	$F_{i\_1°}$ (kN)	F_{i_m} (kN)
1	0.013	55.45	159.65
2	0.031	133.93	159.65
3	0.048	203.91	159.65
4	0.059	233.84	148.19

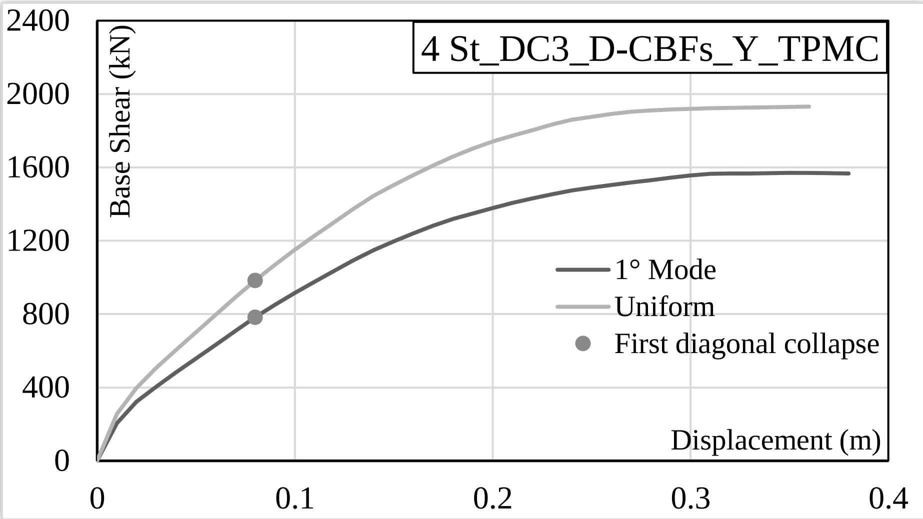

Figure B.20 – Push-over curves for 4 St_DC3_D-CBFs_Y_TRADITIONAL

Table B.40 - Seismic performance data for 4 St_DC3_D-CBFs_Y_TRADITIONAL

CASE	d_1 (m)	V_1 (kN)	d_u (m)	V_u(kN)	μ (-)	q_R (-)
1° Mode	0.08	782.40	0.36	1569.87	4.50	2.01
Uniform	0.08	982.94	0.36	1931.40	4.50	1.96

❖ Structure code: 4 St_DC2_D-CBFs_X_FREEDAM

Base shear seismic action: F_b = 643.65 kN

Table B.41 – Modal displacements and seismic horizontal forces for 4 St_DC2_D-CBFs_X_FREEDAM

Storey	U_1 (m)	$F_{i\_1°}$ (kN)	F_{i_m} (kN)
1	0.014	61.96	163.85
2	0.032	137.68	163.85
3	0.048	207.83	163.85
4	0.059	236.18	152.09

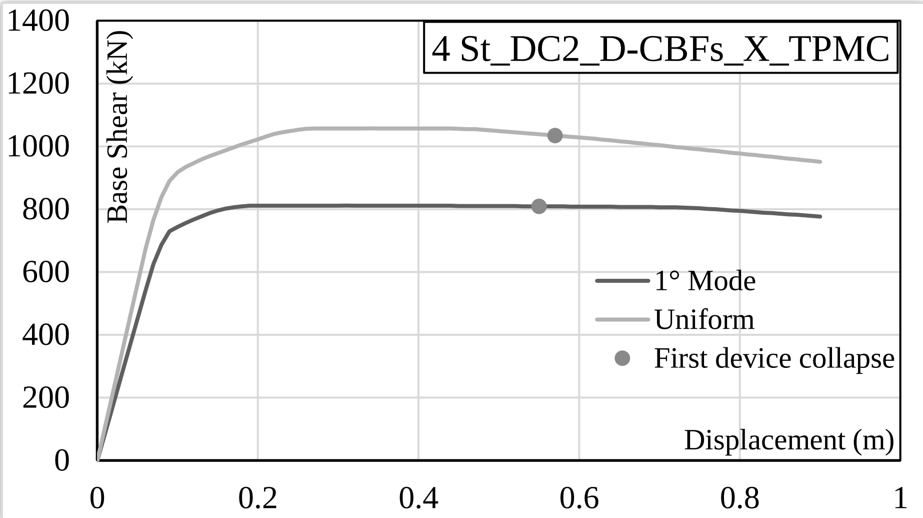

Figure B.21 – Push-over curves for 4 St_DC2_D-CBFs_X_FREEDAM

Table B.42 - Seismic performance data for 4 St_DC2_D-CBFs_X_FREEDAM

CASE	d_1 (m)	V_1 (kN)	d_u (m)	V_u(kN)	μ (-)	q_R (-)
1° Mode	0.07	624.91	0.31	811.45	4.42	1.30
Uniform	0.07	765.88	0.34	1057.14	4.85	1.38

❖ Structure code: 4 St_DC3_D-CBFs_X_FREEDAM

Base shear seismic action: F_b = 534.08 kN

Table B.43 – Modal displacements and seismic horizontal forces for 4 St_DC3_D-CBFs_X_FREEDAM

Storey	U_1 (m)	$F_{i\_1°}$ (kN)	F_{i_m} (kN)
1	0.014	49.25	135.96
2	0.031	111.86	135.96
3	0.048	174.13	135.96
4	0.059	198.84	126.20

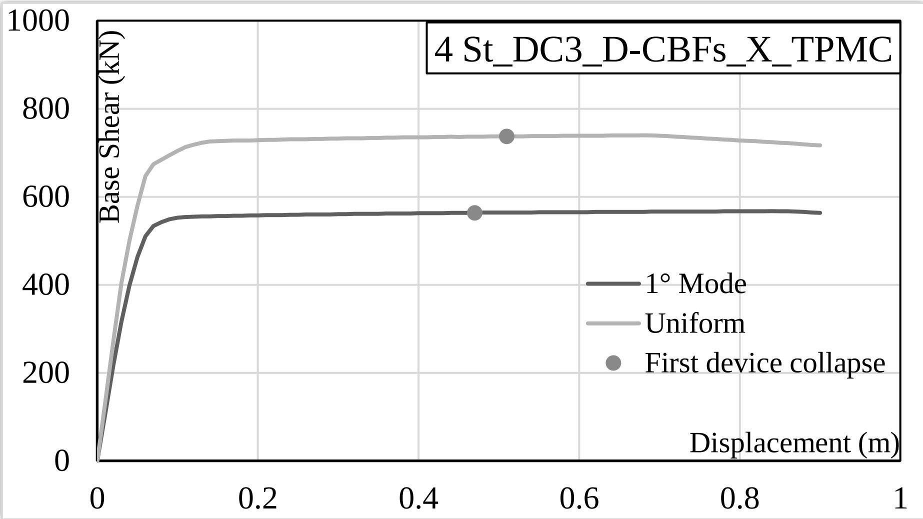

Figure B.22 – Push-over curves for 4 St_DC3_D-CBFs_X_FREEDAM

Table B.44 - Seismic performance data for 4 St_DC3_D-CBFs_X_FREEDAM

CASE	d_1 (m)	V_1 (kN)	d_u (m)	V_u(kN)	μ (-)	q_R (-)
1° Mode	0.03	316.10	0.84	567.20	27.86	1.79
Uniform	0.03	403.76	0.68	739.55	22.55	1.83

❖ Structure code: 4 St_DC2_D-CBFs_Y_FREEDAM

Base shear seismic action: F_b = 643.65 kN

Table B.45 – Modal displacements and seismic horizontal forces for 4 St_DC2_D-CBFs_Y_FREEDAM

Storey	U_1 (m)	$F_{i\_1°}$ (kN)	F_{i_m} (kN)
1	0.014	61.86	163.85
2	0.032	137.50	163.85
3	0.048	207.79	163.85
4	0.059	236.51	152.09

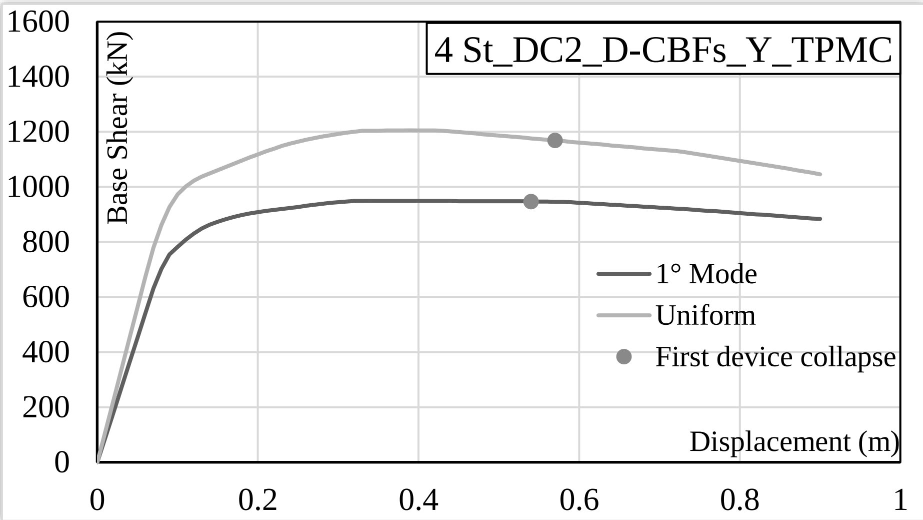

Figure B.23 – Push-over curves for 4 St_DC2_D-CBFs_Y_FREEDAM

Table B.46 - Seismic performance data for 4 St_DC2_D-CBFs_Y_FREEDAM

CASE	d_1 (m)	V_1 (kN)	d_u (m)	V_u(kN)	μ (-)	q_R (-)
1° Mode	0.07	631.61	0.34	949.17	4.85	1.50
Uniform	0.07	778.97	0.39	1205.23	5.56	1.55

❖ Structure code: 4 St_DC3_D-CBFs_Y_FREEDAM

Base shear seismic action: F_b = 534.08 kN

Table B.47 – Modal displacements and seismic horizontal forces for 4 St_DC3_D-CBFs_Y_FREEDAM

Storey	U_1 (m)	$F_{i\_1°}$ (kN)	F_{i_m} (kN)
1	-0.013	48.65	135.96
2	-0.031	111.95	135.96
3	-0.048	174.23	135.96
4	-0.059	199.25	126.20

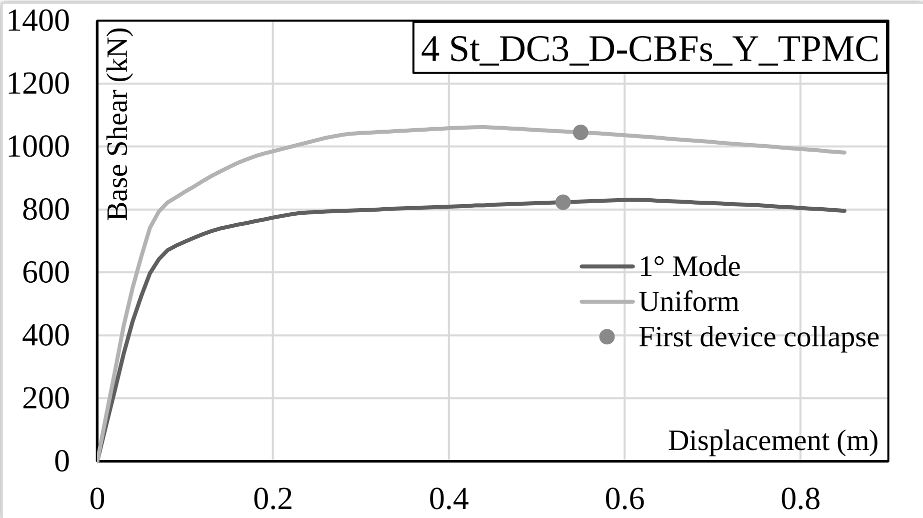

Figure B.24 – Push-over curves for 4 St_DC3_D-CBFs_Y_FREEDAM

Table B.48 - Seismic performance data for 4 St_DC3_D-CBFs_Y_FREEDAM

CASE	d_1 (m)	V_1 (kN)	d_u (m)	V_u(kN)	μ (-)	q_R (-)
1° Mode	0.04	445.04	0.26	793.28	6.48	1.78
Uniform	0.04	551.03	0.25	1020.41	6.23	1.85

Medium Rise Dual Concentrically Braced Frames (MR-D-CBFs)

❖ Structure code: 8 St_DC2_D-CBFs_X_TRADITIONAL

Base shear seismic action: F_b = 677.95 kN

Table B.49 – Modal displacements and seismic horizontal forces for 8 St_DC2_D-CBFs_X_TRADITIONAL

Storey	U_1 (m)	$F_{i\_1°}$ (kN)	F_{i_m} (kN)
1	0.003	10.37	85.51
2	0.009	29.40	85.51
3	0.015	52.41	85.51

4	0.022	76.46	85.51
5	0.030	101.30	85.51
6	0.036	123.86	85.51
7	0.042	141.79	85.51
8	0.045	142.37	79.37

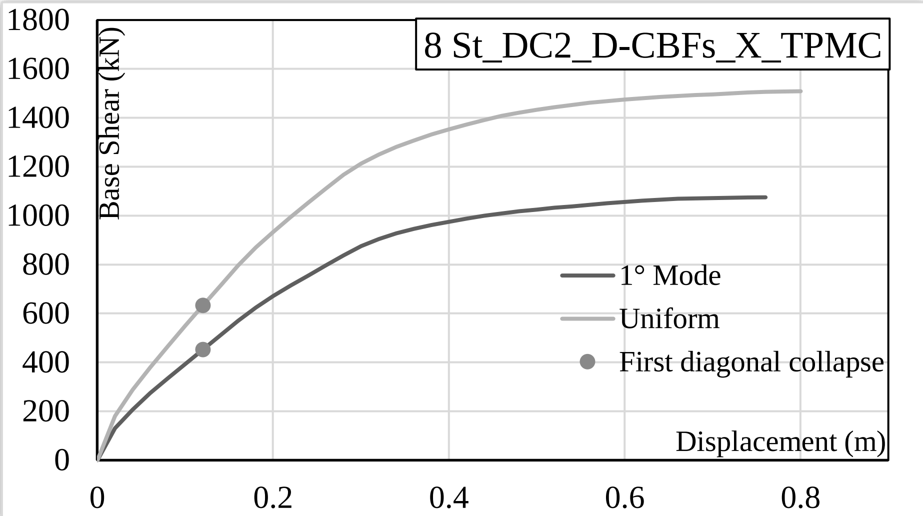

Figure B.25 – Push-over curves for 8 St_DC2_D-CBFs_X_TRADITIONAL

Table B.50 - Seismic performance data for 8 St_DC2_D-CBFs_X_TRADITIONAL

CASE	d_1 (m)	V_1 (kN)	d_u (m)	V_u(kN)	μ (-)	q_R (-)
1° Mode	0.18	624.56	0.74	1074.08	4.11	1.72
Uniform	0.18	869.81	0.80	1508.68	4.44	1.73

❖ Structure code: 8 St_DC3_D-CBFs_X_TRADITIONAL

Base shear seismic action: F_b = 594.42 kN

Table B.51 – Modal displacements and seismic horizontal forces for 8 St_DC3_D-CBFs_X_TRADITIONAL

Storey	U_1 (m)	$F_{i\_1°}$ (kN)	F_{i_m} (kN)

1	-0.003	9.50	74.98
2	-0.009	27.57	74.98
3	-0.015	47.86	74.98
4	-0.022	68.37	74.98
5	-0.028	88.33	74.98
6	-0.034	106.47	74.98
7	-0.039	121.90	74.98
8	-0.043	124.42	69.59

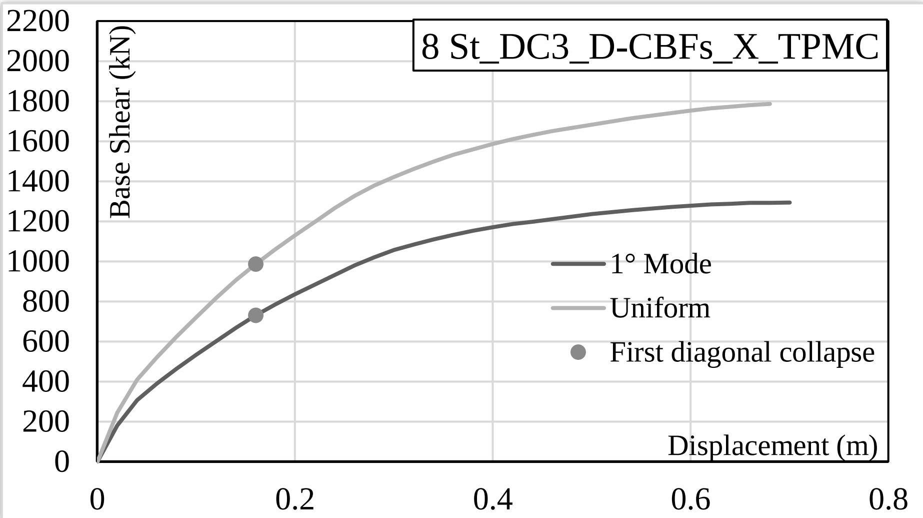

Figure B.26 – Push-over curves for 8 St_DC3_D-CBFs_X_TRADITIONAL

Table B.52 - Seismic performance data for 8 St_DC3_D-CBFs_X_TRADITIONAL

CASE	d_1 (m)	V_1 (kN)	d_u (m)	V_u(kN)	μ (-)	q_R (-)
1° Mode	0.16	730.61	0.66	1291.73	4.12	1.77
Uniform	0.14	907.28	0.66	1780.78	4.71	1.96

❖ Structure code: 8 St_DC2_D-CBFs_Y_TRADITIONAL

Base shear seismic action: F_b = 693.93 kN

Table B.53 – Modal displacements and seismic horizontal forces for 8 St_DC2_D-CBFs_Y_TRADITIONAL

Storey	U_1 (m)	$F_{i\_1°}$ (kN)	F_{i_m} (kN)
1	0.003	10.71	87.53
2	0.009	30.09	87.53
3	0.015	53.47	87.53
4	0.022	77.97	87.53
5	0.030	103.45	87.53
6	0.036	126.77	87.53
7	0.042	145.36	87.53
8	0.045	146.10	81.24

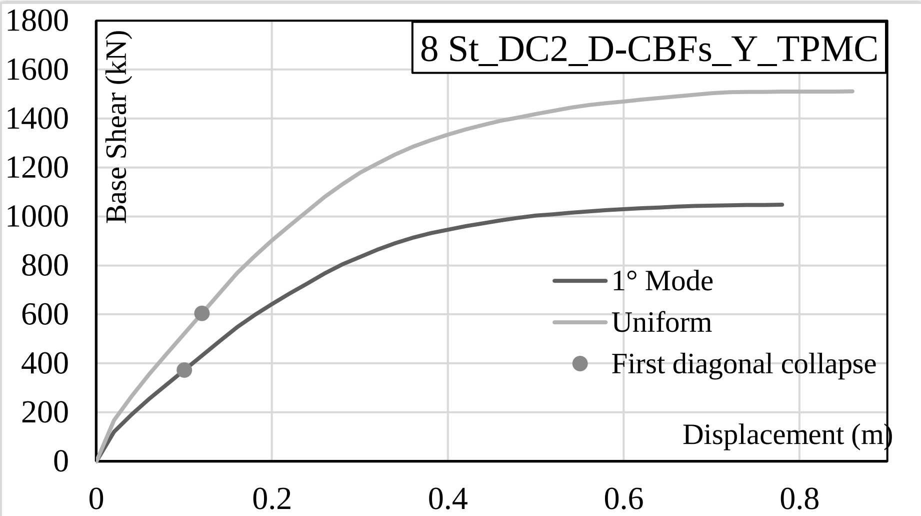

Figure B.27 – Push-over curves for 8 St_DC2_D-CBFs_Y_TRADITIONAL

Table B.54 - Seismic performance data for 8 St_DC2_D-CBFs_Y_TRADITIONAL

CASE	d_1 (m)	V_1 (kN)	d_u (m)	V_u(kN)	μ (-)	q_R (-)
1° Mode	0.18	598.42	0.74	1046.96	4.11	1.75
Uniform	0.16	770.03	0.78	1510.11	4.87	1.96

❖ Structure code: 8 St_DC3_D-CBFs_Y_TRADITIONAL

Base shear seismic action: F_b = 655.80 kN

Table B.55 – Modal displacements and seismic horizontal forces for 8 St_DC3_D-CBFs_Y_TRADITIONAL

Storey	U_1 (m)	$F_{i\_1°}$ (kN)	F_{i_m} (kN)
1	-0.003	11.06	82.72
2	-0.009	30.86	82.72
3	-0.016	53.27	82.72
4	-0.023	75.98	82.72
5	-0.030	98.04	82.72
6	-0.036	117.83	82.72
7	-0.041	133.79	82.72
8	-0.045	134.97	76.78

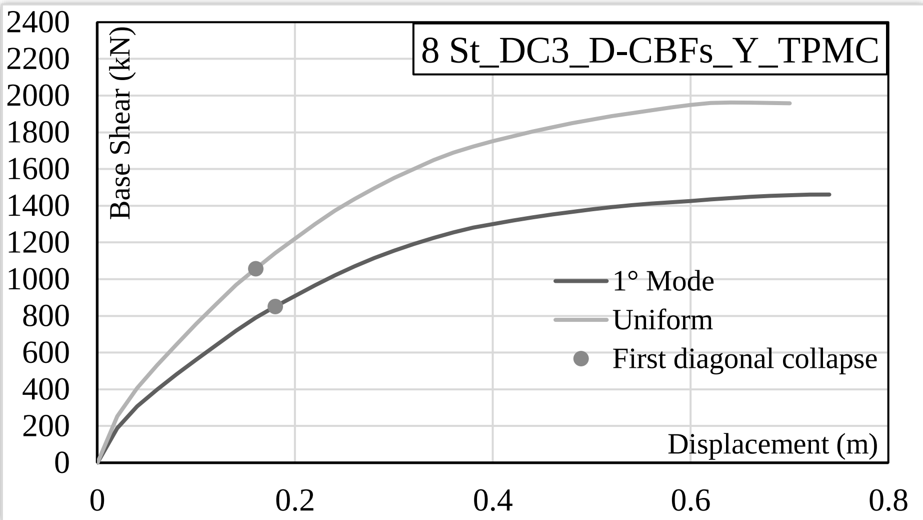

Figure B.28 – Push-over curves for 8 St_DC3_D-CBFs_Y_TRADITIONAL

Table B.56 - Seismic performance data for 8 St_DC3_D-CBFs_Y_TRADITIONAL

CASE	d_1 (m)	V_1 (kN)	d_u (m)	V_u(kN)	μ (-)	q_R (-)
1° Mode	0.16	790.02	0.72	1460.77	4.49	1.85
Uniform	0.14	968.71	0.64	1962.43	4.56	2.03

❖ Structure code: 8 St_DC2_D-CBFs_X_FREEDAM

Base shear seismic action: F_b = 656.71 kN

Table B.57 – Modal displacements and seismic horizontal forces for 8 St_DC2_D-CBFs_X_FREEDAM

Storey	U_1 (m)	$F_{i\_1°}$ (kN)	F_{i_m} (kN)
1	0.003	10.77	82.83
2	0.009	28.94	82.83
3	0.015	50.70	82.83
4	0.022	73.25	82.83
5	0.030	97.19	82.83
6	0.036	119.15	82.83
7	0.042	137.65	82.83
8	0.045	139.07	76.89

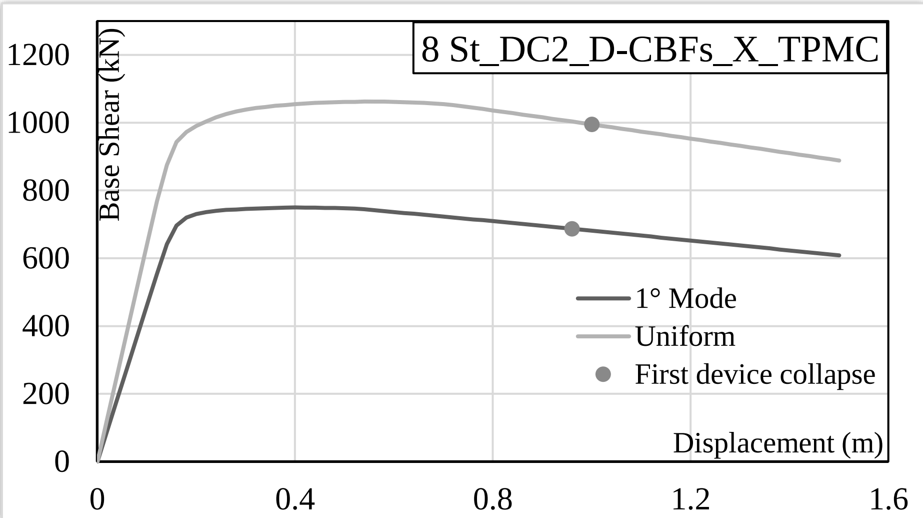

Figure B.29 – Push-over curves for 8 St_DC2_D-CBFs_X_FREEDAM

Table B.58 - Seismic performance data for 8 St_DC2_D-CBFs_X_FREEDAM

CASE	d_1 (m)	V_1 (kN)	d_u (m)	V_u(kN)	μ (-)	q_R (-)

1° Mode	0.14	642.04	0.40	750.02	2.85	1.17
Uniform	0.12	768.69	0.54	1062.45	4.48	1.38

❖ Structure code: 8 St_DC3_D-CBFs_X_FREEDAM

Base shear seismic action: F_b = 501.55 kN

Table B.59 – Modal displacements and seismic horizontal forces for 8 St_DC3_D-CBFs_X_FREEDAM

Storey	U_1 (m)	$F_{i\_1°}$ (kN)	F_{i_m} (kN)
1	0.003	8.24	63.26
2	0.008	21.72	63.26
3	0.014	37.34	63.26
4	0.020	53.60	63.26
5	0.027	71.81	63.26
6	0.034	90.57	63.26
7	0.040	107.57	63.26
8	0.045	110.70	58.72

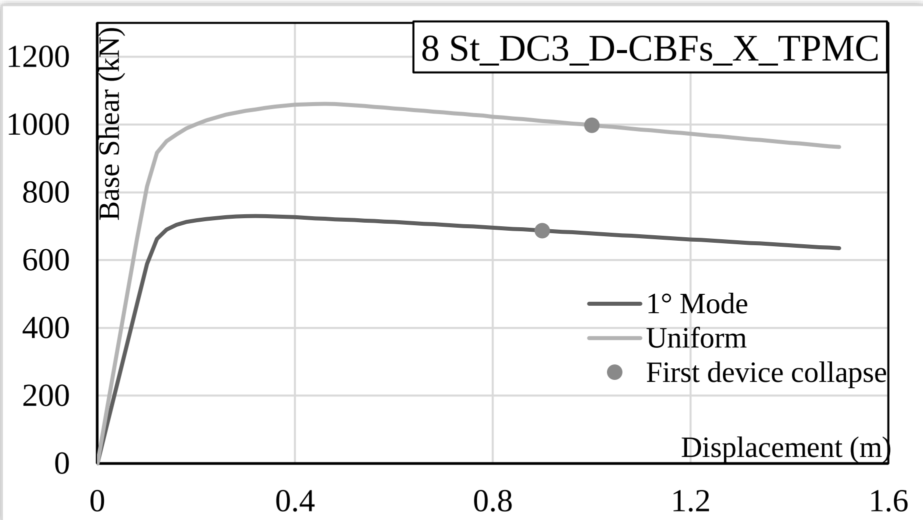

Figure B.30 – Push-over curves for 8 St_DC3_D-CBFs_X_FREEDAM

Table B.60 - Seismic performance data for 8 St_DC3_D-CBFs_X_FREEDAM

CASE	d_1 (m)	V_1 (kN)	d_u (m)	V_u(kN)	μ (-)	q_R (-)
1° Mode	0.12	663.00	0.32	730.13	2.66	1.10
Uniform	0.10	817.51	0.46	1061.10	4.58	1.30

❖ Structure code: 8 St_DC2_D-CBFs_Y_FREEDAM

Base shear seismic action: F_b = 674.26 kN

Table B.61 – Modal displacements and seismic horizontal forces for 8 St_DC2_D-CBFs_Y_FREEDAM

Storey	U_1 (m)	$F_{i\_1°}$ (kN)	F_{i_m} (kN)
1	-0.003	11.24	85.05
2	-0.009	30.13	85.05
3	-0.016	52.77	85.05
4	-0.023	76.18	85.05
5	-0.030	100.28	85.05
6	-0.036	121.57	85.05
7	-0.042	140.21	85.05
8	-0.045	141.88	78.94

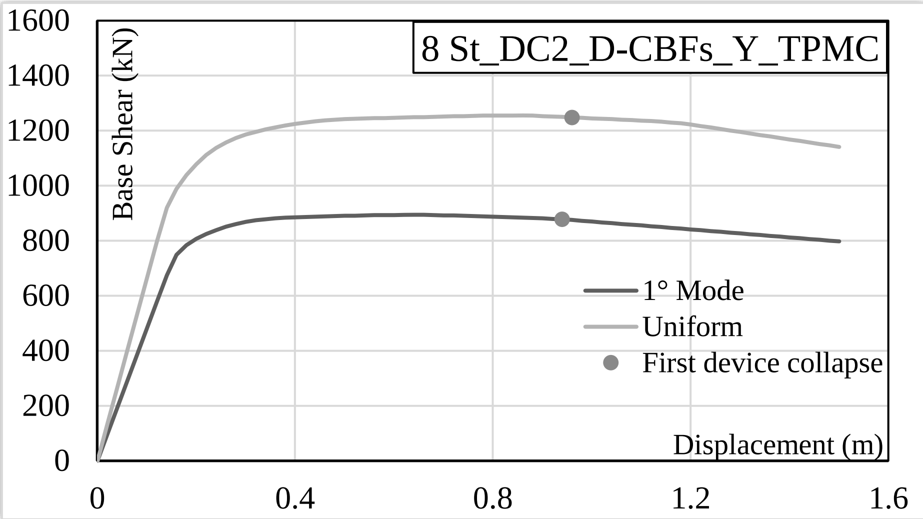

Figure B.31 – Push-over curves for 8 St_DC2_D-CBFs_Y_FREEDAM

Table B.62 - Seismic performance data for 8 St_DC2_D-CBFs_Y_FREEDAM

CASE	d_1 (m)	V_1 (kN)	d_u (m)	V_u(kN)	μ (-)	q_R (-)
1° Mode	0.14	674.76	0.62	894.06	4.41	1.32
Uniform	0.12	798.26	0.86	1255.36	7.13	1.57

❖ Structure code: 8 St_DC3_D-CBFs_Y_FREEDAM

Base shear seismic action: F_b = 561.61 kN

Table B.63 – Modal displacements and seismic horizontal forces for 8 St_DC3_D-CBFs_Y_FREEDAM

Storey	U_1 (m)	$F_{i\_1°}$ (kN)	F_{i_m} (kN)
1	0.003	9.62	70.84
2	0.009	25.06	70.84
3	0.015	42.60	70.84
4	0.021	60.63	70.84
5	0.028	80.62	70.84
6	0.036	101.06	70.84

7	0.042	119.51	70.84
8	0.047	122.51	65.75

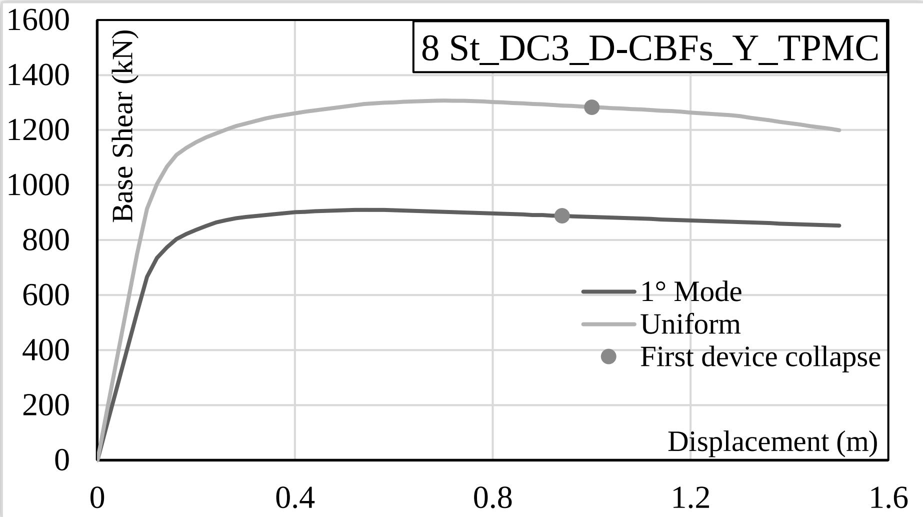

Figure B.32 – Push-over curves for 8 St_DC3_D-CBFs_Y_FREEDAM

Table B.64 - Seismic performance data for 8 St_DC3_D-CBFs_Y_FREEDAM

CASE	d_1 (m)	V_1 (kN)	d_u (m)	V_u(kN)	μ (-)	q_R (-)
1° Mode	0.10	666.03	0.54	909.76	5.37	1.37
Uniform	0.10	914.73	0.70	1307.11	6.96	1.43

APPENDIX C

INCREMENTAL DYNAMIC ANALYSES RESULTS

In this section IDA analyses results in terms of inter-storey drift are reported. For each structure three graphs corresponding to the scale factors 0.5,1 and 1.5 are reported.

- **Structure code: 4 St_DC2_MRFs_X_TRADITIONAL**

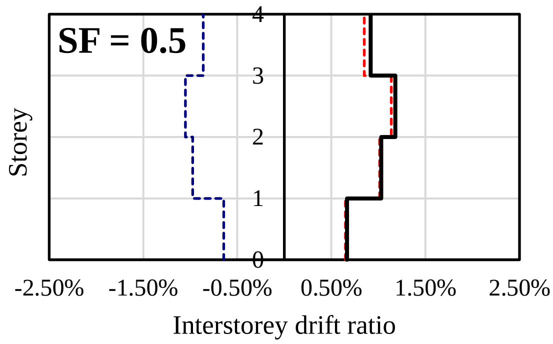

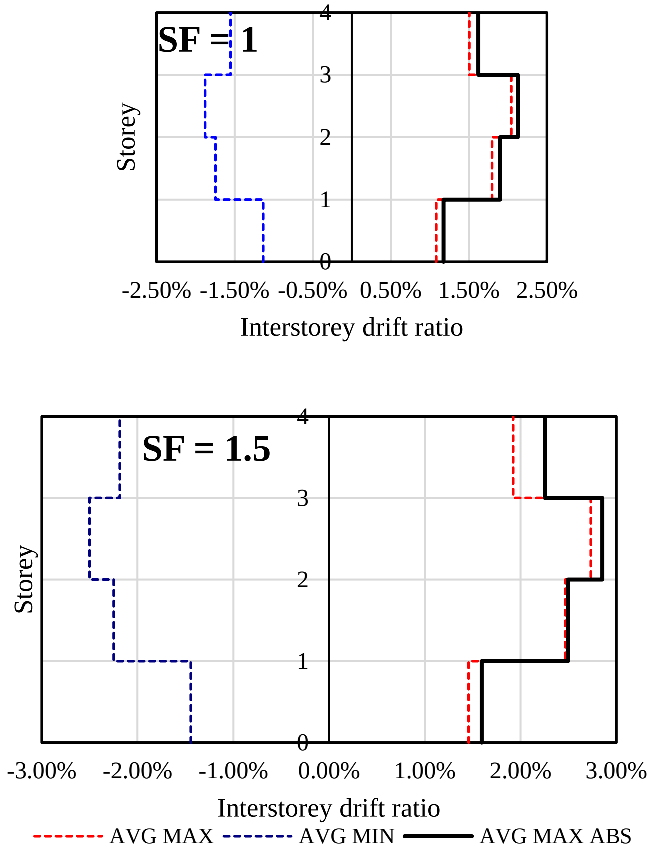

Figure C.1 – Intersorey drift ratio for 4 St_DC2_MRFs_X_TRADITIONAL

❖ **Structure code: 4 St_DC3_MRFs_Y_TRADITIONAL**

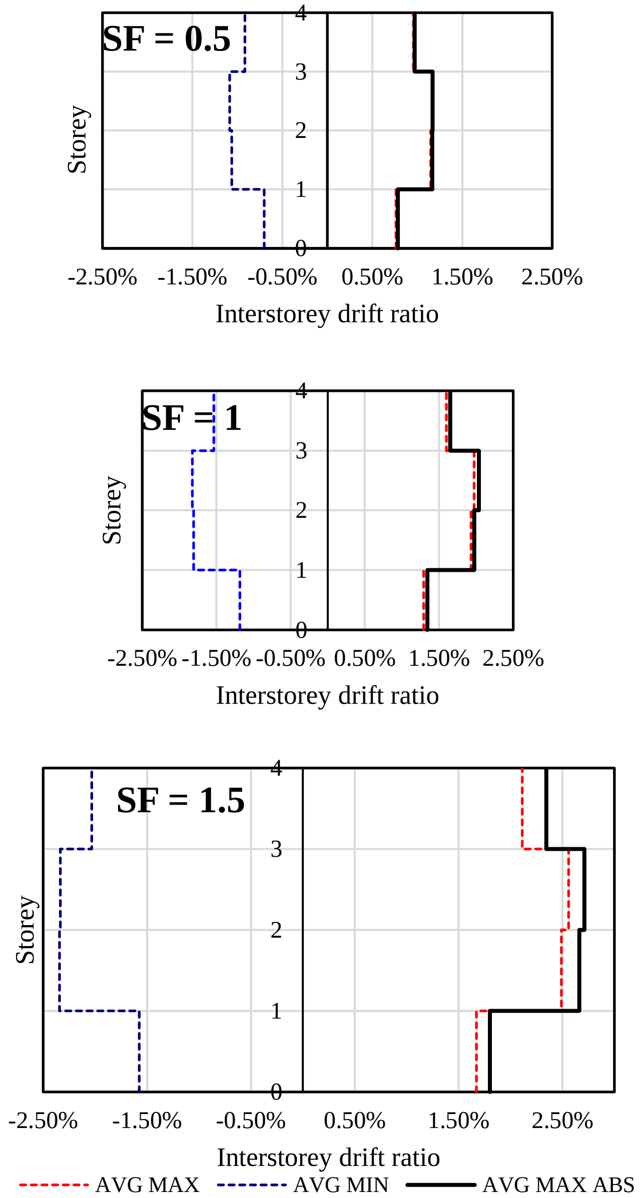

Figure C.2 - Intersorey drift ratio for 4 St_DC3_MRFs_Y_TRADITIONAL

- **Structure code: 8 St_DC2_MRFs_X_TRADITIONAL**

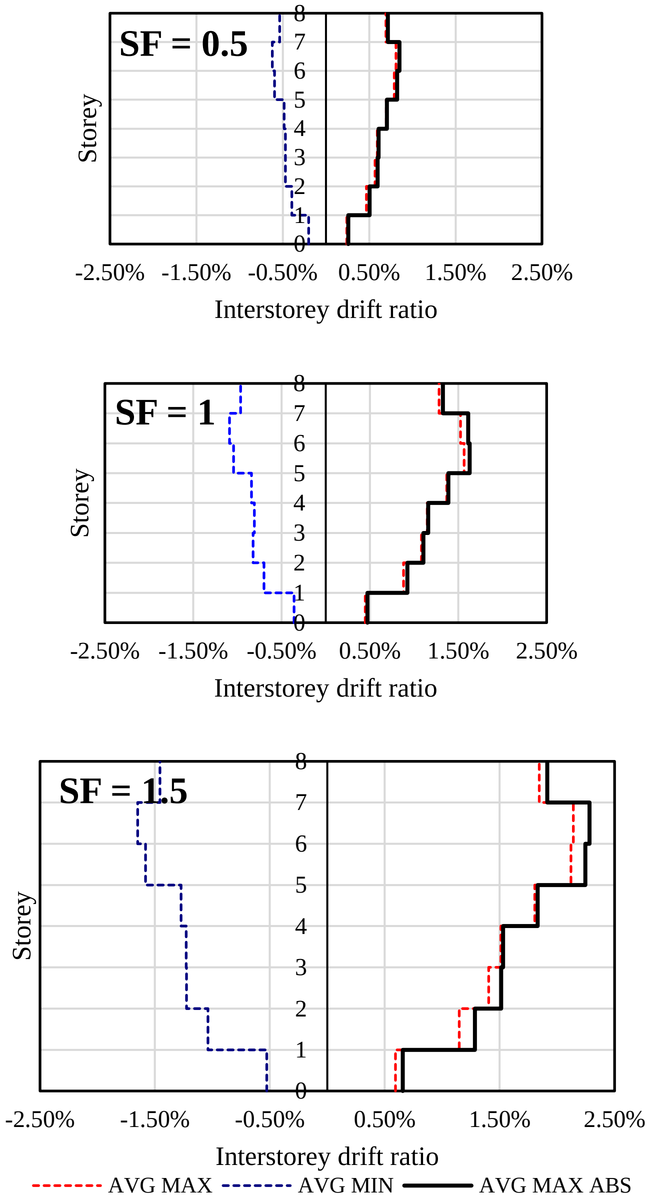

Figure C.3 - Intersorey drift ratio for 8 St_DC2_MRFs_X_TRADITIONAL

❖ Structure code: 8 St_DC3_MRFs_X_TRADITIONAL

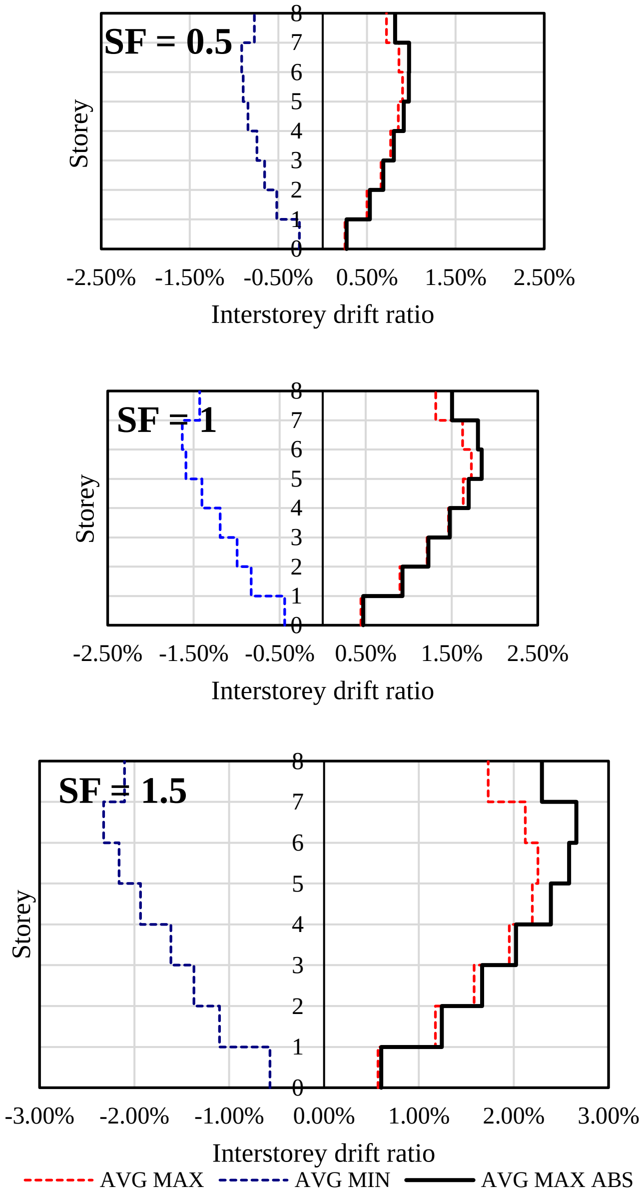

Figure C.4 - Intersorey drift ratio for 8 St_DC3_MRFs_Y_TRADITIONAL

❖ **Structure code: 4 St_DC2_D-CBFs_X_TRADITIONAL**

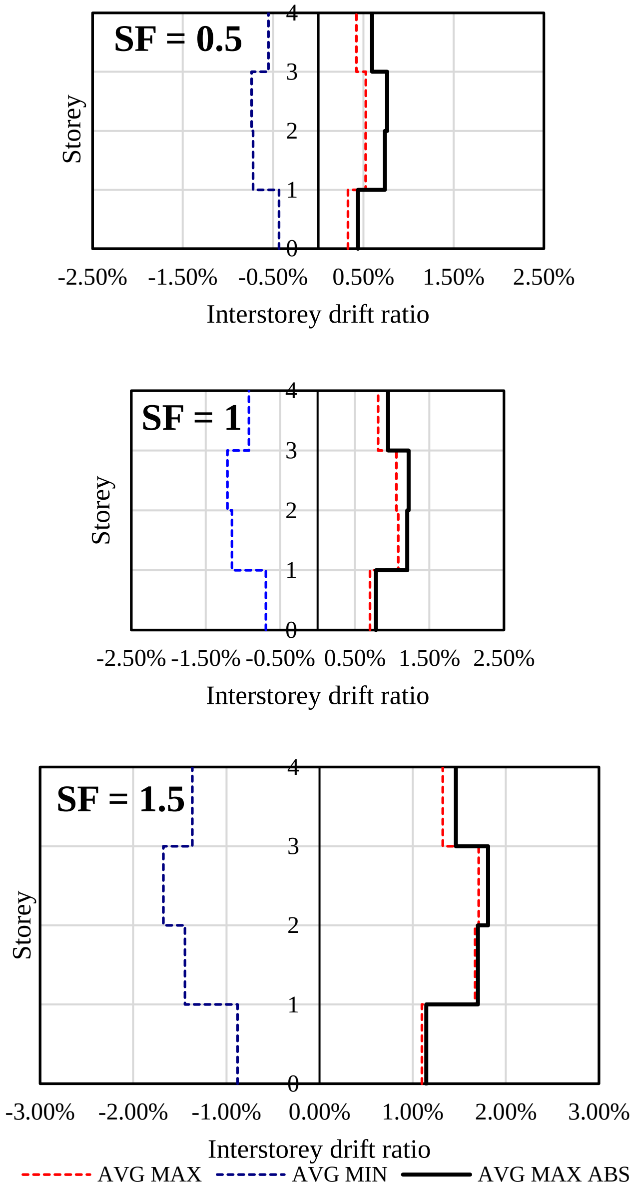

Figure C.5 - Intersorey drift ratio for 4 St_DC2_D-CBFs_X_TRADITIONAL

❖ **Structure code: 8 St_DC2_D-CBFs_X_TRADITIONAL**

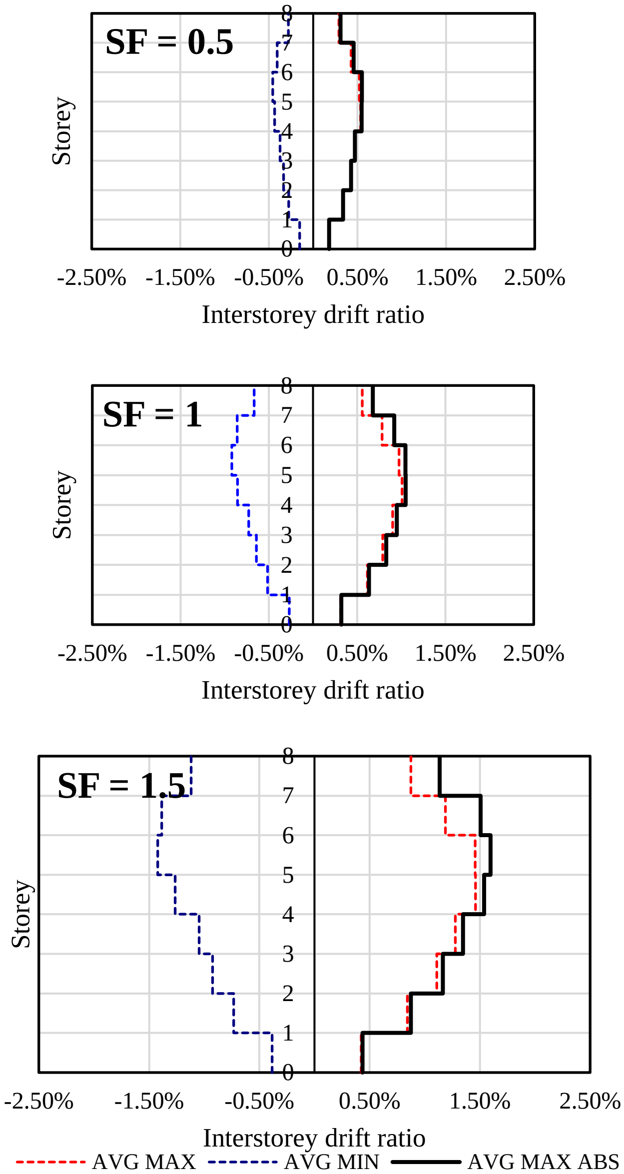

Figure C.6 - Interstorey drift ratio for 8 St_DC2_D-CBFs_X_TRADITIONAL

- **Structure code: 8 St_DC3_D-CBFs_X_TRADITIONAL**

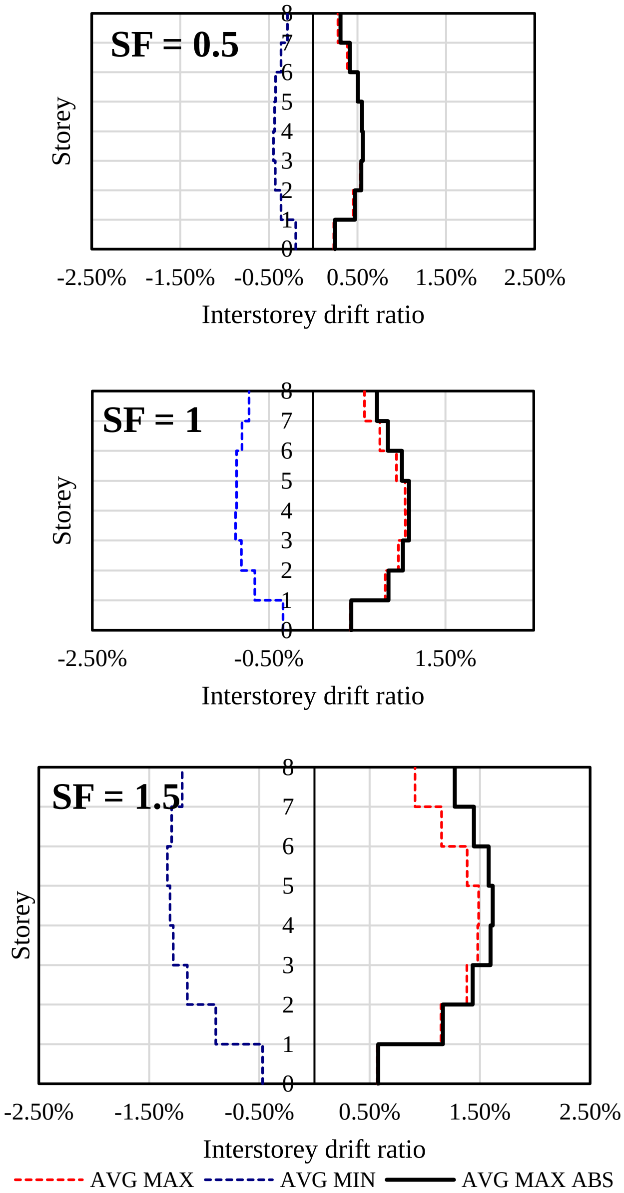

Figure C.7 - Interstorey drift ratio for 8 St_DC3_D-CBFs_X_TRADITIONAL

- **Structure code: 4 St_DC2_MRFs_X_FREEDAM**

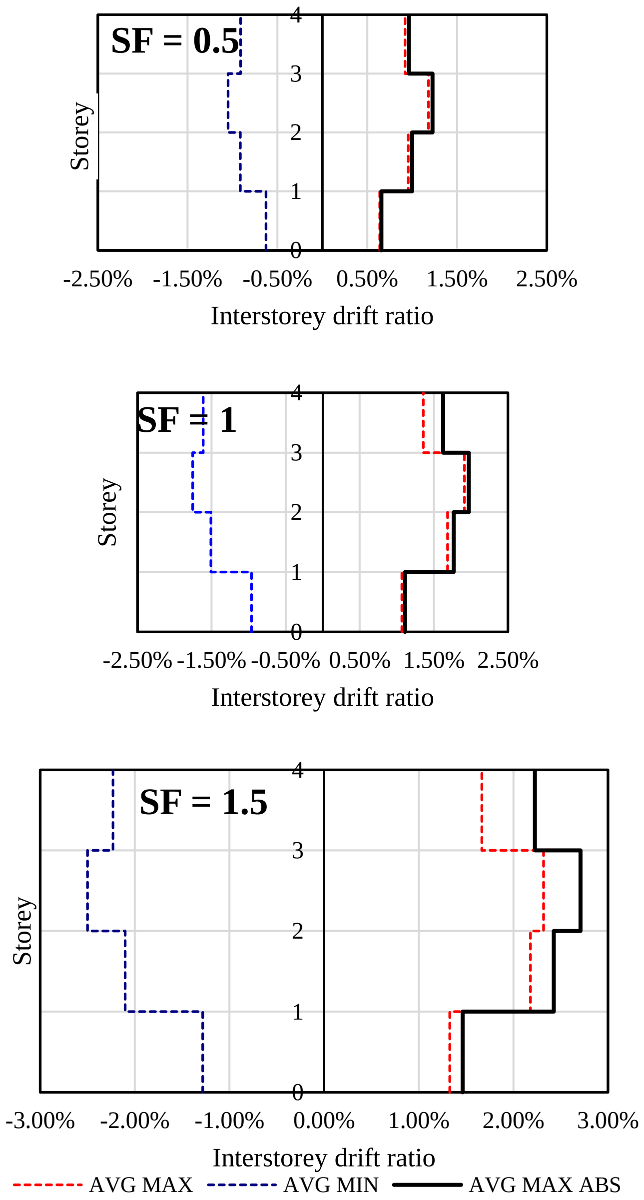

Figure C.8 - Interstorey drift ratio for 4 St_DC2_MRFs_X_FREEDAM

- **Structure code: 4 St_DC3_MRFs_Y_FREEDAM**

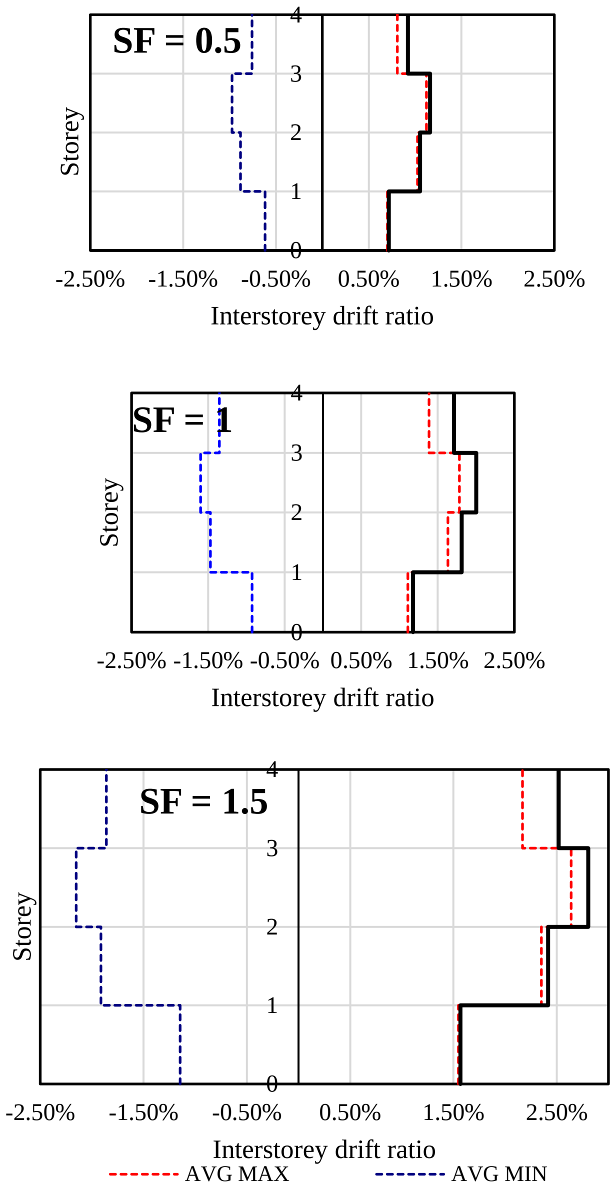

Figure C.9 - Interstorey drift ratio for 4 St_DC3_MRFs_Y_FREEDAM

❖ Structure code: 8 St_DC2_MRFs_X_FREEDAM

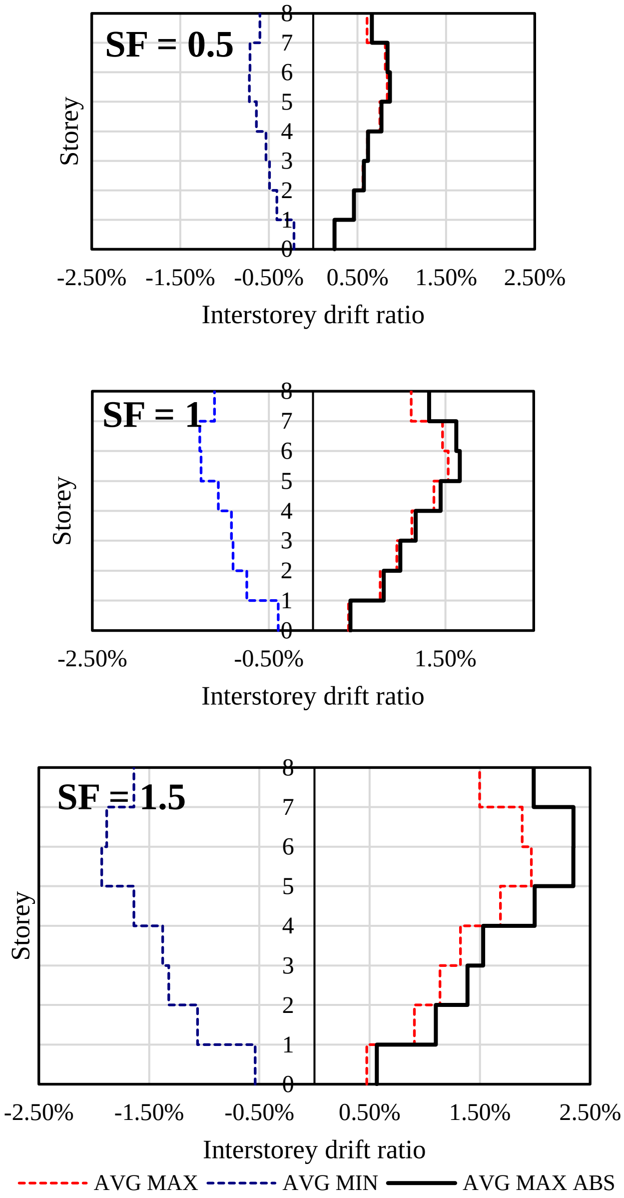

Figure C.10 - Interstorey drift ratio for 8 St_DC2_MRFs_X_FREEDAM

❖ **Structure code: 8 St_DC3_MRFs_X_FREEDAM**

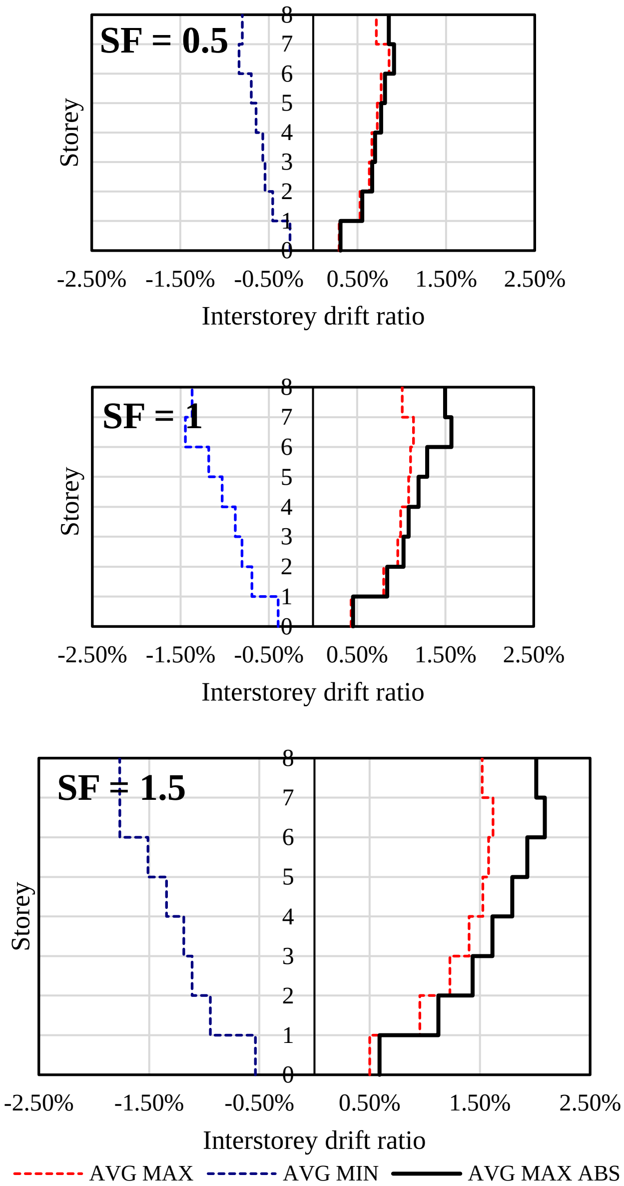

Figure C.11 - Interstorey drift ratio for 8 St_DC3_MRFs_X_FREEDAM

❖ Structure code: 4 St_DC2_D-CBFs_X_FREEDAM

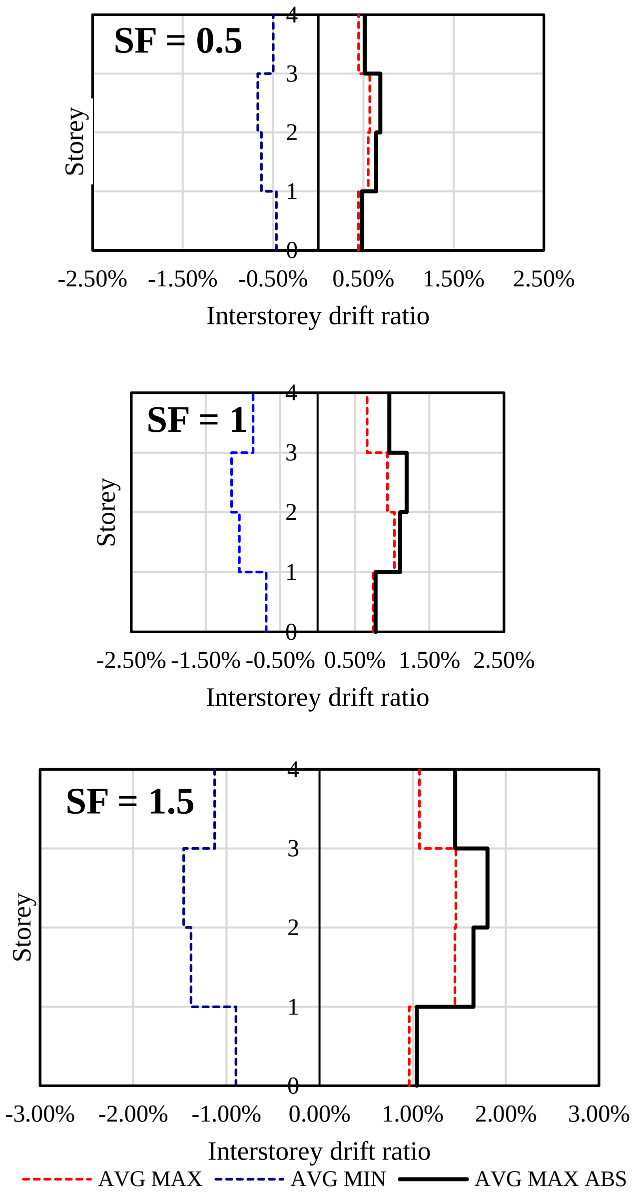

Figure C.12 - Interstorey drift ratio for 4 St_DC2_D-CBFs_X_FREEDAM

❖ Structure code: 8 St_DC2_D-CBFs_X_FREEDAM

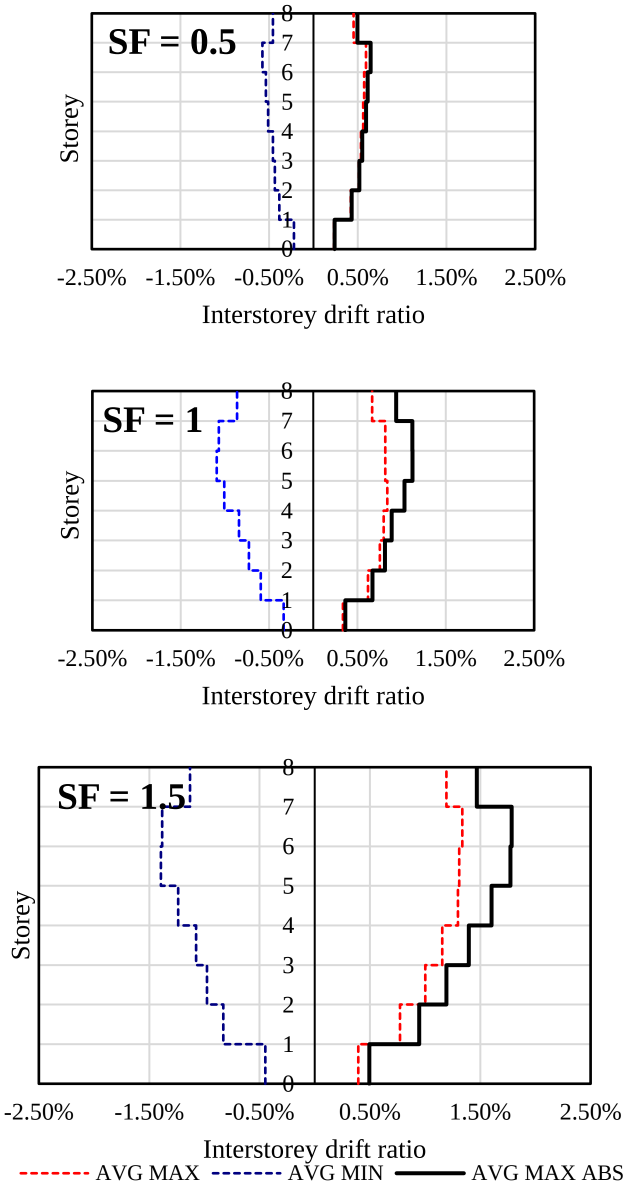

Figure C.13 - Interstorey drift ratio for 8 St_DC2_D-CBFs_X_FREEDAM

❖ Structure code: 8 St_DC3_D-CBFs_X_FREEDAM

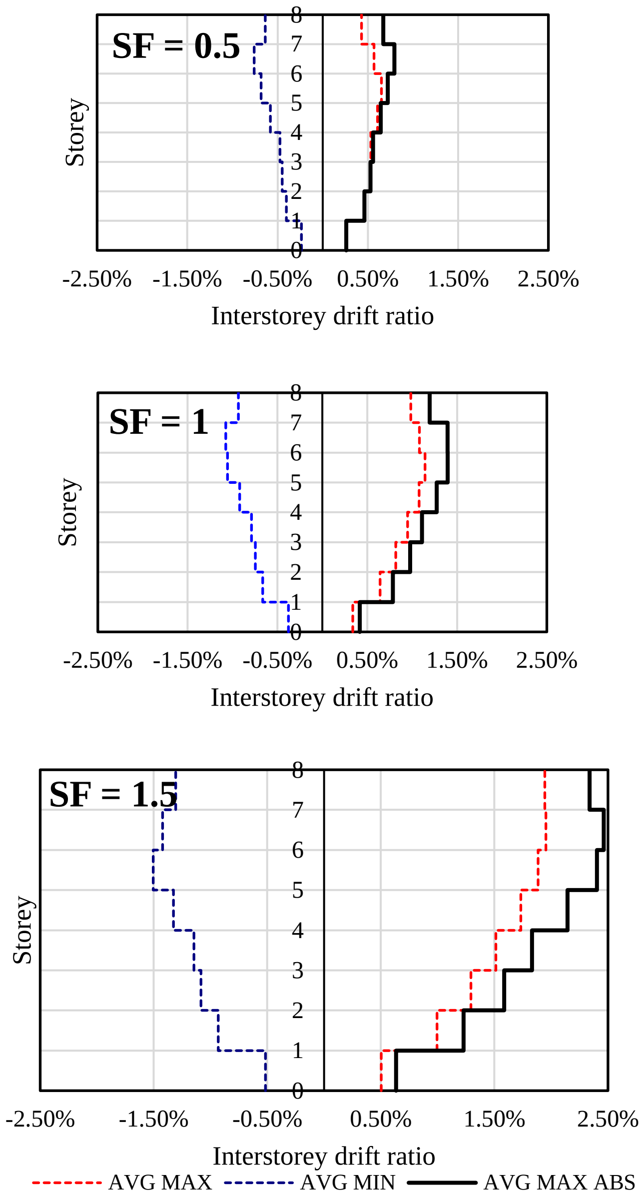

Figure C.14 - Interstorey drift ratio for 8 St_DC3_D-CBFs_X_FREEDAM

ANNEX A

DEVICE D1

Beam range: IPE 270 - IPE 450

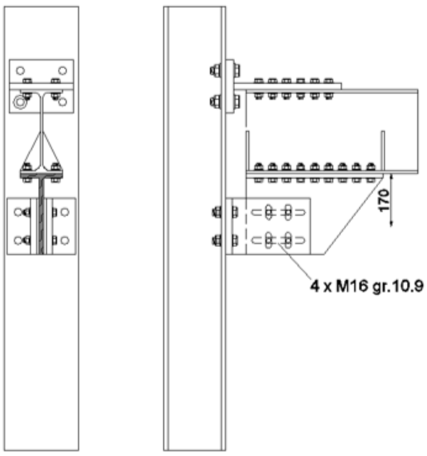

DEVICE D2

Beam range: IPE 360 - IPE 600

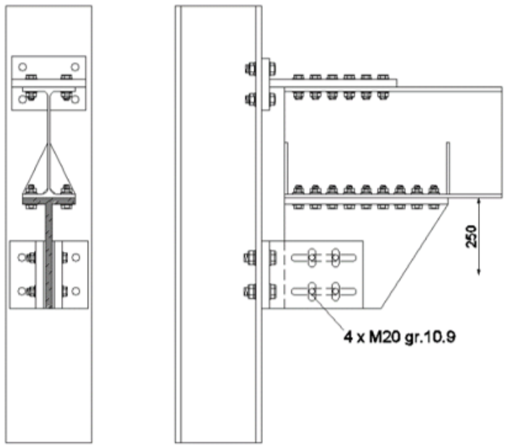

DEVICE D3

Beam range: IPE 400 - IPE 750x173

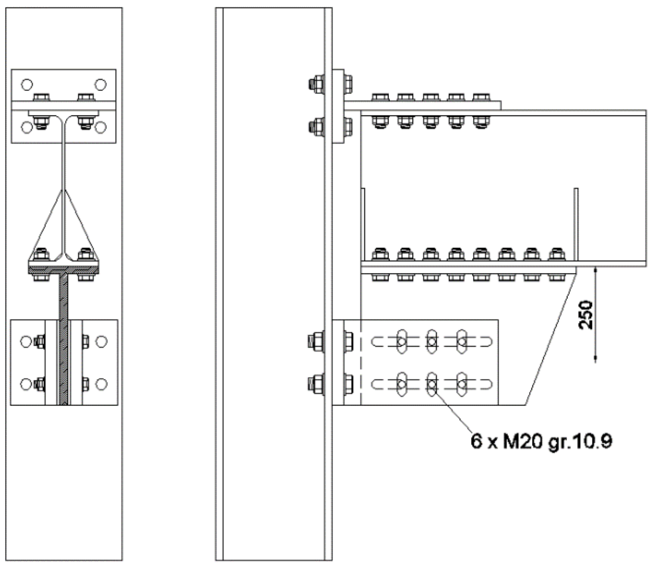

DEVICE D4

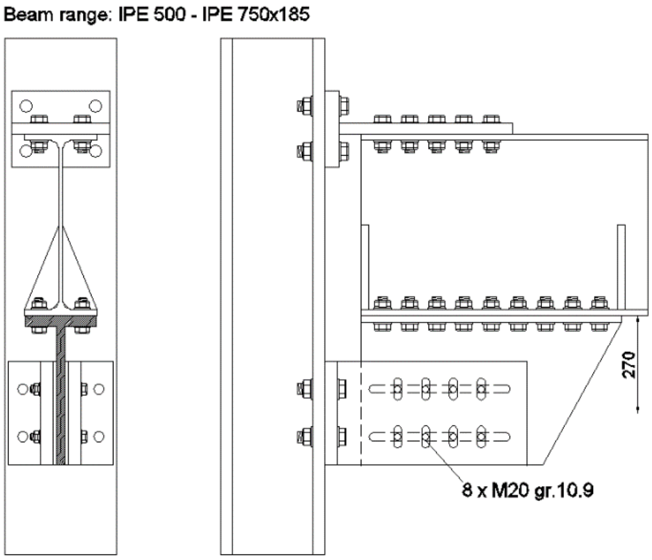

DEVICE D5